The Ins and Outs of Protein Trafficking Pathways: Insights from the FAST Proteins

by

Hirendrasinh B. Parmar

Submitted in partial fulfilment of the requirements
for the degree of Doctor of Philosophy

at

Dalhousie University
Halifax, Nova Scotia
May 2015

TABLE OF CONTENTS

LIST OF FIGURES

ABSTRACT

Sorting and trafficking of integral membrane proteins to the plasma membrane is essential for cellular homeostasis. Our understanding of the pathways and sorting signals that regulate protein trafficking is far from complete, particularly as it relates to protein exit from the Golgi. The reovirus fusion-associated small transmembrane (FAST) proteins are small integral membrane proteins that traffic through the ER-Golgi pathway to the plasma membrane where they cause cell-cell membrane fusion. The small sizes of FAST proteins and their simple structures provide an excellent system to identify factors and pathways affecting plasma membrane trafficking.

Using the reptilian reovirus p14 FAST protein, I discovered that a polybasic motif (PBM), located four residues downstream of the transmembrane domain in the cytoplasmic tail of p14, is required for p14 export from the Golgi to the plasma membrane. Extensive mutagenesis of the PBM indicated that the number, but not the identity or position, of basic residues in the PBM directs p14 trafficking to the plasma membrane, with a minimum of three basic residues being required for efficient Golgi export. Insertion of the PBM into a Golgi-resident ERGIC-53 chimeric protein resulted in protein trafficking to the plasma membrane, indicating the p14 PBM functions as an autonomous Golgi export signal.

I also discovered that the PBM can serve diverse trafficking roles depending on its proximity to the transmembrane domain. The PBM exerts no effect when located at internal positions in the 68-residue p14 cytoplasmic tail, it functions as an ER retention signal when located at the C-terminus, and when present at both membrane-proximal and -distal locations promotes export to and retrieval from the Golgi complex. Interestingly, the conflicting signals provided by membrane-proximal and -distal PBMs induce extensive ER tubulation and segregation of luminal ER components. A single trafficking motif can therefore exert remarkably diverse, position-dependent effects on protein trafficking and membrane compartment morphogenesis.

To determine how the p14 PBM directs Golgi-plasma membrane transport, I examined the effects of various trafficking factors and pathways on this process. Yeast two-hybrid analysis identified Rab11A as a genetic interaction partner of p14. Co-immunoprecipitation (co-IP) determined that p14 interacts preferentially with GTP-bound activated Rab11A in a PBM-dependent manner. Overexpression of dominant-negative Rab11A, but not Rab5, significantly reduced p14 surface expression. Fluorescence resonance energy transfer (FRET) microscopy indicated activated Rab11 directly interacts with p14 dependent on the PBM, the first example of activated Rab11 directly interacting with membrane cargo for Golgi-plasma membrane trafficking. Furthermore, RNA interference revealed that both Rab11 and adaptor protein 1 (AP1), but not AP3 or AP4, are required for efficient p14 trafficking from the *trans*-Golgi network (TGN) to the plasma membrane. This is also the first indication of Rabs regulating adaptor proteins at the TGN for anterograde vesicle traffic, and provides a clear indication that AP1 can mediate anterograde traffic from the Golgi to the plasma membrane. I conclude that the p14 PBM functions as a novel autonomous tribasic Golgi export signal by directing interaction with activated Rab11, resulting in p14 sorting into AP1-coated vesicles at the TGN for trafficking to the plasma membrane, either directly or via endosomal recycling pathways.

LIST OF ABBREVIATIONS USED

ALPS	amphipathic lipid packing sensor
ANOVA	analysis of variance
AP	adaptor protein
APP	amyloid precursor protein
Arf	ADP ribosylation factor
Arl	Arf-like protein
ARV	avian reovirus
Asna1	arsenical pump-driving ATPase protein
AT1R	angiotensin II type 1 receptor
BAR	bin/amphiphysin/Rvs
BIG	brefeldin A-inhibited guanine exchange factor
BroV	Broome reovirus
BRV	Baboon reovirus
BSA	bovine serum albumin
CAML	calcium-modulating cyclophilin ligand
CAR	Coxsackie and adenovirus receptor
CERT	ceramide transfer protein
cGK-II	cGMP dependent protein kinase II
co-IP	co-immunoprecipitation
COP	coat protein
DMEM	Dulbecco's modified eagle medium
DMSO	dimethyl sulfoxide
E. coli	*Escherichia coli*
EDTA	ethylenediaminetetraacetic acid
endo H	endoglycosidase H
ER	endoplasmic reticulum
ERAD	ER associated degradation pathway
ERES	endoplasmic reticulum exit site
ERGIC	ER-Golgi intermediate compartment
EPS15	EGFR pathway substrate 15
FAPP	four-phosphate adaptor protein
FAST	fusion-associated small transmembrane
FBS	fetal bovine serum
FCHO	FCH domain only
FcR	Fc receptor
FIP	family-interacting protein
FRAP	fluorescence recovery after photobleaching
FRET	fluorescence resonance energy transfer
GAE	gamma-adaptin ear homology
GAP	GTPase activating protein
GAT	GGA and Tom1
GBF	Golgi-specific brefeldin A-resistant factor
GEF	guanine exchange factor
GDF	GDI dissociation factor

GDI	GDP dissociation inhibitor
GGA	Golgi-localizing gamma-adaptin ear containing Arf-binding proteins
HBSS	Hank's balanced salt solution
HEK	human embryonic kidney
HEPES	4-(2-hydroxyethyl)-1-piperazineethanesulfonic acid
hIP	human prostacyclin receptor
HPS	Hermansky-Padlock syndrome
hpt	hours post-trnsfection
HRP	horseradish peroxidase
HSC70	heat shock cognate 70
HSP	hereditary spastic paraplegia
IPTG	isopropyl-beta-D-thiogalactopyranoside
kDa	kilodalton
LDLR	low-density lipoprotein receptor
MPER	membrane-proximal ectodomain region
MRV	mammalian reovirus
MVB	multivesicular body
NBV	Nelson Bay reovirus
NFRET	normalized fluorescence resonance energy transfer
NPRA	natriuretic peptide receptor A
OD	optical density
OSBP	oxysterol-binding protein
PBM	polybasic motif
PBS	phosphate-buffered saline
PCR	polymerase chain reaction
PDI	protein disulphide isomerase
PEI	polyethylenimine
PH	pleckstrine-homology
pIgAR	polymeric immunoglobulin A receptor
PI3K	phosphoinositide-3-kinase
PI4KIIIα/β	phosphatidylinositol-4-kinase IIIα/β
PIP	phosphatidylinositol phosphate
PI(3)P	phosphatidylinositol-3-phosphate
PI(4)P	phosphatidylinositol-4-phosphate
PI(5)P	phosphatidylinositol-5-phosphate
$PI(3,4)P_2$	phosphatidylinositol-3,4-bisphosphate
$PI(4,5)P_2$	phosphatidylinositol-4,5-bisphosphate
$PI(3,5)P_2$	phosphatidylinositol-3,5-bisphosphate
$PI(3,4,5)P_3$	phosphatidylinositol-3,4,5-triphosphate
PNGaseF	N-glycosidase F
PTEN	phosphatase and tensin homologue
PVDF	polyvinylidene difluoride
PX	phox-homology
RBD	Rab11 binding domain
REP	Rab escort protein
RRV	Reptilian reovirus

SBT	spectral bleed-through
SD	standard deviation
SDS	sodium dodecyl sulphate
SEM	standard error of the mean
SH3	SRC homology 3
SNARE	soluble N-ethylmaleimide-sensitive factor attachment protein receptor
SNX	sorting nexin
SRP	signal recognition particle
TBS-T	Tris-buffered saline with Tween-20
tER	transitional endoplasmic reticulum
TfR	transferrin receptor
TGN	*trans*-Golgi network
TMD	transmembrane domain
TRC	transmembrane recognition complex
TRP	transient receptor potential
VHS	Vps27, Hrs and STAM
VPS	vacuolar protein sorting
VSV-G	vesicular stomatitis virus glycoprotein
WRB	Tryptophan-rich basic protein

ACKNOWLEDGEMENTS

I sincerely thank my supervisor, Roy, for accepting me as a graduate student and being a wonderful guide by providing meaningful insights and ideas for my project as well as providing independence to pursue a new research direction in the lab. You are an excellent teacher and taught me a lot of skills required to succeed in science. Your support, kindness and enthusiasm made my journey quiet enjoyable. In addition, thank you for all of the fun parties at your place and for explaining Canadian customs, phrases and 'norms' that made my life a lot easier to adjust to the North American culture. The last five and half years have truly been a lifelong learning experience.

I would like to extend my thanks to my committee members, Rick, Neale, Craig and Denis, for their useful comments and feedback, and for taking an interest in my project. Thank you for also providing reagents that I needed for my project. I also thank Karl Matter (University College London) for providing constructs and helpful discussions.

Many thanks go to the Duncan lab members, present and past, for tech transfer and help, and being awesome colleagues, good friends and hilarious people. Also, thanks to all my friends in Halifax and around the globe for continuous support and company. All of you have made this journey so easy and enjoyable.

A special thanks to Jan for inviting me to Nova Scotia. This gave me the opportunity to truly enjoy the natural beauty of the Maritimes, and to meet Roy, which led to this thesis.

A huge thanks to my parents and my brother, Manoj, for always being supportive and believing in me no matter where I am. Thank you for ensuring my good education and well-being. A special heartfelt thanks to my wife, Archita, for her support and making the process of thesis writing so much easier. Finally, a warm thanks to my spiritual guru P. Hariprasadswamiji for always inspiring and showing me the path I wanted to follow.

CHAPTER 1
INTRODUCTION

1.1 Overview

Membrane proteins are essential for numerous cellular functions and use secretory pathways to traffic to their respective subcellular compartments. Our understanding of the molecular mechanisms regulating the various steps of membrane protein trafficking remain incomplete, particularly in regard to protein trafficking from the *trans*-Golgi network (TGN), which is considered the main 'sorting hub' for vesicle traffic. I used a unique family of viral fusion proteins, the reovirus fusion-associated small transmembrane (FAST) proteins, as tools to study intracellular trafficking pathways. My results identified the polybasic motif (PBM) of the p14 FAST protein as a novel tribasic autonomous Golgi export signal that can exert multiple effects on trafficking depending on its membrane-proximity. I further discovered that the PBM regulates interaction of p14 with activated Rab11 and sorting into adaptor protein (AP) 1 complex-coated vesicles for export from the Golgi and transport to the plasma membrane, a novel active Rab11-dependent cargo sorting mechanism at the TGN for biosynthetic anterograde transport. In this chapter, I introduce membrane proteins and secretory pathways, and describe our current understanding of molecular mechanisms regulating protein traffic through the secretory pathway. I also introduce the fusogenic reoviruses and described the characteristics of the FAST proteins they encode.

1.2 Membrane protein trafficking

1.2.1 Membrane proteins

Approximately one third of the human proteome are membrane proteins, which are involved in range of essential cellular functions including allowing cells to specifically communicate with the extracellular environment (Almen et al., 2009). Over 50% of current pharmaceutical drugs target membrane proteins, and aberrant trafficking and subcellular localization of membrane proteins leads to variety of human diseases (described in 1.10). Membranes proteins are subcategorized based on the nature of their interaction with

cellular membranes. Monotopic membrane proteins interact with only one side of the lipid bilayer, while bitopic and multitopic membrane proteins span the membrane bilayer once or multiple times, respectively. Bitopic or multitopic membrane proteins are also known as integral membrane or transmembrane proteins. Bitopic membrane proteins can be further subcategorized depending on their topology (Goder and Spiess, 2001; Higy et al., 2004). The Type I transmembrane proteins are targeted to the endoplasmic reticulum (ER) membrane by an N-terminal signal peptide (described in 1.3) that is subsequently cleaved to generate an ER luminal N-terminus and cytoplasmic C-terminus. The Type II transmembrane proteins are targeted to the ER by a non-cleavable signal anchor that also functions as the transmembrane domain, targeting the C-terminus to the ER lumen and the N-terminus to the cytoplasm. The Type III transmembrane proteins also lack a cleavable signal peptide and use their transmembrane domain as a signal anchor; however, it functions as a reverse signal anchor that targets the N-terminus to the ER lumen to obtain a similar topology as Type I transmembrane proteins. Tail-anchored transmembrane proteins have their transmembrane domain, which also function as a signal anchor, close to the C-terminus and therefore, post-translationally inserted into the ER membrane in contrast to co-translational membrane insertion of Type I, II and III transmembrane proteins (described in 1.3).

Transmembrane protein topology is significantly influenced by a biased distribution of basic residues on the cytoplasmic side of the transmembrane domain, the so-called 'positive-inside' rule (von Heijne, 1986). Early studies by von Heijne revealed that cytoplasmic regions of transmembrane proteins are rich in lysine and arginine residues, and that removal of this highly charged region and the addition of four lysine residues to the extra-cytoplasmic side resulted in the *Escherichia coli (E. coli)* membrane protein leader peptidase assuming the reverse topology (von Heijne, 1989). Similar studies confirmed the positive-inside rule for eukaryotic membrane proteins (Sipos and von Heijne, 1993). More recent bioinformatic analysis of 107 genomes also indicated a biased distribution of basic residues towards the cytoplasmic side of transmembrane proteins, suggesting the positive-inside rule is broadly applicable (Nilsson et al., 2005).

Membrane proteins use intracellular vesicle transport and the secretory pathway to localize to the correct membrane compartment. Once the membrane protein is targeted to

the ER membrane by a signal peptide or signal anchor, the protein is translocated into the ER membrane and traffics through the ER-Golgi pathway, accompanied by necessary post-translational modifications, to its destined cellular compartment (Figure 1.1). Membrane proteins at the plasma membrane can also be endocytosed and recycled back to the plasma membrane, or trafficked through endosomal pathways to lysosomes for degradation (Figure 1.1). Protein transport in the forward direction from the ER to the Golgi to the plasma membrane is known as anterograde transport, while protein transport in the reverse direction from the plasma membrane to endosomes to the Golgi to the ER is known as retrograde transport. Recent advances in molecular cell biology have provided in-depth knowledge of various factors that play key roles in these cellular transport pathways. Details of protein trafficking in the secretory and endocytic pathways and the regulatory molecules involved are discussed in the following sub-sections.

1.2.2 Mechanisms of membrane protein trafficking

The secretory pathway sorts and delivers numerous proteins, termed 'cargo' proteins, to their correct intracellular compartments or for secretion by exocytosis. Cargo proteins are delivered to their final destinations through a series of vesicle budding events from the donor membrane compartment and fusion with an acceptor compartment along the secretory pathway (Figure 1.2). A great deal of research has gone into understanding how cargo proteins are specifically sorted into these budding vesicles. Two contrasting models have been proposed to explain cargo protein sorting and export from the ER, the bulk-flow and receptor-mediated export models (Figure 1.3), and these models have been applied to other cellular compartments from which vesicles bud. The latter model is now widely accepted and considered a better fit for recent data.

The bulk-flow model (Figure 1.3) suggests that cargo proteins move by default from the ER to the Golgi to the plasma membrane and require no signals for export from the ER or the Golgi (Barlowe, 2003; Warren and Mellman, 1999). Sorting signals are only needed for cargo proteins to be diverted from the default pathway for delivery to compartments other than the plasma membrane. Early studies by Rothman and colleagues with a tripeptide containing an acceptor sequence for N-linked glycosylation indicated this tripeptide was glycosylated in the ER and trafficked to the Golgi, where oligosaccharide

chains were processed and the tripeptide was then secreted into the medium (Wieland et al., 1987). They suggested that no trafficking signal was necessary, as this tripeptide was too short to contain any sorting signals for efficient transport from the ER to the Golgi and from the Golgi to the plasma membrane. However, later studies indicated that glycosylated proteins are trafficked from the ER to the Golgi by interaction with cargo receptors such as ERGIC-53 that interact with carbohydrates (Appenzeller et al., 1999), and N-linked glycosylation itself is a plasma membrane targeting signal from the Golgi (Gut et al., 1998). There is no cargo receptor identified to interact with carbohydrates to mediate Golgi to plasma membrane transport. Conformational changes in the cargo protein induced by glycosylation may mediate plasma membrane transport. Another group showed that soluble cargo proteins were not concentrated in ER buds and traffic from the ER to the Golgi through concentration in post ER tubular structures that are devoid of coat proteins supporting the bulk-flow model (Martinez-Menarguez et al., 1999). For such a mechanism, some form of cargo aggregation may be required to pass ER quality control and exit from the ER. If true, cargo aggregation may be facilitated by particular sequence that serve as an export signal for exit from the ER. With many examples identified for sorting signals involved in trafficking from the ER and Golgi, the bulk-flow model has been put on rest (Rodriguez-Boulan and Musch, 2005). Mutations in the basolateral plasma membrane sorting signals resulted in cargo protein localization to the apical plasma membrane suggested that the cargo proteins traffic through constitutive transport from the Golgi to the apical plasma membrane in the absence of sorting signal. However, these cargo proteins were N- or O- glycosylated, which serve as an apical sorting determinant (Fiedler and Simons, 1995; Gut et al., 1998; Matter and Mellman, 1994; Yeaman et al., 1997).

The receptor-mediated export model (Figure 1.3) suggests that each and every cargo protein requires signals for selective incorporation into ER-derived vesicles for ER export (Kuehn and Schekman, 1997). In several instances, these export signals have been shown to directly or indirectly interact with vesicle coat proteins. Resident ER proteins could be excluded by an active retention system, while proteins involved in vesicle formation and fusion that travel with the cargo may contain signals that mediate retrieval from post-ER compartments. The selective concentration of cargo proteins in vesicles surrounded by coat protein II (COPII) complex (defined in 1.4.1), a protein complex that

mediates traffic from the ER to the Golgi, favors this model (Bednarek et al., 1995). In this model, sorting signals in luminal cargo would require a transmembrane receptor that recognizes the signal and can interact with the COPII complex. The membrane proteins such as ERGIC-53, p24 and KDEL receptor recycle between the ER and the Golgi and act as such transmembrane receptors for luminal cargo (Appenzeller et al., 1999; Belden and Barlowe, 2001; Capitani and Sallese, 2009; Muniz et al., 2000; Nichols et al., 1998). For example, the luminal domain of ERGIC-53, a single-pass transmembrane protein, displays lectin activity that recognizes a subset of glycoproteins, allowing ERGIC-53 to function as a transport receptor to promote ER-Golgi transport (Appenzeller et al., 1999; Itin et al., 1996; Nichols et al., 1998). Similarly, KDEL receptor is a seven transmembrane domain protein that functions in retrieval to the ER of luminal proteins containing the tetrapeptide KDEL sequence (Capitani and Sallese, 2009). There are numerous examples of sorting signals, including dibasic-, tribasic-, tyrosine- and dileucine-based sorting signals, that interact with particular components of various coat protein complexes such as COPI, COPII and APs for protein sorting and trafficking (described below and summarized in Figure 1.4). Thus, the receptor-mediated export model is clearly involved in most, and perhaps all, intracellular protein sorting and trafficking mechanisms.

1.3 Protein targeting to the ER

The starting point of the secretory pathway is targeting of secretory and membrane proteins to the ER. The most prominent mechanism of membrane insertion involves co-translational insertion mediated by a cytosolic signal-recognition particle (SRP), ER-localized SRP receptor and ER translocon complex formed by Sec61 (Osborne et al., 2005; Shan and Walter, 2005). The signal sequence or signal anchor sequence present near the N-terminus of most cargo proteins interacts with SRP as it emerges from the ribosome. The ribosome-nascent chain complex is delivered to the ER membrane by interaction between the SRP and SRP receptor. Upon ER membrane arrival, the ribosome-nascent chain complex is delivered to the ER translocon apparatus, and the SRP and SRP receptor are released and recycled. The translocon apparatus then translocates the growing polypeptide into the ER lumen, or in the case of membrane proteins until the stop transfer sequence (i.e. the transmembrane domain) mediates integration into the ER membrane (Saraogi and

Shan, 2011; Shan and Walter, 2005; Shao and Hegde, 2011). Signal sequences may or may not be cleaved by signal peptidase resident on the luminal side of the ER membrane and further cleaved by signal peptide peptidase (Hegde and Bernstein, 2006; Martoglio and Dobberstein, 1998). Some cargo proteins are co-translationally inserted into the ER membrane by an SRP-independent mechanism (Martoglio and Dobberstein, 1998). A recent study identified a network of cytosolic factors that promote SRP-independent protein insertion into the ER (Ast et al., 2013). These ER-targeting mechanisms prevent protein mis-folding or aggregation in the cytoplasm.

Although the majority of secretory pathway proteins are co-translationally inserted into the ER, some proteins are inserted post-translationally. Some soluble secretory proteins contain a moderately hydrophobic signal sequence that escapes co-translational SRP recognition and are therefore post-translationally targeted to the ER. A complex of Sec61, Sec62 and Sec63 at the ER membrane with luminal chaperone BiP mediates post-translational translocation of these soluble secretory proteins (Rapoport, 2007). Tail-anchored membrane proteins, such as SNARE (soluble N-ethylmaleimide-sensitive factor attachment protein receptor) proteins involved in vesicle fusion, contain a C-terminal transmembrane domain that also functions as signal sequence for ER insertion, and is only exposed to the cytosolic targeting factors on termination of protein synthesis and release from ribosomes (Borgese and Fasana, 2011; Kutay et al., 1993; Rabu et al., 2009; Shao and Hegde, 2011; Wattenberg and Lithgow, 2001). The mechanism for ER translocation of tail-anchored proteins was recently revealed. The cytosolic ATPase transmembrane recognition complex (TRC) 40 (also known as arsenical pump-driving ATPase protein, Asna1) recognizes the transmembrane domain of newly synthesized tail-anchored proteins (Borgese and Fasana, 2011; Favaloro et al., 2010; Stefanovic and Hegde, 2007) and directs them to the ER membrane by interaction with the tryptophan-rich basic protein (WRB) and calcium-modulating cyclophilin ligand (CAML) protein in the ER membrane (Vilardi et al., 2011; Yamamoto and Sakisaka, 2012). CAML and WRB interact with each other by their transmembrane domains and synergistically mediate ER membrane insertion of tail-anchored proteins (Yamamoto and Sakisaka, 2012).

1.4 Traffic from the ER

1.4.1 The COPII complex

Once secretory and membrane proteins are targeted to the ER, anterograde transport of these newly synthesized proteins from the ER (also referred to as the biosynthetic transport pathway) is mediated by the COPII complex. Components of COPII, first identified in *S. cerevisiae*, were found to be essential for cell viability and are conserved throughout all known eukaryotes (Duden, 2003). The COPII complex comprises the small GTPase secretion-associated ras-related protein 1 (Sar1), the Sec23/24 complex and the Sec13/31 complex (Barlowe et al., 1994). Formation of COPII coated vesicles is initiated by Sec12, an ER membrane-bound guanine-exchange factor (GEF) for Sar1, which activates Sar1 by GTP binding (Barlowe and Schekman, 1993). Activated Sar1 binds to the ER membrane where it recruits the Sec23/24 complex and subsequently the Sec13/31 complex, leading to coat polymerization and vesicle bud formation (Barlowe et al., 1994). Secretory and membrane cargo proteins containing short linear ER export signals (described in more detail in 1.4.4) that interact with components of the COPII complex are incorporated during vesicle formation (Dong et al., 2012; Duvernay et al., 2009a; Duvernay et al., 2009b; Giraudo and Maccioni, 2003; Miller et al., 2002; Nishimura and Balch, 1997; Nufer et al., 2003; Sevier et al., 2000; Zhang et al., 2011). After vesicle budding, GTP hydrolysis by Sar1, facilitated by Sec23 and Sec31, promotes coat depolymerization (Antonny et al., 2001) and vesicle fusion with the acceptor compartment mediated by SNARE proteins (Jahn and Scheller, 2006; Malsam et al., 2008).

Structural studies on components of the COPII complex have provided useful insights into the mechanism of coat formation. The crystal structure of Sec12 reveals that potassium binding in the cytosolic domain is critical for Sec12 GEF activity to activate Sar1 (McMahon et al., 2012). Upon GTP binding, the N-terminal helix of Sar1 swings out, exposing hydrophobic residues that lead to attachment of Sar1 to the ER membrane (Huang et al., 2001). The amphipathic helix region of the Sar1 N-terminus recruits the Sec23/24 heterodimer complex that forms a bow-tie shape containing a concave membrane-proximal positively charged inner surface (Bi et al., 2002; Bi et al., 2007). This curved positively charged surface would initiate membrane curvature favoring membrane deformation and vesiculation for ER exit. The Sec23/24 complex then binds with the Sec13/31 to form a

heterotetramer, which forms the outer coat layer consisting of cuboctahedral geometry (Stagg et al., 2006). The sizes of the cages are approximately 600 Å (Antonny et al., 2003; Matsuoka et al., 2001; Stagg et al., 2006), which brings into question the mechanism of transport for large cargos, such as procollagen, that have sizes of ~3000 Å (Jones et al., 2003; Stephens and Pepperkok, 2002). The mechanism was explained by cryogenic electron tomographic reconstitution of Sec13/31 tubules 3300 Å in length and 300 Å in diameter (O'Donnell et al., 2011). Also, cryogenic electron microscopy studies of Sec13/31 along with Sec23 revealed that Sec23 binding induces Sec13/31 to form vesicles/tubules with a variety of geometries (Bhattacharya et al., 2012), providing a further mechanism for transport of large cargo from the ER. A recent report showed that mature glycosylphosphatidylinositol-anchored proteins in the ER lumen bind to cargo receptor membrane protein p24 that stimulates COPII complex recruitment for ER export (Manzano-Lopez et al., 2015) suggesting that cargo proteins can regulate assembly and required sizes of the COPII cage.

1.4.2 ER exit sites

COPII budding occurs at specific sites of the ER called the transitional ER (tER) or ER exit site (ERES) that include post-ER structures prior to fusion with or becoming the ER-Golgi intermediate compartment (ERGIC) (Budnik and Stephens, 2009). After translation, all secretory and membrane cargo proteins enter into the ERES, which is devoid of ribosomes (Orci et al., 1991), for sorting and export from the ER. The ER exit sites are part of larger export complexes comprising buds bearing tER components facing towards the ERGIC (Balch et al., 1994; Bannykh et al., 1996; Schweizer et al., 1991). The post-ER compartment in the vicinity of the ERES includes tubulo-vesicular membranes coated with COPII complex and free COPII coated vesicles (Mironov et al., 2003; Zeuschner et al., 2006). However, a recent report challenges this model of cytosolic release of COPII vesicles from the ERES that tether and fuse with the neighboring ERGIC. Through high-speed and super-resolution microscopy, Kurokawa *et al.* report a ‘hug and kiss’ model for the *cis*-Golgi that approaches and contacts the ERES to capture cargo proteins by simultaneous collapse of the COPII cage (Kurokawa et al., 2014). However, it is possible that free COPII vesicles could be released and immediately captured by the *cis*-Golgi.

Moreover, this study was conducted using *S. cerevisiae* that does not have highly organized ERESs and Golgi structures (Preuss et al., 1992; Rossanese et al., 1999). Similar experiments need to be performed in mammalian cells to more clearly define the nature of cargo export from the ERES.

The peripheral ER membrane protein Sec16 plays an important role in organization of the ERES. As with COPII components, Sec16 was first identified in a *S. cerevisiae* screen for secretory pathway mutants and shown to localize to the ER (Espenshade et al., 1995; Novick et al., 1980). Two mammalian orthologues, Sec16A and Sec16B, have been identified and also localize to ERESs (Bhattacharyya and Glick, 2007; Hughes et al., 2009; Iinuma et al., 2007; Watson et al., 2006). Both yeast and mammalian Sec16 interact with COPII components Sec23, Sec24, Sec13 and Sec31, and overexpression or depletion of Sec16 disorganizes ERESs (Bharucha et al., 2013; Bhattacharyya and Glick, 2007; Espenshade et al., 1995; Gimeno et al., 1996; Hughes et al., 2009; Iinuma et al., 2007; Shaywitz et al., 1997). Sec16 stabilizes the Sar1-GTP-Sec23/24 complex on liposomes, by preventing premature GTP hydrolysis (Kung et al., 2012; Supek et al., 2002; Yorimitsu and Sato, 2012). Moreover, fluorescence recovery after photobleaching (FRAP) experiments indicate that recycling of Sec16 from the membrane is slower than that of Sec23, and there is a greater immobile pool of Sec16 on ER membranes (Hughes et al., 2009). These observations suggest that Sec16 is a scaffolding protein that provides a platform for COPII assembly. In contrast, the 'anchor-away' technique (Haruki et al., 2008), where a protein of interest remains cytosolic by anchoring to ribosomes upon addition of rapamycin, used to analyze whether Sec16 is a scaffolding protein, showed that removal of COPII from ERESs also results in removal of Sec16, while loss of Sec16 from ERES does not displace COPII (Bharucha et al., 2013). This observation suggests that the COPII complex mediates recruitment of Sec16, not the other way around, and proposes that Sec16 does not organize COPII but rather COPII turnover can account for Sec16 effects on ERES. More studies clearly need to be done to define more precisely the sequence of events that regulate ERES assembly and function.

Another important regulator of ERES is phosphatidylinositol-4-phosphate (PI(4)P). PI(4)P plays an important role in Golgi vesicular trafficking by recruiting Arf1 GTPase and pleckstrin homology (PH) domain-containing accessory proteins four-phosphate-

adaptor protein (FAPP) 1 and FAPP2 which are primarily involved in lipid transport (Godi et al., 2004; He et al., 2011). Evidence shows that PI(4)P also regulates ER export. Addition of the FAPP1-PH domain inhibits COPII vesicle budding *in vitro* (Blumental-Perry et al., 2006). Also, PI4P is enriched on ER membranes upon Sar1 activation. The presence of the PI(4)P phosphatase Sac1 results in reduced vesicle production *in vitro* (Blumental-Perry et al., 2006), and knockdown of ER-associated phosphatidylinositol-4-kinase IIIα (PI4KIIIα), which synthesizes PI(4)P, reduces the number of ERESs in cells (Farhan et al., 2008). Therefore, production of PI(4)P at the ERES by PI4KIIIα may assist Sar1 membrane constriction and nucleation of COPII assembly that mediates ER export.

1.4.3 The ER-Golgi intermediate compartment (ERGIC)

The destination of ER export vesicles is a vesicular-tubular cluster of membranes that is known as the ERGIC. The type I membrane protein ERGIC-53 is required for maintaining the structural integrity of the ERGIC, in addition to cargo sorting from the ER (Appenzeller et al., 1999; Hauri et al., 2000; Nichols et al., 1998). In addition to ERGIC-53, cargo receptor membrane proteins Surf4 and p25, which recycle in the early secretory pathway similar to ERGIC-53, are also required to maintain the ERGIC architecture (Mitrovic et al., 2008). ERGIC-53 interacts directly with Sec23 at the ER for cargo sorting into COPII vesicles that travel to the ERGIC. Cargo proteins are dissociated in the ERGIC and sorted for trafficking to the Golgi or back to the ER, and ERGIC-53 is recycled back to the ER (Kappeler et al., 1997). Two models have been proposed for cargo transport from the ER to the Golgi complex via the ERGIC. The transport complex model proposes that ERGIC clusters are transient cargo containers formed by homotypic fusion of COPII vesicles, which then migrate to and fuse with or give rise to the *cis*-Golgi. The stable compartment model suggests the ERGIC is best considered as a separate membrane compartment that receives cargo from the ER and generates anterograde cargo destined for the Golgi (Appenzeller-Herzog and Hauri, 2006). The transport complex model was initially based on observations showing large carriers transporting cargo from the ERES to the Golgi, and these carriers were identical to the ERGIC clusters defined by ERGIC-53 (Bannykh et al., 1998; Stephens and Pepperkok, 2001). The stable compartment model originated from results showing that low temperature inhibition of ERGIC-to-Golgi

trafficking did not inhibit ER-to-ERGIC transport and did not increase the number of ERGIC clusters (Klumperman et al., 1998). More recent studies have not resolved which of this models is correct. For example, ERGIC transport carriers can directly be formed from COPII-dependent protrusions, and p25 plays a role in *de novo* ERGIC formation (Lavoie et al., 1999; Mironov et al., 2003). However, inhibiting homotypic fusion of COPII vesicles did not prevent transport complex formation (Mironov et al., 2003), supporting the stable compartment model. Large anterograde carriers can leave the ERGIC-53 containing compartment behind while moving to the Golgi (Ben-Tekaya et al., 2005), again consistent with the stable compartment model. However, knockdown of the ER-ERGIC recycling cargo adaptor Surfs4 with ERGIC-53 or p25 results in reduced numbers of ERGIC clusters (Mitrovic et al., 2008), suggesting the ERGIC clusters are transient, more in-line with the transport complex model for traffic through the ERGIC. Hence, the precise mechanisms governing the formation and function of the ERGIC remain unresolved.

1.4.4 ER export signals

Numerous ER export signals have been identified in the cytosolic tail of various membrane proteins, and several of these signals have been shown to interact with components of the COPII complex for ER export. For instance, dibasic motifs (R/K)X(R/K) in glycosyltransferases and RNKR in Crumbs, a type I membrane protein required for *Drosophila* epithelial polarity, interact with Sar1 for ER export (Giraudo and Maccioni, 2003; Kumichel et al., 2015; Quintero et al., 2010). Diacidic-based motifs (DXE, DXD, FXYENEV), dileucine-based motifs (FX_6LL, EX_3LL, FNX_2LLX_3L), diphenylalanine motifs (QX_7FF), ϕXϕXϕ motifs [FXFXF, (V/L/F)X(I/L)X(M/L)] and other motifs, such as the tribasic RRR, YNNSNPF, LXX(L/M)E, IXM, R(I/L) motifs, have been identified as ER export signals in membrane proteins and many of them have been shown to directly interact with the Sec24 subunit of COPII complex to exit from the ER (Barlowe, 2003; Bermak et al., 2001; Dong et al., 2012; Duvernay et al., 2004; Farhan et al., 2007; Ma et al., 2001; Mancias and Goldberg, 2008; Mossessova et al., 2003; Nishimura and Balch, 1997; Nishimura et al., 1999; Nufer et al., 2003; Robert et al., 2005; Schulein et al., 1998; Stockklausner et al., 2001; Sucic et al., 2011; Wang et al., 2004; Zhang et al., 2011). Sec24 was recently shown to simultaneously bind to two sorting signals

(DXE and IFRTL) to drive ER export, suggesting that high levels of efficient capture and specificity are employed in the ER export process (Pagant et al., 2015).

1.4.5 ER retention/retrieval signals

The retention and retrieval of ER proteins is largely mediated by sorting signals containing basic residues that interact with components of the COPI complex, a coat protein complex that mediates retrograde traffic from the Golgi to the ER (described in 1.5.1). For example, the di-lysine motifs KXKXX or KKXX at the C-terminus of the cytosolic tail of membrane proteins is an ER retention signal that functions by interacting with components of the COPI complex to retrieve proteins to the ER (Cosson and Letourneur, 1994; Jackson et al., 1990; Teasdale and Jackson, 1996; Zerangue et al., 2001). The function of these di-lysine motifs depends on the length and structure of the cytoplasmic domain (Shikano and Li, 2003; Vincent et al., 1998), and they can also mediate direct ER retention in addition to retrieval to the ER (Andersson et al., 1999). Recent structural studies reveal electrostatic binding pockets in COPI subunits that bind terminally located di-lysine motifs (KKXX and KXKXX), with a specific requirement of two-residue spacing from the C-terminus (Jackson et al., 2012). Another dibasic motif, RXR, also functions as an ER retention/retrieval signal (Bichet et al., 2000; Margeta-Mitrovic et al., 2000; Scott et al., 2001; Zerangue et al., 2001; Zerangue et al., 1999) that depends on the length of the cytoplasmic tail (Shikano and Li, 2003). Similarly, the type II membrane protein glucosidase I contains cytosolic N-terminal di-arginine motifs (RR, RXR, RXXR) in plants and a tri-arginine motif (RRR) in humans that both function as ER retention signals (Boulaflous et al., 2009; Hardt et al., 2003). Thus, terminal basic residues are widely employed for ER retention and retrieval.

1.5 Traffic from the Golgi

The Golgi complex serves as the main sorting station for anterograde transport of newly synthesized proteins destined for the plasma membrane or other organelles (De Matteis and Luini, 2008; Jackson, 2009; Surma et al., 2012). It also plays an important role in receiving traffic from the endocytic pathways. The Golgi complex is composed of a variable number of Golgi stacks, referred to as *cis*, *medial* and *trans* stacks. The *cis* and

trans sides of the Golgi complex are associated with tubulovesicular structures called the ERGIC and the *trans*-Golgi network (TGN), respectively, representing cargo entry and exit at both sides. As described above, ER-to-Golgi anterograde traffic is mediated by COPII coated vesicles while retrograde traffic from the Golgi to the ER is mediated by COPI coated vesicles (Figure 1.4). Traffic from the TGN to endosomes, lysosomes and the plasma membrane is mediated by hetero-tetrameric AP complexes or monomeric adaptor GGA (Golgi-localizing γ-adaptin ear-containing Arf-binding) proteins that link vesicles with clathrin coat proteins, while traffic from endosomes to the TGN is mediated by retromer complex (Figure 1.4). Details of these coat complexes are described below.

1.5.1 The COPI complex

COPI coat proteins are involved in cargo trafficking in the Golgi-to-ER retrieval pathway, as well as retrograde flow between the Golgi compartments. COPI vesicles are composed of the small GTPase Arf1 (ADP ribosylation factor 1) and a coatomer complex of ~600 kDa containing seven subunits, α-, β-, β'-, γ-, δ-, ε- and ζ-COP. All components of COPI are essential for yeast cell viability, except for ε-COP, and are conserved in all known eukaryotes, similar to the COPII components (Duden, 2003). Activation of Arf1 is mediated by GEFs of the BIG (brefeldin A–inhibited GEF) family localized to the *trans* side of the Golgi, and GBF (Golgi-specific brefeldin A–resistance factor) family members localized to early Golgi compartments (Bui et al., 2009; Gillingham and Munro, 2007). The coatomer is recruited as a single complex to the membrane (Hara-Kuge et al., 1994). However, based on homology to other coat protein complexes, two 'subdomains' can be distinguished: the adaptor subcomplex (β-, γ-, δ- and ζ-COP) and a cage like subcomplex (α-, β'- and ε-COP) (Faini et al., 2013). The adaptor subcomplex of COPI binds to two Arf1 molecules (Sun et al., 2007; Zhao et al., 1997), which was confirmed through structural determination by X-ray crystallography (Yu et al., 2012). The structure of the γ-ζ-COP-Arf1 complex revealed residues in γ-COP for Arf1 binding, and similar residues were predicted by homology in β-COP and confirmed by mutagenesis for Arf1 binding (Yu et al., 2012). The α-β'-COP complex forms a triskelion with three copies by converging through axial ends of the β-propeller domain of β'-COP, which shares partial similarities with the cages formed by both clathrin and COPII (Lee and Goldberg, 2010).

The β-propeller structure of the β'-COP subunit was also shown to bind with a di-lysine sorting motif (Jackson et al., 2012), indicating a role for β'-COP in cargo selection in addition to cage formation. Single-particle electron microscopy of the complete heptameric COPI complex reveals a globular mass, representing the adaptor subcomplex surmounted by an extended domain representing the cage subcomplex, and with substantial conformational flexibility likely required for scaffolding function (Yip and Walz, 2011). GTP hydrolysis by Arf1, promoted by Arf1 GTPase activating proteins (ArfGAPs), results in COPI coat depolymerization (Cukierman et al., 1995; Reinhard et al., 2003; Tanigawa et al., 1993). ArfGAP1 contains an amphipathic lipid packing sensor (ALPS) motif that senses curved membranes and serves as a mechanism to associate with COPI vesicles (Bigay et al., 2005; Bigay et al., 2003), while ArfGAP2/3 associates directly with the COPI complex for coat depolymerization (Frigerio et al., 2007; Kliouchnikov et al., 2009; Pevzner et al., 2012; Weimer et al., 2008).

1.5.2 The adaptor proteins (APs)

APs are another key component in vesicle trafficking, and form the coat around post-Golgi vesicles as well as playing an important role in cargo sorting. APs are hetero-tetrameric complexes with two large subunits (~100 kDa), a medium (~50 kDa) and a small subunit (~20kDa) (Hirst et al., 2013; Robinson, 2004). There are five distinct APs: AP1 mediates traffic between tubular endosomes and the TGN, although the trafficking direction is unclear (Canuel et al., 2008; Robinson et al., 2010); AP2 is involved in vesicle formation at the plasma membrane for endocytosis (described below in 1.7.1); AP3 mediates traffic from the TGN and/or early endosome to late endosomes; AP4 mediates traffic from the TGN to endosomes, lysosomes and basolateral membranes; and AP5 is localized to late endosomes but the precise function is unclear (Hirst et al., 2011; Hirst et al., 2013; Nakatsu and Ohno, 2003; Ohno, 2006; Popova et al., 2013; Robinson, 2004). AP1 and AP3 also have cell-type specific isoforms; AP1-B is expressed in polarized epithelial cells and mediates basolateral sorting, while AP3-B is expressed in neurons and mediates synaptic-vesicle biogenesis (Ohno, 2006; Robinson, 2004).

The regulation and functional mechanisms vary between different APs. The assembly of AP3 and AP4 on the membrane is regulated by activation of the Arf1 GTPase,

while assembly of AP1 is regulated by both Arf1 and PI(4)P (Wang et al., 2003). In contrast, assembly of the AP2 complex is regulated by phosphatidylinositol-4,5-bisphosphate ($PI(4,5)P_2$) (Honing et al., 2005). Positively charged patches of basic residues in AP1 and AP2 are involved in binding to respective PIPs (Heldwein et al., 2004). AP5 assembly on the membrane was not inhibited by brefeldin A treatment and, therefore, remain independent of Arf1 GTPase (Hirst et al., 2011). Moreover, AP1, AP2 and AP3 interact with clathrin molecules to form clathrin coated vesicles, while AP4 and AP5 do not interact with clathrin (Hirst et al., 2011; Robinson, 2004). Crystal structures of AP1 and AP2 core complexes comprising the N-termini of the large subunits plus intact medium and small subunits display similar structures, defined as an inactive conformation in which the cargo binding site is inaccessible (Collins et al., 2002; Heldwein et al., 2004). Upon membrane recruitment of AP1 by Arf1, or AP2 by PI(4,5)P2, changes in the conformation of the AP complexes expose the cargo binding site with pockets for tyrosine and tyrosine+3 bulky amino acid of YXXϕ motif (Jackson et al., 2010; Ren et al., 2013). The coat layer formed by AP complexes is removed by dephosphorylation of AP components and of phosphatidylinositol phosphates (PIPs) that reduces adaptors affinity to vesicles (Ghosh and Kornfeld, 2003; Verstreken et al., 2003).

1.5.3 GGA proteins

Membrane transport between the TGN and endosomes is also mediated by monomeric clathrin adaptor proteins called GGA proteins. There are three GGA isoforms found in humans (GGA1, GGA2 and GGA3) and two in the yeast (Gga1 and Gga2). All GGAs are 60-80 kDa in size and have common structural and functional domains; a VHS (Vps-27, Hrs and STAM) domain, a GAT (GGA and Tom1) domain, a hinge region, and a GAE (γ-adaptin ear homology) domain (Bonifacino, 2004; Nakayama and Wakatsuki, 2003). The membrane recruitment of GGAs is mediated by GAT domain interaction with membrane-bound activated Arf1, and this interaction hinders the action of Arf-GAPs providing transient stabilization of a GGA-Arf-GTP complex (Jacques et al., 2002). Upon membrane recruitment of GGA, the VHS domain comes into close proximity with the membrane and sorts cargo proteins by interaction with di-leucine-based sorting signals in the cytoplasmic tails of membrane cargo proteins (He et al., 2002; Nielsen et al., 2001;

Puertollano et al., 2001a; Takatsu et al., 2001; Zhu et al., 2001) and this interaction is enhanced by phosphorylation of a serine residue within the di-leucine motif (von Arnim et al., 2004; Wahle et al., 2005). A clathrin-box like sequence in the hinge region of membrane-bound GGA recruits clathrin by interaction with the terminal domain of clathrin to form clathrin coated vesicles (Mullins and Bonifacino, 2001; Puertollano et al., 2001b; Stahlschmidt et al., 2014). The WNSF motif in the hinge region binds to the GAE domain for auto-regulation of GGA function (Inoue et al., 2007). The GAE domain also binds to a variety of accessory proteins via the DFGXϕ motif, which may facilitate vesicle budding, cargo sorting, coat assembly and disassembly (Bonifacino, 2004).

1.5.5 Golgi sorting signals

In spite of the Golgi being the main sorting hub for cargo proteins and the identification of various coat proteins functioning at the Golgi, few Golgi sorting signals have been identified. Two types of motifs, di-leucine based ((D/E)XXXL(L/I) and DXXLL) and tyrosine based (YXXϕ) motifs interact with GGAs and APs, respectively, for protein sorting from the Golgi to the basolateral plasma membrane and for endocytosis (Anitei and Hoflack, 2011; De Matteis and Luini, 2008; Rodriguez-Boulan and Musch, 2005). Tyrosine-based motifs were first identified in low-density-lipoprotein receptor (LDLR), the polymeric-immunoglobulin-A receptor (pIgAR), and the transferrin receptor (TfR) (Matter and Mellman, 1994); and di-leucine-based motif in Fc receptor (FcR) (Hunziker and Fumey, 1994; Matter et al., 1994). These motifs were also shown to target E-cadherin and vesicular stomatitis virus glycoprotein (VSV-G) to basolateral membranes (Miranda et al., 2001; Thomas and Roth, 1994). Alternatively, single-leucine-based motifs were also identified in stem cell factor and CD147 for basolateral targeting (Deora et al., 2004; Wehrle-Haller and Imhof, 2001). Substitution mutations of these basolateral sorting motifs results in mis-sorting of proteins to apical membranes rather than accumulation in the Golgi, owing to their O- or N-linked glycans that function in apical targeting (Carvajal-Gonzalez et al., 2012; De Matteis and Luini, 2008; Rodriguez-Boulan and Musch, 2005), implying that these basolateral targeting motifs are Golgi sorting signals rather than Golgi export signals. Recently, a novel tyrosine-based motif (YX[F/Y/L][F/L]E) was identified in amyloid precursor protein (APP) for its traffic from the TGN to the endosomes (Burgos

et al., 2010). Alanine substitution of this motif inhibited APP traffic to the endosomes and resulted in accumulation in the Golgi.

1.6 Traffic through the Golgi

Mechanisms for protein trafficking through the Golgi complex remain highly debatable and various models have been proposed (Glick and Luini, 2011). The vesicular trafficking model and the cisternal-maturation model (Figure 1.5) are the oldest and remain extensively discussed (Jackson, 2009; James Morre and Mollenhauer, 2007; Simon, 2008). At present, the cisternal-maturation model is better accepted and explains most of the experimental data reported so far.

The vesicular transport model (Figure 1.5), in which the Golgi is viewed as being composed of distinct stable compartments and cargo proteins move from one compartment to the next in COPI coated vesicles, was widely accepted for a long time (Dunphy and Rothman, 1985; Farquhar, 1985; Farquhar and Palade, 1981; Rothman, 1981; Rothman and Wieland, 1996). This model was extended with the view that COPI could mediate bidirectional transport; anterograde transport of cargo proteins and retrograde transport of vesicle trafficking components (Orci et al., 2000; Pelham and Rothman, 2000). Polarized distribution of glycosylation enzymes supports this model, such that each Golgi compartment contains a unique set of Golgi-resident enzymes that process cargo proteins in an assembly line fashion (Kleene and Berger, 1993; Nilsson et al., 2009; Rabouille et al., 1995). Some studies have showed COPI vesicles containing secretory cargo proteins, supporting the view that cargo proteins traffic in a forward direction via vesicles between the Golgi compartments (Malsam et al., 2005; Orci et al., 1997; Ostermann et al., 1993). However, other studies failed to detect any secretory cargo in COPI coated vesicles (Dahan et al., 1994; Gilchrist et al., 2006; Martinez-Menarguez et al., 2001). Also, the traffic of large cargo proteins such as procollagen through Golgi cisternae could not be explained by the vesicular transport model (Becker et al., 1995; Bonfanti et al., 1998; Mironov et al., 2001). Moreover, the transient nature of yeast Golgi cisternae, a fused Golgi network in microsporidia, tubular connections between cisternae in mammalian cells, and the mobility of Golgi-resident enzymes between compartments are also not explained by this stable

compartment model (Beznoussenko et al., 2007; Losev et al., 2006; Matsuura-Tokita et al., 2006; Trucco et al., 2004; Wooding and Pelham, 1998).

In contrast, the cisternal-maturation model (Figure 1.5) suggests that one set of Golgi-resident proteins replaces another as cargo traffics within the Golgi complex, is a better fit for most of these observations. Homotypic fusion of COPII vesicles or ER-derived carriers would form a *cis*-Golgi cisterna that matures into the TGN and disintegrates into vesicles and other type of carriers. As the cargo moves forward, the Golgi-resident proteins are retrieved to the younger cisternae by COPI vesicles (Bonfanti et al., 1998; Gilchrist et al., 2006; Glick and Malhotra, 1998; Malsam et al., 2005; Martinez-Menarguez et al., 2001; Rabouille and Klumperman, 2005). In fact, Golgi cisternal maturation with cargo and retrieval of Golgi-resident enzymes were visualized in live-cell imaging experiments (Losev et al., 2006; Matsuura-Tokita et al., 2006). However, this model still cannot explain the fused Golgi network in microsporidia or tubular connections between Golgi cisternae (Beznoussenko et al., 2007; Trucco et al., 2004). The extended cisternal-maturation model with tubular transport could accommodate these results (Glick and Luini, 2011). Moreover, studies by Lippincott-Schwartz and coworkers suggest a dramatic revision of these traditional models by proposing a rapid-partitioning model for traffic within the Golgi (Patterson et al., 2008). They observed cargo diffusion into and out of Golgi export domains and exit from the Golgi with exponential kinetics, and proposed that secretory cargo partitions into processing and export domains upon arrival at the Golgi and exit from every level of the Golgi to their final destinations (Lippincott-Schwartz and Phair, 2010; Patterson et al., 2008). In this rapid-partitioning model, the Golgi operates as a single compartment that contradicts the observation of polarized distribution of Golgi enzymes and the existence of discrete Golgi cisternae. Moreover, the rapid-partitioning model also cannot explain the slower traffic of large cargo such as procollagen (Bonfanti et al., 1998; Mironov et al., 2001; Trucco et al., 2004). The cisternal-maturation model with tubular transport between cisternae could explain cargo diffusion within the Golgi and the exponential kinetics of smaller secretory cargo exit and, therefore, seems a more plausible model for traffic through the Golgi.

1.7 Endocytic pathways

Cells take up extracellular materials as well as cell surface-expressed proteins by various mechanisms of endocytosis. Endocytic mechanisms can be classified into two subgroups, clathrin-mediated endocytosis (described below) and clathrin-independent endocytosis. Many clathrin-independent endocytosis mechanisms remain less well characterized in terms of their molecular details and cargo specificity, and will not be further discussed. During endocytosis, internalized vesicles immediately fuse with or become early endosomes, which are considered a main sorting station for the endocytic pathway (Huotari and Helenius, 2011). Early endosomes contain membrane microdomains, each enriched in various trafficking regulators such as Rab4, Rab5, Rab7, Rab11, retromer complex and caveolae (Hayer et al., 2010; Rojas et al., 2008; Vonderheit and Helenius, 2005), and sort cargo proteins to the plasma membrane, recycling endosomes or the TGN. Early endosomes mature into late endosomes, which can then fuse with lysosomes to form endolysosomes for degradation of luminal contents (Huotari and Helenius, 2011). Alternatively, inward budding into late endosomes generates multi-vesicular bodies containing luminal vesicles that are released from cells as exosomes, following fusion of the limiting multi-vesicular body membrane with the plasma membrane.

1.7.1 Clathrin-mediated endocytosis

Clathrin-mediated endocytosis is the most studied mechanism of endocytosis. Formation of clathrin-coated pits is initiated by recruitment of AP2 to the plasma membrane by $PI(4,5)P_2$ (Honing et al., 2005). However, more recent studies have shown that the initiation stage may involve a putative nucleation module composed of FCH-domain-only (FCHO) proteins, EGFR pathway substrate 15 (EPS15) and intersectins that assemble at the plasma membrane due to their preferences to PI(4,5)P2 (Henne et al., 2010; Reider et al., 2009; Stimpson et al., 2009). Proteins of the putative nucleation module then recruit AP2 to the membrane, which changes the conformation of the AP2 core complex to expose the cargo binding sites and mediates cargo selection by interaction with di-leucine- and tyrosine-based motifs (Jackson et al., 2010; Kelly and Owen, 2011; Traub, 2009). The conformational changes in AP2 following membrane recruitment and cargo

binding also relieves auto-inhibition of clathrin association, triggering clathrin recruitment and formation of clathrin-coated pits (Kelly et al., 2014). A variety of accessary proteins are also assembled during clathrin-coated vesicle formation for endocytosis (McMahon and Boucrot, 2011; Traub, 2011). For instance, the GTPase dynamin is recruited by BAR-domain-containing proteins such as endophillin and sorting nexin (SNX) 9, which bind to curved membranes and likely mediate neck formation. The SRC homology 3 (SH3) domain of these BAR proteins interacts with proline-rich regions of dynamin, which mediates scission of clathrin-coated vesicles by GTP hydrolysis (Bashkirov et al., 2008; Ferguson et al., 2009; Hinshaw and Schmid, 1995; Sundborger et al., 2011; Sweitzer and Hinshaw, 1998). Dynamin also mediates vesicle fission at the plasma membrane for various clathrin-independent endocytic mechanisms (Mercer et al., 2010). Endophillin was also recently shown to mediate clathrin-independent endocytic mechanisms (Boucrot et al., 2015; Renard et al., 2015). Once the endocytic vesicle is detached from the plasma membrane, ATPase heat-shock cognate 70 (HSC70) and its cofactor auxilin mediate disassembly of the clathrin coat (Schlossman et al., 1984; Ungewickell et al., 1995). Auxilin is recruited after vesicle budding by binding to the terminal domain and ankle of the clathrin triskelium, and localizes under the 'hub' of neighboring triskelia where the uncoating reaction is initiated upon HSC70 recruitment (Fotin et al., 2004; Rapoport et al., 2008; Scheele et al., 2001; Taylor et al., 2011; Xing et al., 2010). The vesicle is then ready to fuse with the target endosomal compartment for further processing.

1.7.2 The retromer complex

Another trafficking regulator, the retromer complex, mediates sorting and trafficking of proteins from endosomes. The retromer complex was first identified in yeast as an endosomal coat-protein complex required for cargo retrieval from endosomes to the TGN (Seaman et al., 1998). The hetero-pentameric retromer complex is composed of a vacuolar protein sorting (VPS) trimer VPS26-VPS29-VPS35 subcomplex and a SNX dimer subcomplex mainly composed of SNX1/2-SNX5/6 (Burd and Cullen, 2014; Collins, 2008; Seaman, 2012). SNX3 and SNX27 are present in alternative retromer complexes (Harterink et al., 2011; Steinberg et al., 2013). SNXs contain a Bin/Amphiphysin/Rvs (BAR) domain that can induce and/or sense membrane curvature and tubules (Carlton et

al., 2004; van Weering et al., 2012), and a phox-homology (PX) domain that binds to phosphatidylinositol-3-phosphate (PI(3)P) (Carlton et al., 2004; Cullen, 2008; Seet and Hong, 2006). The SNX dimer complex associates with endosomal membranes by binding to PI(3)P and recruits the VPS trimer complex to the membrane (Haft et al., 2000; Harterink et al., 2011; Seaman et al., 1998; Vardarajan et al., 2012). However, VPS trimers were also shown to be associated with late endosomal membranes via Rab7 (Balderhaar et al., 2010; Liu et al., 2012; Nakada-Tsukui et al., 2005; Rojas et al., 2008; Seaman et al., 2009; Zelazny et al., 2013). The VPS trimer functions in cargo sorting, mainly through VPS35 interaction with simple hydrophobic cargo-sorting motifs (Nothwehr et al., 2000; Seaman, 2007), and VPS26, SNX3 and SNX27 also play a role in cargo selection (Fjorback et al., 2012; Steinberg et al., 2013; Temkin et al., 2011). In addition to cargo retrieval from endosomes to the TGN, retromers influence a wide array of cellular functions such as establishment of cell polarity, cargo recycling from endosomes to the plasma membrane and transcytosis (Lohia et al., 2012; Pocha et al., 2011; Seaman, 2012; Verges et al., 2004; Zhou et al., 2011).

1.7.3 Endocytic sorting signals

Various sorting signals that function at distinct steps of the endocytic pathway have been identified. For example, di-leucine- and tyrosine-based motifs ((D/E)XXL(L/I), YXXϕ, NPXY) interact with AP2 subunits and endocytose plasma membrane proteins into clathrin-coated vesicles (Bonifacino and Traub, 2003; Kelly and Owen, 2011; Traub, 2009). Protein recycling to the plasma membrane from recycling endosomes is mediated by sorting motifs such as LF, RF, KR, PLSLL (Dai et al., 2004; Li et al., 2007), and from early endosomes by DSLL, NPXY and proline-rich motifs that interact with clathrin or retromer coat complexes (Gage et al., 2001; Parachoniak et al., 2011; Temkin et al., 2011; van Kerkhof et al., 2005). Interestingly, a single motif can have dual sorting functions. For example, the GDAY motif in the natriuretic peptide receptor A (NPRA) serves a dual role as an endocytosis signal and a recycling signal (Pandey et al., 2005), while a YXXϕ motif in the Coxsackie- and adenovirus-receptor (CAR) protein can sort cargo from the TGN to the basolateral membrane via interaction with AP1-A, and from recycling endosomes to

the basolateral membrane via interaction with AP1-B (Carvajal-Gonzalez et al., 2012; Diaz et al., 2009).

1.8 Rab GTPases

Rab GTPases are considered as the master regulator of vesicular trafficking. They are the largest sub-family of the Ras superfamily, comprising approximately 70 members in humans (Bhuin and Roy, 2014; Wandinger-Ness and Zerial, 2014). Rabs exist in two forms, an activated GTP-bound form and an inactive GDP-bound form. GEFs convert inactive GDP-bound Rabs to the active GTP-bound form, while GTPase-activating proteins (GAPs) enhance the Rab GTPase activity converting the active Rab back to the inactive GDP-bound state (Figure 1.6). The inactive form of Rabs is kept in the cytoplasm by their association with GDP-dissociation inhibitors (GDIs) (Ullrich et al., 1993). In their active form, Rab GTPases localize to the cytosolic face of membranes via geranylgeranyl moieties covalently attached to each of two C-terminal cysteines (Kinsella and Maltese, 1992; Lane and Beese, 2006; Sasaki et al., 1990; Seabra et al., 1991). Individual Rabs localize to distinct membranes that is thought to be mediated by GDIs, GDI dissociation factors (GDFs), Rab escort proteins (REPs) and GEFs, making Rabs useful markers for specific membrane compartments (Barr, 2013; Pfeffer, 2013; Seabra and Wasmeier, 2004; Sivars et al., 2005; Ullrich et al., 1993; Wu et al., 2010).

Various Rabs have been shown to mediate diverse range of trafficking-related processes such as vesicle formation, cargo selection, vesicle motility, vesicle uncoating and vesicle tethering and fusion (Hutagalung and Novick, 2011; Stenmark, 2009). Cargo selection is a key process for protein sorting during vesicle formation, which is usually mediated by components of coat complexes as described above. However, there is increasing evidence of Rabs interacting with cargo molecules for cargo sorting during vesicle formation (Aloisi and Bucci, 2013). Rab5 and Rab11 are involved in the endocytic trafficking pathway and are particularly relevant to results discussed in this thesis, and are described below in more detail.

1.8.1 Rab5

Rab5 is involved in a range of functions in vesicular trafficking. For example, Rab5 sequesters transferrin receptor into clathrin-coated pits (McLauchlan et al., 1998). Rab5 also binds to the human prostacyclin receptor and frizzled GPCRs, independent of Rab5 GTP/GDP bound status (O'Keeffe et al., 2008; Purvanov et al., 2010; Strutt and Vincent, 2010), while internalization of the angiotensin II type 1A receptor is dependent on binding to the GDP-bound form of Rab5 (Seachrist et al., 2002). Other Rab5 trafficking functions include promoting vesicle motility along microtubules (Nielsen et al., 1999), vesicle tethering to acceptor membranes (Gorvel et al., 1991; Rubino et al., 2000) and uncoating of clathrin-coated vesicles (Semerdjieva et al., 2008). Rab5 activation also promotes focal-adhesion disassembly and concomitant cell migration (Mendoza et al., 2014). These functions are regulated by different effectors of Rab5 and highlight the variety of functions that can be mediated by the same Rab molecule. How Rabs recruit distinct effectors in different processes remains unknown.

1.8.2 Rab11

Rab11 has three subfamily members, Rab11A, Rab11B and Rab11C (also known as Rab25). Rab11A and Rab11B share 89% sequence identity but have only 61% and 66% sequence identity, respectively, with Rab25 (Kelly et al., 2012; Welz et al., 2014). While Rab11A is ubiquitously expressed (Kikuchi et al., 1988; Sakurada et al., 1991), Rab11B is predominantly expressed in brain, heart and testes (Lai et al., 1994), and Rab25 is expressed in kidney, lung and gastric track (Goldenring et al., 1993).

Rab11 and its effector molecules mediate a variety of cellular functions, including cargo sorting and recycling (Lindsay and McCaffrey, 2002; Mammoto et al., 1999; Welsh et al., 2007; Welz et al., 2014), vesicle motility on microtubules (Hales et al., 2002; Lapierre and Goldenring, 2005; Schonteich et al., 2008), cytokinesis (Horgan and McCaffrey, 2012), cancer cell migration (Caswell et al., 2008; Laflamme et al., 2012; Westlake et al., 2007) and primary ciliogenesis (Knodler et al., 2010). The Rab11 family-interacting proteins (FIPs) are Rab11 effectors that bind to Rab11 via a conserved Rab11-binding domain (RBD). The crystal structure of this interaction indicates a heterotetrameric complex formed of a central parallel FIP dimer with Rab11 on either side (Eathiraj et al.,

2006; Horgan and McCaffrey, 2009; Jagoe et al., 2006). Rab11 was shown to be associated with TGN membranes (Urbe et al., 1993) and to mediate traffic of VSV-G from the TGN to the plasma membrane (Chen et al., 1998). However, whether Rab11 interacts with VSV-G was not determined. While Rab11 is known to regulate the recycling of numerous cargo proteins (Aloisi and Bucci, 2013; Kelly et al., 2012), few cargo proteins have been shown to directly interact with Rab11 by GST pull-down assays, mostly with the GDP-bound inactive form of Rab11 (Hamelin et al., 2005; Parent et al., 2009; van de Graaf et al., 2006; Wikstrom et al., 2008). To date, Rab11 interactions with cargo proteins are implicated in cargo recycling to the plasma membrane, but not anterograde transport from the TGN.

1.9 Phosphatidylinositol phosphates (PIPs)

PIPs are involved in a variety of cellular functions such as signaling, cytoskeletal dynamics and membrane trafficking (Balla, 2013; Waugh, 2015). PIPs are phosphorylated derivatives of phosphatidylinositol (PI), which can be phosphorylated in combination at hydroxyl groups of the 3rd, 4th and 5th carbon positions of the inositol ring to produce seven different PIPs: PI(3)P, PI(4)P, phosphatidylinositol-5-phosphate (PI(5)P), phosphatidylinositol-3,4-bisphosphate ($PI(3,4)P_2$), $PI(4,5)P_2$, phosphatidylinositol-3,5-bisphosphate ($PI(3,5)P_2$) and phosphatidylinositol-3,4,5-triphosphate ($PI(3,4,5)P_3$). PIPs are interconverted by specific kinases and phosphatases that add or remove phosphate groups to maintain distinct PIP populations in different organelles. For example, PI(3)P is predominantly present in endosomes, PI(4)P at the TGN, and $PI(4,5)P_2$ and $PI(3,4,5)P_3$ at the plasma membrane (Brill et al., 2011). Multiple effector proteins interact with PIPs via PIP-interacting domains and localize to particular organelles. For instance, PH domains of lipid-transfer proteins such as oxysterol-binding protein (OSBP), ceramide-transfer protein (CERT) or four-phosphate-adaptor protein (FAPP) bind with PI(4)P resulting in protein localization to the Golgi complex where they play essential roles in lipid synthesis and membrane traffic (Carvajal-Gonzalez et al., 2012; Hanada et al., 2009; Ngo et al., 2010). The PH domain of Akt binds specifically with $PI(3,4,5)P_3$ and mediates signaling pathways for cell growth, proliferation and survival (Park et al., 2008; Varnai et al., 2005; Vivanco and Sawyers, 2002). The PX-domain or FVYE-domain proteins such as SNXs specifically interact with PI(3)P to localize to endosomes to mediate membrane traffic (Cullen, 2008;

Lemmon, 2007). In addition, the PX-domain of Vam7p, a SNARE molecule, interacts with PI(3)P for docking onto yeast vacuole for homotypic fusion (Boeddinghaus et al., 2002). PH, PX and FYVE domains are approximately 60-130 amino acids in length and fold into distinct tertiary structures to interact with particular PIP molecules through interface of basic residues (Bravo et al., 2001; Burd and Emr, 1998; Ferguson et al., 1995; Kutateladze et al., 1999). PI(3)P, PI(4)P and PI(4,5)P2 were shown to mediate vesicle formation at distinct cellular compartments by recruitment of retromer, AP1 and AP2 coat complex components, respectively, implying their important roles in initiation of vesicle formation (Carlton et al., 2004; Honing et al., 2005; Wang et al., 2003).

1.10 Defects in membrane trafficking

Membrane trafficking pathways are tightly regulated and important for proper cellular function. Various diseases in humans are due to defects in these trafficking pathways. For example, genetic mutations in the Sec23 and Sec24 subunits of COPII complex are linked to cranio-lentico-sutural dysplasia and osteogenesis imperfecta, respectively, in which ER export of cargo proteins such as procollagen is defective (Garbes et al., 2015). Genetic mutations in AP3 subunits lead to mis-localization of endosomal/lysosomal transmembrane proteins such as tyrosinase, CD63 and Lamp1/2 to the plasma membrane and cause Hermansky-Padlock syndrome (HPS) (Cobbold et al., 2003; Starcevic et al., 2002). Mutations in AP4 and AP5 are associated with hereditary spastic paraplegia (HSP), an inherited neurodegenerative disorder (Hirst et al., 2013). Loss of the retromer complex results in amyloidogenic processing of APP, contributing to the pathogenesis of Alzheimer's disease (Choy et al., 2012; He et al., 2005; Muhammad et al., 2008; Siegenthaler and Rajendran, 2012; Small et al., 2005; Wen et al., 2011). A genetic mutation, Asp620Asn, in the retromer subunit VPS35 is linked to Parkinson's disease (Vilarino-Guell et al., 2011; Wen et al., 2011). Missorting of many transmembrane proteins is also linked to several genetic diseases (Mellman and Nelson, 2008), including hereditary familial hypercholesterolemia and retinitis pigmentosa diseases, in which low-density-lipoprotein receptor (LDLR) and rhodopsin, respectively, are missorted to the apical membrane (Koivisto et al., 2001; Sung and Tai, 2000).

1.11 Trafficking Summary

Anterograde traffic from the ER to the Golgi is mediated by numerous sorting signals that specifically interact with components of COPII coat complex. In contrast, few Golgi sorting signals have been identified, with no definitive export signals for traffic to plasma membrane, even after identification of multiple type of coat complexes such as APs, GGAs, COPI and retromer that function at the Golgi for vesicular trafficking. Moreover, sorting signals can have dual sorting functions that may depend on the length and tertiary structure of the cytoplasmic tail. Various regulatory molecules such as Arfs, Rabs and PIPs play important roles in these complex and tightly regulated trafficking processes. Many aspects of vesicular trafficking such as cargo sorting, spatiotemporal regulation of vesicle formation, assembly and disassembly remain ill-defined, particularly as it relates to the traffic from the Golgi to the plasma membrane.

1.12 Fusogenic reoviruses and FAST proteins

1.12.1 Fusogenic ortho- and aquareoviruses

Orthoreoviruses and *Aquareoviruses* are two related genera in the virus family *Reoviridae*, a large diverse group of nonenveloped viruses with double-stranded RNA genomes containing 10 or 11 genome segments, respectively (Nibert and Duncan, 2013). Historically, reovirus terminology comes from 'respiratory enteric orphan' viruses that were first isolated from human respiratory and gastrointestinal tracks, and called orphan viruses since they were not associated with any disease. These prototypical mammalian reoviruses (MRVs) are one of six recognized species of orthoreoviruses, and they infect a wide range of mammalian hosts. The other five species of orthoreoviruses are named according to their host species (avian, reptilian and baboon reoviruses, abbreviated ARV, RRV and BRV, respectively) or location of first isolation (Nelson Bay reovirus and Broome reovirus, abbreviated NBV and BroV, respectively). The latter two species were isolated from bats, and are distinct from other bat reovirus isolates that belong to the MRV species (Kohl et al., 2012; Steyer et al., 2013). Aside from MRV, all of the other orthoreovirus species induce cell-cell fusion and syncytium formation (Ciechonska and Duncan, 2014; Duncan, 1999; Duncan et al., 2004). The two recognized species of aquareoviruses are also fusogenic (Samal et al., 2005). These fusogenic ortho- and

aquareoviruses are the only known examples of nonenveloped viruses that induce syncytium formation.

The prototypical MRVs are generally nonpathogenic following natural infections, generating subclinical infections or mild respiratory or gastrointestinal symptoms. In contrast, the fusogenic reoviruses are associated with a variety of clinical syndromes and disease states such as pneumonia, neurological disorders, enteric syndromes and meningoencephalomyelitis (Benavente and Martinez-Costas, 2007; Chua et al., 2007; Lamirande et al., 1999; Leland et al., 2000; Vieler et al., 1994). There is also a correlation between syncytium formation and virulence of the fusogenic reoviruses (Duncan and Sullivan, 1998).

The fusogenic bat reoviruses were isolated following zoonotic transmission to humans in association with acute respiratory disease, with some indication of possible human-human transmission (Cheng et al., 2009; Chua et al., 2007; Chua et al., 2008; Chua et al., 2011; Wong et al., 2012; Yamanaka et al., 2014). A small-scale survey in Malaysia also indicated a 13% seroprevalence of infection by fusogenic bat reoviruses (Chua et al., 2007), suggesting zoonotic transmission may be common. The correlation between cell-cell fusion and pathogenicity and the evidence of zoonotic transmission suggest fusogenic reoviruses represent a potential threat as emerging human pathogens (Smith and Wang, 2013).

1.12.2 FAST protein family

The fusion-associated small transmembrane (FAST) proteins represents a unique family of proteins that are responsible for the cell-cell fusion and syncytiogenic activity of fusogenic reoviruses (Boutilier and Duncan, 2011; Ciechonska and Duncan, 2014). Currently, there are six members in the FAST protein family (Figure 1.7), named according to their molecular mass in kDa; p10 proteins encoded by avian and Nelson Bay orthoreoviruses, p13 of Broome orthoreovirus, p14 of reptilian orthoreovirus, p15 of baboon orthoreovirus, and the p16 and p22 proteins of aquareoviruseses (Dawe and Duncan, 2002; Duncan et al., 2004; Guo et al., 2013; Racine et al., 2009; Shmulevitz and Duncan, 2000; Thalmann et al., 2010). FAST proteins are nonstructural proteins that are expressed only during active virus infection. Upon their expression in vertebrate cells,

FAST proteins traffic through the ER-Golgi secretory pathway to the plasma membrane where they cause cell-cell membrane fusion (Corcoran and Duncan, 2004; Dawe et al., 2005).

FAST protein-mediated cell-cell fusion maintains cell viability, providing a means for cell-cell virus transmission without the need for virus particle release and reentry. However, extensive FAST protein-mediated syncytiogenesis in transfected cell monolayers triggers membrane instability and apoptosis leading to a burst of virus release (Salsman et al., 2005). Moreover, recent data suggest FAST proteins and reovirus particles are released from cells in exosomes (Jolene Read, PhD thesis, Dalhousie University). These observations suggest that fusogenic reoviruses first exploit cell-cell fusion events for localized spread followed by systemic spread by release of large numbers of virus progeny through leaky syncytia and possibly infectious exosomes, either or both of which could explain the correlation between virulence and the FAST proteins (Brown et al., 2009).

The fusogenic reoviruses also employ an interesting mechanism to regulate FAST protein-mediated cell-cell fusion, and to coordinate the virus replication cycle with syncytiogenesis. Unlike enveloped virus fusion proteins (White et al., 2008), the FAST proteins are 'unregulated' protein fusogens, meaning they are not controlled by pH, receptor-binding or interaction with other viral proteins (Ciechonska and Duncan, 2014). However, FAST proteins are all encoded on polycistronic mRNAs that encode one or two additional viral proteins in addition to the FAST protein, from independent open reading frames (Boutilier and Duncan, 2011). In all cases, the FAST protein open reading frame is 5'-proximal and contains a non-optimized translation start site (Racine et al., 2009). Moreover, FAST protein expression is also down-regulated by the ER-associated degradation pathway (ERAD) (Shmulevitz et al., 2004). The combination of weak translation and protein degradation slows accumulation of FAST proteins in the plasma membrane, thereby delaying the onset and rate of syncytium formation during virus infection, which may allow sufficient time for progeny virus production prior to cell disruption.

With no conserved sequence similarity, FAST proteins do share some structural similarity. All FAST proteins are type III membrane proteins that use their single

transmembrane domain as a reverse signal anchor sequence for co-translational insertion into the ER membrane, acquiring an N-exoplasmic/C-cytoplasmic topology in the ER membrane and at the plasma membrane (Corcoran and Duncan, 2004; Dawe et al., 2005). FAST proteins all contain exceptionally small ectodomains on extracellular side (19-37 residues), and equal-sized or considerably longer (36-141 residues) cytoplasmic endodomains (Figure 1.7). These domains contain a number of shared motifs, but each FAST protein has its own unique repertoire and arrangement of these motifs. For example, each FAST protein contain a hydrophobic patch, a short stretch of mostly hydrophobic or apolar residues, that is located in the cytoplasmic domains of p13, p15, p16 and p22, but is located in the ectodomains of p10 and p14. All FAST proteins also contain motifs for fatty acid acylation; N-terminal myristoylation motifs in p13, p14, p15, and p22, and a cytoplasmic cysteine-based palmitoylation motif in p10 and p16. Most FAST proteins also contain a proline-rich motif, located in the cytoplasmic domains of p14 and p16 but in the ectodomains of p13 and p15. Each FAST protein also contains a cluster of 3-7 basic residues, termed as the polybasic motif (PBM). Interestingly, this is the only motif that is located in a similar position in all FAST proteins (i.e., membrane-proximal in the cytoplasmic tail).

Considerable effort has gone into defining the roles of the various FAST protein motifs in the cell-cell fusion process. Most of these studies have focused on the ARV and NBV p10, RRV p14, and BRV p15 FAST proteins. For example, the palmitoylation motif in p10, and the myristoylation motifs in p14 and p15, have been shown to be essential for fusion activity, although their precise roles have not been determined (Corcoran et al., 2004; Dawe and Duncan, 2002; Shmulevitz et al., 2003). The ectodomains of p10 and p14 control multimerization, and both proteins localize to specialized membrane microdomains, termed lipid rafts (Corcoran et al., 2011; Corcoran et al., 2006; Key and Duncan, 2014). In the case of p10, the membrane-proximal ectodomain region (MPER) controls both raft localization and multimerization to create cholesterol-dependent fusion platforms (Key and Duncan, 2014). The ectodomain hydrophobic patches of p10 and p14 form a cystine noose and a proline-hinged loop, respectively, while the p15 ectodomain polyproline motif forms a polyproline type II helix. These motifs all function as fusion peptides to mediate lipid mixing between apposed membranes (Barry et al., 2010; Corcoran

et al., 2004; Key et al., 2015; Top et al., 2012). Recent results indicate the p15 cytoplasmic hydrophobic patch is essential for pore formation and functions as a novel type of fusion-inducing lipid-packing sensor that partitions into highly curved membranes, such as those present in the rim of a fusion pore (Jolene Read, PhD thesis, Dalhousie University). The cytoplasmic hydrophobic patches in p13, p16 and p22 may serve a similar function, as shown for a previously unrecognized amphipathic helix in the same location in p14. Together, these motifs function from both sides of the membrane to drive the fusion process.

1.13 Objectives

Of all the FAST protein motifs, the spatially conserved polybasic motif (PBM) is the least understood. Previous studies indicated that substitution mutations of the p10 PBM result in loss of syncytiogenic activity (Shmulevitz et al., 2003). However, the basis for the loss of function was not determined. A previous graduate student showed that substitution of the PBM of p14 also results in loss of syncytia formation, and p14 proteins with an alanine-substituted PBM were inefficiently trafficked to the plasma membrane, preferentially localizing instead in the Golgi apparatus (Christopher Barry, PhD thesis, Dalhousie University). These preliminary observations provided the rationale for my research.

My objective was to more clearly define the role(s) of the p14 PBM in protein trafficking. I was able to demonstrate that the p14 PBM is a novel Golgi export signal, not a plasma membrane retention signal, which requires a minimum of three basic residues that function in a relatively sequence-independent manner to mediate efficient Golgi export and transport to the plasma membrane. I also determined that the Golgi export ability of the p14 PBM is transferable to a heterologous Golgi resident protein, implying it is an autonomous Golgi export signal. Moreover, I showed that the trafficking function of the p14 PBM is exquisitely sensitive to membrane proximity and can function to mediate ER/Golgi export, ER retention, and/or ER retrieval depending on its location in the p14 cytoplasmic tail. Lastly, I determined the molecular determinants and cellular pathway through which p14 traffics to the plasma membrane. I demonstrated for the first time that activated Rab11 can directly interact with a cargo protein to mediate cargo sorting into

AP1-coated vesicles that can mediate anterograde traffic from the TGN to the plasma membrane, events that were all dependent on the p14 PBM. Together, these findings support a receptor-mediated Golgi export hypothesis and provide novel insights into cellular trafficking mechanisms at the Golgi complex, one of the least understood steps in the secretory pathway.

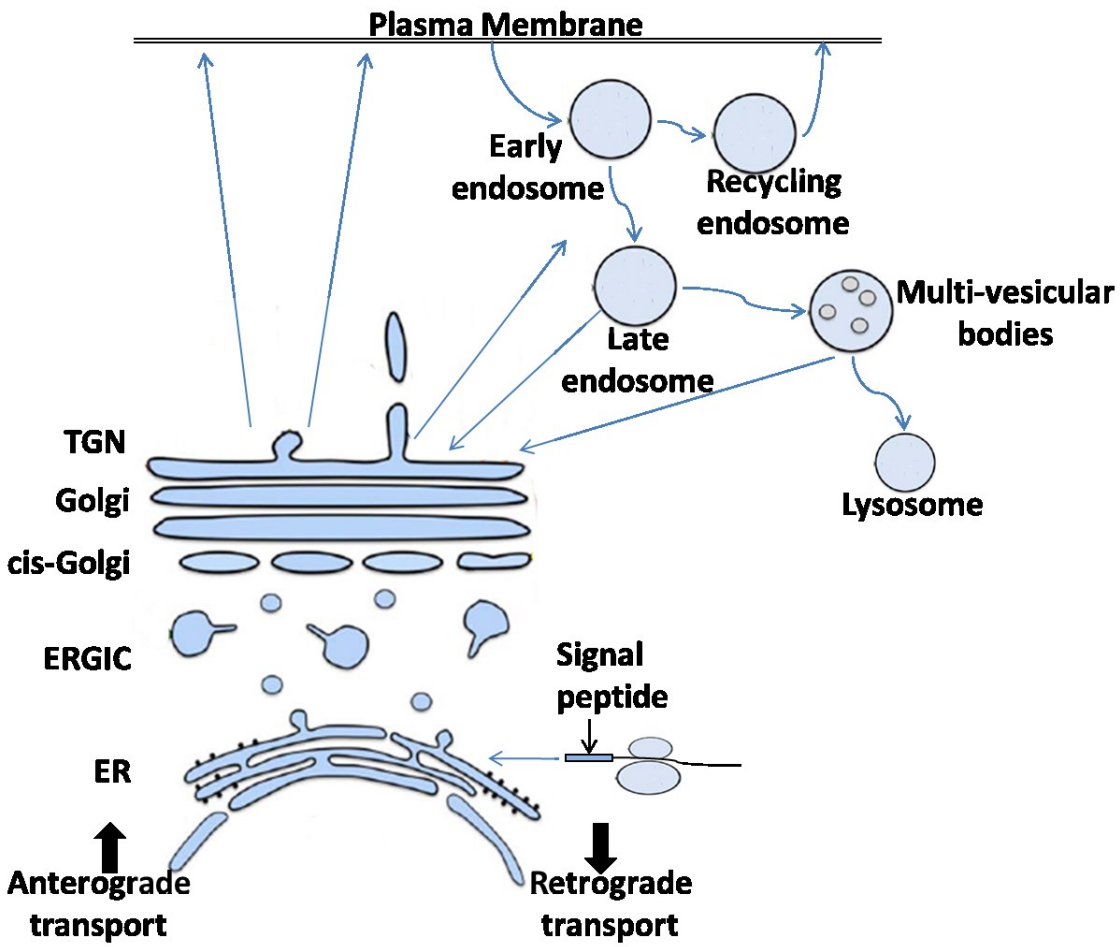

Figure 1.1 Overview of cellular secretory and endocytic pathways. Signal peptides direct protein translocation into the ER and cargo proteins are then transported to the Golgi complex via the ERGIC. Proteins may be post-translationally modified in the ER and the Golgi and are then trafficked from the TGN to the cell surface. Cell surface-expressed proteins and extracellular materials can be internalized by endocytosis and either recycled back to the plasma membrane or sorted to intracellular organelles such as late endosomes, lysosomes or TGN. Protein transport in the forward direction from the ER to the plasma membrane is referred to as anterograde transport, while protein transport in the reverse direction is referred to as retrograde transport. ER: Endoplasmic Reticulum, TGN: trans-Golgi Network, ERGIC: ER-Golgi intermediate compartment [modified from (Goud and Gleeson, 2010) with permission].

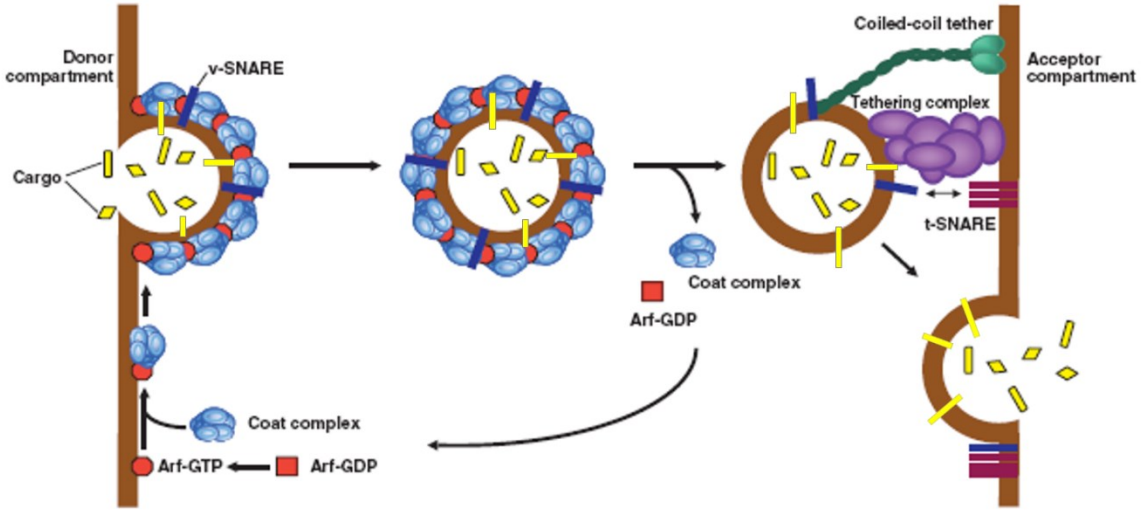

Figure 1.2: Vesicle budding and fusion. Activation of a small G protein (such as Arf1 or Sar1) (red) by exchange of GDP for GTP results in recruitment of a coat complex (blue) to the membrane by the GTP-bound form of the G protein. Membrane curvature and sorting of cargo (yellow) into the forming bud ensues, followed by fission of the coated bud to form a vesicle. Hydrolysis of GTP eventually leads to release of the coat from the vesicle. The vesicle is targeted to the acceptor-compartment membrane by tethering complexes (long coiled-coil, green; multi-subunit, purple). For simplicity, the coat is not shown at this stage, but note that the coat may in some cases remain on the vesicle during the tethering process, with uncoating occurring after tethering. Vesicle SNARE proteins (v-SNARE; dark blue bars) engage tripartite target-localized SNARE proteins (t-SNARE; maroon bars), which leads to fusion of the vesicle and acceptor compartment membranes, and to release of cargo into the acceptor compartment [modified from (Jackson, 2009) with permission].

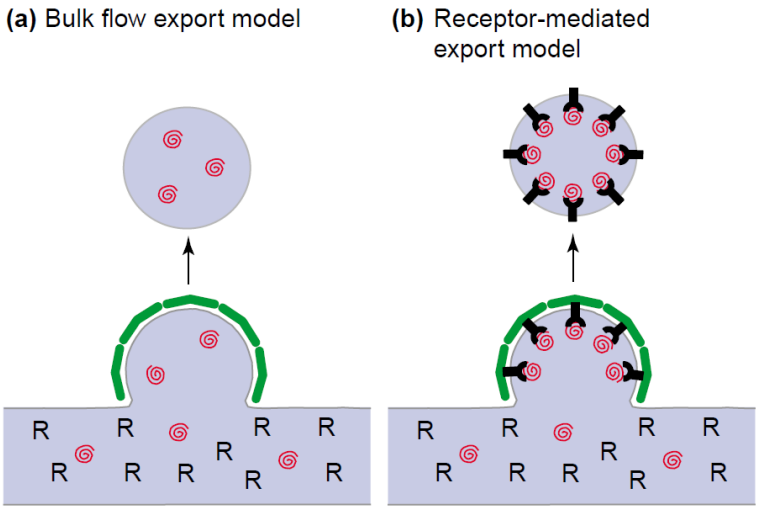

Figure 1.3 Bulk-flow and receptor-mediated export models for ER export of secretory cargo proteins. (a) In the bulk-flow model, soluble cargo molecules depart in vesicles at a concentration equal to that found in the ER lumen. (b) The receptor-mediated export model results in concentrative sorting of soluble cargo during vesicle formation and relies on receptor-like proteins to link cargo to the membrane coat complex. In both models, ER-resident proteins (designated 'R') might not be efficiently packaged into ER-derived vesicles owing to the effect of retention and/or exclusion mechanisms [adapted from (Barlowe, 2003) with permission].

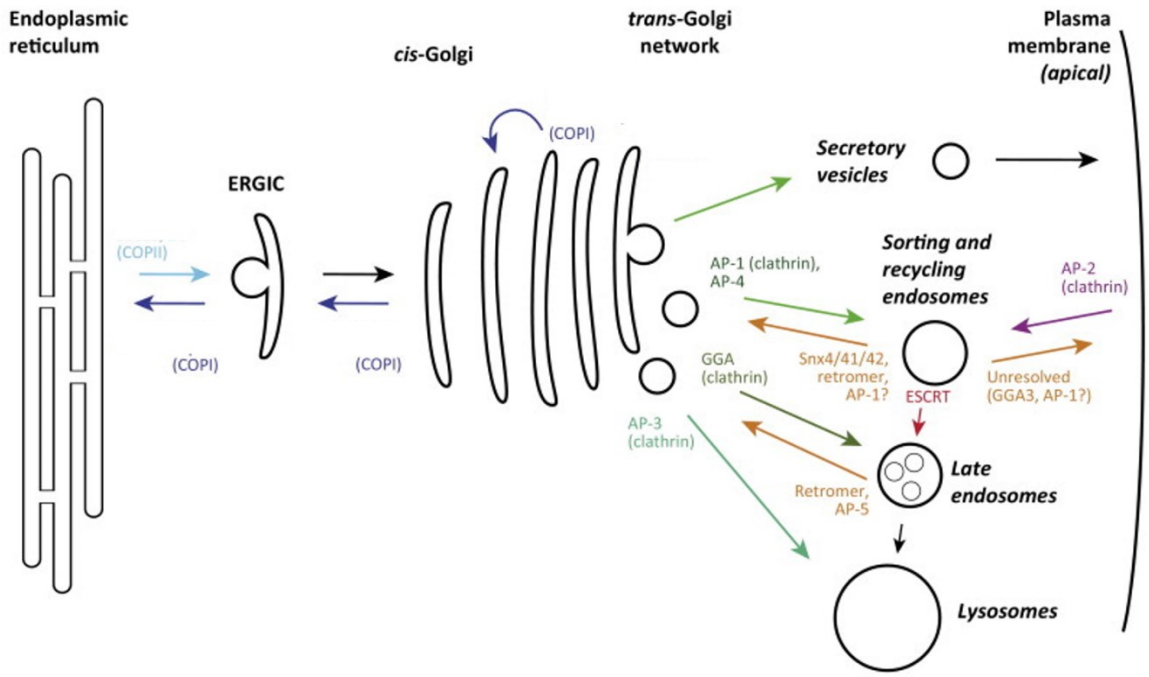

Figure 1.4 Overview of coat complexes involved in various stage of the secretory and endocytic pathway. The COPII complex mediates anterograde traffic from the ER to the ERGIC while COPI complexes mediate retrograde traffic from the Golgi to the ER. Traffic from the Golgi is mediated by adaptor protein 1 (AP1), AP3, AP4 and GGAs. AP2 mediates endocytosis while the retromer complex mediates retrograde traffic from the endosomes to the Golgi [modified from (Paczkowski et al., 2015) with permission].

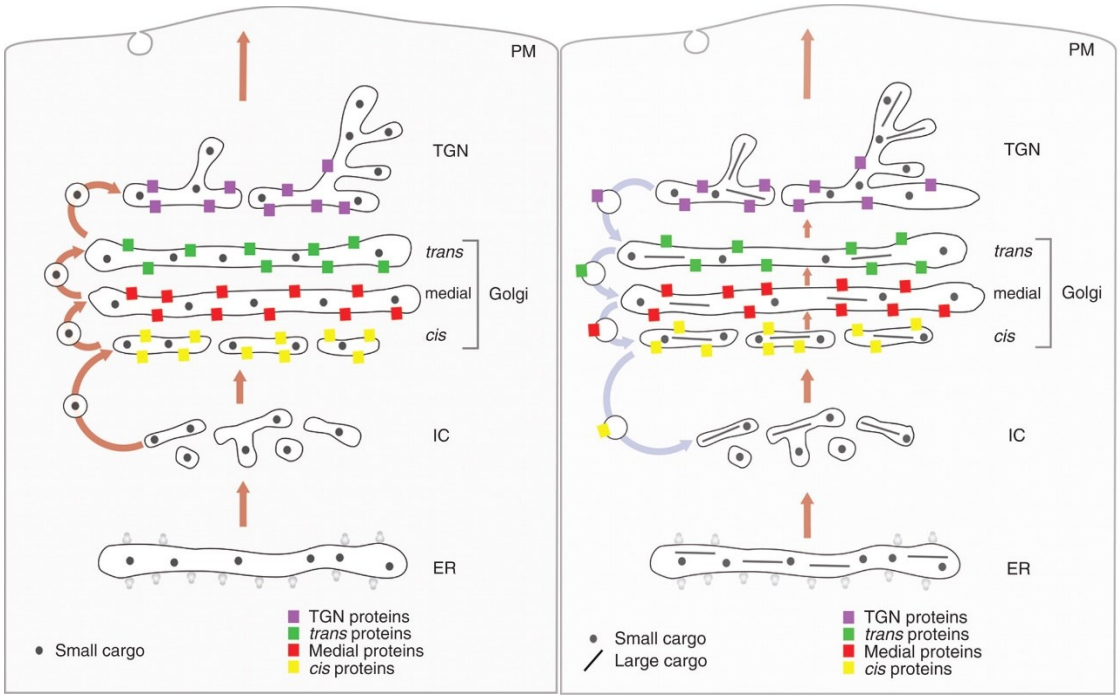

Figure 1.5 Models for traffic through the Golgi. The vesicular transport model (left): Secretory cargoes travel from the ER to the intermediate compartment (IC) and *cis*-Golgi in dissociative carriers. Golgi compartments are stable and biochemically distinct. Secretory cargoes move across the stack by means of COPI vesicles that bud from one compartment and fuse with the next, whereas resident Golgi proteins stay in place by being excluded from budding vesicles. The cisternal-maturation model (right): Secretory cargoes exit the ER in dissociative carriers, which coalesce with one another and with COPI vesicles derived from the *cis*-Golgi to form the intermediate compartment, which coalesces in turn to form a new *cis*-cisterna. In subsequent rounds of COPI-mediated recycling, the new cisterna matures by receiving *medial* and then *trans*-Golgi proteins from older cisternae while exporting *cis* and then *medial*-Golgi proteins to younger cisternae. Meanwhile, the cisterna progresses through the stack, carrying forward both small and large secretory cargoes. In the final stage of maturation, the cisterna is a TGN element that breaks down into anterograde and retrograde transport carriers [modified from (Glick and Luini, 2011) with permission].

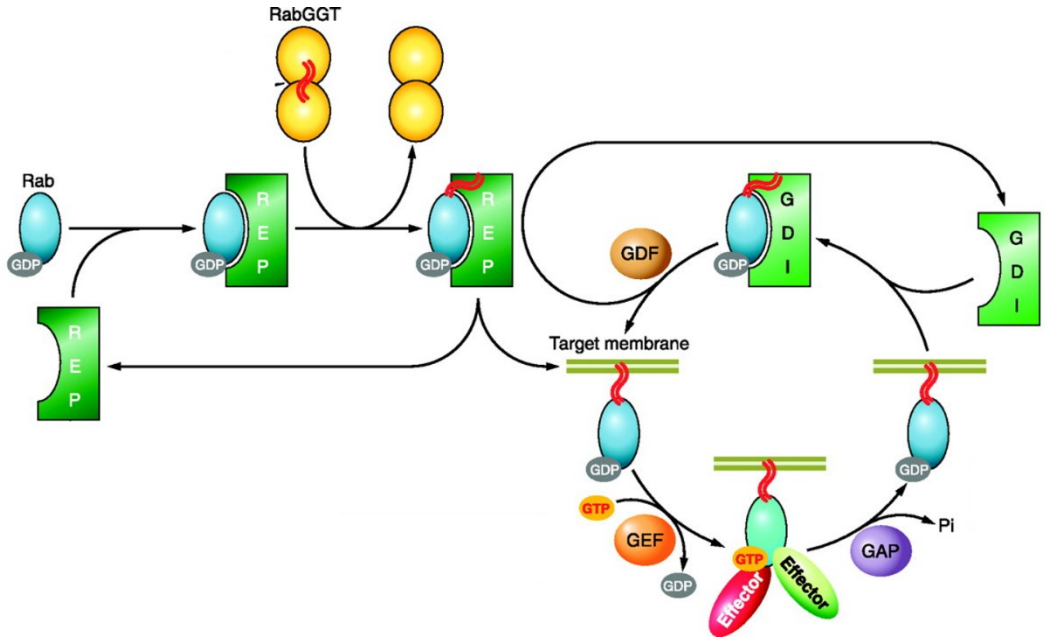

Figure 1.6 The Rab activation cycle. The newly synthesized Rab protein associates with Rab escort protein (REP) that directs it to Rab geranylgeranyl transferase (RabGGT) to receive its prenyl tails (red wavy lines). REP delivers the Rab to its target membrane. Throughout this process, the Rab is GDP-bound. A guanine-nucleotide exchange factor (GEF) catalyzes exchange of GDP for GTP to activate the Rab. The GTP-bound Rab interacts with effector proteins that mediate membrane traffic in the pathway regulated by its associated Rab. The Rab then interacts with its associated GTPase-activating protein (GAP) that catalyzes hydrolysis of GTP to GDP by the Rab. The Rab is then removed from the membrane by guanine nucleotide dissociation inhibitor (GDI) in preparation for the next cycle. The insertion of the Rab into the target membrane is mediated by a GDI-dissociation factor (GDF) that releases the Rab from GDI [modified from (Hutagalung and Novick, 2011)].

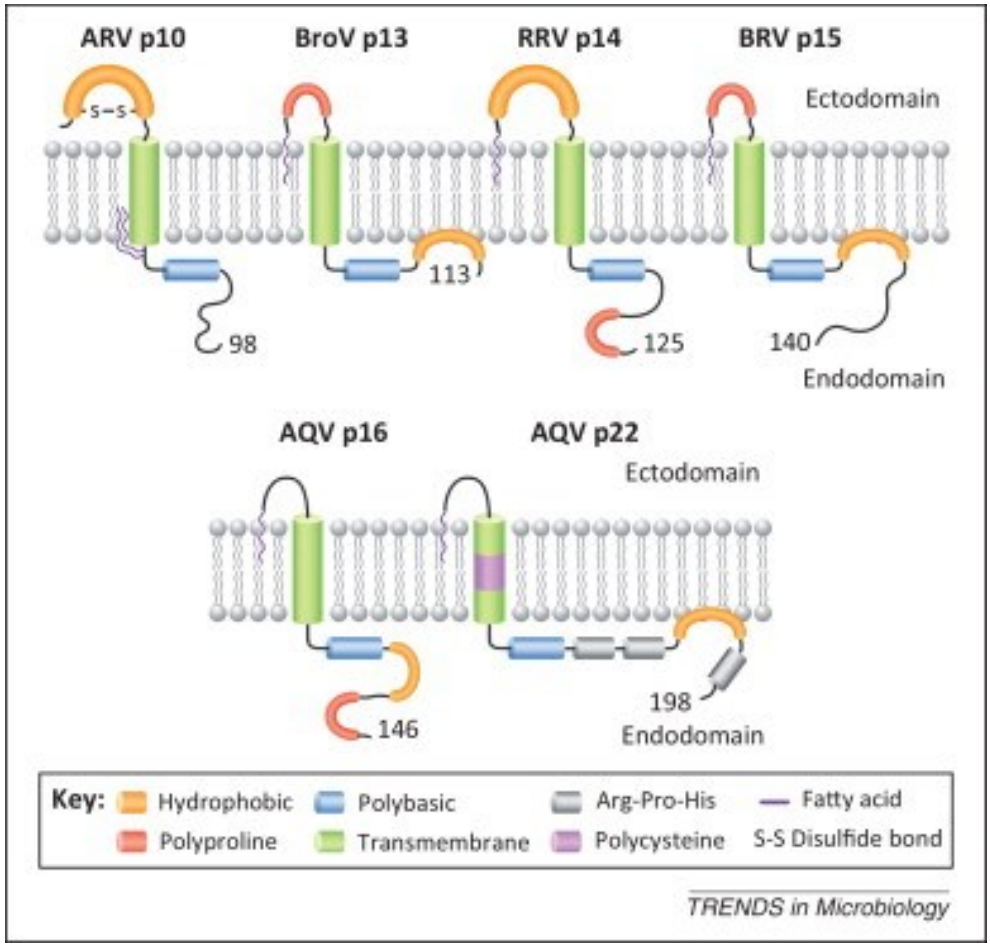

Figure 1.7 The reovirus fusion-associated small transmembrane (FAST) proteins. Diagrams of the orthoreovirus (top) and aquareovirus (bottom) FAST proteins, depicting their topology in the plasma membrane. Structural motifs contained within their N-terminal ectodomains and C-terminal cytoplasmic endodomains are color coded as described in the legend. Numbers indicate the number of residues in each protein. ARV- avian reovirus, BroV- Broome reovirus, RRV- reptilian reovirus, BRV- baboon reovirus, AQV- aquareovirus [adapted from (Ciechonska and Duncan, 2014) with permission].

CHAPTER 2
MATERIALS AND METHODS

2.1 Cells:

Quail fibroblast (QM5) and African green monkey kidney epithelial (Vero) cell lines were grown in Earle's Medium 199 (Life Technologies, Carlsbad, CA) supplemented with 10% or 5% fetal bovine serum (FBS) (Sigma-Aldrich, St. Louis, MO), respectively, at 37°C with 5% CO_2. HeLa cells were grown in Dulbecco's modified Eagle medium (DMEM) (Life Technologies) supplemented with 10% FBS, and human embryonic kidney (HEK) 293T cells were grown in DMEM supplemented with 10% FBS and 25 mM HEPES (Life Technologies) at 37°C with 5% CO_2. All cell lines were maintained in 175 cm^2 flask and sub-cultured using Trypsin-EDTA (Life Technologies) every 2-3 days to prevent over-confluency and cell death. Cells were maintained without use of antibiotics. Generally, QM5 cells were used for syncytial analysis (good transfection efficiency and very permissive for fusion), Vero cells and HeLa cells were used for immunofluorescence microscopy (large cytoplasms), HeLa cells were also used for siRNA and dominant-negative experiments (human cells compatible with the siRNAs and dominant-negative proteins), and HEK cells were used for co-immunoprecipitation assays (human cells compatible with commercial antibodies and with good transfection efficiency).

2.2 Antibodies:

The rabbit polyclonal α-p14 and α-p14 ectodomain antisera were previously described (Corcoran and Duncan, 2004; Top et al., 2005). Primary antibodies against actin (Sigma-Aldrich), myc epitope tag (Sigma-Aldrich), PI4KIIIβ (BD Biosciences, Franklin Lakes, NJ), TGN46 (AbD Serotec, Oxford, UK), protein disulfide isomerase (PDI; Enzo Life Sciences, Farmingdale, NY), KDEL (Stressgen, Victoria, BC), Rab11A (BD Biosciences, Franklin Lakes, NJ), AP1γ (Sigma-Aldrich), AP3δ (DSHB, University of Iowa, Iowa City, IA), AP4ε (Abcam, Cambridge, UK), and horseradish peroxidase (HRP)–conjugated goat α-rabbit (Jackson ImmunoResearch, West Grove, PA), HRP-conjugated goat α-mouse (Santa Cruz Biotech, Dallas, Texas), Alexa Fluor 488–conjugated goat α-mouse and donkey α-sheep, Alexa Fluor 555–conjugated donkey α-rabbit, and Alexa Fluor

647–conjugated goat α-rabbit and chicken α-mouse (Life Technologies) secondary antibodies were obtained from the indicated suppliers.

2.3 Plasmids and Cloning

2.3.1 Vectors

The wild-type (wt) p14 construct, and non-fusogenic mutants p14-G2A (point substitution eliminates the myristoylation consensus sequence) and p14-V9T (point substitution introduces a functional glycosylation signal) were cloned into pcDNA3 mammalian expression vector as described previously (Corcoran and Duncan, 2004). The Rab11A construct in pcDNA3 was cloned from PC3 cells by reverse transcriptase polymerase chain reaction (RT-PCR) and kindly provided by Julie Boutilier (Dalhousie University). All p14 mutant proteins and Rab11 constructs were cloned into pcDNA3 vector. Rab5 and Rab5-S34N constructs in pcDNA3 were kindly provided by Denis Dupré (Dalhousie University). Bacterial expression vector pGEX-2T was kindly provided by Jolene Read (Dalhousie University).

2.3.2 Site-directed mutagenesis

Various p14 polybasic mutants were created by substitution of residues in the p14 polybasic motif (QKRRERRRQ) to alanine using QuickChange site-directed mutagenesis (Stratagene, La Jolla, CA) according to manufacturer's instructions. These mutant protein names and sequences for the polybasic region are: p14PA (QAAAEAAAQ); p14-RRE (QKAAARRRQ); p14-RER (QKRAAARRQ); p14-RRQ (QKRRERAAA); p14-KRR (QAAAERRRQ); p14-RRR (QKRREAAAQ); PA+K,R,R (QKAARAARQ); PA+KR (QKRAAAAAQ); PA+RR (QRRAAAAAQ); PA+RR' (QAAAAARRQ); PA+K,R (QKAAAAARQ); PA+RAR (QAAAERARQ); PA+KAK (QAAAEKAKQ); PA+K (QKAAAAAAQ); and PA+R (QAAAAAARQ). These constructs in the wt p14 backbone were again subjected to site-directed mutagenesis to introduce G2A or V9T mutations. Rab11A dominant-negative (Rab11A-S25N) and constitutively-active (Rab11A-Q70L) mutants were also created by site-directed mutagenesis. Custom primers for site-directed mutagenesis were purchased from Integrated DNA technologies (IDT, Coralville, IA). Plasmids were amplified with the designed primers using PfuUltra High Fidelity DNA

polymerase (Agilent Technologies, Santa Clara, CA) according to the manufacturer's polymerase chain reaction (PCR) protocol. PCR products were treated with DpnI enzyme (New England Biolabs, Ipswich, MA) at 37°C overnight to digest parental plasmid DNA, and were transformed into competent cells of *Escherichia coli* (*E. coli*) strain DH5α. Pure cultures of transformed *E. coli* DH5α were prepared to isolate plasmid DNA using the QIAprep spin miniprep kit (QIAGEN, Hilden, Germany). These plasmid inserts, and all subsequent plasmid inserts, were sequenced before use (MCLAB, San Francisco, CA or GENEWIZ, South Plainfield, NJ).

2.3.3 Polybasic motif insertion in the p14 cytoplasmic tail

p14extPB and p14PAextPB were created using p14 and p14PA as templates, respectively, for PCR with reverse primers that added the PBM to the C-terminus of the protein. The PBM (QKRRERRRQ) was also inserted between cytoplasmic tail residues 74–75 (p14/75PB and p14PA/75PB) or 91–92 (p14/92PB and p14PA/92PB) in the p14 and p14PA backbones using reverse PCR primers containing the PBM nucleotide sequence. All these p14 and p14PA constructs were subjected to site-directed mutagenesis to introduce V9T or G2A substitutions.

2.3.4 ERGIC chimera constructs

N-terminally myc-tagged ERGIC-53 chimera (ERGIC-53 ectodomain, CD4 transmembrane domain and polyalanine cytoplasmic tail) and the glycosylated ERGIC-53 chimera (D61N and VNATASA insertion in the ectodomain) constructs were kindly provided by Karl Matter (University College London, London, UK) in plasmid pCB6. These constructs were subcloned into pcDNA3 vector and sequenced before use. The non-glycosylated ERGIC-53 chimera construct was used as a template for PCR with primers that replaced the membrane-proximal di-arginine sequence in the cytoplasmic tail with the p14 membrane-proximal region containing the PBM (KYLQKRRERRRQ) or Ala substitutions of the PBM (KYLQAAAEAAAQ).

2.3.5 Fluorescently-tagged constructs

EGFP, mCherry and p14 tagged with EGFP or mCherry at the C-terminus in pcDNA3 were kindly provided by Timothy Key (Dalhousie University). p14PA-EGFP was created by replacing p14 with p14PA in the p14-EGFP construct by restriction digestion and ligation. mCherry-Rab11A and mCherry-Rab11A-S25N were created by ligating the Rab11 genes to the 3'-terminus of the mCherry gene in pcDNA3. The PH domain of Akt tagged with GFP in pcDNA3 vector was obtained from Addgene (Cambridge, MA).

2.3.6 Glutathione S-transferase (GST)-tagged constructs

The cytoplasmic endodomains of p14 and p14PA were codon-optimized and chemically synthesized (BioBasic, Markham, ON) for bacterial protein expression. Codon-optimized genes were subcloned into the pGEX-2T vector to add a GST-tag at the N-terminus of the p14 or p14PA endodomains.

2.3.6 Glycerol stocks

Pure cultures of transformed *E. coli* DH5α cells were mixed with equal volumes of LB media with 50% glycerol in cryovials and stored at -80°C. A sample from this glycerol stock was used as inoculum whenever needed to prepare cultures for plasmid extraction using QIAGEN plasmid midiprep kit (QIAGEN).

2.4 Transfections

2.4.1 Transient transfections

QM5 cells grown on culture plates to ~60% confluency were transfected with Lipofectamine (Life Technologies) or polyethyleneimine (PEI; Polysciences Inc., Warrington, PA), Vero cells grown on cover slips were transfected with jetPRIME (PolyPlus Transfection, Illkirch, France), HEK cells grown on culture plates were transfected with PEI, and HeLa cells grown on culture plates or cover slips were transfected with Lipofectamine LTX (Life Technologies), all according to manufacturer's instructions. Briefly, transfection mixes were prepared in OptiMEM (Life Technologies) medium with 0.5 µg of DNA and 3 µg of PEI, 1 µg of DNA and 3 µl of Lipofectamine or Lipofectamine LTX, or 1µg of DNA and 2 µl of jetPRIME for one well of a 12-well culture plate. Cells

were washed and supplemented with fresh serum free growth medium before adding transfection mixes. After incubation for 4-6 h, the transfection mix was removed and cells were supplemented with serum-containing growth medium for another 18-20 h for analysis by respective assays. Transfection mixes were scaled according to the various sizes of culture plates. Doses of plasmid DNA for transfection were titrated according to the respective assay as indicated in the text.

2.4.2 Stable transfection

For stable transfections with ERGIC-53 chimeric constructs, at 24 hours post-transfection (hpt), the growth medium on QM5 or Vero cells was replaced with growth medium containing 1 mg/ml G418 (Life Technologies), and transfected cells were cultured under selective conditions for 5 days with subculturing in the selective medium as required.

2.4.3 siRNA transfection

siRNAs against Rab11A and/or Rab11B (Sigma-Aldrich), AP1γ, AP3δ or AP4ε (SMARTpool, Dharmacon, Lafayette, CO) were transfected into HeLa cells grown on culture plates or coverslips using DharmaFECT1 transfection reagent (Dharmacon) for 48 h according to manufacturer's instructions. Transfection mix with 25 nM siRNA and 2 µl of DharmaFECT1 was used for one well of 12-well culture plate. Cells were then analyzed by western blotting or re-transfected with p14-G2A or p14PA-G2A for 24 h before analysis by flow cytometry for cell surface immunofluorescence or by immunofluorescence microscopy for intracellular localization as described below.

2.5 Syncytial assay

Transfected QM5 cell monolayers at 8 hpt were rinsed with Hank's balanced salt solution (HBSS), fixed with methanol, and stained using Wright–Giemsa stain. A syncytial index was determined by counting the number of syncytial nuclei (i.e., cells containing >4 nuclei/cell) in five random microscopic fields at 20X magnification, as previously described (Corcoran and Duncan, 2004). Results are reported as percent fusion relative to wt p14 based on the mean number of syncytial nuclei per field from two or more independent experiments using triplicate samples.

2.6 SDS-PAGE and Western blotting

2.6.1 Protein expression analysis

QM5 cells were lysed at 8 hpt with RIPA buffer (50 mM Tris, pH 8.0, 150 mM NaCl, 1 mM EDTA, 1% NP-40, 0.5% IGEPAL) containing 1 μM protease inhibitors (aprotinin, pepstatin, and leupeptin) for 45 min on ice. Equivalent protein loads were determined by Lowry assays (BioRad, Hercules, CA) and analyzed by SDS–PAGE (15% acrylamide) and western blotting. HeLa or HEK cells grown and treated in culture plates were harvested by adding 2X Laemmli sample buffer, for efficient cell lysis, directly onto the cells. Cells were then scraped, syringed or sonicated and boiled before analysing by SDS-PAGE (7.5% or 15% acrylamide). Gels were electrophoresed at 160V for 1 h using a Mini-PROTEAN 3 cell (BioRad) and transferred onto PVDF membranes at 100V for 1 h using a wet-transfer apparatus (BioRad) according to manufacturer's instructions. Membranes were blocked with 5% milk in TBST (Tris-buffered saline, 0.1% Tween-20; 20 mM Tris, 150 mM NaCl, pH 7.6) for 1 h at room temperature. Membrane blots were then probed with α-p14 antiserum (1:10,000 or 1:20,000) or with antibodies against actin (1:2500 or 1:5000), the myc epitope tag (1:2500), Rab11A (1:5000), AP1γ (1:5000), AP3δ (1:1000) or AP4ε (1:1000) at 4°C overnight. HRP-conjugated goat α-rabbit (1:10,000) or goat α-mouse (1:5,000) secondary antibodies were incubated for 1 h at room temperature. Membranes were developed using ECL-plus reagent (GE Healthcare, Little Chalfont, UK) and imaged using a Typhoon 9410 variable-mode imager (GE healthcare) or a Kodak 4000-mm Pro CCD imager (Kodak, Rochester, NY). Blots were quantified from two or three independent experiments using densitometry analysis in ImageJ (National Institutes of Health, Bethesda, MD) and results reported as band density relative to control sample. Images in figures are manipulated in Photoshop using only linear adjustments on the entire image.

2.6.2 Endoglycosidase H assay

QM5 cells were lysed at 24 hpt with RIPA buffer as described for protein expression analysis (2.6.1), and before SDS–PAGE, lysates were treated at 37˚C for 2 h with endoglycosidase H (endo H) or N-glycosidase F (PNGase F) according to the

manufacturer's specifications (NEB). Membranes were developed using ECL-Plus reagent, imaged and analyzed as in 2.6.1.

2.6.3 Co-immunoprecipitation assay

HEK cells transfected with p14-G2A, p14PA-G2A or empty vector were harvested at 24 hpt by following a Rho-activation assay protocol (Cytoskeleton, Denver, CO). Briefly, cells were washed quickly with ice-cold phosphate buffered saline (PBS), lysed in the dishes on ice with ice-cold lysis buffer (50 mM Tris-HCL, pH 8.0, 0.5 M NaCl, 10 mM $MgCl_2$, 2% Igepal), collected into microcentrifuge tubes by scrapping, syringed and centrifuged at 14000 Xg for 5 min in a table-top microcentrifuge. Supernatants were snap-frozen in liquid nitrogen and stored at -80°C until use, or incubated right after harvesting with Dynabeads (Life Technologies) pre-bound to Rab11 antibody or IgG for 1 h at 4°C. Samples were washed three times with lysis buffer and eluted by boiling the beads in 2X Laemmli sample buffer for efficient elution. Eluted samples were analysed by SDS-PAGE and western blotting using α-p14 antiserum. A portion of each cell lysate was removed prior to adding beads and directly analyzed by western blotting with α-p14 antiserum, and α-Rab11 and α-actin antibodies to serve as a protein expression and detection control for the co-immunoprecipitations.

For Rab11 activation, a GTPγS loading protocol was followed according to manufacturer's instruction (Cytoskeleton). Cell lysates were loaded with 10 mM EDTA and GTPγS (100 μM) or GDP (1 mM) and incubated at 30°C for 30 min. Nucleotide loading was stopped by adding $MgCl_2$ (60 mM final) prior to overnight incubation of cell lysates with Rab11 antibody at 4°C. Dynabeads were added to the lysates the next day for 1 h at 4°C. Samples were eluted by boiling beads with 2X Laemmli sample buffer and analyzed by western blotting with α-p14 antiserum.

2.7 Flow cytometry

2.7.1 Cell surface immunofluorescence

Transfected QM5 cells were cultured for 24 h in growth medium containing a 1:20 dilution of α-p14 ectodomain antiserum to prevent syncytium formation. Alternately, QM5 cells transfected with the non-fusogenic p14-G2A or p14-V9T constructs were cultured for

24 h in normal growth medium. HeLa cells co-transfected with p14-G2A (0.2 µg DNA/well of 12 well plate) and Rab11, Rab11 S25N, Rab11 Q70L, Rab5 or Rab5 S34N (0.8 µg DNA) were cultured for 24 h. HeLa cells transfected with Rab11, AP1γ, AP3δ or AP4ε siRNA for 48 h and re-transfected with p14-G2A (0.2 µg DNA) were cultured for an additional 24 h in normal growth medium. Live cells were then incubated at 4˚C for 30 min in blocking buffer (5% normal goat serum, 1% bovine serum albumin [BSA], 0.02% NaN_3 in HBSS) and stained with a 1:1000 dilution of α-p14 ectodomain antiserum, α-p14 full-length antiserum, or α-myc antibody (for the chimeric ERGIC-53 constructs) and a 1:2000 dilution of Alexa 647–conjugated goat α-rabbit secondary antibody, each for 1 h at 4˚C. Cells were washed 6X with blocking buffer after each antibody incubation. Cells were quickly rinsed with PBS and resuspended in PBS containing 10 mM EDTA and fixed with 3.7% formaldehyde, and 10,000 cells were analyzed by flow cytometry (FACSCalibur; BD Biosciences) using De-Novo software. Cells transfected with empty vector were used as negative controls to set the fluorescence gate to <5%, and the same gate was applied to quantify surface fluorescence of p14-transfected cells. Background fluorescence from vector-transfected cells was subtracted before mean percent surface fluorescence was calculated.

2.7.2 Intracellular immunofluorescence

QM5 cells were transfected with non-fusogenic p14-G2A or p14PA-G2A for 24 h in normal culture medium. Cells were then resuspended in PBS with 10 mM EDTA and fixed with 1% paraformaldehyde in PBS for 15 min at room temperature. Cells were pelleted, washed with PBS, and permeabilized in blocking buffer containing 0.1% saponin for 30 min at room temperature. Cells were then labelled with 1:1000 dilution of α-p14 antiserum and 1:2000 dilution of Alexa 647–conjugated goat α-rabbit secondary antibody, each for 1 h at room temperature in blocking buffer containing 0.1% saponin. Cells were resuspended in PBS and analyzed by flow cytometry as indicated for cell surface immunofluorescence (2.7.1).

2.7.3 Endocytosis inhibition assay

QM5 cells were transfected with non-fusogenic p14-G2A or p14PA-G2A, and at 24 hpt cells were incubated with 80 μM dynasore (Santa Cruz Biotechnology, Dallas, TX) or 0.8% dimethyl sulfoxide (DMSO; Sigma-Aldrich) at 37˚C for 1 h in serum-free growth medium. Cells were then treated and analyzed for p14 plasma membrane expression as described for cell surface immunofluorescence (2.7.1).

2.7.4 Transferrin binding assay

To confirm dynasore inhibited dynamin-dependent endocytosis, vector-transfected QM5 cells were serum-starved for 30 min and then incubated with 80 μM dynasore or 0.8% DMSO at 37˚C for 30 min. Alexa 555–conjugated transferrin (Life Technologies) was then added (20 μg/ml) to cells for 20 min at 4˚C. Cells were then harvested and analyzed as described in cell surface immunofluorescence (2.7.1).

To confirm RAB5-S34N inhibited endocytosis, at 24 hpt HeLa cells transfected with Rab5 or Rab5-S34N were incubated at 4°C for 10 min and then incubated with Alexa-647 conjugated transferrin (20 μg/ml; Life technologies) for 20 min at 4°C. Cells were then washed with PBS, resuspended with PBS containing 10 mM EDTA, fixed with 3.7% formaldehyde, and analyzed by flow cytometry as described for cell surface immunofluorescence (2.7.1).

2.8 Cellular microscopy

2.8.1 Intracellular immunofluorescence microscopy

At 24 hpt, transfected Vero cells cultured on glass coverslips (Thermo Scientific, Hampton, NH) were fixed with 3.7% formaldehyde for 20 min at room temperature and permeabilized for 20 min at room temperature with 0.1% Triton X-100. Cells were washed 3X with PBS and blocked for 30 min in blocking buffer (1% BSA in PBS) and co-stained with rabbit α-p14 antiserum (1:200) or rabbit α-myc antibodies (1:1000) and with 1:1000 dilutions of mouse monoclonal antibodies against a Golgi marker (PI4KIIIβ), TGN marker (TGN46), or ER marker (PDI or KDEL) and subsequently with 1:1000 dilutions of Alexa 488–conjugated goat α-mouse and Alexa 647–conjugated goat α-rabbit secondary antibodies. Cells were washed 3X with PBS after each antibody incubation. Coverslips

were mounted on glass slides using fluorescence mounting medium (Dako, Glostrup, Denmark) or Prolong gold antifade reagent (Life Technologies) and then visualized and photographed using a Zeiss LSM 510 META confocal microscope or a Zeiss Axioplan II MOT and AxioCam HRC Color Camera. Images were acquired with either 63X or 100X objective lens. Laser intensity was set to minimize saturated pixels, and detector gain was set to have minimal background in control samples using image acquisition software. The same parameters were used for subsequent image acquisition within the experiment. Images were analyzed by ImageJ to generate fluorescence intensity graphs. The Pearson's correlation coefficient for colocalization was determined from 5–10 cells on raw images using the Fiji version of ImageJ (Schindelin et al., 2012). If required, background was corrected using the rolling ball background plug-in, and colocalization thresholds were set using the Coloc_2 plug-in (Costes et al., 2004).

HeLa cells grown on coverslips were transfected with p14-G2A or p14PA-G2A (0.2 μg DNA) and fixed, permeabilized and washed as above. Cells were blocked for 30 min at room temperature and co-labelled in blocking buffer with α-p14 antiserum (1:200) and α-PI4KIIIβ (1:1000), α-TGN46 (1:1000), α-Rab11 (1:100) and/or α-AP1γ (1:1000) primary antibodies for 1 h at room temperature. Cells were then incubated with appropriate Alexa-conjugated secondary antibodies (1:1000) for 1 h at room temperature. Coverslips were mounted on glass slides using ProLong Gold antifade reagent (Life Technologies). Cells were imaged using a Zeiss LSM 510 META confocal microscope and 40X or 63X objective lens. Laser intensity and detector gain were set as described above. Colocalization was quantified in ten cells each from two independent experiments by calculating Pearson's correlation coefficients on raw images using the Coloc_2 plugin for ImageJ. Images in all figures were manipulated in Photoshop using only linear adjustments on the entire image.

2.8.2 Antibody internalization assay

Vero cells cultured on glass coverslips were transfected with non-fusogenic p14-G2A or p14PA-G2A and incubated for 24 h with normal growth medium. Cells were then incubated with blocking buffer and subsequently with 1:200 dilution of α-p14 antiserum in blocking buffer, each for 30 min at 37°C. Cells were fixed with 4% paraformaldehyde for

15 min at room temperature and washed 3X with PBS. Cells were processed further as non-permeabilized cells or after permeabilization with 0.1% Triton X-100 in PBS for 15 min at room temperature using Alexa Fluor 488–conjugated goat α-rabbit antibody for 1 h at room temperature. Coverslips were then mounted and analyzed as described for intracellular immunofluorescence staining (2.8.1).

2.8.3 Fluorescence resonance energy transfer (FRET) assay

2.8.3.1 Image acquisition

HeLa cells grown on coverslips were co-transfected with C-terminally tagged p14-EGFP (0.2 µg DNA) and N-terminally tagged Rab11-mCherry (0.2 µg DNA) constructs. Cells were fixed at 24 hpt with 3.7% formaldehyde, washed 3X with PBS and mounted directly on glass slides using ProLong Gold antifade reagent. Images were acquired with a Zeiss LSM 510 META confocal microscope in wide field mode using a 100X oil-immersion, 1.4 NA Plan Apochromat objective lens. Cells transfected with free EGFP, free mCherry, free EGFP and mCherry together, and EGFP linked to mCherry were used for microscope set up and controls. For a bimolecular FRET positive control, p14-EGFP and p14-mCherry were co-transfected as a known homomultimeric protein. Cells were also co-transfected with p14-EGFP/mCherry-Rab11-S25N and p14PA-EGFP/mCherry-Rab11 for FRET analysis. Cells co-transfected with free EGFP/mCherry-Rab11 and p14-EGFP/free mCherry were used as a FRET negative control. EGFP was excited using a 40 mW Argon laser at 488 nm, and mCherry was excited using a helium-neon (HeNe) 548 nm laser. The PixFRET plugin (Feige et al., 2005) for ImageJ was used to determine spectral bleed-through values and normalized FRET (NFRET) intensities for each pixel, as described below.

2.8.3.2 Spectral bleed-through determination

Donor and acceptor spectral bleed-through (SBT) values were visually minimized using free-EGFP- and free-mCherry-transfected cells, respectively, during image acquisition. Stacks of two images for each cell were captured for free-EGFP- and free-mCherry-transfected samples: a FRET image using donor excitation and acceptor emission lasers and filters, and a donor or acceptor image using the appropriate lasers and excitation

and emission filters. The SBT values were determined after background subtraction for each stack by selecting a background area in the image using PixFRET. The donor and acceptor SBT values were modeled with the ImageJ PixFRET plugin using an exponential relationship for fluorophore intensity after excluding background values at low fluorophore intensity and applying a Gaussian blur.

2.8.3.3 FRET normalization

After determination of SBT values, FRET intensities were determined for p14 and Rab11 interactions. A series of three images was acquired for each cell imaged: (1) donor image with donor excitation and donor emission; (2) acceptor image with acceptor excitation and acceptor emission; and (3) a FRET image with donor excitation and acceptor emission. Ten cells were imaged for each sample condition from two separate experiments (total of twenty cells imaged). Background subtraction and a Gaussian blur for donor, acceptor and FRET channels were performed on each image prior to FRET analysis. FRET intensities of each pixel were normalized by dividing the FRET-channel pixel intensity by the square-root of the product of the corresponding donor- and acceptor-channel pixels using equation:

$$NFRET = \frac{I_{FRET} - I_{EGFP} \times BT_{EGFP} - I_{mCherry} \times BT_{mCherry}}{\sqrt{I_{EGFP} \times I_{mCherry}}}$$

This normalization of FRET intensities allowed comparison between samples with differences in protein expression levels (Xia and Liu, 2001). NFRET images were converted to 8-bit images for histogram analysis to obtain mean NFRET values for individual cells.

2.8.4 Intracellular fluorescence microscopy

HeLa cells co-transfected with Akt-PH-GFP and p14-mCherry were fixed at 24 hpt with 3.7% formaldehyde, washed 3X with PBS and mounted on glass slides with ProLong gold antifade reagent. Images were acquired with a Zeiss LSM 510 META confocal microscope using a 63X oil-immersion objective lens.

2.9 p14 endodomain expression and purification

Bacterial expression plasmid pGEX-2T with the codon-optimized sequence for the p14 or p14PA endodomains was transformed into *E. coli* expression strain BL21 (DE3), plated on an LB agar medium containing ampicillin (100 μg/ml) and incubated overnight at 37°C. A single colony was used to inoculate a small volume of LB medium containing ampicillin for overnight growth, and this culture (1/100 dilution) was used to inoculate a large volume of LB medium containing ampicillin that was grown to an optical density (OD) of 0.6-0.8. Cells were then induced with 1 mM isopropyl-β-D-thiogalactopyranoside (IPTG) for protein expression for 3-4 h and pelleted at 6000 Xg for 15 min. Bacterial pellets were then processed for protein purification using Glutathione Sepharose 4B (GE healthcare) beads according to the manufacturer's instructions.

2.10 Protein-lipid overlay assay

Phosphatidylserine (PS), PI(3)P, PI(4)P, PI(3,4)P_2, PI(4,5)P_2, PI(3,5)P_2 and PI(3,4,5)P_3 (Avanti polar lipids, Alabaster, AL) were dissolved in chloroform and spotted on nitrocellulose membranes (GE Healthcare) at 3.13, 6.25, 12.50, 25, 50 or 100 pmol amounts using a Hamilton syringe (Hamilton, Reno, NV). Membranes were dried overnight and then blocked with 1% fatty acid free BSA (Fisher Scientific) in PBS for 30 min at room temperature, then incubated with 0.5 μg/ml of *E. coli*-expressed GST-tagged p14 or p14PA endodomain in blocking buffer for 1 h at room temperature. After 3X washes with PBS, membranes were incubated with α-p14 antiserum and subsequently with HRP-conjugated goat α-rabbit secondary antibody for 1 h each at room temperature. Membranes were washed 3X with PBS after each antibody incubation and developed as described in western blotting for protein expression analysis (2.6.1).

2.11 Statistics

Statistical analysis and sample comparison were performed using Prism software (GraphPad, San Diego, CA). Standard deviation (SD) values were calculated for averaging sample values within the experiment and standard error of the mean (SEM) values were calculated for averaging sample values between experiments. Groups of two samples were

analyzed with a paired two-tailed t-test, and groups of more than two samples were analyzed using ANOVA with a Tukey post-test.

CHAPTER 3
RESULTS

3.1 The p14 polybasic motif (PBM) is a novel autonomous tribasic Golgi export signal [subset of these data published in (Parmar et al., 2014b)]

3.1.1 The p14 PBM is required for p14 fusion activity and localization to the cell surface

All FAST proteins contain a cluster of membrane-proximal basic residues in the cytosolic C-terminal tail. Previous studies indicated the PBM of p10 is essential for fusogenic activity (Shmulevitz et al., 2003). However, the basis of this loss of function was not determined. The p14 PBM contains two tribasic clusters separated by an acidic residue (KRRERRR). To analyze the involvement of the PBM in p14-mediated cell-cell fusion, alanine substitutions of either tribasic cluster (constructs p14-KRR and p14-RRR), or both together (p14PA, Figure 3.1A) were created using site-directed mutagenesis. These constructs were transfected into QM5 cells and the extent of syncytia formation was determined by counting syncytial nuclei per microscopic field of Giemsa-stained monolayers (Figure 3.1B and C). p14-KRR and p14-RRR showed slight, but statistically significant, reductions in syncytiogenic activity compared to authentic p14 while p14PA failed to induce syncytium formation. All three p14 alanine mutants were expressed at approximately equivalent levels based on western blotting (Figure 3.1D), although p14PA was consistently expressed at slightly lower (~30% reduction) levels in multiple western blots. The modest reduction in p14PA expression was unlikely to explain the complete loss of fusion activity, and the decreases in fusion induced by the p14-KRR and p14-RRR constructs did not correlate with expression levels, suggesting the p14 PBM plays a role in fusion activity.

To determine the basis for the loss of p14PA fusion activity, cell surface expression of p14PA was determined by flow cytometry using p14 ectodomain antibody. Since p14 causes rapid syncytium formation commencing at 4 hour post-transfection (hpt) and large syncytia cannot be processed by flow cytometry, p14 ectodomain antibody was added to cells at 3 hpt to prevent syncytia formation, which allowed longer incubations to improve

detection and quantification of cell surface fluorescence. Replacement of three basic residues in the PBM (p14-KRR and p14-RRR) had no effect on p14 surface fluorescence (Figure 3.2C), indicating the slight reduction in syncytiogenesis (Figure 3.1C) is due to effects on fusion activity, not on trafficking. In contrast, replacement of all six basic residues in the PBM decreased p14 surface expression by >95% (Figure 3.2A and C). Flow cytometry analysis of immunostained, permeabilized cells indicated ~20% decrease in p14PA expression compared to wt p14 (Figure 3.2B and D), similar to the western blotting results (Figure 3.1D). Basic residues on the cytosolic side of the TMD can determine protein topology, according to the 'positive inside' rule (Nilsson et al., 2005; von Heijne, 1989). To determine whether the p14 PBM affects protein topology, p14 full-length antibody, which recognizes epitopes in the p14 cytoplasmic tail, was used to detect p14PA on the cell surface. Use of p14 full-length antibody also failed to detect p14PA on the cell surface (Figure 3.2E), indicating loss of the PBM did not result in plasma membrane trafficking of p14 in the reverse topology. These results indicate that the PBM is required for p14 plasma membrane localization.

3.1.2 The p14 PBM functions as a Golgi export signal

Since p14PA is expressed but not localized to cell surface, I determined its intracellular localization using immunofluorescence microscopy. Vero cells were used due to their flatter, uniform morphology and larger cytoplasm compared to QM5 cells, providing better visualization of intracellular compartments. Also, p14-G2A was used instead of wt p14. This myristoylation-minus mutant traffics to the cell surface with equal efficiency as wt p14 but is devoid of cell-cell fusion activity (Corcoran and Duncan, 2004), allowing for longer incubations post-transfection without the need to use of high concentrations of p14 antibody to block syncytium formation. p14-G2A showed a reticular staining pattern throughout cells that extended out to the cell periphery, characteristic of a membrane protein trafficking from the ER to the plasma membrane. p14-G2A also showed minimal colocalization with phosphatidylinositol 4-kinase IIIβ (PI4KIIIβ), a Golgi marker, with a Pearson's correlation coefficient (R) of 0.19 (Figure 3.3, top row). Values for R ranges from 1, which indicates a complete linear correlation for colocalization, to -1, which indicates a complete inverse correlation for colocalization, and values near 0 indicate no

correlation for colocalization (Dunn et al., 2011). In contrast, p14PA-G2A showed very faint cytoplasmic staining with no detectible staining at the cell periphery, and it strongly colocalized with PI4KIIIβ (R=0.55) and with the *trans*-Golgi marker TGN46 (R=0.70) (Figure 3.3). The absence of the PBM therefore results in p14 accumulation in the TGN and Golgi, and an inability to traffic to the plasma membrane.

Golgi accumulation of p14 in the absence of the PBM could be due to an inability of p14 to exit the Golgi, or rapid retrieval of p14 from the plasma membrane to the Golgi via the endocytic pathway. To differentiate these two possibilities, dynamin-dependent endocytosis was inhibited using dynasore, a small molecule inhibitor of dynamin. The transferrin receptor, which undergoes dynamin-dependent endocytic recycling, was used as a positive control for endocytosis inhibition by dynasore. Vector-transfected cells treated with dynasore showed a dramatic increase in cell surface binding of fluorescent transferrin (Figure 3.4B and D), indicating dynasore effectively inhibited dynamin-dependent endocytosis of transferrin receptor. Treatment with dynasore only marginally increased cell surface fluorescence of p14-G2A and had no effect on cell surface fluorescence of p14PA-G2A (Figure 3.4A and C), suggesting dynamin-dependent endocytosis did not contribute to the absence of p14PA on the plasma membrane. To determine whether dynamin-independent mechanisms promote p14PA endocytosis, transfected cells were incubated with p14 antibody at 37°C for 30 min before fixation, permeabilization and application of a fluorescent-secondary antibody. There was no evidence of p14PA presence on the cell surface or endocytic uptake of p14 antibody and Golgi accumulation (Figure 3.4E). Together, these results imply p14PA does not traffic to the plasma membrane, and that the PBM is a Golgi export signal not a plasma membrane retention signal.

3.1.3 The p14 PBM directs Golgi export of a heterologous protein

I wanted to determine whether the p14 PBM is sufficient for Golgi export of a heterologous protein, by transferring the p14 PBM into the cytosolic tail of a Golgi resident membrane protein. This heterologous protein should lack any Golgi resident signal that might compete with the Golgi export characteristics of the PBM. A previously described ERGIC-53 chimera, comprising the myc-tagged ERGIC-53 ectodomain, CD4 transmembrane domain and cytoplasmic domain with two arginine residues linked to a tail

with ten alanine residues, fulfilled these requirements. Replacement of the transmembrane domain and cytosolic tail of ERGIC-53 removes determinants that recycle ERGIC-53 between the ER and Golgi, resulting in accumulation in the Golgi in stably transfected MDCK cells (Gut et al., 1998). Addition of two glycosylation sites into the ERGIC-53 ectodomain promotes Golgi export of ERGIC-53 chimera to the plasma membrane. The two arginine residues in the cytoplasmic tail of the ERGIC-53 chimera were replaced with the p14 membrane-proximal cytoplasmic tail region containing the PBM (KYLQKRRERRRQ) or the alanine-mutated version of the PBM (KYLQAAAEAAAQ) (Figure 3.5A). The glycosylated ERGIC-53 chimera was used as a positive control for Golgi export.

All ERGIC-53 chimeric constructs were stably expressed in QM5 cells at approximately equivalent levels based on western blotting (Figure 3.5B). Cell surface analysis confirmed low levels of plasma membrane localization of the ERGIC-53 chimera (E-53), and a significant increase in the plasma membrane localization of the glycosylated ERGIC-53 chimera (Gly-E) (Figure 3.5C). Addition of the p14 PBM to the ERGIC-53 chimera (E-p14) resulted in equivalent levels of plasma membrane localization as Gly-E, while plasma membrane localization of the ERGIC-53 chimera with an alanine-substituted version of the PBM (E-PA) was significantly reduced relative to Gly-E and E-p14, and only moderately increased relative to E-53 (Figure 3.5C). These cell surface fluorescence results were confirmed by immunofluorescence microscopy of stably transfected Vero cells. Both E-53 and E-PA showed significant colocalization with the Golgi marker PI4KIIIβ (R=0.78 and 0.75, respectively) while Gly-E and E-p14 showed a reticular staining pattern throughout cells with apparent plasma membrane staining and limited Golgi co-localization (Figure 3.6). Based on Pearson's correlation coefficients, the PBM functioned as well or better than the glycosylation signals to mediate Golgi export (R=0.22 vs 0.57, respectively). The p14 PBM can therefore function as an autonomous Golgi export signal to promote plasma membrane trafficking of a heterologous protein.

3.1.4 The p14 PBM functions as a tribasic Golgi export signal

To characterize more precisely the Golgi export features of the p14 PBM, twelve additional polybasic mutants were generated by site-directed mutagenesis (Figure 3.7).

These mutants varied in the number, location and identity of basic residues in the PBM. When cell surface fluorescence of all fifteen p14 PBM mutants were rank ordered, there was a striking correlation between the number of basic residues in the PBM and plasma membrane localization (Figure 3.7). This correlation was largely independent of the location or identity of the basic residues within the PBM. Addition of one basic residue in the p14PA construct increased p14 surface expression from <5% to ~20%, addition of two basic residues in several locations in the PBM increased surface expression to ~40-60% of wt p14, and addition of three or more basic residues resulted in equivalent surface expression as wt p14 (Figure 3.7). Moreover, there was no correlation between the net charge of the PBM and plasma membrane localization, meaning the presence of the glutamic acid had no effect. Thus, Golgi export is dependent on the number of basic residues, not their identity or location or the net charge of the PBM.

All p14 polybasic mutants were expressed at variable levels that correlated with their number of basic residues. Steady-state expression levels of mutants with two or fewer basic residues in the PBM were reduced by ~40% compared to wt p14 (Figure 3.8A and B). Lower expression of these mutants is expected due to their accumulation in the Golgi, which presumably leads to some quantity of the protein being directed to lysosomes for degradation. However, there was no correlation between reduced expression and the levels of cell surface fluorescence. For example, mutants with one basic residue had the same level of expression but reduced cell surface expression compared to mutants with two basic residues (Figures 3.7 and 3.8). Mutants with three or more basic residues were expressed at the same level (Figure 3.8), and trafficked to the plasma membrane with equal efficiency (Figure 3.7), as wt p14. There was only one exception to this trend, the PA+K,R,R mutant, which has three basic residues but is not efficiently trafficked to the plasma membrane and showed decreased steady-state expression relative to wt p14 (Figures 3.7 and 3.8). The basis for this abnormality is unknown. This construct lacked the acidic residue separating the two tribasic clusters of the PBM, but other constructs (p14-RRE and p14-RER) lacking this acidic residue trafficked normally. However, this acidic residue was changed to a basic residue in PA+K,R,R, and this was the only mutant with three basic residues that did not contain adjacent basic residues, suggesting clustering of basic residues may influence the efficiency of this tribasic Golgi export signal.

The cell surface fluorescence results were confirmed by immunofluorescence microscopy of permeabilized cells using representative polybasic mutants in the p14-G2A backbone. As expected, p14PA-G2A colocalized extensively with the Golgi marker PI4KIIIβ (Figure 3.9). Addition of one basic residue to the PBM (PA+K-G2A) resulted in some diffuse cytoplasmic staining along with Golgi staining (Figure 3.9). Addition of two basic residues (PA+K,R-G2A) increased punctate, distributed cytoplasmic staining with reduced Golgi staining (Figure 3.9). Addition of three basic residues (p14-KRR-G2A) resulted in punctate staining throughout the cell with apparent plasma membrane staining and very little Golgi staining, a similar staining pattern as p14-G2A (Figure 3.9). These qualitative results were confirmed quantitatively by calculating Pearson's correlation coefficients, which showed a progressive decrease in colocalization of p14 with the Golgi marker with progressive addition of basic residues to the PBM (Figure 3.9). Efficient Golgi export of p14 is therefore dependent on the three basic residues in the PBM.

3.1.5 The p14 PBM might mediate interactions with phosphatidylinositol 3,4,5-triphosphate (PI(3,4,5)P_3) to promote p14 plasma membrane localization or fusion activity

Since Golgi export of p14 is dependent on the number of basic residues present in the juxtamembrane PBM, ionic interaction of the PBM with anionic lipids could potentially play a role in p14 trafficking to the plasma membrane. I conducted a series of preliminary experiments to test this hypothesis. The cytoplasmic tails of p14 and p14PA were GST-tagged and expressed and purified using *E. coli* and GST affinity chromatography. These purified GST-tagged p14 and p14PA endodomains were overlaid on nitrocellulose membranes spotted with various concentrations of different phosphatidylinositol phosphates (PIPs), and bound p14 endodomains were detected by immunoblotting. Phosphatidylserine (PS) was used as an anionic lipid control. Results indicated that only PI(3,4,5)P_3 interacted strongly with p14, and this interaction was substantially decreased for the p14PA cytoplasmic tail (Figure 3.10). Since PI(3,4,5)P_3 is concentrated in the plasma membrane, the protein-lipid overlay assay suggests PBM interactions with PI(3,4,5)P_3 could affect p14 plasma membrane localization or fusion activity. This speculation is supported by preliminary fluorescence-microscopy results using the GFP-

tagged PH domain of Akt, which binds to $PI(3,4,5)P_3$, co-expressed with mCherry-tagged p14 in HeLa cells to analyze their colocalization. Interestingly, in HeLa cells co-expressing these constructs, $PI(3,4,5)P_3$ strongly colocalized with p14 at the plasma membrane, particularly at sites of cell-cell adhesion (Figure 3.11). These results suggest the PBM might recruit or colocalize with $PI(3,4,5)P_3$ at cell-cell junctions, the sites of p14-mediated cell-cell fusion (Salsman et al., 2008), and that $PI(3,4,5)P_3$ might have a role during p14-mediated cell-cell fusion.

3.2 The p14 PBM exerts diverse effects on protein trafficking depending on membrane-proximity [subset of these data published in (Parmar et al., 2014a)]

3.2.1 Membrane-distal p14 PBM functions an ER retention signal

Previous studies indicate that the distance from the TMD of a dibasic ER export signal in a cytosolic tail can influence the function of this trafficking motif (Shikano and Li, 2003; Vincent et al., 1998). We sought to determine the effects of membrane-proximity on the trafficking functions of the p14 PBM. The p14 PBM was added to the C-terminus of the p14PA construct (p14PAextPB), where the PBM was separated by 68 residues from the TMD instead of four residues away as in wt p14 (Figure 3.12). Cell surface fluorescence analysis of this p14PAextPB construct indicated the membrane-distal PBM did not promote p14 trafficking to the plasma membrane (Figure 3.13A). To examine ER-to-Golgi trafficking, we introduced the V9T substitution mutation into p14 and p14PAextPB. Previous studies indicated that the V9T substitution mutation introduces a functional glycosylation site in p14 (Corcoran and Duncan, 2004). Flow cytometry analysis indicated p14-V9T traffics equally, if not slightly better, than authentic p14 to the plasma membrane (Figure 3.13B). Western blot analysis of QM5 cells transfected with p14-V9T detected two distinct bands for p14 (Figure 3.13C). Treatment of cell lysates with N-glycosidase F (PNGaseF), which cleaves both high mannose and N-linked carbohydrates from glycoproteins, confirmed that the slower migrating band was a glycosylated version of p14 (Figure 3.13C). The slower migrating p14 species was partially resistant to endoglycosidase H (endo H) treatment, which indicates sugar modifications in the Golgi complex to an endo H-resistant complex oligosaccharide (Figure 3.13C). In contrast, the

slower migrating species of p14PAextPB-V9T was completely sensitive to endo H treatment, indicating an inability to traffic to the Golgi complex (Figure 3.13C). Fluorescence microscopy of Vero cells transfected with p14PAextPB-V9T also indicated a reticular staining pattern throughout the cell without any colocalization with a Golgi marker, characteristic of an ER staining pattern (Figure 3.13D). These results suggested that the membrane-distal PBM can function as an ER retention signal.

Since glycosylation can contribute to protein sorting and trafficking (Gut et al., 1998), I sought to confirm these results in a non-glycosylated p14 construct. Therefore, p14PAextPB was created in a p14-G2A backbone. Western blots of QM5 cells transfected with p14PAextPB-G2A indicated approximately equal levels of protein expression to p14-G2A, and flow cytometry analysis confirmed that p14PAextPB-G2A was not expressed on the plasma membrane (data not shown). Furthermore, immunofluorescence microscopy of transfected Vero cells showed extensive colocalization of p14PAextPB-G2A with the ER marker PDI (protein disulfide isomerase) and limited colocalization with the Golgi marker PI4KIIIβ, in contrast to p14PA-G2A (same construct but lacking the C-terminal PBM) which showed intense colocalization with PI4KIIIβ but limited colocalization with PDI (Figure 3.14). These results clearly indicate that the C-terminal PBM can function as an ER retention signal.

3.2.2 Membrane-proximity dictates whether the p14 PBM can function as a sorting signal

To further examine effects of membrane proximity on PBM function, the PBM was inserted at internal locations in the endodomains of p14-G2A and p14PA-G2A (Figure 3.12). Flow cytometry analysis indicated that the PBM, when inserted 17 (p14PA/75PB-G2A) or 34 (p14PA/92PB-G2A) residues downstream of the TMD, was not able on its own to promote p14 trafficking to the plasma membrane (Figure 3.15A). Similarly, an internal PBM did not interfere with plasma membrane localization of p14-G2A (constructs p14/75PB-G2A and p14/92PB-G2A), which retains the normal membrane-proximal PBM in addition to the extra internal PBM (Figure 3.15A). All these constructs were expressed at approximately equivalent levels based on western blotting (Figure 3.15B). Fluorescence microscopy results indicated that both p14PA/75PB-G2A and p14PA/92PB-G2A intensely

colocalized with the Golgi marker PI4KIIIβ while minimally colocalizing with the ER marker PDI, a similar staining pattern as p14PA-G2A (Figure 3.16). The p14/75PB-G2A and p14/92PB-G2A constructs showed diffuse staining throughout the cytoplasm radiating out to the cell periphery, a similar staining pattern as p14-G2A (Figure 3.17). Thus, the PBM at an internal position in the endodomain does not promote Golgi export of p14PA nor interfere with plasma membrane localization of p14.

3.2.3 A membrane-distal PBM functions as an ER retrieval signal that dominates over a membrane-proximal PBM Golgi export signal

Results indicated that a membrane-proximal PBM is a Golgi export signal while a membrane-distal PBM functions as an ER retention signal. To analyze how p14 trafficking is effected by the presence of both membrane-proximal and membrane-distal PBMs, the PBM was added to the C-terminus of p14-V9T (Figure 3.12). Flow cytometry analysis of p14extPB-V9T indicated this mutant was not expressed on the plasma membrane (Figure 3.18A). As shown previously (Figure 3.13C), endo H assays confirmed that the slower migrating species of p14-V9T was partially resistant to endo H (Figure 3.18B). As expected, the glycosylated form of p14PA-V9T was also partially resistant to endo H (Figure 3.18B). Interestingly, the slower migrating, glycosylated species of p14extPB-V9T was also partially resistant to endo H (Figure 3.18B), indicating this mutant was trafficked to the Golgi complex. Surprisingly, fluorescence microscopy of Vero cells transfected with p14extPB-V9T showed extensive colocalization with the ER marker PDI and no apparent colocalization with the Golgi marker PI4KIIIβ (Figure 3.19). These results indicate that the membrane-distal PBM can also function as an ER retrieval signal that dominates over the Golgi export function of a membrane-proximal PBM.

3.2.4 Conflicting ER retrieval and Golgi export signals induce ER tubulation and segregation

Interestingly, the ER staining pattern in the p14extPB-V9T expressing cells appeared extensively tubular compared to the punctate ER staining in non-transfected cells in the same field of view (Figure 3.19). The Golgi staining pattern was indistinguishable in non-transfected cells or cells transfected with p14extPB. To examine this tubular ER

phenotype more closely, the KDEL ER marker, which is an antibody raised against ER membrane protein KDEL receptor, was used in addition to PDI to stain the ER in p14-V9T or p14extPB-V9T transfected cells. Fluorescence microscopy images indicated punctate ER staining throughout the cell for p14-V9T transfected cells with PDI and KDEL markers (Figure 3.20). In contrast, the PDI marker showed an extensive tubular ER appearance with extensive colocalization with p14extPB-V9T. Moreover, the KDEL staining pattern was dramatically changed compare to p14-V9T with a limited number of perinuclear aggregates and limited colocalization with p14extPB-V9T (Figure 3.20). Thus, conflicting trafficking signals can have dramatic effects on ER morphology.

3.3 The PBM directs interaction with activated Rab11 for p14 sorting into AP1-coated vesicles and Golgi-plasma membrane transport.

3.3.1 Rab11 is required for p14 plasma membrane localization

I sought to define the pathway for p14 transport by determining which cellular proteins and trans-factors mediate p14 trafficking to the plasma membrane. A yeast two-hybrid screen performed by Julie Boutilier (Dalhousie University), using the p14 cytoplasmic endodomain as bait, identified Rab11A as an interaction partner. To determine whether Rab11 has any importance in p14 trafficking to plasma membrane, I knocked down Rab11A function in p14-G2A-transfected HeLa cells by overexpressing a dominant-negative mutant, Rab11A-S25N. Analysis of p14 surface expression by flow cytometry using the p14 ectodomain antiserum indicated overexpression of Rab11A-S25N significantly reduced p14-G2A surface expression, while overexpression of wt Rab11A or a constitutively active Rab11A-Q70L mutant had no effect on p14 trafficking to the plasma membrane (Figure 3.21A). Western blots confirmed overexpression of Rab11A, Rab11A-S25N and Rab11A-Q70L (Figures 3.21C and 3.22A).

To confirm the Rab11A dominant-negative results, Rab11 was knocked down using siRNA against Rab11A and Rab11B, either individually or in combination. Knockdown of either Rab11A or Rab11B decreased p14 surface expression in HeLa cells, with a combined knockdown exerting the strongest effect (Figure 3.21B). Westerns blots confirmed knockdown of Rab11A (Figures 3.21D and 3.22B), and the extent of

knockdown approximated the relative effects on p14 plasma membrane expression. Thus, both Rab11 isoforms exert effects on p14 plasma membrane trafficking.

To determine whether the Rab11 results are specific, Rab5 and a Rab5 dominant-negative mutant, Rab5-S34N, were overexpressed in HeLa cells. Overexpression of Rab5 or Rab5-S34N had no effect on p14 surface expression (Figure 3.23A). To confirm that Rab5 function was inhibited by Rab5-S34N, a transferrin-binding assay was performed. Rab5 mediates endocytosis and inhibiting Rab5 function increases the levels of transferrin receptor on the cell surface (Somsel Rodman and Wandinger-Ness, 2000). As expected, transferrin surface binding was significantly increased by overexpression of Rab5-S34N (Figure 3.23B), indicating Rab5-S34N was capable of inhibiting wt Rab5 activity. Hence, Rab11, but not Rab5, plays a role in p14 plasma membrane trafficking.

3.3.2 The PBM is required for p14 colocalization with Rab11

To examine more closely the relationship between Rab11 and p14 trafficking, fluorescence microscopy was performed on HeLa cells transfected with p14-G2A or p14PA-G2A using antibodies against p14 and Rab11A. As shown in Figure 3.24, p14-G2A showed extensive colocalization with Rab11A in the perinuclear region. Comparing cells expressing p14 to those with undetectable p14 expression in the same field of view, it also appeared that p14 resulted in Rab11 redistribution and accumulation in the perinuclear region (Figure 3.24A). In contrast, p14PA-G2A showed minimal colocalization with Rab11 and did not appear to have a pronounced effect on Rab11 redistribution in cells (Figure 3.24A). These qualitative results were confirmed quantitatively by calculating Pearson's correlation coefficients for p14 and Rab11 colocalization in ten cells each from two independent experiments (Figure 3.24B). These results suggested p14 recruits Rab11A to the perinuclear region in a PBM-dependent manner.

3.3.3 Activated Rab11 directly interacts with p14 in a PBM-dependent manner

To determine whether Rab11 interacts with p14, co-immunoprecipitation (co-IP) assays were performed using HEK cells, a human cell line with good transfection efficiencies. Cell lysates expressing p14-G2A or p14PA-G2A were immunoprecipitated with α-Rab11A antibody and western blots probed with α-p14 antiserum. The co-IP results

indicated that p14-G2A co-immunoprecipitates with Rab11A (Figure 3.25). The specificity of the co-immunoprecipitation was confirmed using a heterologous IgG antibody, which showed only low level co-precipitation of p14 (Figure 3.25). Notably, co-immunoprecipitation of p14PA-G2A was substantially reduced relative to p14-G2A, to the low levels observed using control IgG. These data suggest that p14 interacts with Rab11 in a PBM-dependent manner.

Since Rab11 is a GTPase that is active when bound to GTP and inactive when bound to GDP, I sought to analyze which form of Rab11 interacts with p14. Co-IP assays were performed following addition of GTPγS (a non-hydrolysable analogue of GTP) or GDP to cell lysates expressing p14-G2A or p14PA-G2A. The presence of GTPγS resulted in a substantial increase in the amount of p14 that co-precipitated with Rab11 compared to lysates containing GDP (Figure 3.25), suggesting p14 interacts preferentially with the active form of Rab11A. No such increase in co-precipitation of p14PA-G2A was observed in the presence of GTPγS, which still co-precipitated with Rab11 at levels equivalent to the IgG control (Figure 3.25). The PBM of p14 therefore promotes interaction with activated Rab11.

Aliquots of cell lysates were taken before performing co-IPs to confirm equal protein input using α-p14 antiserum, and α-Rab11A and α-actin antibodies (Figure 3.25). Surprisingly, distinct double bands were observed for p14PA-G2A, which were not present in p14-G2A samples and were not previously observed when analyzing p14PA or p14PA-G2A (see Figures 3.1D and 3.15B). In previous western blots of transfected cells expressing p14PA or p14PA-G2A , cells were QM5 cells and were harvested at 8 hpt verses HEK cells harvested at 24 h in Figure 3.25. The prominent lower band for p14PA in HEK cells could therefore be a cell-type specific effect, or possibly time-dependent cleavage or degradation of p14PA. The latter was confirmed by comparison of HEK cells transfected with p14PA or p14PA-G2A and harvested at 8 or 24 hpt for western blotting. As shown in Figure 3.26, the lower band increases in intensity and becomes prominent with longer incubation times in the p14PA and p14PA-G2A samples. A small percent of p14 is processed to generate soluble endodomain that is detectable at 12 hpt but not at 8 hpt (Top et al., 2009). Abnormal Golgi accumulation of p14PA somehow may enhance the percent

of p14 being processed to generate soluble endodomain that may represent the lower prominent band with longer incubations.

To analyze whether the interaction between p14 and Rab11 is direct and occurs inside cells, I developed a fluorescence resonance energy transfer (FRET) protocol using fluorescently-tagged p14 and Rab11 proteins. FRET analysis detects protein-protein interactions that occur over a distance of <5-10 nm, the distance of stable protein-protein interactions (Sekar and Periasamy, 2003). EGFP was added to the C-terminus of p14 or p14PA, and mCherry was added to the N-terminus of Rab11A or Rab11A-S25N. Fluorescently-tagged Rab11 does not alter its endogenous cellular localization pattern (Rzomp et al., 2003), and EGFP-tagged p14 still traffics to the plasma membrane and retains fusion activity, albeit at a reduced efficiency (Timothy Key, Dalhousie University, personal communication). Donor and acceptor spectral bleed-through (SBT) values and normalized FRET (NFRET) intensities were determined using the PixFRET plugin for ImageJ (Feige et al., 2005), as described in detail in Materials and Methods. Mean NFRET intensities were obtained from ten cells each from two independent experiments for quantitative measurements (Figure 3.27B). Cells co-transfected with p14 tagged with EGFP (p14-EGFP) and mCherry (p14-mCh) were used as a positive control (Figure 3.27), as previous studies indicated p14 forms homomultimers that are detectible by FRET inside cells (Ciechonska et al., 2014; Corcoran et al., 2011; Key and Duncan, 2014). For negative controls, cells co-transfected with free EGFP and mCherry-Rab11, and p14-EGFP and free mCherry were used that provided no FRET signals (Figure 3.28). Cells co-transfected with mCherry-Rab11A and p14-EGFP emitted FRET signals at the same level as p14-EGFP and p14-mCherry homomultimers (Figure 3.27). In contrast, cells transfected with mCherry-Rab11A-S25N and p14-EGFP failed to provide any FRET signals above background (Figure 3.27). Moreover, cells transfected with mCherry-Rab11A and p14PA-EGFP also failed to provide any FRET signals (Figure 3.27) indicating that the p14 PBM is required for p14 interaction with Rab11. These *in cellula* results confirmed that p14 interacts with activated Rab11 in a PBM-dependent manner, and the distance restraints of FRET imply these two proteins interact directly with each other.

3.3.4 Rab11 knockdown results in p14 accumulation in the Golgi

Rab11 knockdown inhibits p14 plasma membrane localization (Figure 3.21), but does this reflect a role for Rab11 in p14 Golgi export or does Rab11 mediate post-Golgi p14 trafficking through the endosomal recycling pathway? To address this question, I examined p14 subcellular localization in Rab11 knockdown cells. Confocal microscopy of HeLa cells transfected with control siRNA and p14-G2A showed the characteristic reticular staining pattern for p14 with minimal colocalization with the PI4KIIIβ Golgi marker (Figure 3.29A). In contrast, cells transfected with Rab11 siRNA and p14-G2A showed concentrated perinuclear staining with extensive colocalization between p14 and PI4KIIIβ that approached the level of colocalization observed between p14PA-G2A and PI4KIIIβ (Figure 3.29). These results suggest that Rab11 mediates PBM-dependent p14 trafficking from the Golgi to the plasma membrane.

3.3.5 AP1 knockdown leads to Golgi accumulation of p14

Vesicle trafficking between the Golgi, plasma membrane, and lysosomal and endosomal compartments requires one of several adaptor proteins (APs) that are part of the vesicle coats. Among various AP complexes, AP1, AP3 and AP4 are known to mediate trafficking from the Golgi to endosomes or plasma membrane (Ohno, 2006; Popova et al., 2013). To determine which of these AP complexes mediates p14 plasma membrane trafficking, siRNAs targeting the gamma, delta or epsilon subunits were used to knockdown AP1, AP3 or AP4 complexes, respectively. Knockdown of the AP1γ, AP3δ and AP4ε adaptor complex subunits was confirmed by western blotting (Figures 3.30B and 3.31). Only AP1 knockdown resulted in a significant decrease (>50%) in p14-G2A plasma membrane expression as analyzed by flow cytometry (Figure 3.30A). When examined by immunofluorescence confocal microscopy and quantified by Pearson's correlation coefficients, RNAi-mediated knockdown of AP1 (but not AP3 or AP4) resulted in extensive p14 colocalization with the Golgi marker PI4KIIIβ (Figure 3.32). As with p14PA-G2A (Figure 3.29), AP1 knockdown resulted in concentrated co-localization of p14-G2A with the Golgi complex (Figure 3.32). These results imply that p14 trafficking between the Golgi and plasma membrane is mediated by AP1-coated vesicles.

3.3.6 p14 colocalizes with AP1 and Rab11 at the *trans*-Golgi network (TGN)

Knockdown of either Rab11 or AP1 results in p14 accumulation in the Golgi, suggesting both likely mediate p14 trafficking from the Golgi to the plasma membrane. However, it was possible that Rab11 and AP1 might mediate p14 transport from a post-Golgi endosomal compartment to the plasma membrane, with knockdown of Rab11 or AP1 resulting in p14 retrieval back to the Golgi. To address this issue, HeLa cells transfected with p14-G2A were triple-stained with antibodies against p14, TGN46, and Rab11 or AP1. Confocal microscopy images showed obvious colocalization of p14 with Rab11 and AP1 at the TGN (Figure 3.33). Taken together, the above results imply that Rab11 and AP1 mediate p14 biosynthetic anterograde traffic from the Golgi to the plasma membrane.

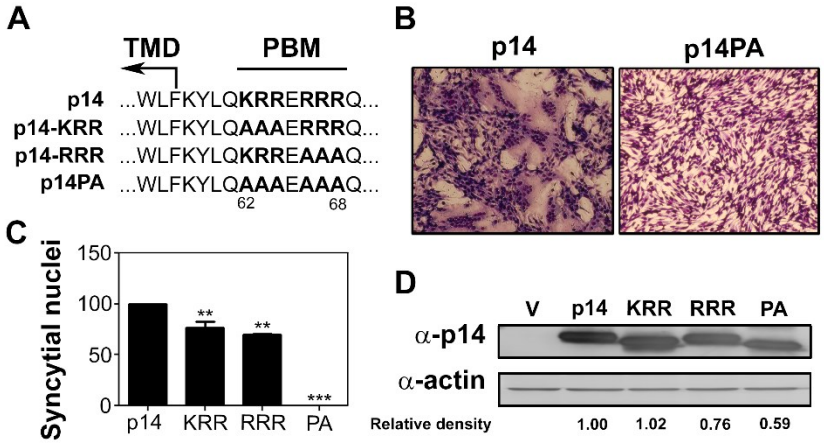

Figure 3.1: The p14 PBM is required for cell–cell fusion. (A) Amino acid sequence of the p14 PBM and the indicated polybasic mutants. Numbers indicate residue position in p14. Boundary of the TMD and location of the PBM are indicated. **(B)** QM5 cells transfected with wt p14 or p14PA were Giemsa-stained at 8 hpt and imaged by bright-field microscopy at 200X magnification. **(C)** QM5 cells transfected with p14 or the indicated polybasic mutants (p14-KRR [KRR], p14-RRR [RRR], or p14PA [PA]) were imaged as in panel B, and syncytial nuclei were quantified from five random fields. Results are mean number of syncytial nuclei ± SEM from two independent experiments performed in triplicate. Statistical significance is indicated relative to p14 (**$p < 0.01$; ***$p < 0.005$). **(D)** Lysates of QM5 cells transfected with the indicated p14 constructs as in panel C were processed for western blotting at 8 hpt using α-p14 or α-actin antibody. Numbers at the bottom indicate relative band intensity normalized to wt p14.

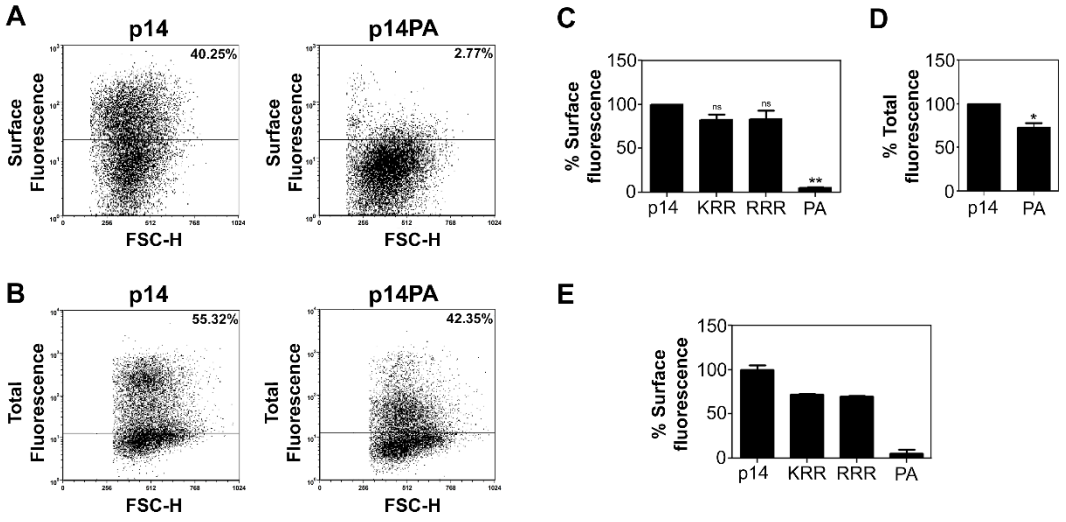

Figure 3.2: The PBM is required for p14 surface expression. (A) QM5 cells transfected with p14 or p14PA were surface-labeled using α-p14 ectodomain antiserum and Alexa 647–conjugated secondary antibody, fixed, and analyzed by flow cytometry. Percent cell surface fluorescence is indicated after background subtraction of empty vector-transfected cells and was determined from scatter plots of relative fluorescence vs. forward scatter (FSC) using the indicated gating (horizontal line). **(B)** QM5 cells transfected with p14-G2A or p14PA-G2A were fixed and permeabilized in suspension at 24 hpt. Cells were stained with full-length α-p14 antiserum, which recognizes both the N-terminal ectodomain and C-terminal endodomain, and Alexa 647–conjugated secondary antibody. Scatter plots and percentage cell surface fluorescence are shown as in panel A. **(C)** Surface fluorescence of QM5 cells transfected with the indicated p14 constructs was quantified as in panel A. Results are mean percent cell surface fluorescence ± SEM relative to wt p14 from two independent experiments performed in triplicate. Statistical significance is indicated relative to wt p14 (**$p < 0.01$; ns, not significant). **(D)** As in panel C, except cells were permeabilized before immunostaining to detect total fluorescence of QM5 cells transfected with p14-G2A and p14PA-G2A. Results are mean percent cell fluorescence ± SEM from three independent experiments performed in triplicate. Statistical significance is indicated relative to wt p14 (*$p < 0.05$). **(E)** As in panel C, except cells were stained with an anti-p14 antiserum that recognizes both the N-terminal ectodomain and C-terminal endodomain. Results are mean percent cell surface fluorescence ± SD relative to wt p14 for triplicate samples from a single experiment.

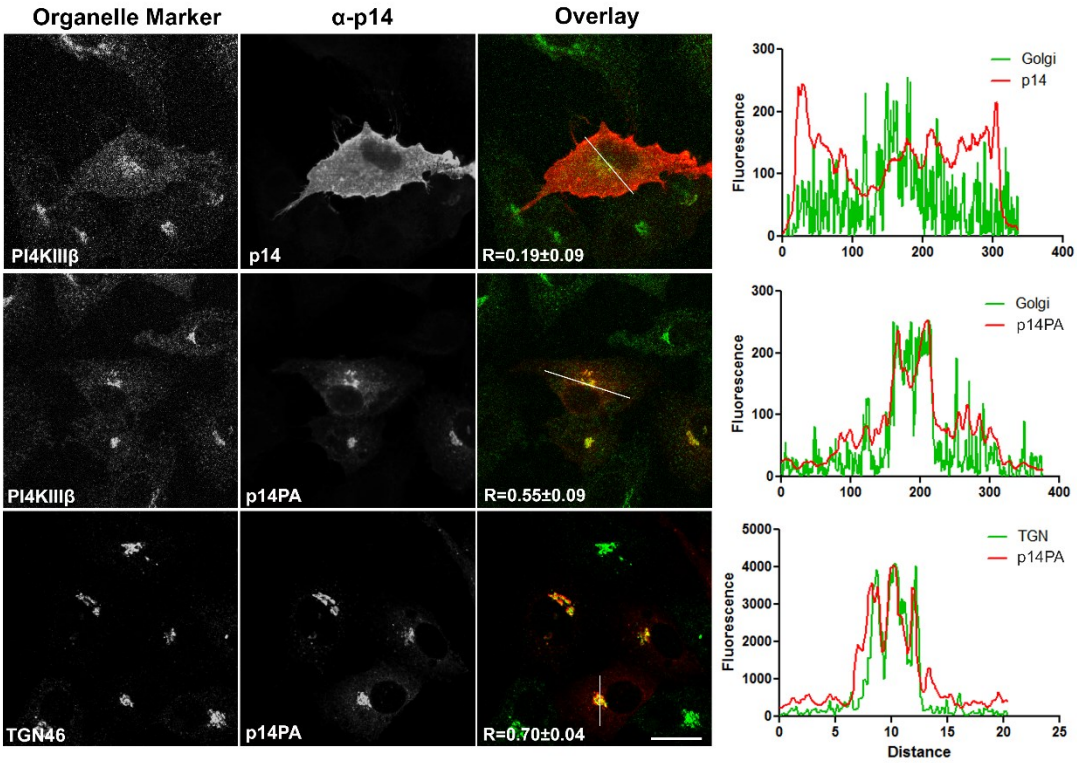

Figure 3.3: Absence of the PBM concentrates p14 in the Golgi complex. Vero cells transfected with p14-G2A or p14PA-G2A were fixed and immunostained at 24 hpt using α-p14 antiserum (red) and the indicated organelle markers (green) for the Golgi complex (PI4KIIIβ) and TGN (TGN46). Right column shows merged images. Scale bars, 20μm. Graphs show relative fluorescence intensities for organelle markers and p14 imaged along the white line in the corresponding merged images. Pearson's correlation coefficients (R) are shown as the mean ± SEM from 10 cells (from two independent experiments) and are indicated on the merged images. Images in the top two rows provided by Christopher Barry (Dalhousie University).

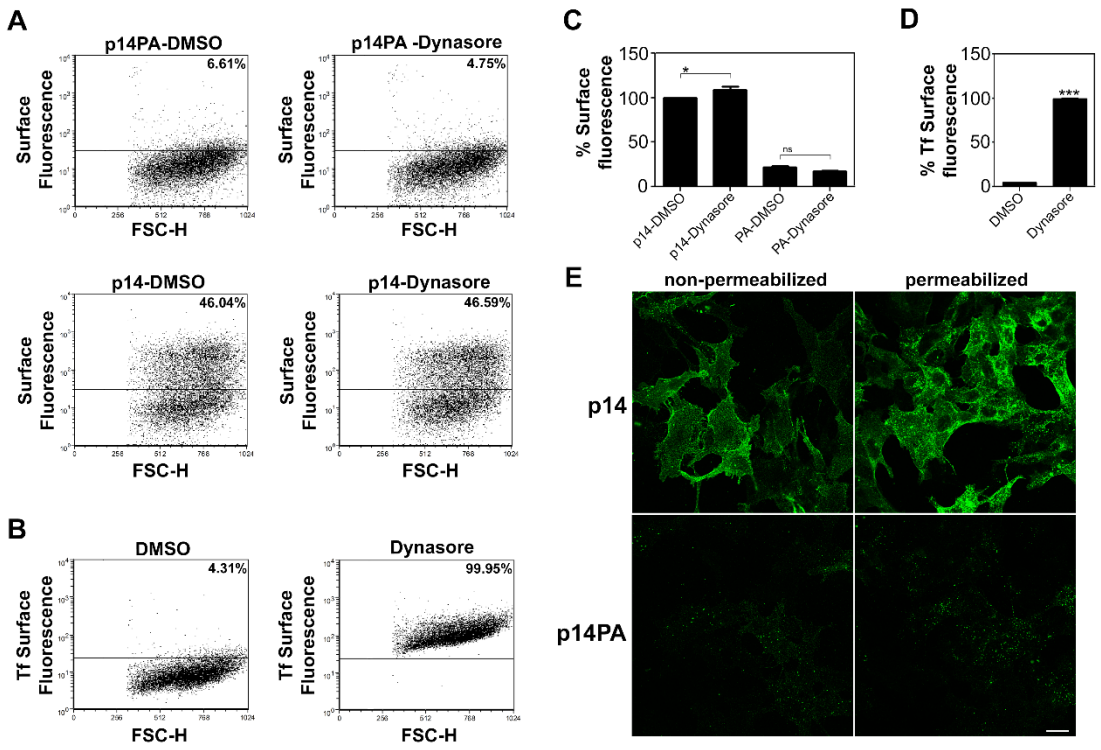

Figure 3.4: Endocytic pathways do not influence plasma membrane localization of p14PA. (A) QM5 cells transfected with p14-G2A (bottom row) or p14PA-G2A (top row) were treated for 1 h in serum-free medium with the dynamin inhibitor dynasore (80 μM) or DMSO at 24 hpt, live cells were stained with α-p14 ectodomain antiserum and Alexa Fluor 647–conjugated secondary antibody, and cell surface fluorescence was analyzed by flow cytometry. Percent cell surface fluorescence is indicated as in Figure 3.2A. **(B)** Vector-transfected QM5 cells were treated with DMSO or dynasore as in panel A. Live cells were stained using Alexa Fluor 555–conjugated transferrin and analyzed by flow cytometry to detect surface-bound transferrin. Percent cell surface fluorescence is indicated as in Figure 3.2A. **(C)** Surface fluorescence of QM5 cells transfected with p14-G2A or p14PA-G2A quantified as in panel A. Mean percent cell surface fluorescence ± SEM from three independent experiments performed in triplicate. Statistical significance is shown between the indicated paired samples (*$p < 0.05$; ns, not significant). **(D)** Transferrin receptor cell surface fluorescence quantified as in panel B. Mean percent cell surface fluorescence ± SEM from three independent experiments performed in triplicate (***$p < 0.005$). **(E)** Vero cells transfected with p14-G2A or p14PA-G2A were incubated with α-p14 antiserum at 24 hpt for 30 min at 37°C. Cells were then fixed and stained with Alexa Fluor 488-conjugated antibody with (permeabilized) or without (non-permeabilized) prior Triton X-100 treatment. Scale bar, 20 μm.

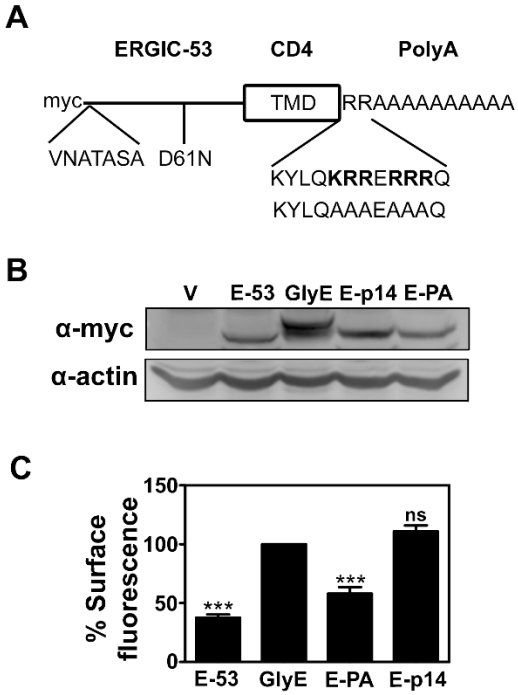

Figure 3.5: p14 PBM traffics a Golgi-resident protein to the plasma membrane. (A) Schematic diagram of the N-terminally myc-tagged chimeric ERGIC-53 protein containing the ERGIC-53 ectodomain, CD4 TMD, and polyalanine (polyA) cytoplasmic tail. The glycosylated ERGIC-53 chimera has two glycosylation sites (VNATASA and D61N) introduced into the ectodomain. The ERGIC-p14 and ERGIC-p14PA constructs replace the two membrane-proximal endodomain arginine residues in the parental ERGIC-53 chimera with the membrane-proximal p14 sequence containing the PBM (KYLQKRRERRRQ) or the Ala-substituted version of this motif (KYLQAAAEAAAQ). **(B**) QM5 cells stably transfected with empty vector (V), parental ERGIC-53 chimera (E-53), glycosylated ERGIC-53 chimera (GlyE), ERGIC-53 with the p14 PBM (E-p14) or the Ala-substituted PBM (E-PA) were processed for western blotting using α-myc or α-actin antibody. **(C)** As in panel B, except QM5 cells transfected with the indicated chimeric ERGIC-53 constructs were processed for flow cytometry after live-cell staining with α-myc antibody and Alexa 647–conjugated secondary antibodies. Mean percent cell surface fluorescence relative to GlyE transduced cells ± SEM from triplicate samples was calculated from three independent experiments. Statistical significance is indicated relative to GlyE (*$p < 0.05$; ***$p < 0.005$).

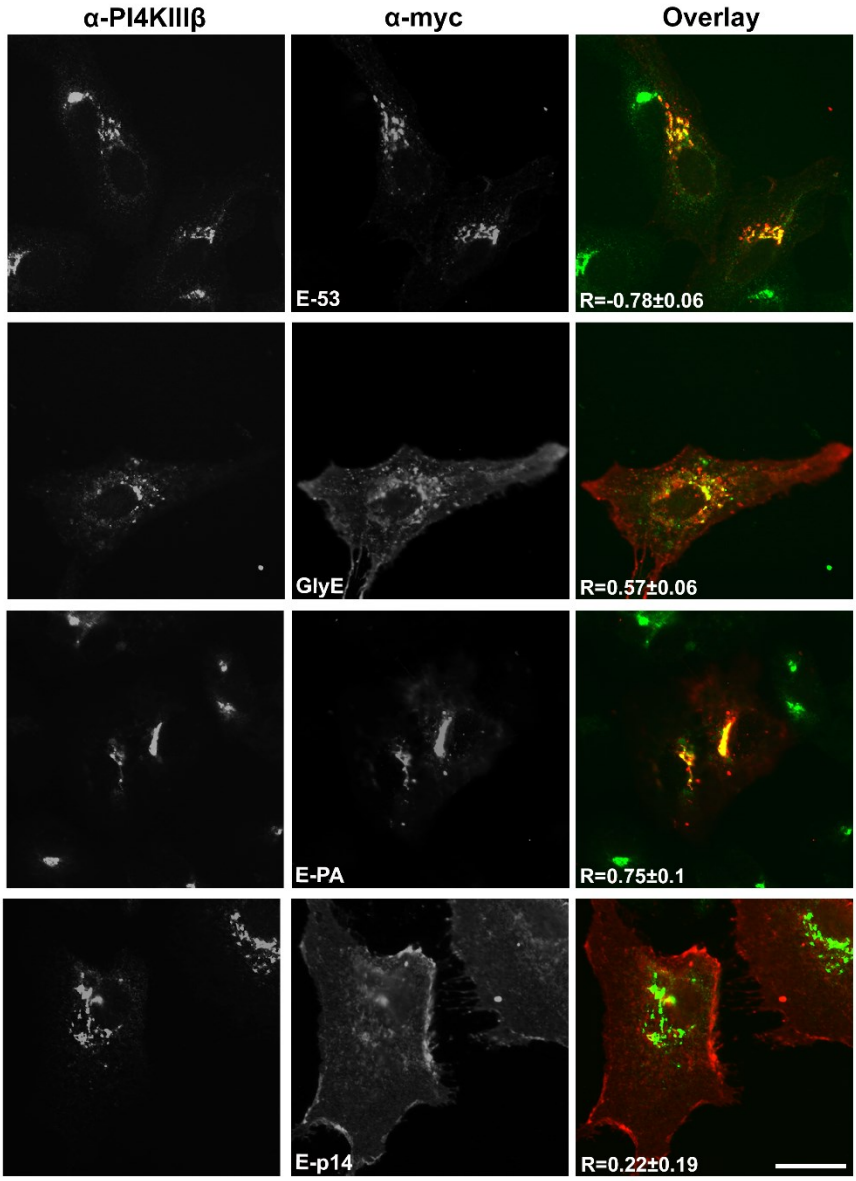

Figure 3.6: The p14 PBM is sufficient to function as a Golgi export signal. Vero cells transfected with the indicated chimeric ERGIC-53 constructs as in Figure 3.5 were immunostained with α-myc antibody (red) and the PI4KIIIβ Golgi marker (green). Right column shows merged images. Pearson's correlation coefficients (R) are shown in the merged images of each construct as the mean ± SEM from nine cells (from two independent experiments). Scale bars, 20 μm.

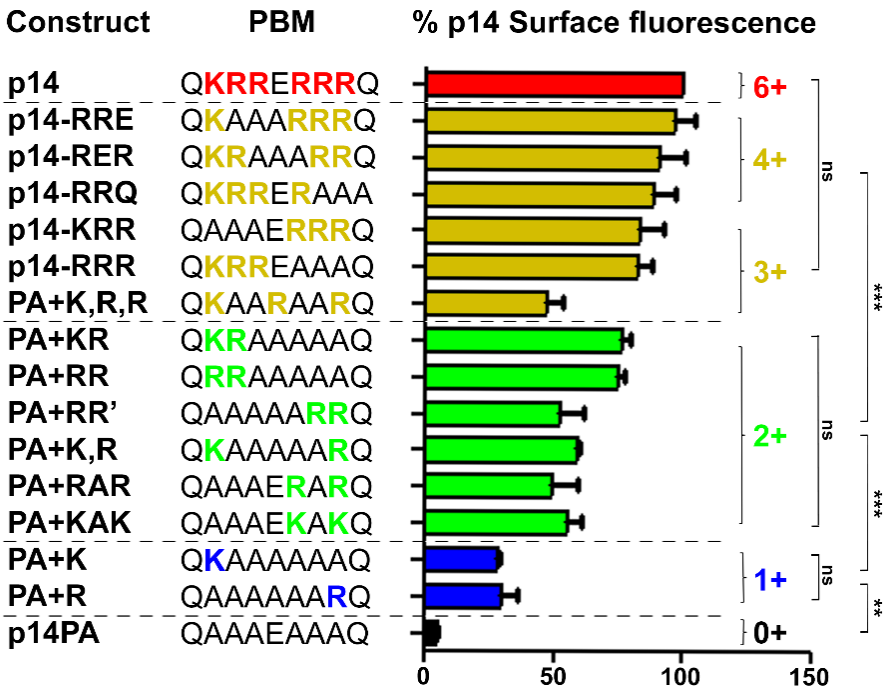

Figure 3.7: Three basic residues are required for maximal p14 cell surface expression. Amino acid sequences of the p14 PBM and the indicated polybasic mutants are shown on the left. The number of positive residues in the PBM are color coded and indicated. Cell surface fluorescence of QM5 cells transfected with the indicated p14 constructs was quantified by flow cytometry as described in Figure 3.2A. Results are mean percent cell surface fluorescence ± SEM relative to wt p14, after background subtraction of empty vector-transfected cells, from three or more independent experiments performed in triplicate. Numbers on the right indicate the number of positive residues present within respective groups of PBMs. One-way ANOVA indicated no significant difference (ns) between constructs sharing the same number of basic residues (except for PA+K,R,R in the 3+ group). Statistical significance is indicated between groups (**$p < 0.01$; ***$p < 0.005$).

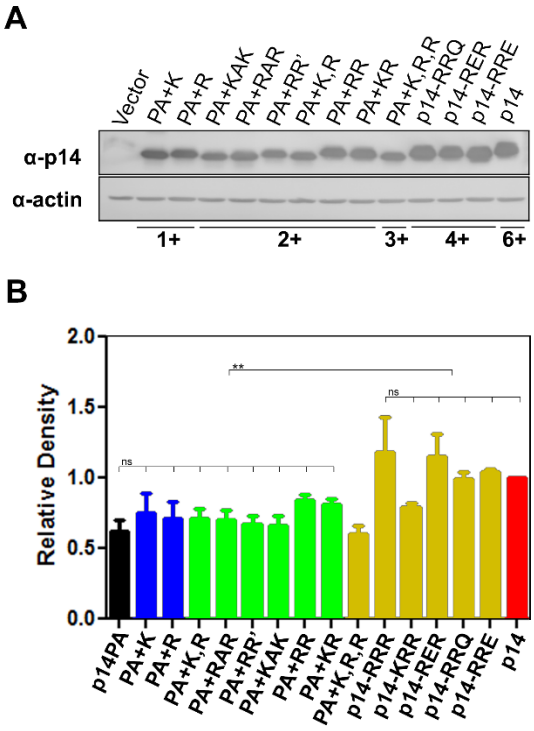

Figure 3.8: Quantification of steady-state p14 expression levels by western blotting. **(A)** QM5 cells transfected with the indicated p14 constructs were harvested at 8 hpt and processed for western blotting using α-p14 antiserum or α-actin antibody. Numbers at the bottom indicate the number of positive residues present in the PBM. **(B)** Western blots from three independent experiments obtained as in panel A were quantified by ImageJ, and results are presented as band density ± SEM normalized to wt p14. Statistical significance was determined using one-way ANOVA on the indicated subgroups (ns, not significant; ** $p<0.01$).

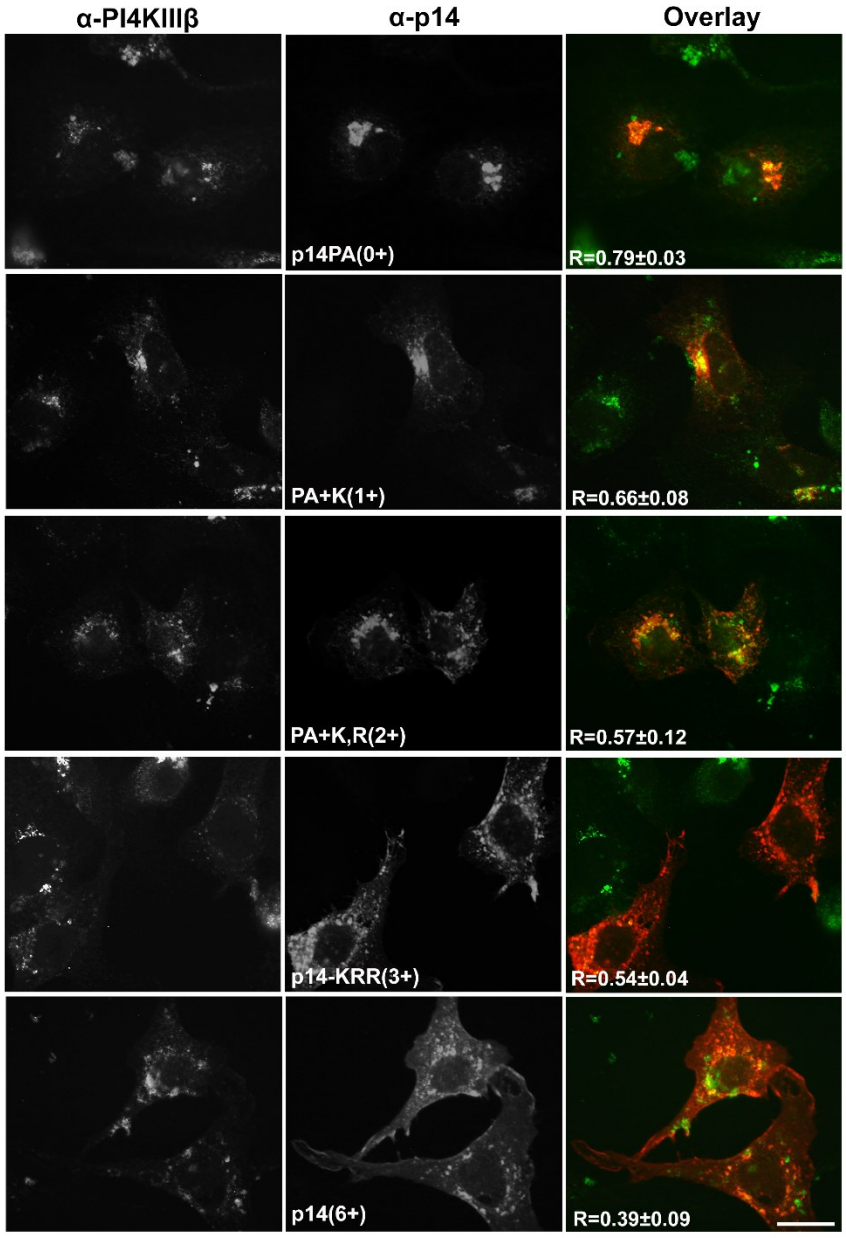

Figure 3.9: Basic residues have an additive effect on p14 Golgi export. Vero cells transfected with p14-G2A and the indicated p14-G2A polybasic mutants were immunostained with α-p14 antiserum (red) and the PI4KIIIβ Golgi marker (green) at 24 hpt. Right column shows merged images. Pearson's correlation coefficients (R) for each construct were calculated from five transfected cells and are shown as mean ± SD on the merged images. Scale bar, 20 μm.

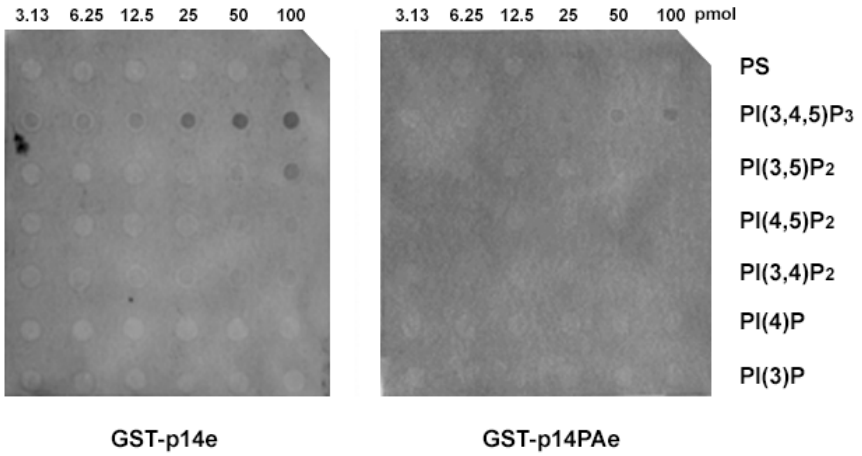

Figure 3.10: Preferential interaction of the p14 endodomain with PI(3,4,5)P_3 is dependent on the PBM. The cytoplasmic endodomains of p14 (GST-p14e) or p14PA (GST-p14PAe) tagged with glutathione S-transferase (GST) were expressed in *E. coli* and incubated with nitrocellulose membranes spotted with the indicated concentrations of various phosphatidylinositol lipids or phosphatidylserine (PS). Membranes were developed using α-p14 antiserum and HRP-conjugated secondary antibody.

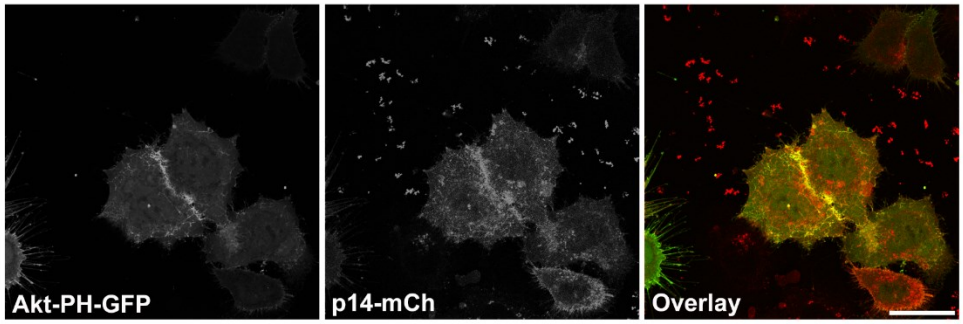

Figure 3.11: PI(3,4,5)P_3 colocalizes with p14 at the plasma membrane in regions of cell-cell contact. HeLa cells co-transfected with Akt-PH-GFP (green) (PH domain that binds to PI(3,4,5)P_3) and p14 tagged with mCherry (red) (p14-mCh) were fixed at 24 hpt and imaged by confocal microscopy. Right column shows merged images. Scale bar, 20 μm.

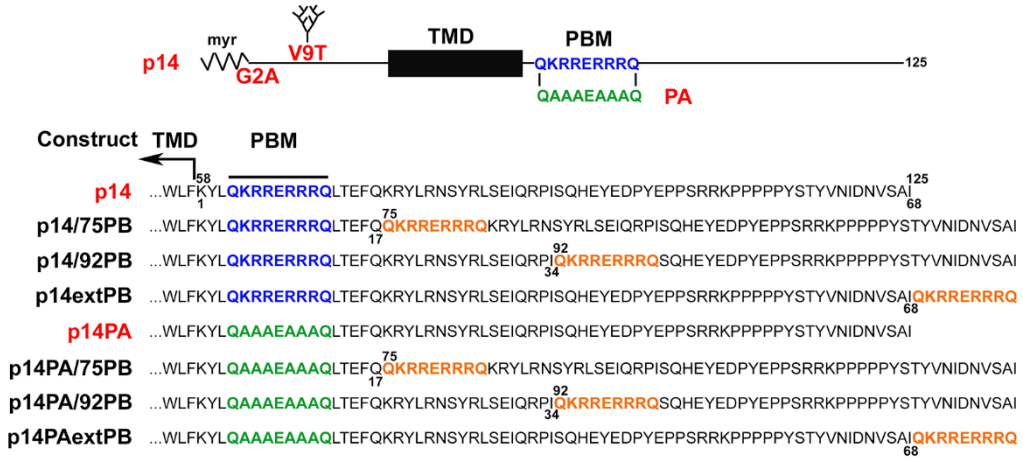

Figure 3.12: Motif arrangements in p14 and mutated p14 constructs. The top panel depicts motif arrangements in the full-length, 125-residue p14 protein, including N-terminal myristoylation (myr), transmembrane domain (TMD) and PBM. The sequence of the PBM and the polyalanine substitution (PA) of this motif are shown. G2A and V9T are the locations of point substitutions that eliminate the myristoylation motif (G2A) or introduce an N-linked glycosylation site (V9T), depicted as a branched tree. These p14 backbones (wt p14, p14PA, p14-G2A, and p14-V9T) were used as templates for insertion of PBMs in various locations. The lower panel depicts the sequence of the p14 cytoplasmic endodomain. Numbers on the top of the sequence indicate amino-acid positions relative to full-length protein. Numbers below the sequence indicate amino-acid position relative to the first residue in the endodomain. The boundary of the TMD and location of the PBM are indicated. The PBM was inserted in various locations in the endodomain (orange sequences), either in a wt p14 backbone containing the membrane-proximal PBM (blue sequences), or in a p14PA backbone containing polyalanine substitution of the PBM (green sequences). The p14 and p14PA backbones contained either the G2A or V9T substitutions depicted above, as specified in the text and figure legends.

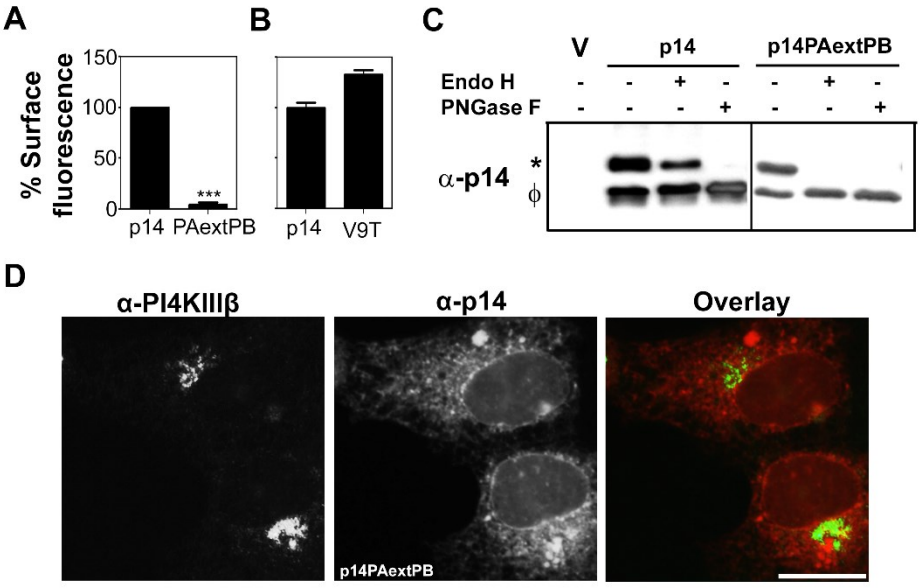

Figure 3.13: Membrane-proximity influences the trafficking function of the p14 PBM. **(A)** Percent cell surface fluorescence analysis of p14 and p14PAextPB (PAextPB), as described in Figure 3.2A. Statistical significance by t-test is indicated relative to p14 (***$p < 0.005$; $n = 3$). **(B)** Percent cell surface fluorescence analysis of p14 and p14-V9T (V9T) as described in Figure 3.2A. **(C)** Cell lysates of QM5 cells transfected with empty vector (V), p14-V9T or p14PAextPB-V9T were harvested at 24 hpt, and equal protein amounts were left untreated or treated with endo H or PNGase F, as described in Materials and Methods, before western blotting with α-p14 antiserum. Glycosylated (*) and nonglycosylated (φ) p14 are indicated on the left. **(D)** Vero cells transfected with p14PAextPB-V9T and immunostained at 24 hpt using α-p14 antiserum (red) and the ER marker PDI (green). Right column shows merged image. Scale bar, 20 μm. Results in panels B and C provided by Christopher Barry (Dalhousie University).

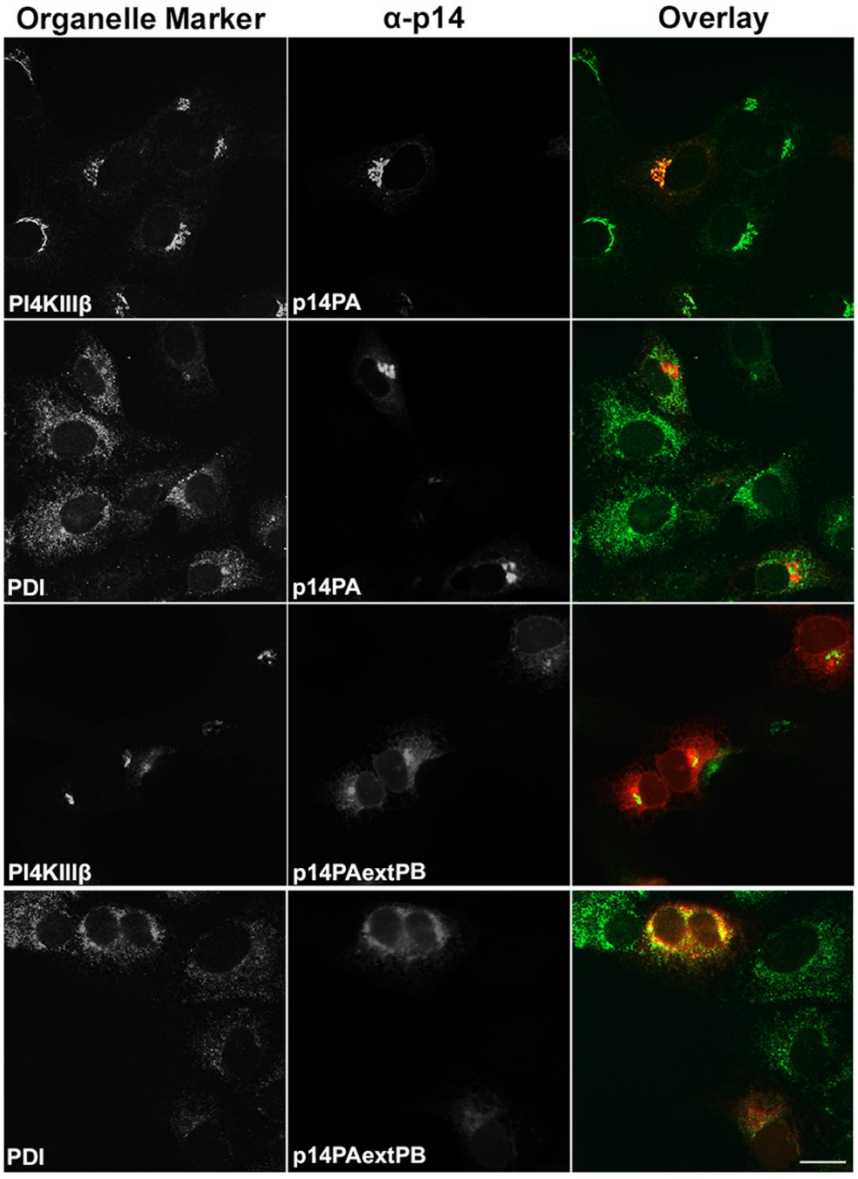

Figure 3.14: p14 accumulates in the ER when the PBM is membrane-distal. Vero cells transfected with p14PB or p14PAextPB in a p14-G2A backbone (see Figure 3.12) were fixed and stained at 24 hpt with α-p14 antiserum (red) and the indicated organelle markers (green) for the Golgi (PI4KIIIβ) or the ER (PDI). Right column shows merged images. Scale bar, 20 μm.

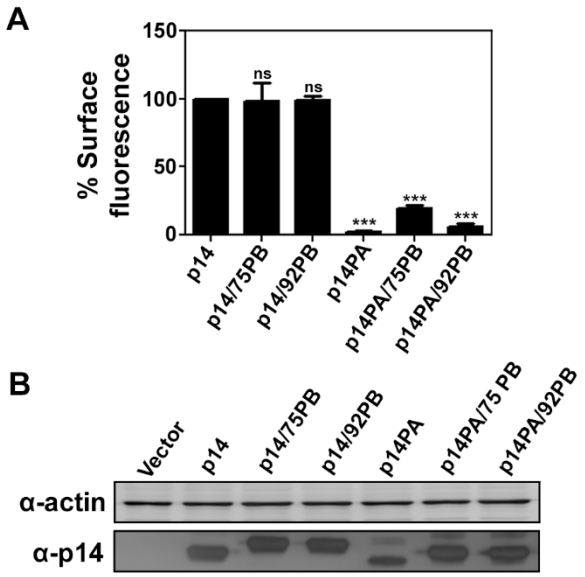

Figure 3.15: An internal PBM does not alter p14 trafficking to the plasma membrane. **(A)** QM5 cells transfected with p14-G2A or the indicated p14 mutants in a p14-G2A backbone (see Figure 3.12) were surface stained at 24 hpt as in Figure 3.2A. Percent cell surface fluorescence relative to p14 is presented as mean ± SEM from three independent experiments in triplicate. Statistical significance by one-way ANOVA and Tukey post-test is shown relative to p14 (***$p<0.005$, ns - not significant). **(B)** QM5 cells transfected with p14 and the same constructs as in panel A were harvested at 8 hpt and lysates were processed for western blotting using α-p14 antiserum or α-actin antibody.

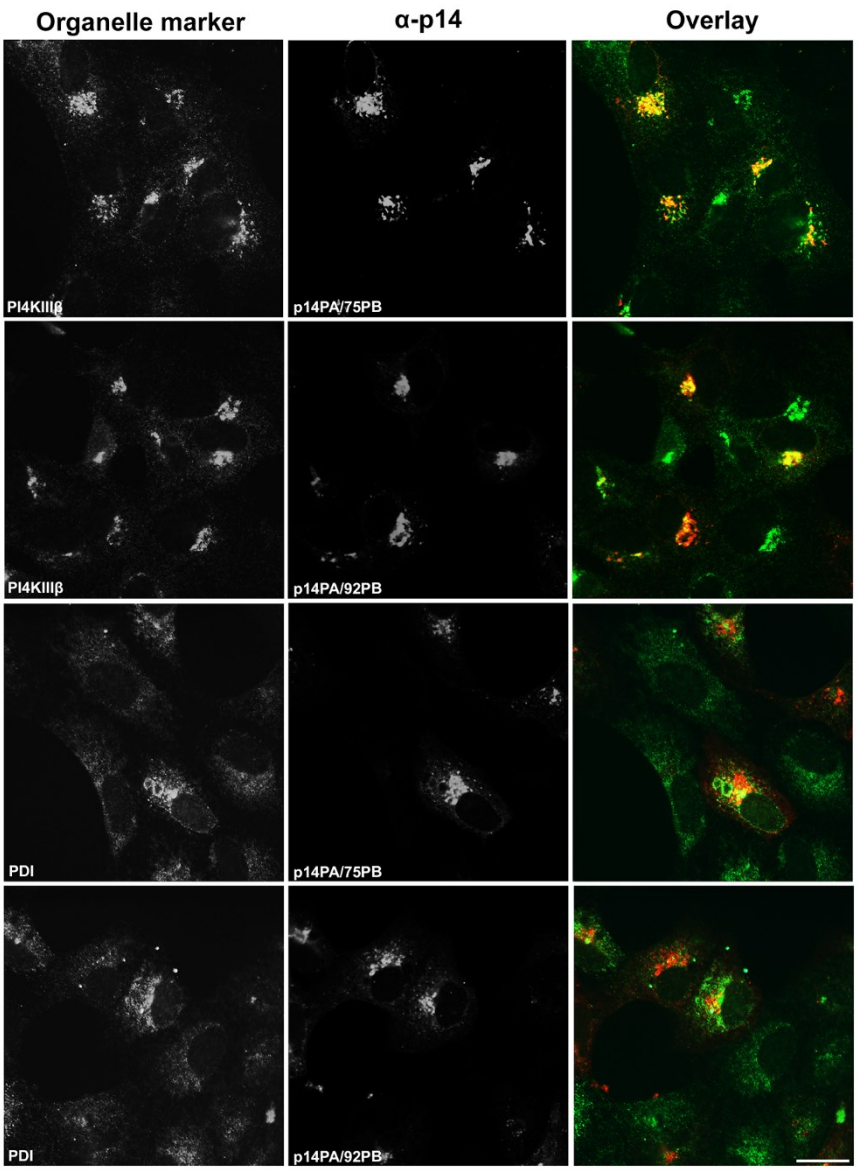

Figure 3.16: An internal PBM cannot function as a Golgi export signal. Vero cells transfected with p14PA/75PB or p14/PA92PB in a p14-G2A backbone (see Figure 3.12) were immunostained as in Figure 3.14 using α-p14 antiserum (red) and the indicated organelle markers (green). Right column shows merged images. Scale bar, 20 μm.

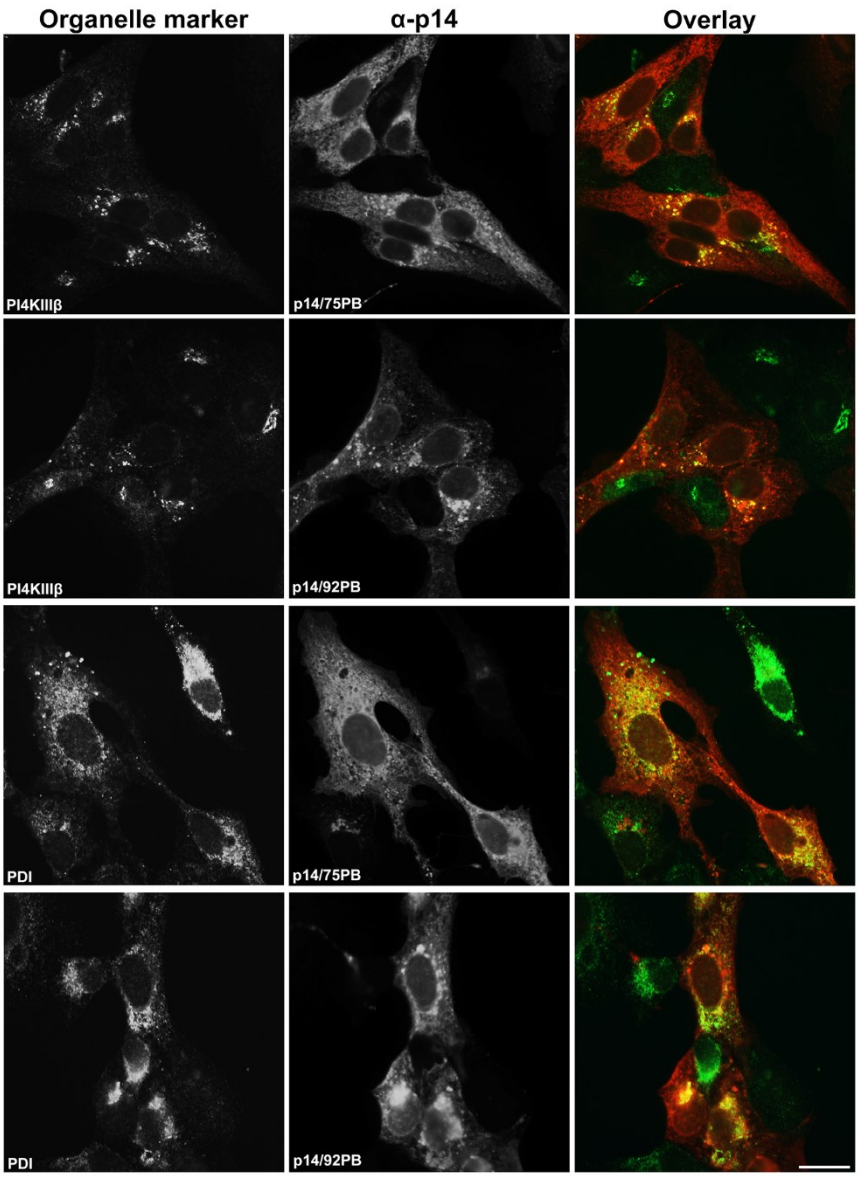

Figure 3.17: An internal PBM does not interfere with the Golgi export function of a membrane-proximal PBM. Vero cells transfected with p14/ 75PB or p14/92PB in a p14-G2A backbone (see Figure 3.12) were immunostained with α-p14 antiserum (red) and the indicated organelle markers (green) as in Figure 3.14. Right column shows merged images. Scale bar, 20 μm.

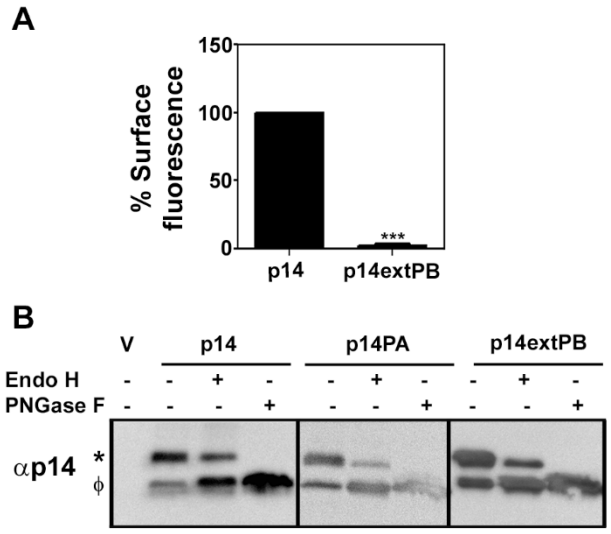

Figure 3.18: Membrane-distal and -proximal PBMs alter ER-Golgi p14 trafficking. **(A)** QM5 cells transfected with p14-V9T or p14extPB in a p14-V9T backbone (see Figure 3.12) were surface stained at 24 hpt as in Figure 3.2A. Percent cell surface fluorescence relative to p14-V9T is presented as mean ± SEM from three independent experiments in triplicate. Statistical significance from student t-test is shown relative to p14 (***$p<0.005$) **(B)** Endo H resistance of p14, p14PA or p14extPB, all in a p14-V9T backbone, as in Figure 3.13C. V, empty vector; *, glycosylated p14; ϕ, non-glycosylated p14. Blot provided by Christopher Barry (Dalhousie University).

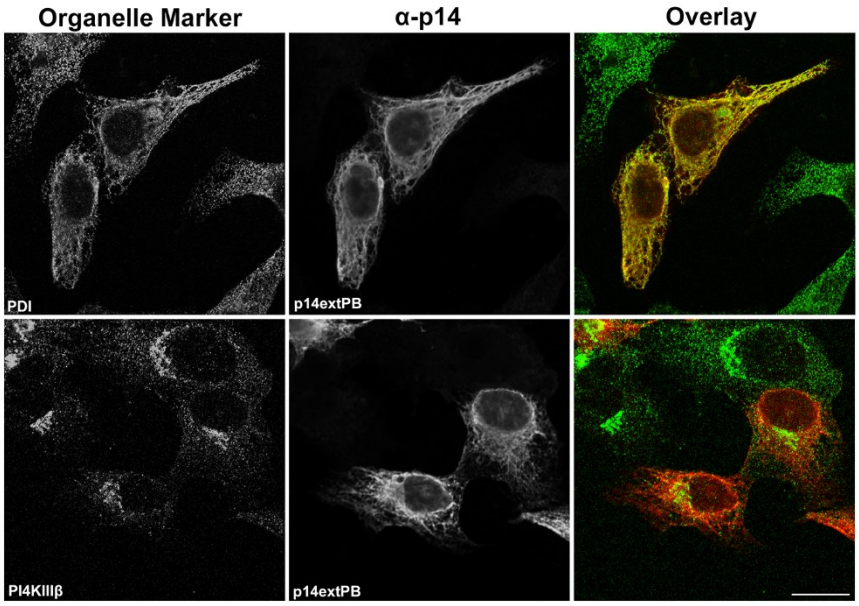

Figure 3.19: Membrane-distal PBM dominates over membrane-proximal PBM. Vero cells were transfected with p14extPB in a p14-V9T backbone and immunostained with α-p14 antiserum (red) and the indicated organelle markers (green) as in Figure 3.14. Right column shows merged images. Scale bar, 20 μm. Figure provided by Christopher Barry (Dalhousie University).

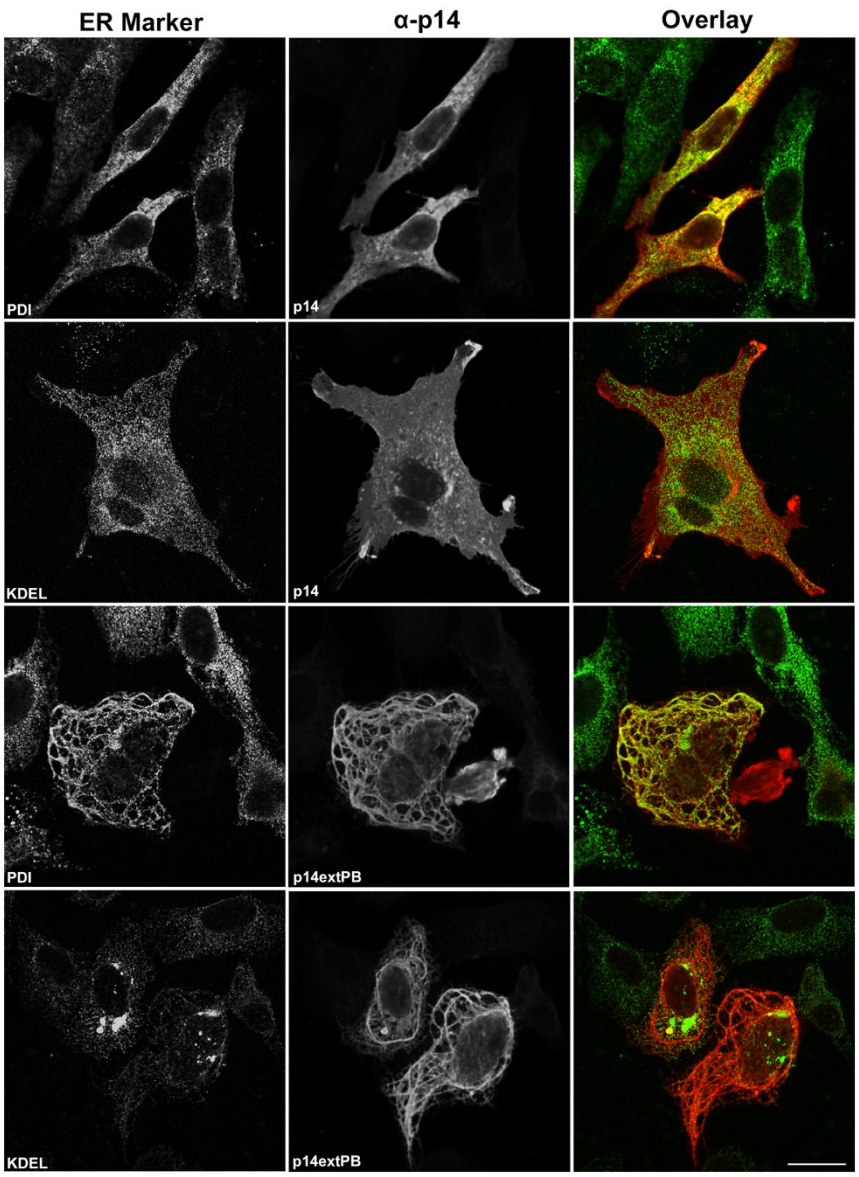

Figure 3.20: p14extPB induces ER tubulation and segregation. Vero cells transfected with p14 or p14extPB, both in a p14-V9T backbone were immunostained with α-p14 antiserum (red) and the indicated organelle markers (green) as in Figure 3.14. Right column shows merged images. Scale bar, 20 μm. Figure provided by Christopher Barry (Dalhousie University).

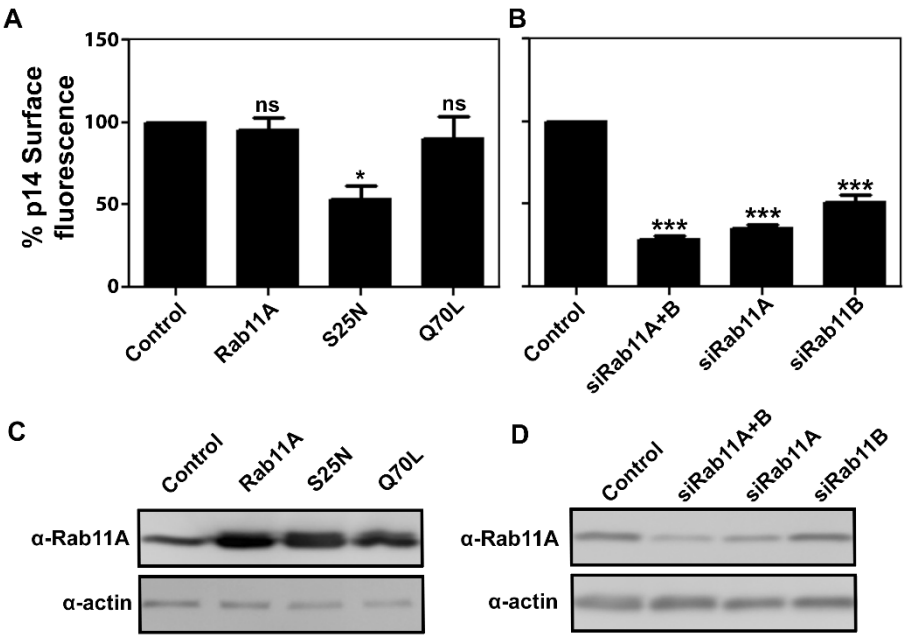

Figure 3.21: Knockdown of Rab11 reduces p14 surface expression. (A) HeLa cells co-transfected with plasmids p14-G2A and empty vector (Control), Rab11A, Rab11A-S25N (S25N) or Rab11A-Q70L (Q70L) were stained at 24 hpt with α-p14 ectodomain antiserum and Alexa-647 secondary antibody and analyzed by flow cytometry. Percent cell surface fluorescence relative to control after background subtraction is presented as mean ± SEM from three independent experiments performed in triplicate. Statistical significance by one-way ANOVA and Tukey post-test is shown relative to control (*$p<0.05$, ns - not significant). **(B)** HeLa cells were transfected with non-targeting siRNA (Control) or siRNA targeting Rab11A (siRab11A), Rab11B (siRab11B) or both (siRab11A+B, and 48 hpt were co-transfected with p14-G2A. Cells were stained and analyzed as in panel A 24 h after the co-transfection. (***$p<0.001$ relative to control). **(C)** HeLa cells transfected with the indicated Rab11 constructs were harvested at 24 hpt and analyzed by western blotting with α-Rab11A and α-actin antibodies. **(D)** HeLa cells transfected with the indicated siRNAs were harvested at 48 hpt and analyzed by western blotting with α-Rab11A and α-actin antibodies.

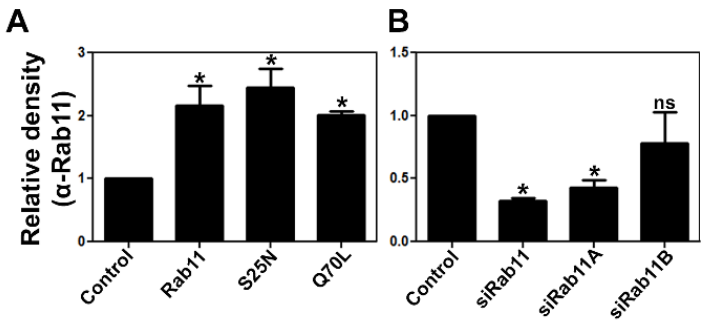

Figure 3.22: Confirmation of Rab11 overexpression and knockdown by western blot quantification. (A) HeLa cells transfected with Rab11A, Rab11A-S25N (S25N), Rab11A-Q70L (Q70L) or empty vector (control) were harvested at 24 hpt and analyzed by western blotting with α-Rab11A antibody. Relative density for western blots obtained from two independent experiments are shown as mean ± SEM. Statistical significance by one-way ANOVA and Tukey post-test is indicated relative to empty vector transfected control sample (*$p<0.05$). **(B)** HeLa cells transfected with siRNA for Rab11A (siRab11A), Rab11B (siRab11B) or both Rab11A and B (siRab11) or control siRNA were harvested at 48 h, analyzed by western blotting with α-Rab11A antibody, and analyzed as in panel A (ns - not significant).

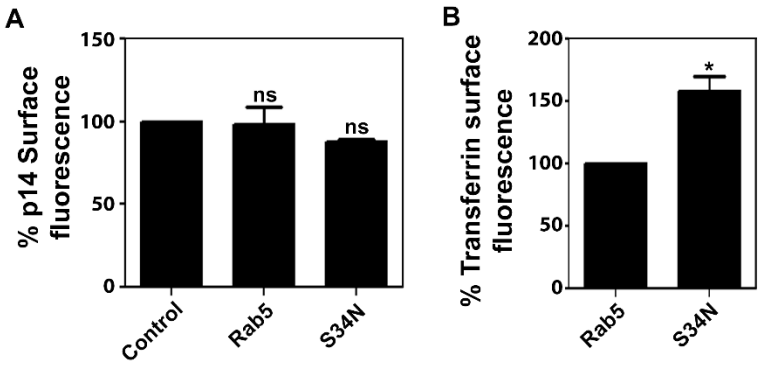

Figure 3.23: Knockdown of Rab5 has no effect on p14 surface expression. (A) HeLa cells co-transfected with p14-G2A and Rab5, Rab5-S34N (S34N) or empty vector (Control) were stained and analyzed by flow cytometry for cell surface fluorescence as in Figure 3.21A (ns - not significant). **(B)** HeLa cells transfected with Rab5 or Rab5-S34N (S34N) constructs were labelled with Alexa-647-conjugated transferrin at 24 hpt and analyzed by flow cytometry. Percent transferrin surface fluorescence relative to Rab5-transfected cells is indicated as mean ± SEM from three independent experiments performed in triplicate. Statistical significance by Student t-test is indicated (*$p<0.05$).

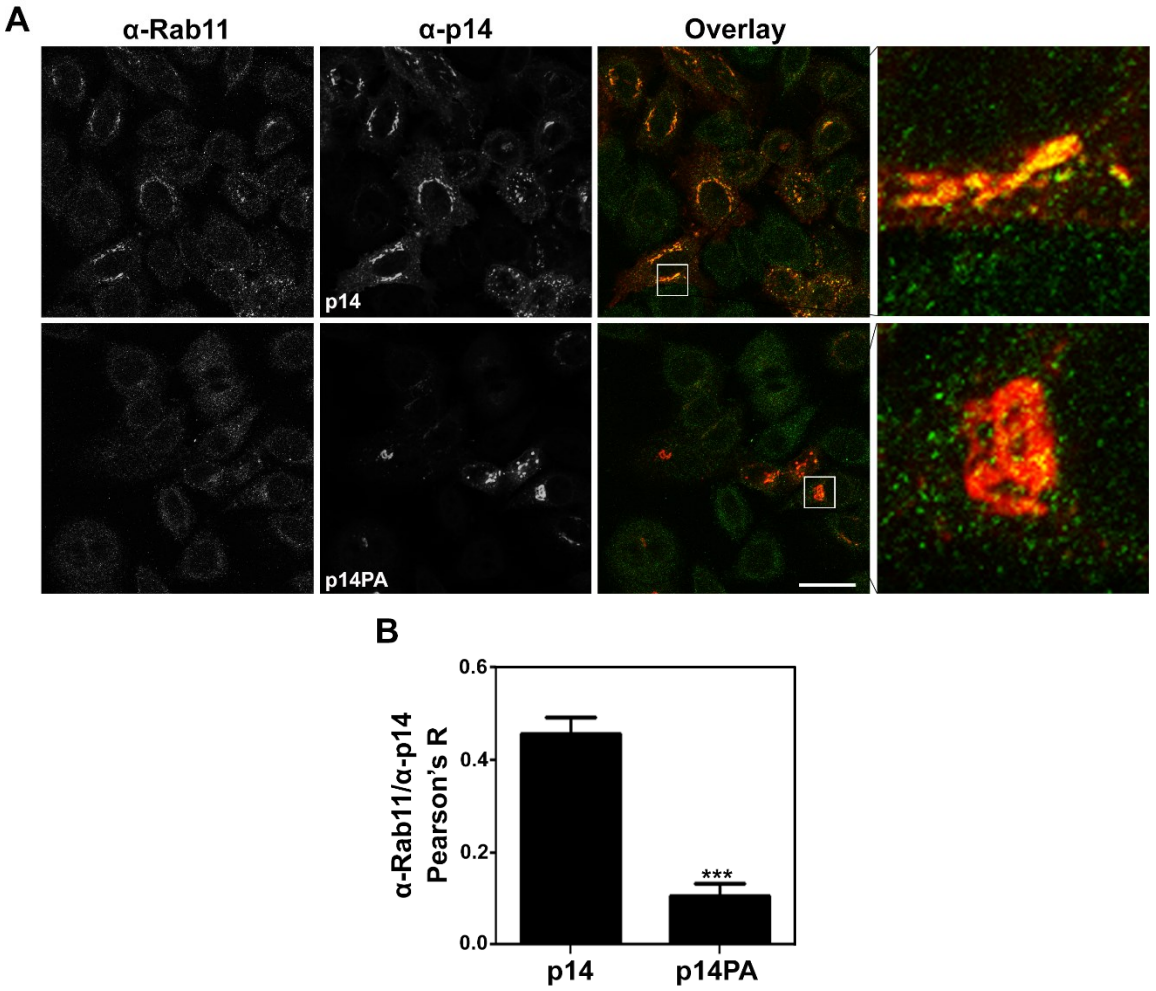

Figure 3.24: p14 colocalizes with Rab11 *in cellula* in a PBM-dependent manner. (A) HeLa cells transfected with p14-G2A (p14) or p14PA-G2A (p14PA) were fixed, permeabilized and stained with α-Rab11 (green) antibody and α-p14 (red) antiserum at 24 hpt. Right, merged images. Scale bar, 20 μm. **(B)** Pearson's correlation coefficient as mean ± SEM for colocalization between Rab11 and p14 or p14PA calculated from twenty cells (ten cells in each of two independent experiments). Statistical significance is indicated by Student t-test (***$p<0.001$).

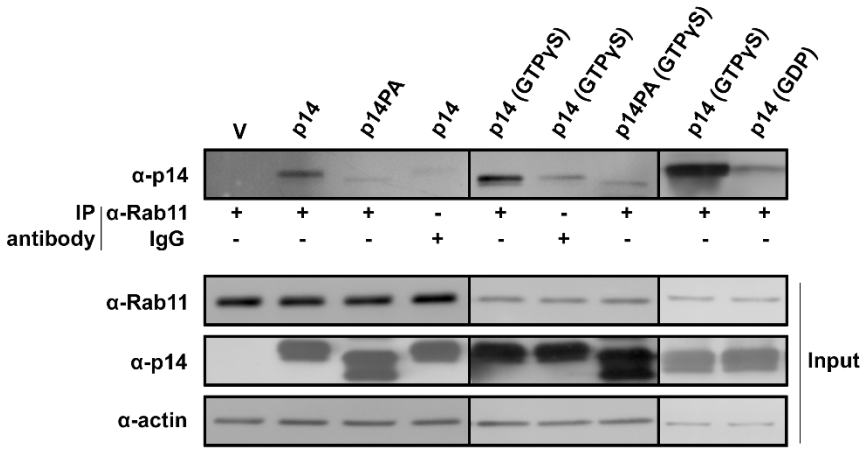

Figure 3.25: p14 co-immunoprecipitates preferentially with activated Rab11 in a PBM-dependent manner. Lysates of HEK cells transfected with p14-G2A (p14), p14PA-G2A (p14PA) or empty vector (V) were obtained at 24 hpt and treated with GTPγS, GDP or no treatment and immunoprecipitated with α-Rab11A antibody. IgG antibody was used as a negative control. Co-IP samples (top panel) and lysates prior to co-IP (bottom three panels) were subjected to western blotting with α-p14 antiserum, and α-Rab11 and α-actin antibodies.

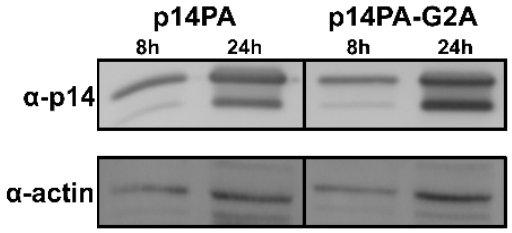

Figure 3.26: p14PA is significantly degraded over time. HEK cells were transfected with p14PA or p14PA-G2A, harvested at 8 hpt or 24 hpt and analyzed by western blotting with α-p14 antiserum and α-actin antibody.

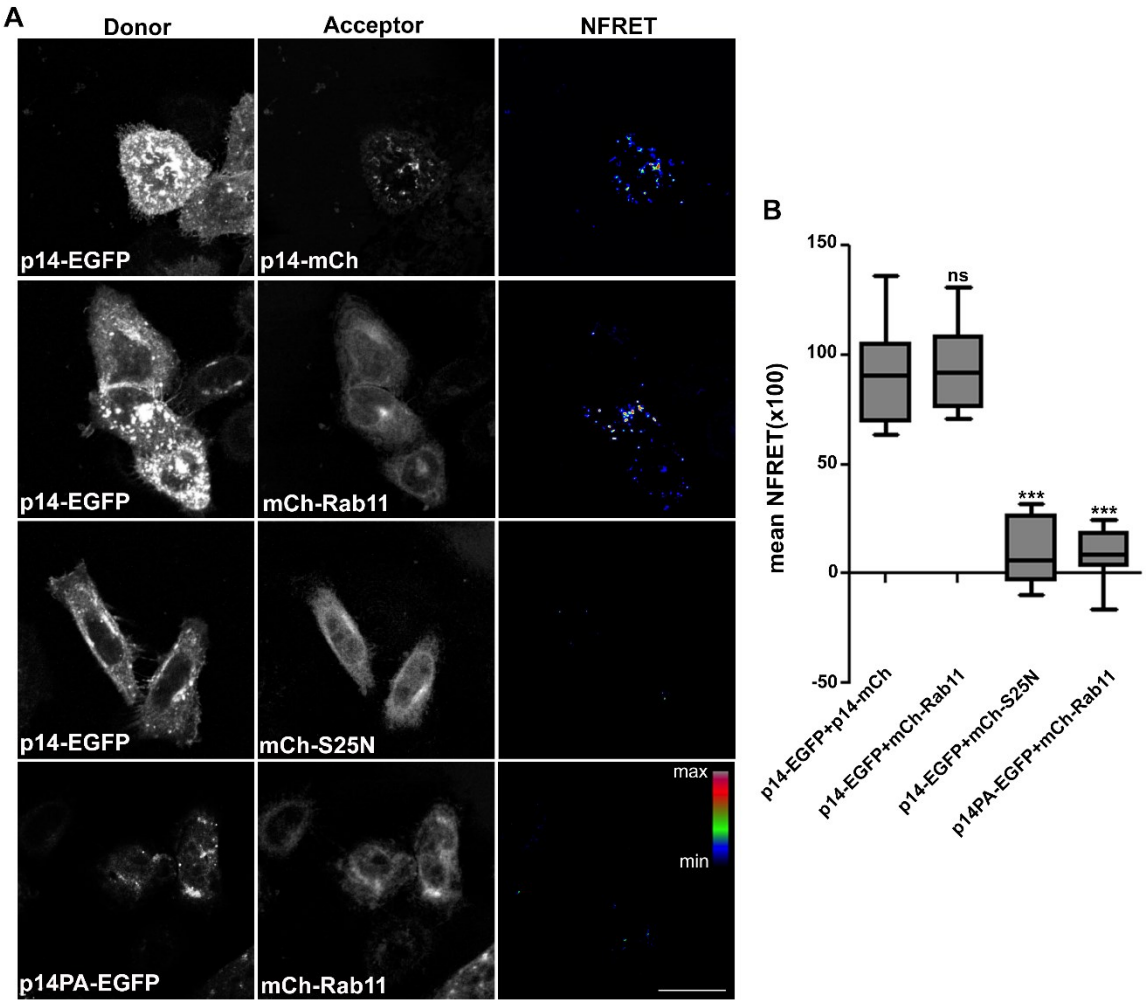

Figure 3.27: p14 directly interacts with Rab11 *in cellula* in a PBM-dependent manner. **(A)** HeLa cells co-transfected with p14 or p14PA tagged with EGFP and Rab11 or Rab11-S25N (S25N) tagged with mCherry (mCh) were fixed at 24 hpt and imaged for sensitized emission FRET along with donor and acceptor images. Right panel shows calculated normalized FRET (NFRET) images. Cells co-transfected with p14 tagged with EGFP (p14-EGFP) and mCherry (p14-mCh) were used as a positive FRET control for a known multimeric membrane protein. NFRET range is indicated by color gradations. Scale bar, 20 µm. **(B)** Mean NFRET values were calculated for 20 cells (10 ten cells from each of two independent experiments) for the indicated co-transfected samples. Boxes indicate standard deviations, horizontal lines indicate means and whiskers indicate minimum and maximum NFRET values. Statistical significance by one-way ANOVA and Tukey post-test relative to the p14 homomultimer control is indicated (***$p<0.001$, ns - not significant).

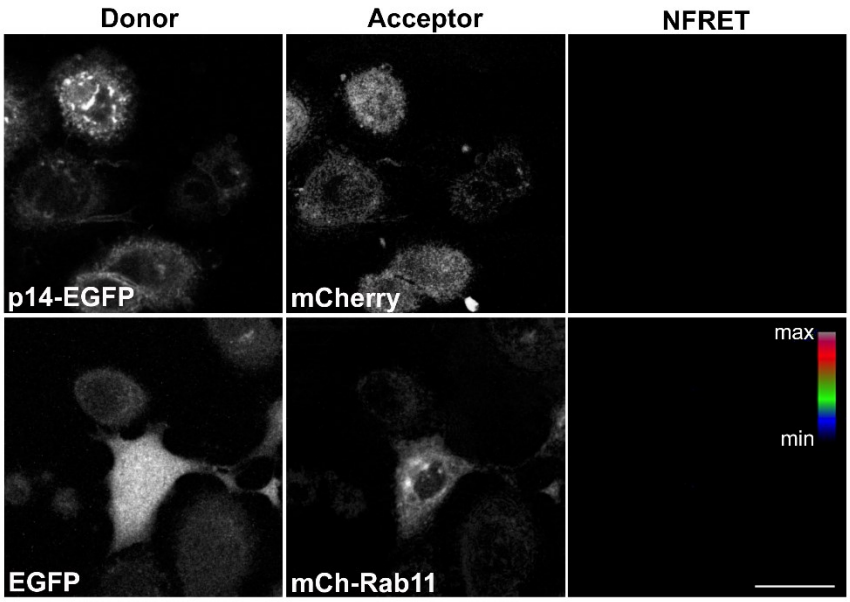

Figure 3.28: Negative controls for FRET microscopy. HeLa cells co-transfected with p14-EGFP and mCherry or EGFP and mCh-Rab11 constructs were fixed at 24 hpt and imaged for sensitized emission FRET along with donor and acceptor images. Right panel shows calculated normalized FRET (NFRET) images. NFRET range is indicated by color gradations. Scale Bar, 20 μm.

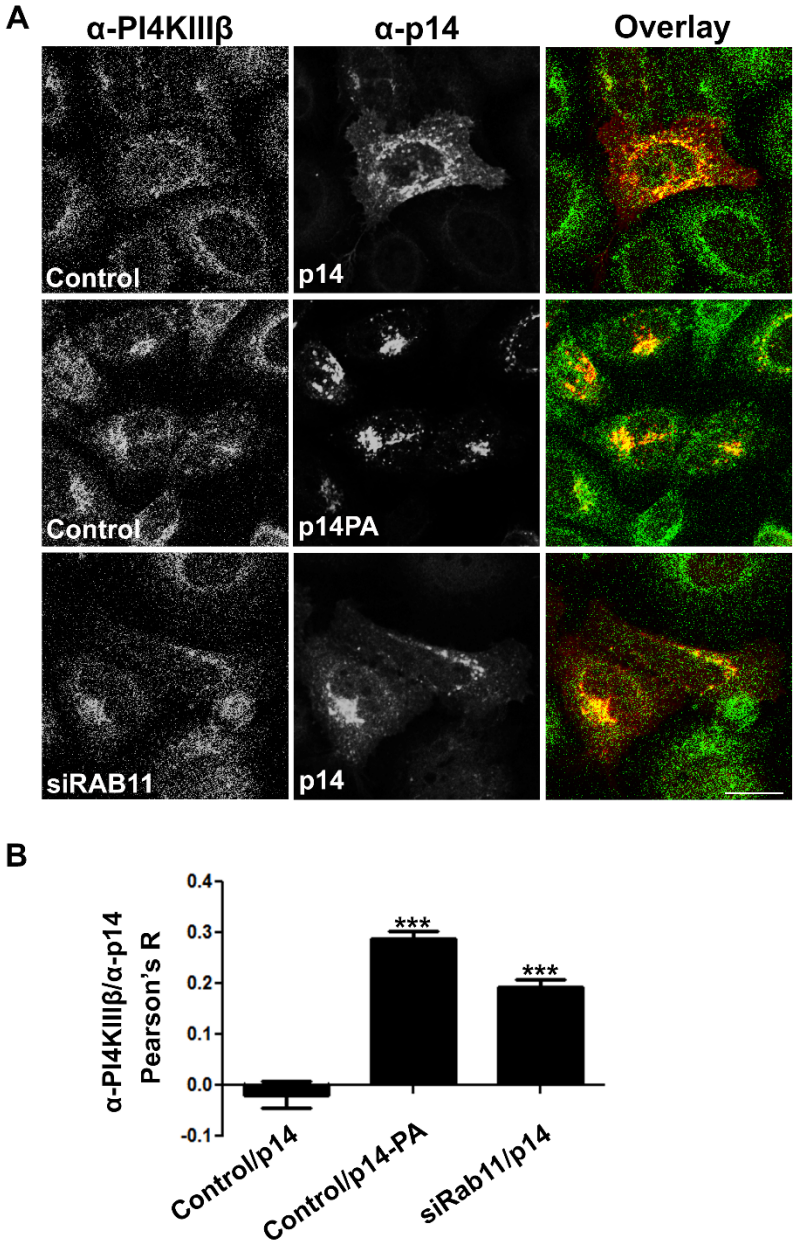

Figure 3.29: Rab11 knockdown results in p14 accumulation in the Golgi. (A) HeLa cells transfected for 48 h with siRNA for Rab11A and B (siRab11) or control siRNA were re-transfected with p14-G2A (p14) or p14PA-G2A (p14PA) for 24 h and fixed, permeabilized and stained with α-p14 (red) antiserum and α-PI4KIIIβ (green) antibody. Right, merged images. Scale bar, 20μm. **(B)** Pearson's correlation coefficients as mean ± SEM for colocaliztion between the Golgi marker PI4KIIIβ and p14 for the indicated samples calculated from 20 cells (10 ten cells from each of two independent experiments). Statistical significance assessed by one-way ANOVA and Tukey post-test is indicated relative to cells co-transfected with control siRNA and p14-G2A (***$p<0.001$).

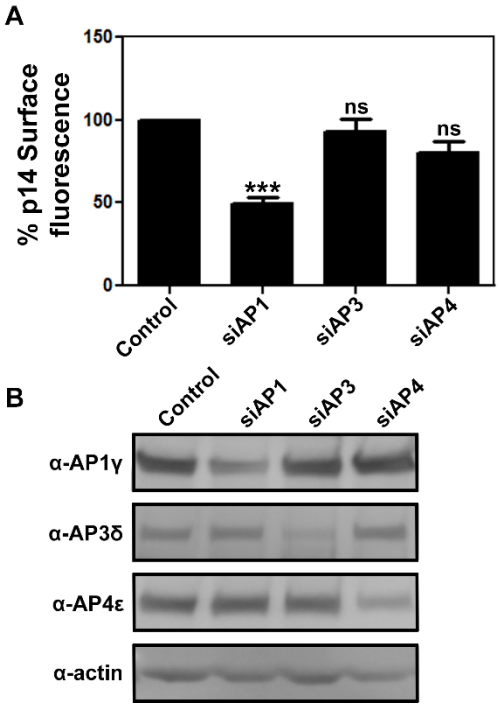

Figure 3.30: Knockdown of AP1, but not AP3 or AP4, reduces p14 surface expression. **(A)** HeLa cells transfected for 48 h with control siRNA or siRNA targeting AP1γ (siAP1), AP3δ (siAP3), or AP4ε (siAP4) were re-transfected with p14-G2A for 24 h and then analyzed for p14 cell surface fluorescence by flow cytometry as in Figure 3.21A. Percent cell surface fluorescence relative to control siRNA-transfected cells is indicated as mean ± SEM from three independent experiments performed in triplicate. Statistical significance by one-way ANOVA and Tukey post-test is indicated relative to control siRNA-transfected cells. (***$p<0.001$, ns - not significant). **(B)** Lysates of HeLa cells transfected with the indicated siRNAs were subjected to western blotting with α-AP1γ, α-AP3δ, α-AP4ε or α-actin antibodies at 48 hpt.

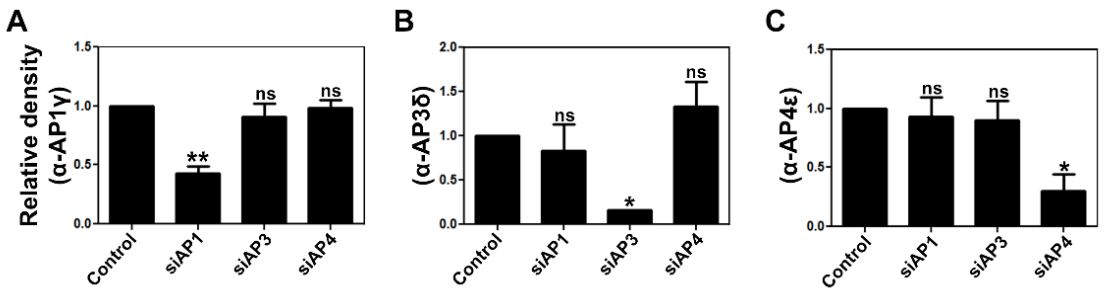

Figure 3.31: Quantification of AP1, AP3 and AP4 knockdown by western blotting. HeLa cells transfected with control siRNA or siRNA targeting AP1γ (siAP1), AP3δ (siAP3), AP4ε (siAP4) were harvested at 48 hpt and analyzed by western blotting using α-AP1γ antibody **(A)**, α-AP3δ antibody **(B)**, or α-AP4ε antibody **(C)**. Relative density from two independent experiments is shown as mean ± SEM. Statistical significance by one-way ANOVA and Tukey post-test is indicated relative to control siRNA sample (*$p<0.05$, **$p<0.01$, ns - not significant).

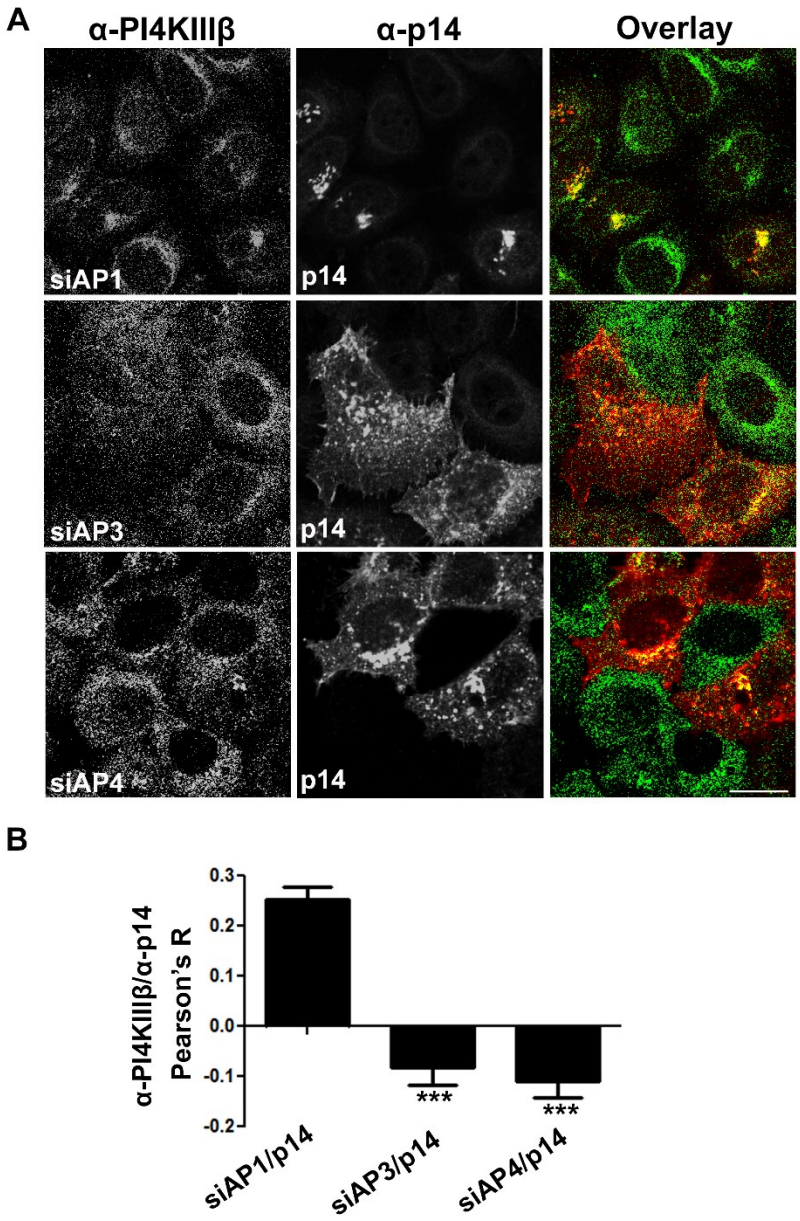

Figure 3.32: Knockdown of AP1 results in p14 accumulation in the Golgi complex. **(A)** HeLa cells transfected with siRNA targeting AP1γ (siAP1), AP3δ (siAP3) or AP4ε (siAP4) were re-transfected at 48 hpt with p14-G2A (p14) for 24 h and fixed, permeabilized and stained with α-p14 (red) antiserum and α-PI4KIIIβ (green) antibody. Right, merged images. Scale bar, 20 μm. **(B)** Pearson's correlation coefficients for colocalization between Golgi marker PI4KIIIβ and p14 is shown as mean ± SEM for the indicated samples calculated from 20 cells (10 ten cells from each of two independent experiments). Statistical significance by one-way ANOVA and Tukey post-test is indicated relative to cells co-transfected with AP1γ siRNA and p14-G2A (***$p<0.001$).

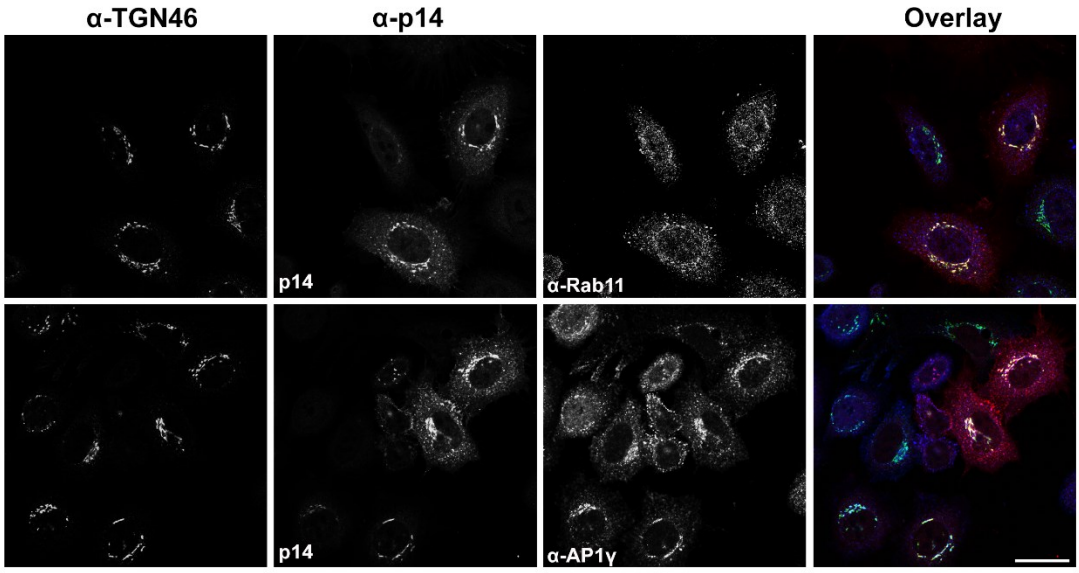

Figure 3.33: p14 colocalizes with Rab11 and AP1 at the TGN. HeLa cells transfected with p14-G2A (p14) were fixed, permeabilized and stained with α-p14 (red) antiserum, α-TGN46 (green), and α-Rab11 (blue) or α-AP1γ (blue) antibodies at 24 hpt. Right, merged images. Scale bar, 20 μm.

CHAPTER 4
DISCUSSION

4.1 Overview

The reovirus FAST proteins are a unique family of viral membrane fusion proteins involved in viral pathogenesis. They are the smallest known membrane fusogens and the only non-structural viral fusion proteins. FAST proteins traffic through the ER-Golgi pathway to the plasma membrane where they promote virus dissemination by causing cell-cell membrane fusion. Unlike most integral membrane proteins, FAST proteins are not glycosylated and lack an N-terminal signal peptide for membrane insertion. They instead use their single transmembrane domain as a reverse signal anchor, resulting in small N-terminal ectodomains and equal-sized or larger C-terminal cytoplasmic endodomains. The simple structure and domain organization of FAST proteins provides an excellent model for studying plasma membrane trafficking determinants.

This thesis describes a comprehensive analysis of the role of the p14 FAST protein PBM in trafficking to the plasma membrane. Several significant conclusions can be drawn from my studies: (1) the p14 PBM is a novel tribasic autonomous Golgi export signal; (2) the PBM exerts positional-dependent effects on protein trafficking and ER morphogenesis; (3) interactions of the PBM with $PI(3,4,5)P_3$ might play a significant role in p14 localization in the plasma membrane and p14-mediated cell-cell fusion; (4) anterograde Golgi-to-plasma membrane transport of p14 involves a PBM-dependent direct interaction with activated Rab11 and sorting into AP1-coated vesicles at the TGN. These results provide several novel insights into factors, processes and pathways involved in Golgi-plasma membrane trafficking, and they provide the first model for FAST protein trafficking.

4.2 The p14 PBM is a novel tribasic autonomous Golgi export signal

All FAST proteins contain a cluster of membrane-proximal basic residues whose function has been undefined. Previous studies indicated the PBM of the p10 FAST protein is required for cell-cell fusion (Shmulevitz et al., 2003). We now show a similar involvement of the p14 PBM in p14-mediated cell-cell fusion (Figure 3.1). The FAST

protein PBMs were speculated to play a role in FAST protein topology, since basic residues on the cytosolic side of a transmembrane domain are dominant determinants of membrane protein topology (Nilsson et al., 2005; von Heijne, 1989). However, p14 antiserum that detects both the N- and C-termini of p14 failed to detect p14PA on the plasma membrane in either the correct N-exoplasmic/C-cytoplasmic or reverse N-cytoplasmic/C-exoplasmic topology (Figure 3.2E). Endo H assays also revealed that the p14PA-V9T N-terminus is glycosylated and, therefore, assumes the correct luminal N-terminus and cytoplasmic C-terminus topology (Figure 3.18B). I predict that a single Lys residue upstream of the PBM at the boundary of the transmembrane domain might be sufficient to maintain the correct topology of p14. Thus, I demonstrated for the first time that the PBM is not required for maintaining p14 topology but is required for plasma membrane localization. Moreover, this trafficking phenotype is not cell-type specific as the same phenotype was observed in QM5 muscle fibroblast, Vero kidney epithelial, HeLa cervical cancer epithelial, and HEK 293T transformed embryonic kidney epithelial cells.

Basic residue-dependent sorting motifs are well described to function as ER export, retention or retrieval signals by directly interacting with components of COPI and COPII complexes (Andersson et al., 1999; Dong et al., 2012; Duvernay et al., 2009b; Giraudo and Maccioni, 2003; Jackson et al., 2012). However, several lines of evidence indicate that the PBM is a Golgi, not ER, export signal. First, endo H assays with p14PA-V9T indicated p14 traffics to the Golgi in the absence of the PBM and, therefore, the PBM is not required for ER export (Figure 3.18B). Second, immunofluorescence microscopy showed extensive colocalization of p14PA with Golgi and TGN markers indicating p14PA is trafficked to, and accumulates in, the Golgi complex (Figure 3.3). Third, inhibiting dynamin-dependent endocytosis using dynasore did not cause p14PA to accumulate on the plasma membrane (Figure 3.4A and C), and an antibody-internalization assay failed to detect recycling of p14PA from the plasma membrane to the Golgi (Figure 3.4E), implying the PBM is not a plasma membrane retention signal but is a *bona fide* Golgi export signal.

Sorting signals involved in trafficking from the Golgi have been reported, however, they function more as sorting signals than as export signals *per se*. Tyrosine or di-leucine based cytosolic sorting signals function in biosynthetic anterograde trafficking pathways from the Golgi, targeting proteins to basolateral membranes (Bonifacino and Traub, 2003;

Rodriguez-Boulan and Musch, 2005). However, mutation of these sorting signals result in protein mis-sorting to apical membranes rather than failure to exit the Golgi, indicating they are not Golgi export signals (Carvajal-Gonzalez et al., 2012; Rodriguez-Boulan and Musch, 2005). As far as I am aware, there is no clear identification of a linear sorting signal required for Golgi export to the plasma membrane. Two residues, tyrosine and serine, in the luminal N-terminus of α2-adrenergic receptors are required for exit from the Golgi, however, luminal residues cannot act as an independent linear sorting signal that can interact with coat protein components for Golgi export (Dong and Wu, 2006). The mechanism by which a luminal YS signal mediates Golgi export remains unknown. Specific conformational changes mediated by the YS motif may be responsible for Golgi export. Also, two basic residues in the cytosolic N-terminus of inward rectifier potassium channel Kir2.1 are involved in Golgi export, but substitution of these basic residue only qualitatively decreases Golgi export (~50%), indicating this motif enhances, but is not required for, Golgi export to the plasma membrane (Stockklausner and Klocker, 2003). Furthermore, a more recent study revealed that these basic residues are actually part of a bipartite Golgi export signal that includes cytosolic C-terminal sequences juxtaposed with the basic residues in the tertiary structure (Ma et al., 2011). In contrast, I showed that mutation of the PBM decreases p14PA plasma membrane localization by >95% (Figure 3.2C) and results in accumulation in the Golgi (Figure 3.3). Extensive mutagenic analysis revealed a stepwise progression in Golgi export and plasma membrane localization of p14 with progressive addition of basic residues to p14PA where maximual plasma membrane levels were observed with three basic residues (Figures 3.7 and 3.9). Thus, the p14 PBM is a tribasic signal required for Golgi export. Most notably, the p14 PBM is transferable to a heterologous Golgi resident protein. Insertion of the wt p14 PBM, but not an alanine substituted version, into the Golgi localized ERGIC-53 chimera led to Golgi export and plasma membrane localization (Figures 3.5 and 3.6) as efficiently as addition of a glycosylation signal previously reported to promote Golgi export of this construct (Gut et al., 1998). The p14 PBM therefore is sufficient to provide a Golgi export phenotype to a Golgi resident protein, implying the p14 PBM is an autonomous Golgi export signal. Thus, the p14 PBM is the first example of an autonomous signal required for Golgi export to plasma membrane, and the first post-Golgi trafficking signal based on a tribasic motif.

4.3 The p14 PBM exerts positional-dependent effects on protein trafficking

The effect of membrane proximity on the function of cytosolic trafficking signals has been noted previously. For example, KKXX motifs function as ER retention or retrieval signals when located distal, but not proximal, to the transmembrane domain (Vincent et al., 1998). A Lys residue is required to be located at the -3 and -4 or -5 positions in the KKXX motif for electrostatic interaction with components of the COPI coat protein complex for ER retrieval (Jackson et al., 2012; Jackson et al., 1990). The p14 PBM does not conform to these consensus arrangements but still inhibits ER export and results in p14 accumulation in the ER (Figures 3.13 and 3.14) when located at the C-terminus of the p14PA. The p14PBM therefore provides a new example of a basic residue-dependent, C-terminal ER retention motif (Figure 4.1), with the caveat that ER retention could mean rapid retrieval from an adjacent post-ER compartment (e.g., the ERGIC).

Surprisingly, Golgi export and ER retention functions cancel each other out when membrane-proximal and -distal PBMs are present together. Endo H and surface expression analysis of p14extPB indicated trafficking to the Golgi but not to the plasma membrane (Figure 3.18), inferring the membrane-distal PBM did not promote ER retention and the membrane-proximal PBM did not promote Golgi export. Interestingly, immunofluorescence microscopy revealed p14extPB accumulation in the ER (Figure 3.19), indicating that the membrane-distal PBM in p14extPB functions as an ER retrieval signal that dominates over the Golgi export ability of the membrane-proximal PBM. The p14extPB construct also revealed an additional role of a membrane-proximal PBM as an ER export signal. Since p14PA traffics to the Golgi, a membrane-proximal PBM is not required for ER export. However, p14extPB traffics to the Golgi while p14PAextPB is retained in the ER, suggesting the membrane-proximal PBM in p14extPB promotes ER export (Figure 4.1). Thus, a membrane-proximal PBM can function as a Golgi or ER export signal, and a membrane-distal PBM can function as an ER retention or retrieval signal (Figure 4.1).

Basic sorting motifs are only active within a defined functional zone relative to the transmembrane domain or C-terminus of membrane proteins (Shikano and Li, 2003; Vincent et al., 1998). Positional effects of sorting signals on ER trafficking are attributed

to their interaction with different COPI or COPII components (Dong et al., 2012; Giraudo and Maccioni, 2003; Jackson et al., 2012; Quintero et al., 2010). For example, KKXX and KXKXX motifs must be present at the C-terminus to interact with subunits of the COPI complex (Jackson et al., 2012; Jackson et al., 1990; Ma and Goldberg, 2013), and mediate ER retention/retrieval when located 17 residues, but not 37 residues from the transmembrane domain (Shikano and Li, 2003). Conversely, the ϕRXR (ϕ-aromatic residue) motif involved in ER retention/retrieval is not required to be at the C-terminus, and is functional when located >45 residues from the C-terminus but not when located <25 residues from the TMD (Michelsen et al., 2005; Shikano and Li, 2003; Zerangue et al., 2001). These positional effects presumably reflect the organization of vesicles coats and which component of the vesicle coat interacts with the sorting signal. For example, glycosyltransferases have a short cytoplasmic tail and their membrane proximal (R/K)X(R/K) motifs interact with a Sar1 binding pocket facing towards the ER membrane while cargoes such as Sed5 and Bet1 SNAREs have longer cytoplasmic tails and membrane-distal YNNSNPF and LXX(L/M)E motifs, respectively, that interact with the Sec24 subunit of the COPII complex for ER export (Miller et al., 2003; Mossessova et al., 2003; Quintero et al., 2010).

My results indicate that the PBM positioned at internal locations in the p14 endodomain has no effect on trafficking. When located >17 residues from the transmembrane domain (p14/75PB) or >34 residues from the transmembrane domain or the C-terminus (p14/92PB), the PBM had no effect on the Golgi export function of the membrane-proximal PBM (Figures 3.15A and 3.17), and did not function as an ER retention signal when the membrane-proximal PBM was absent (Figures 3.15A and 3.16). The p14 PBM shares features with di-lysine (KKXX or KXKXX) and di-arginine (ϕRXR) ER retention/retrieval motifs, but is distinct from both. The C-terminal PBM functions as an ER retention/retrieval signal, similar to di-lysine motifs. However, the PBM does not require lysine residues strictly at -3 and -4 or -5 positions from the C-terminus, as is the case for di-lysine motifs (Jackson et al., 2012; Jackson et al., 1990). Moreover, di-lysine motifs function best when located between 17-37 residues from the transmembrane domain (Shikano and Li, 2003), while the p14 PBM functions when located 68 residues from the transmembrane domain. The ability of the PBM to function as an ER retention/retrieval

signal when membrane distal is a feature shared with the ϕRXR motif. However, the presence of an acidic residue at ϕ or X positions results in a non-functional motif (Zerangue et al., 2001). In contrast, the PBM is functional with the presence of a glutamic acid within the motif (KRRERRR). In addition, ϕRXR motifs function when located at internal positions in the cytosolic endodomain (Michelsen et al., 2005; Shikano and Li, 2003), which is not the case for the p14 PBM. I note that in addition to these two well-described ER retention/retrieval motifs, an unrelated tri-arginine motif also functions as an ER targeting motif. However, replacement of this tri-arginine motif with lysine or histidine results in a non-functional motif, indicating that the positive charge is not important for ER targeting (Hardt et al., 2003). The p14 PBM therefore represents an example of a novel class of ER trafficking motif based on basic residues. My results also revealed that a single sorting motif can have remarkably diverse trafficking functions between the ER and Golgi, and for the first time beyond the Golgi, dependent solely on membrane-proximity. An outstanding question to be answered is whether all sorting signals are affected by membrane-proximity. In addition, it is unclear whether the sequence-independent, tribasic properties of the p14 PBM Golgi export signal also apply to the function of this motif during ER-Golgi trafficking. Additional studies using my panel of PBM mutants in ER-Golgi trafficking studies would address this issue.

Interestingly, ER morphology was dramatically changed in cells expressing a p14 construct containing conflicting membrane-proximal and –distal trafficking signals. Expression of p14extPB in cells induced extensive ER tubulation and a change in distribution of ER resident KDEL receptor from broadly distributed punctate staining that collapsed into a few large perinuclear patches (Figures 3.19 and 3.20). Alterations of ER morphology with extensive tubule formation and segregation of ER components has been previously reported. For example, treatment of cells with the small-molecule inhibitor dispergo induces ER tubulation, loss of ER cisternae and generation of ER patches (Lu et al., 2013). These ER patches contain condensed ER tubules, the Sec61β component of the translocon, and the ER markers KDEL receptor and calreticulin. The broadly distributed, reticular staining pattern of these luminal markers collapses into these ER patches following dispergo treatment (Lu et al., 2013). Overexpression of reticulons, ER membrane proteins that interact with DP1 membrane proteins to induce or stabilize membrane

curvature to form ER tubules, also induces extensive ER tubulation and segregation of the KDEL marker into perinuclear patches (Hu et al., 2008; Voeltz et al., 2006; Zurek et al., 2011).

In the cells expressing p14extPB, ER morphology was remarkably similar to that observed following dispergo treatment or reticulon overexpression. However, dispergo treatment inhibits ER-to-Golgi transport resulting in loss of the Golgi (Lu et al., 2013), which is not the case with p14extPB. Endo H assays indicated that traffic of p14extPB to the Golgi was not inhibited (Figure 3.18B), and the staining pattern of the Golgi indicated that Golgi morphology was intact in cells expressing p14extPB (Figure 3.19). The basis for the dramatic changes in ER morphology induced by dispergo or p14extPB is unknown. Interestingly, p14PAextPB also accumulated in the ER, similar to p14extPB, but did not alter ER morphology. It therefore seems likely that dynamic trafficking of p14extPB in and out of the ER is responsible for the ER tubulation phenotype. It is unknown how p14extPB shuttling results in ER tubulation. One possibility is p14extPB may somehow upregulate reticulons involved in forming ER tubules, although why only p14extPB might induce this response is unclear. Another possibility is that p14extPB may inhibit atlastin-mediated ER membrane fusion due to the opposite effects of p14 and atlastin on membrane curvature induction in the ER. Atlastin, a dynamin-like GTPase that induces membrane curvature and fusion, mediates fusion of the tip of one ER tubule to the side of another tubule, creating three-way junctions and a polygonal ER network (Chen et al., 2013). Atlastin and p14 induce opposite membrane curvature. Atlastin is inserted in the cytoplasmic leaflet of ER membranes and promotes membrane curvature toward the cytoplasm to mediate ER-ER fusion, while p14 spans the membrane with bulky aromatic side chain containing residues towards the cytoplasmic leaflet that promotes membrane budding away from the cytoplasm to mediate cell-cell fusion (Clancy et al., 2010) (Figure 4.2). By potentially opposing the curvature changes induced by atlastin, p14extPB would inhibit atlastin-mediated ER membrane fusion, leading to a decrease in formation of the polygonal ER network and resulting in accumulation of long ER tubules. While these opposing curvature effects would apply to other p14 constructs as well, only p14extPB appears to continually shuttle between the ER and Golgi. The reversible ER-Golgi trafficking of p14extPB might expand the spatial distribution of p14extPB, thereby amplifying the impacts of this

"curvature war" on ER morphogenesis by extending it throughout the cell. Experiments with overexpression or knockdown of reticulons or atlastin would provide additional information that might help to understand this process, as might examining p14extPB constructs that have reduced numbers and ratios of positive charges in the conflicting trafficking signals.

4.4 A potential role for PBM interactions with PI(3,4,5)P_3

PI(3,4,5)P_3 is an important regulator of cellular signaling pathways for cell survival, migration, growth and proliferation (Assinder et al., 2009; Cantley, 2002; Duronio, 2008; Engelman et al., 2006; Yuan and Cantley, 2008). Upon PI(3,4,5)P_3 synthesis by PI3K, downstream signaling effectors interact with PI(3,4,5)P_3 via a PH domain (Lemmon, 2007). Basic residues separated in the primary structure of these PH domains form an array of basic side chains in the tertiary structure creating a binding pocket to interact with PI(3,4,5)P_3 (Lemmon, 2007). The specificity of the Akt and GRP1 PH domains for binding with PI(3,4,5)P_3 compare to PI(4,5)P_2 is provided by a glutamic acid residue adjacent to the binding pocket (Carpten et al., 2007; Landgraf et al., 2008; Pilling et al., 2011). The PBM (KRRERRR) contains a glutamic acid and mediated stronger interaction of the p14 endodomain with PI(3,4,5)P_3 among other PIPs in the protein-lipid overlay assay (Figure 3.11). These results suggest that the PBM (KRRERRR) could be a novel linear PI(3,4,5)P_3 interaction motif that has basic residues for binding and glutamic acid for specificity without the requirement for structural arrangements as in PH domains.

Interestingly, the polybasic mutant p14-RER that lacks glutamic acid in the PBM (KRAAARR) localized to the plasma membrane as well as wt p14 (Figure 3.7) while its fusion activity was significantly reduced (Christopher Barry, PhD thesis, Dalhousie University). Moreover, immunofluorescence microscopy using a fluorescently-tagged Akt-PH domain indicated that PI(3,4,5)P_3 and p14 colocalized in the plasma membrane at sites of cell-cell contact (Figure 1.11). These results suggest that interactions of the PBM with PI(3,4,5)P_3 may not be involved in trafficking to the plasma membrane, but instead are required for p14 fusion activity by mediating lateral sorting of p14 at the plasma membrane to form a cell-cell fusion platform. The PI(3,4,5)P_3 and p14 localization at cell-cell contact sites has been reported previously (Czech, 2000; Salsman et al., 2008).

Moreover, PI(3,4,5)P3 and p14 are also associated with specialized membrane microdomains at the plasma membrane (Corcoran et al., 2006; Hope and Pike, 1996). These reports strengthen the idea that PI(3,4,5)P3 may facilitate PBM-dependent p14 recruitment to lipid rafts and cell-cell contact sites at the plasma membrane to facilitate cell-cell fusion. In addition, actin remodeling is required for p14-mediated cell-cell fusion (Salsman et al., 2008) and PI(3,4,5)P3 is involved in actin cytoskeleton regulation (Piccolo et al., 2002), further suggesting that PI(3,4,5)P_3 may not only recruit p14 to cell-cell contact sites but also facilitate the p14-mediated cell-cell fusion process. PIPs have been shown to be required for yeast vacuole fusion. For instance, PI(4,5)P_2 concentrates at the vesicle docking site and blocking PI(4,5)P_2 with antibody, neomycin or phospholipase impairs vacuole fusion (Fratti et al., 2004; Mayer et al., 2000). Similarly, PI(3)P recruits the Vam7p SNARE to the vacuole membrane for fusion by interacting with its PX domain (Boeddinghaus et al., 2002). PI(3,4,5)P_3 could exert a similar role in FAST protein mediated cell-cell fusion. I note that results in this section are preliminary and need to be confirmed. Liposome-floatation assays would confirm the p14 interaction with PI(3,4,5)P_3 in a membrane-mimicking environment. Analyzing p14-mediated cell-cell fusion while depleting PI(3,4,5)P_3 levels by knockdown of phosphoinositide-3-kinase (PI3K) or by overexpression of phosphatase and tensin homologue (PTEN) may indicate a functional requirement for PI(3,4,5)P_3 in p14-mediated cell-cell fusion.

4.5 Anterograde Golgi-to-plasma membrane transport of p14 involves PBM-dependent direct interaction with activated Rab11 and sorting into AP1-coated vesicles at the TGN

Various studies have shown Rab11 interaction with cargo proteins. However, these studies implicate Rab11 in cargo recycling back to the plasma membrane, and in most of these studies the GDP-bound inactive form of Rab11 was shown to interact with the respective cargo proteins. For example, GST-pulldown studies showed a direct interaction of GDP-bound Rab11 with TRPV5 and TRPV6, two Ca^{2+}-selective members of the transient receptor potential (TRP) channel superfamily, and these interactions influenced trafficking to the plasma membrane and Ca^{2+} uptake (van de Graaf et al., 2006). Similar approaches showed Rab11 interactions with the β2-adrenergic receptor and the β-isoform

of the thromboxane A2 receptor, two G protein-coupled receptors, were required for receptor recycling back to the plasma membrane (Hamelin et al., 2005; Parent et al., 2009). The inactive GDP-bound form of Rab11 was also shown to interact with cGMP-dependent protein kinase II (cGK-II) and influenced its recycling and signaling functions, but whether there was a direct interaction was not analyzed (Yuasa et al., 2008). Studies with human prostacyclin receptor (hIP) indicate a direct interaction of hIP with both GTP- and GDP-bound forms of Rab11 regulates hIP recycling to the plasma membrane (Wikstrom et al., 2008), suggesting hIP interactions with Rab11 are independent of the guanine nucleotide bound forms.

By determining that the direct interaction of p14 with the GTP-bound activated form of Rab11 is required for p14 Golgi export to the plasma membrane, I was able to define the pathway used by p14 for Golgi-to-plasma membrane trafficking. Co-IP results indicated that p14 preferentially interacts with the GTP-bound active form of Rab11 (Figure 3.26), and FRET results strongly imply that this interaction is direct (Figure 3.27). Additional studies using GST-pulldowns would provide additional evidence of this direct interaction. However, the GST-pulldown approach is a contrived, *in vitro* interaction under non-physiological conditions while the FRET approach detects atomic-scale interactions under physiological conditions. In conjunction with the co-localization and co-IP results (Figures 3.24 and 3.25), and with the noted redistribution of Rab11 in cells expressing p14 (Figure 3.24), I believe the FRET results strongly imply that p14 directly interacts with Rab11. I am aware of two studies reporting that the GTP-bound active form of Rab11 interacts with cargo proteins, the voltage-gated potassium channel Kv1.5 and the IL-8 receptor (McEwen et al., 2007; Takahashi et al., 2007). In both cases, these interactions involved recycling back to the plasma membrane, not Golgi-to-plasma membrane transport, and whether Rab11 interacted directly with either Kv1.5 or IL8 was not analyzed.

I also defined a role for Rab11 in cargo interaction for anterograde Golgi-to-plasma membrane trafficking, a poorly characterized directional Rab11 pathway. The only example I am aware of that shows Rab11 can mediate cargo export from the Golgi is with VSV-G (Chen et al., 1998). Overexpression of dominant-negative Rab11-S25N, but not wt Rab11 or constitutively-active Rab11-Q70L, resulted in ~50% decrease in VSV-G plasma membrane expression and increased accumulation in the Golgi, similar to my results with

p14 (Figures 3.21A and 3.29B). Dupre *et al.* also shows that overexpression of Rab11-S25N decreases plasma membrane expression of β_2 adrenergic receptor (β_2AR) (Dupre et al., 2006). However, whether β_2AR was accumulated in the Golgi or endosomes was not analyzed. In my studies, Rab11 could have mediated recycling of endocytosed p14, with the absence of Rab11 resulting in p14 accumulation in the Golgi complex from the endosomes. However, inhibiting endocytosis by Rab5 knockdown or dynasore showed little, if any, effects on p14 plasma membrane or Golgi localization (Figures 3.4 and 3.23A), indicating p14 endocytosis is minimal and unlikely to contribute to the significant effects seen by Rab11 knock-down on p14 Golgi accumulation. Moreover, p14 colocalized with and redistributed Rab11 to the TGN (Figure 3.33), suggesting p14 interacts with Rab11 *en route* to the plasma membrane. Whether endocytosis had any effects on VSV-G plasma membrane or Golgi localization, whether VSV-G colocalized with Rab11 at the TGN and whether Rab11 interacted with VSV-G were not analyzed in studies by Chen *et al*. Hence, I showed for the first time that the GTP-bound active form of Rab11 directly interacts with a cargo protein for biosynthetic anterograde trafficking of cargo from the Golgi to the plasma membrane.

Various Rabs have been shown to interact with cargo proteins for regulation of intracellular trafficking, however, no consensus trafficking motif has been defined so far (Aloisi and Bucci, 2013). The few known Rab interacting motifs include a di-leucine motif in the C-terminus of the β2-adrenergic receptor (β2AR) that interacts with Rab1 for anterograde trafficking from the ER (Hammad et al., 2012). Interestingly, basic residues Arg333 and Lys348 in the cytoplasmic tail of the β2AR were also shown to be important for interaction with Rab11 and for recycling to the plasma membrane (Parent et al., 2009). These basic residues are part of a bipartite Rab11 binding motif, and a specific structural arrangement may therefore be required for their interaction with Rab11. A stretch of ten amino-acids (KKPAPCFEVE) at the C-terminus of the angiotensin II type 1 receptor (AT1R) was also shown to be important for interaction with multiple Rabs, including Rab4, Rab5, Rab7 and Rab11, for regulation of endocytic trafficking (Esseltine et al., 2011). Essseltine *et al*. also showed that residues Pro354 and Cys355, not the basic residues within this stretch of ten amino acids, were important for binding to Rabs. A five amino acid motif (MLERK) in the cytoplasmic tail of TRPV5 and TRPV6 was also shown to be essential

for Rab11 interactions and trafficking to plasma membrane (van de Graaf et al., 2006). Substitution mutation of all five residues of MLERK to glycine residues resulted in decreased plasma membrane localization of TRPV5 and TRPV6. However, whether recycling or the anterograde biosynthetic pathway was affected by this substitution, and whether the two basic residues in the MLERK motif were important for Rab11 binding, was not determined. In contrast, I was able to show that substitution of the PBM with alanine residues resulted in loss of p14 interaction with Rab11 (Figures 3.25 and 3.27) and resulted in p14 accumulation in the Golgi (Figure 3.29), suggesting the PBM is required for p14 interaction with Rab11 and trafficking from the Golgi to the plasma membrane. The p14 PBM (KRRERRR) does not share any similarity with any previously characterized Rab interaction motifs, indicating it represents a novel Rab11 interaction motif. Additional studies using the large panel of PBM mutants I created might help define the precise nature of this novel Rab11 interaction motif. The simple linear structure of this motif is also compatible with X-ray crystallography approaches using Rab11 and PBM peptides to define molecular interactions governing this interaction.

Expression of p14 also altered the staining pattern of Rab11 in cells (Figure 3.24), suggesting p14 may recruit Rab11 to the TGN for efficient export from the Golgi. Moreover, the Golgi staining pattern in cells expressing p14 suggest changes in Golgi morphology that resemble Golgi fragmentation (Figure 3.3 and 3.9). Interestingly, *Chlamydia* also induces Golgi fragmentation, which is dependent on Rab11 and Rab6 (Rejman Lipinski et al., 2009). Golgi morphology needs to be more carefully analyzed with and without Rab11 knockdown during FAST protein expression, and p14 could provide a new tool to study biogenesis of the Golgi complex.

The AP1 complex is known to mediate traffic between the Golgi and endosomes. However, the trafficking direction is unclear (Robinson et al., 2010). Some studies indicate that knockdown of AP1 results in cargo accumulation in endosomes, suggesting AP1 involvement in retrograde traffic from endosomes to the TGN (Foote and Nothwehr, 2006; Meyer et al., 2000). A novel approach referred to as 'knocksideways', where siRNA-resistant AP1 was rerouted to mitochondria by rapamycin-induced heterodimerization, also indicated a role for AP1 role in retrograde transport (Robinson et al., 2010). However, other studies showed cargo accumulation in the Golgi or reduced plasma membrane localization

of cargo following AP1 knockdown, suggesting a role for AP1 in anterograde traffic from the TGN to the endosomes or plasma membrane (Canuel et al., 2008; Lubben et al., 2007). My results indicate that p14 colocalized with AP1 at the TGN (Figure 3.33), and AP1 depletion using siRNA led to inhibited p14 transport to the plasma membrane and p14 accumulation in the Golgi (Figures 3.30 and 3.32). These results provide further compelling evidence that AP1 plays a role in biosynthetic anterograde protein trafficking from the Golgi to the plasma membrane.

While both Rab11 and AP1 have been shown to be involved in traffic from the Golgi complex (Canuel et al., 2008; Chen et al., 1998; Urbe et al., 1993), whether they function together to sort and traffic a specific cargo protein from the Golgi complex has not been reported previously. My results suggest this is the case for p14. Whether Rab11 is directly responsible for AP1 coat assembly at the TGN remains to be determined. There are recent reports indicating Rabs play a role in coat protein assembly. For example, Rab7 was recently shown to be required for retromer coat complex assembly on endosomes (Harrison et al., 2014). Another recent study indicates that Rab4 regulates small GTPase cascades to recruit adaptor complexes to early endosomes (D'Souza et al., 2014). Rab4 activates ADP-ribosylation factor (Arf)-like protein Arl1 that recruits BIG1 and BIG2, Arf GEFs that activate Arf1 and Arf3 to recruit AP1 and AP3 complexes to early endosomes. My results suggest a similar small GTPase cascade mechanism may be regulated by Rab11 at the TGN to recruit the AP1 complex. Rab11 has actually been shown to regulate a Rab cascade for ciliogenesis, where activated Rab11 was shown to interact with Rabin8 to activate its GEF function for Rab8, which promotes primary ciliogenesis (Knodler et al., 2010). The yeast homologue for Rab11, Ypt31/32, has also recently been shown to stimulate Sec7 Arf-GEF activity that activates Arf1 to recruit adaptor complexes to the TGN (McDonold and Fromme, 2014). These studies suggest that Rab11 might be activating Arf-GEFs homologues to activate Arf1 for recruitment of AP1 to the TGN. This would be the first indication that Rabs can regulate adaptor complex assembly for vesicle formation at the TGN. The exceptionally clean phenotype provided by p14PA, or by Rab11 and AP1 knockdowns on wt p14 trafficking, suggests this system coupled with live-cell imaging techniques, such as fluorescence recovery after photobleaching (FRAP) or

photoactivation, might be a useful means of elucidating how Rab11 and AP1 function together to promote Golgi export of p14 to the plasma membrane.

4.6 Model for p14 traffic from the Golgi to the plasma membrane

Based on the results presented herein, I propose a model for p14 sorting and trafficking from the Golgi to the plasma membrane based on a novel cargo protein/activated Rab11/AP1 ternary complex mediating Golgi export to the plasma membrane (Figure 4.3). The journey of a FAST protein to the plasma membrane starts with co-translational insertion into the ER membrane followed by trafficking to the Golgi complex. How p14 is exported from the ER is still not clear, since the PBM is not required for ER export. The cytoplasmic domain of p14 does contain a diacidic motif (EYE, residues 95 to 97), which seems a likely candidate to function as an ER export signal as diacidic motifs mediate ER export (Nishimura and Balch, 1997). Results obtained with the p14extPB construct also suggest the PBM may exert an enhancing effect on ER export. Moreover, since numerous ER export motifs are based on tyrosine residues, individual mutations of six tyrosine residues scattered within the p14 cytoplasmic domain may reveal other potential p14 ER export signals. Since the Sec24 subunit of COPII complex interacts with diacidic and tyrosine-based sorting signals for ER export, it is a likely candidate to interact with the p14 cytoplasmic tail for ER export. A series of mutational and protein-protein interaction analyses, such as co-IP and FRET assays, are required to confirm these speculations.

Regardless of how p14 exits the ER, when p14 reaches the TGN, it interacts with activated Rab11, most likely via direct interactions with the PBM, which results in p14 sorting into AP1-coated vesicles. Cargo sorting usually occurs via interaction of sorting motifs in the cargo with components of vesicle coat protein complexes during vesicle formation, and the p14 PBM may also mediate direct interactions with AP1. Additional activation of a small GTPase cascade and/or regulatory molecules, such as Rab11 shown here, may well be involved in cargo sorting during vesicle formation. Conversely, cases where the GDP-bound form of Rabs interacts with cargo proteins suggest that cargo proteins can be autoregulated by recruiting Rabs and activating them for sorting into vesicles. The $AT_{1A}R$ was shown to preferentially interact with GDP-bound Rab5 and

promote Rab5 GTP-binding and thereby, cargo itself can function as a GEF (Seachrist et al., 2002) indicating cargo sorting is complex and selective process. Once incorporated into AP1 coated vesicles, p14 is transported to the plasma membrane either directly or via the endocytic recycling pathway.

4.7 Additional outstanding questions

Being a respiratory and enteric virus, epithelial cells are the primary target for infection by reoviruses. Considering the function of FAST proteins in cell-cell fusion, FAST proteins should traffic to the basolateral rather than apical plasma membrane in polarized epithelial cells. Does the p14 PBM function as a basolateral targeting signal? Analysis of p14 expression in polarized cells would provide an answer to this question. If true, it would be interesting to analyze whether the glycosylated polyalanine mutant (p14PA-V9T) traffics to the apical plasma membrane since carbohydrates can mediate apical targeting of proteins (Gut et al., 1998). In addition, AP1-B mediates basolateral traffic from the Golgi (Gonzalez and Rodriguez-Boulan, 2009), and therefore would likely mediate p14 basolateral traffic. It would also be interesting to determine which coat proteins are involved in p14PA-V9T apical trafficking.

When two different sorting signals are present, one dominates over the other, and the basis for this dominance effect remains unknown. My data indicate that the ER retrieval function of a membrane-distal PBM dominates over the Golgi export function of the membrane-proximal PBM. Similarly, ER retention determinants in the transmembrane domain of T-cell receptor subunit α dominate over a diacidic (DXE) ER export signal (Nishimura and Balch, 1997). In addition, basolateral sorting signals dominate over apical sorting carbohydrates in polarized epithelial cells (Gut et al., 1998). The direct and stronger interaction between the sorting motif and coat proteins may play a role in determining dominance. For example, the interaction of membrane-proximal PBM with active Rab11 that sorts p14 into AP1 vesicles may not be as strong as the interaction of membrane-distal PBM with COPI complex. The efficiency of these interactions needs to be determined by *in vitro* interaction assays.

The p14 PBM also appears to have a function in cell-cell fusion, in addition to its role in Golgi export to the plasma membrane. The reduced fusion ability of p14-KRR and

p14-RRR, despite their localization to the plasma membrane at levels equivalent to wt p14 (Figure 3.1 and 3.2), implies the PBM plays a role in cell-cell fusion, not just in p14 trafficking. Interaction of the p14 PBM with $PI(3,4,5)P_3$ suggests that $PI(3,4,5)P_3$ localized at sites of cell-cell contact may promote PBM-dependent p14 recruitment to these sites, which are also sites of cell-cell fusion (Salsman et al., 2008). As mentioned before, the p10 PBM is essential for syncytia formation (Shmulevitz et al., 2003). Substitution of the p10 PBM with alanine residues resulted in ~50% reduced transport to the plasma membrane but completely abolished the fusion activity. In addition, alanine substitution of the p15 PBM has no effect on plasma membrane localization but abrogates fusion activity (Seohee Kang, Honour's thesis, Dalhousie University). Which trafficking motifs control transport of these other FAST proteins, and how the FAST proteins PBMs promote membrane fusion independent of trafficking, remains to be determined.

4.8 Conclusion

The receptor-mediated export model for protein trafficking suggests specific interactions between cargo proteins and coat complexes that are required for cargo export from the ER also applies to each step of the secretory or endocytic pathways. Definitive examples of this mechanism functioning for Golgi export, in particular the sorting signals involved and the pathways utilized, are lacking or poorly characterized. My studies identified the first example of an autonomous, tribasic Golgi export signal, they provided the first demonstration that membrane-proximity governs proper functioning of a Golgi export signal and can effect organelle morphology, and they defined a novel cargo protein/activated Rab11/AP1 ternary complex mediating Golgi export to the plasma membrane. Viral proteins such as VSV-G and influenza hemagglutinin (HA) have been extensively used to study protein trafficking pathways. I propose the small size and simple organization of the FAST proteins provide some distinct advantages that can be exploited to explore fundamental aspects of membrane protein sorting and trafficking. My studies also suggest that the PBM is not just a trafficking motif but likely also plays an important role in FAST protein mediated cell-cell fusion. These fascinating small viral fusion proteins should continue to provide novel insights into intracellular protein trafficking pathways and mechanisms of protein-mediated membrane fusion.

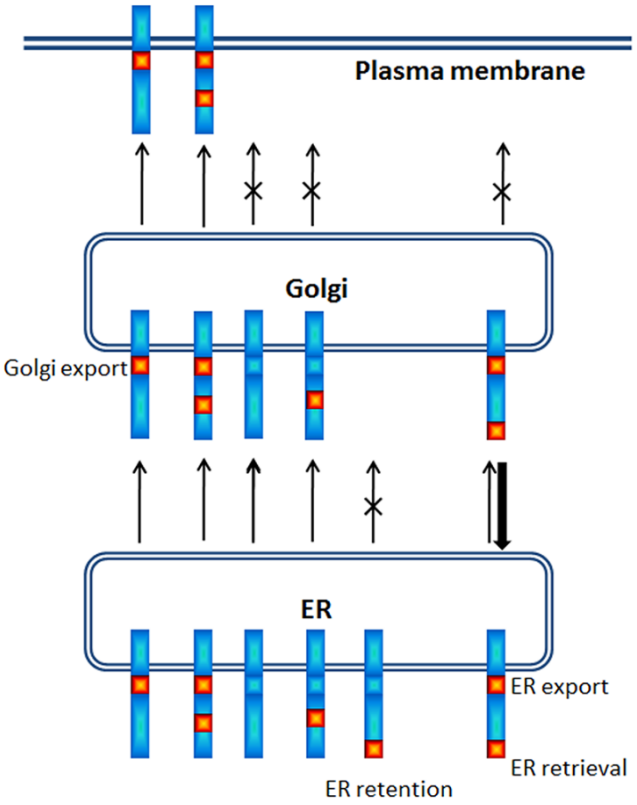

Figure 4.1 Summary of position-dependent effects of the PBM on p14 trafficking. Depicted are the trafficking properties of p14 constructs (blue) containing the PBM (red) in membrane-proximal, C-terminal or internal locations in the p14 cytoplasmic endodomain, as described in the text. Arrows indicate trafficking of the various constructs between the ER, Golgi and plasma membrane, with an X indicating inhibition and thin and thick arrows indicating relative strength of directional trafficking. The positional-dependent functions of the PBM at specific locations in Golgi export, ER retention, ER export or ER retrieval are indicated.

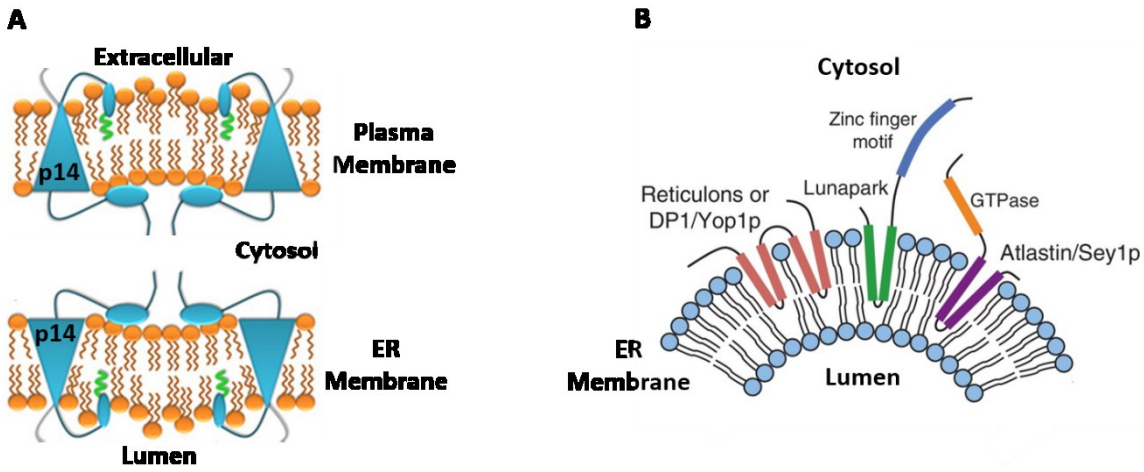

Figure 4.2 Opposite membrane curvature induction by p14 and atlastin in the ER membrane. **(A)** Membrane curvature induced by p14 at the plasma membrane and ER membrane [modified from (Clancy et al., 2010) with permission]. **(B)** Membrane curvature induced and required by atlastin at ER membranes for fusion with another ER membrane [modified from (Chen et al., 2013) with permission].

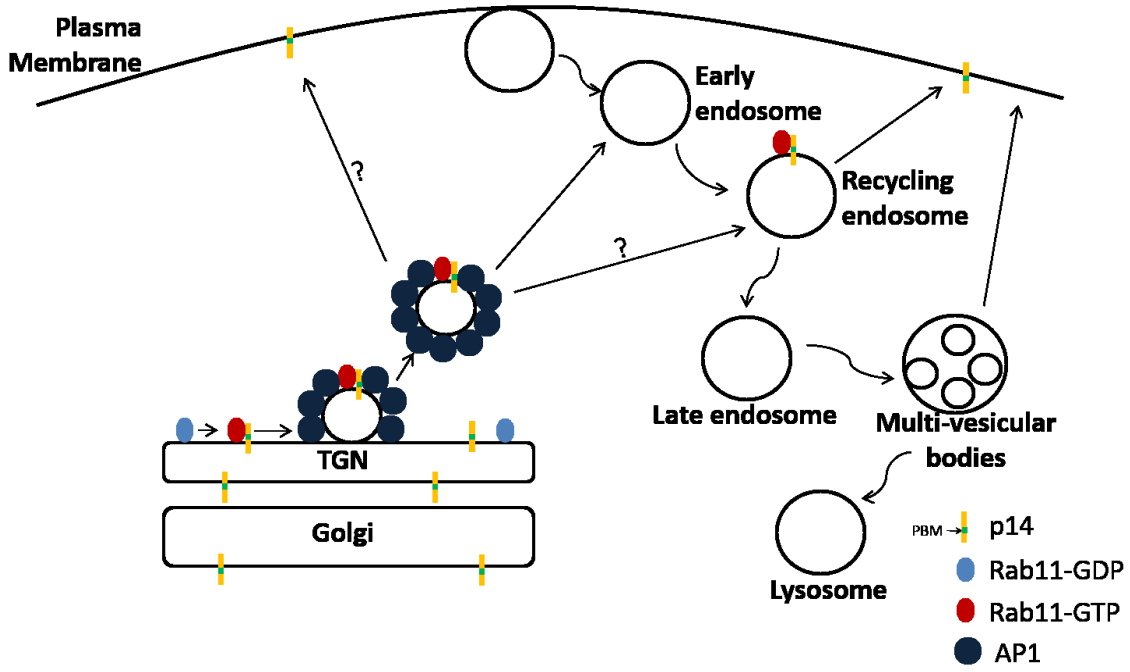

Figure 4.3. Model for p14 plasma membrane trafficking. The p14 polybasic motif directs interaction with activated Rab11 bound to the TGN membrane. This interaction promotes p14 sorting into vesicles being formed by the AP1 adaptor complex, which then traffic from the TGN to the plasma membrane, either directly or via the endosomal recycling pathway. Clathrin coat around AP1 is not shown due to simplicity.

REFERENCES

Almen, M.S., K.J. Nordstrom, R. Fredriksson, and H.B. Schioth. 2009. Mapping the human membrane proteome: a majority of the human membrane proteins can be classified according to function and evolutionary origin. *BMC biology*. 7:50.

Aloisi, A.L., and C. Bucci. 2013. Rab GTPases-cargo direct interactions: fine modulators of intracellular trafficking. *Histology and histopathology*. 28:839-849.

Andersson, H., F. Kappeler, and H.P. Hauri. 1999. Protein targeting to endoplasmic reticulum by dilysine signals involves direct retention in addition to retrieval. *The Journal of biological chemistry*. 274:15080-15084.

Anitei, M., and B. Hoflack. 2011. Exit from the trans-Golgi network: from molecules to mechanisms. *Current opinion in cell biology*. 23:443-451.

Antonny, B., P. Gounon, R. Schekman, and L. Orci. 2003. Self-assembly of minimal COPII cages. *EMBO reports*. 4:419-424.

Antonny, B., D. Madden, S. Hamamoto, L. Orci, and R. Schekman. 2001. Dynamics of the COPII coat with GTP and stable analogues. *Nature cell biology*. 3:531-537.

Appenzeller-Herzog, C., and H.P. Hauri. 2006. The ER-Golgi intermediate compartment (ERGIC): in search of its identity and function. *Journal of cell science*. 119:2173-2183.

Appenzeller, C., H. Andersson, F. Kappeler, and H.P. Hauri. 1999. The lectin ERGIC-53 is a cargo transport receptor for glycoproteins. *Nature cell biology*. 1:330-334.

Assinder, S.J., Q. Dong, Z. Kovacevic, and D.R. Richardson. 2009. The TGF-beta, PI3K/Akt and PTEN pathways: established and proposed biochemical integration in prostate cancer. *The Biochemical journal*. 417:411-421.

Ast, T., G. Cohen, and M. Schuldiner. 2013. A network of cytosolic factors targets SRP-independent proteins to the endoplasmic reticulum. *Cell*. 152:1134-1145.

Balch, W.E., J.M. McCaffery, H. Plutner, and M.G. Farquhar. 1994. Vesicular stomatitis virus glycoprotein is sorted and concentrated during export from the endoplasmic reticulum. *Cell*. 76:841-852.

Balderhaar, H.J., H. Arlt, C. Ostrowicz, C. Brocker, F. Sundermann, R. Brandt, M. Babst, and C. Ungermann. 2010. The Rab GTPase Ypt7 is linked to retromer-mediated receptor recycling and fusion at the yeast late endosome. *Journal of cell science*. 123:4085-4094.

Balla, T. 2013. Phosphoinositides: tiny lipids with giant impact on cell regulation. *Physiological reviews*. 93:1019-1137.

Bannykh, S.I., N. Nishimura, and W.E. Balch. 1998. Getting into the Golgi. *Trends in cell biology*. 8:21-25.

Bannykh, S.I., T. Rowe, and W.E. Balch. 1996. The organization of endoplasmic reticulum export complexes. *The Journal of cell biology*. 135:19-35.

Barlowe, C. 2003. Signals for COPII-dependent export from the ER: what's the ticket out? *Trends in cell biology*. 13:295-300.

Barlowe, C., L. Orci, T. Yeung, M. Hosobuchi, S. Hamamoto, N. Salama, M.F. Rexach, M. Ravazzola, M. Amherdt, and R. Schekman. 1994. COPII: a membrane coat formed by Sec proteins that drive vesicle budding from the endoplasmic reticulum. *Cell*. 77:895-907.

Barlowe, C., and R. Schekman. 1993. SEC12 encodes a guanine-nucleotide-exchange factor essential for transport vesicle budding from the ER. *Nature*. 365:347-349.

Barr, F.A. 2013. Review series: Rab GTPases and membrane identity: causal or inconsequential? *The Journal of cell biology*. 202:191-199.

Barry, C., T. Key, R. Haddad, and R. Duncan. 2010. Features of a spatially constrained cystine loop in the p10 FAST protein ectodomain define a new class of viral fusion peptides. *The Journal of biological chemistry*. 285:16424-16433.

Bashkirov, P.V., S.A. Akimov, A.I. Evseev, S.L. Schmid, J. Zimmerberg, and V.A. Frolov. 2008. GTPase cycle of dynamin is coupled to membrane squeeze and release, leading to spontaneous fission. *Cell*. 135:1276-1286.

Becker, B., B. Bolinger, and M. Melkonian. 1995. Anterograde transport of algal scales through the Golgi complex is not mediated by vesicles. *Trends in cell biology*. 5:305-307.

Bednarek, S.Y., M. Ravazzola, M. Hosobuchi, M. Amherdt, A. Perrelet, R. Schekman, and L. Orci. 1995. COPI- and COPII-coated vesicles bud directly from the endoplasmic reticulum in yeast. *Cell*. 83:1183-1196.

Belden, W.J., and C. Barlowe. 2001. Role of Erv29p in collecting soluble secretory proteins into ER-derived transport vesicles. *Science*. 294:1528-1531.

Ben-Tekaya, H., K. Miura, R. Pepperkok, and H.P. Hauri. 2005. Live imaging of bidirectional traffic from the ERGIC. *Journal of cell science*. 118:357-367.

Benavente, J., and J. Martinez-Costas. 2007. Avian reovirus: structure and biology. *Virus research*. 123:105-119.

Bermak, J.C., M. Li, C. Bullock, and Q.Y. Zhou. 2001. Regulation of transport of the dopamine D1 receptor by a new membrane-associated ER protein. *Nature cell biology*. 3:492-498.

Beznoussenko, G.V., V.V. Dolgikh, E.V. Seliverstova, P.B. Semenov, Y.S. Tokarev, A. Trucco, M. Micaroni, D. Di Giandomenico, P. Auinger, I.V. Senderskiy, S.O. Skarlato, E.S. Snigirevskaya, Y.Y. Komissarchik, M. Pavelka, M.A. De Matteis, A. Luini, Y.Y. Sokolova, and A.A. Mironov. 2007. Analogs of the Golgi complex in microsporidia: structure and avesicular mechanisms of function. *Journal of cell science*. 120:1288-1298.

Bharucha, N., Y. Liu, E. Papanikou, C. McMahon, M. Esaki, P.D. Jeffrey, F.M. Hughson, and B.S. Glick. 2013. Sec16 influences transitional ER sites by regulating rather than organizing COPII. *Molecular biology of the cell*. 24:3406-3419.

Bhattacharya, N., O.D. J, and S.M. Stagg. 2012. The structure of the Sec13/31 COPII cage bound to Sec23. *Journal of molecular biology*. 420:324-334.

Bhattacharyya, D., and B.S. Glick. 2007. Two mammalian Sec16 homologues have nonredundant functions in endoplasmic reticulum (ER) export and transitional ER organization. *Molecular biology of the cell*. 18:839-849.

Bhuin, T., and J.K. Roy. 2014. Rab proteins: the key regulators of intracellular vesicle transport. *Experimental cell research*. 328:1-19.

Bi, X., R.A. Corpina, and J. Goldberg. 2002. Structure of the Sec23/24-Sar1 pre-budding complex of the COPII vesicle coat. *Nature*. 419:271-277.

Bi, X., J.D. Mancias, and J. Goldberg. 2007. Insights into COPII coat nucleation from the structure of Sec23.Sar1 complexed with the active fragment of Sec31. *Developmental cell*. 13:635-645.

Bichet, D., V. Cornet, S. Geib, E. Carlier, S. Volsen, T. Hoshi, Y. Mori, and M. De Waard. 2000. The I-II loop of the Ca2+ channel alpha1 subunit contains an endoplasmic reticulum retention signal antagonized by the beta subunit. *Neuron*. 25:177-190.

Bigay, J., J.F. Casella, G. Drin, B. Mesmin, and B. Antonny. 2005. ArfGAP1 responds to membrane curvature through the folding of a lipid packing sensor motif. *The EMBO journal*. 24:2244-2253.

Bigay, J., P. Gounon, S. Robineau, and B. Antonny. 2003. Lipid packing sensed by ArfGAP1 couples COPI coat disassembly to membrane bilayer curvature. *Nature*. 426:563-566.

Blumental-Perry, A., C.J. Haney, K.M. Weixel, S.C. Watkins, O.A. Weisz, and M. Aridor. 2006. Phosphatidylinositol 4-phosphate formation at ER exit sites regulates ER export. *Developmental cell*. 11:671-682.

Boeddinghaus, C., A.J. Merz, R. Laage, and C. Ungermann. 2002. A cycle of Vam7p release from and PtdIns 3-P-dependent rebinding to the yeast vacuole is required for homotypic vacuole fusion. *The Journal of cell biology*. 157:79-89.

Bonfanti, L., A.A. Mironov, Jr., J.A. Martinez-Menarguez, O. Martella, A. Fusella, M. Baldassarre, R. Buccione, H.J. Geuze, A.A. Mironov, and A. Luini. 1998. Procollagen traverses the Golgi stack without leaving the lumen of cisternae: evidence for cisternal maturation. *Cell*. 95:993-1003.

Bonifacino, J.S. 2004. The GGA proteins: adaptors on the move. *Nature reviews. Molecular cell biology*. 5:23-32.

Bonifacino, J.S., and L.M. Traub. 2003. Signals for sorting of transmembrane proteins to endosomes and lysosomes. *Annual review of biochemistry*. 72:395-447.

Borgese, N., and E. Fasana. 2011. Targeting pathways of C-tail-anchored proteins. *Biochimica et biophysica acta*. 1808:937-946.

Boucrot, E., A.P. Ferreira, L. Almeida-Souza, S. Debard, Y. Vallis, G. Howard, L. Bertot, N. Sauvonnet, and H.T. McMahon. 2015. Endophilin marks and controls a clathrin-independent endocytic pathway. *Nature*. 517:460-465.

Boulaflous, A., C. Saint-Jore-Dupas, M.C. Herranz-Gordo, S. Pagny-Salehabadi, C. Plasson, F. Garidou, M.C. Kiefer-Meyer, C. Ritzenthaler, L. Faye, and V. Gomord. 2009. Cytosolic N-terminal arginine-based signals together with a luminal signal target a type II membrane protein to the plant ER. *BMC plant biology*. 9:144.

Boutilier, J., and R. Duncan. 2011. The reovirus fusion-associated small transmembrane (FAST) proteins: virus-encoded cellular fusogens. *Current topics in membranes*. 68:107-140.

Bravo, J., D. Karathanassis, C.M. Pacold, M.E. Pacold, C.D. Ellson, K.E. Anderson, P.J. Butler, I. Lavenir, O. Perisic, P.T. Hawkins, L. Stephens, and R.L. Williams. 2001. The crystal structure of the PX domain from p40(phox) bound to phosphatidylinositol 3-phosphate. *Molecular cell*. 8:829-839.

Brill, J.A., R. Wong, and A. Wilde. 2011. Phosphoinositide function in cytokinesis. *Current biology : CB*. 21:R930-934.

Brown, C.W., K.B. Stephenson, S. Hanson, M. Kucharczyk, R. Duncan, J.C. Bell, and B.D. Lichty. 2009. The p14 FAST protein of reptilian reovirus increases vesicular stomatitis virus neuropathogenesis. *Journal of virology*. 83:552-561.

Budnik, A., and D.J. Stephens. 2009. ER exit sites--localization and control of COPII vesicle formation. *FEBS letters*. 583:3796-3803.

Bui, Q.T., M.P. Golinelli-Cohen, and C.L. Jackson. 2009. Large Arf1 guanine nucleotide exchange factors: evolution, domain structure, and roles in membrane trafficking and human disease. *Molecular genetics and genomics : MGG*. 282:329-350.

Burd, C., and P.J. Cullen. 2014. Retromer: a master conductor of endosome sorting. *Cold Spring Harbor perspectives in biology*. 6.

Burd, C.G., and S.D. Emr. 1998. Phosphatidylinositol(3)-phosphate signaling mediated by specific binding to RING FYVE domains. *Molecular cell*. 2:157-162.

Burgos, P.V., G.A. Mardones, A.L. Rojas, L.L. daSilva, Y. Prabhu, J.H. Hurley, and J.S. Bonifacino. 2010. Sorting of the Alzheimer's disease amyloid precursor protein mediated by the AP-4 complex. *Developmental cell*. 18:425-436.

Cantley, L.C. 2002. The phosphoinositide 3-kinase pathway. *Science*. 296:1655-1657.

Canuel, M., S. Lefrancois, J. Zeng, and C.R. Morales. 2008. AP-1 and retromer play opposite roles in the trafficking of sortilin between the Golgi apparatus and the lysosomes. *Biochemical and biophysical research communications*. 366:724-730.

Capitani, M., and M. Sallese. 2009. The KDEL receptor: new functions for an old protein. *FEBS letters*. 583:3863-3871.

Carlton, J., M. Bujny, B.J. Peter, V.M. Oorschot, A. Rutherford, H. Mellor, J. Klumperman, H.T. McMahon, and P.J. Cullen. 2004. Sorting nexin-1 mediates tubular endosome-to-TGN transport through coincidence sensing of high-curvature membranes and 3-phosphoinositides. *Curr.Biol.* 14:1791-1800.

Carpten, J.D., A.L. Faber, C. Horn, G.P. Donoho, S.L. Briggs, C.M. Robbins, G. Hostetter, S. Boguslawski, T.Y. Moses, S. Savage, M. Uhlik, A. Lin, J. Du, Y.W. Qian, D.J. Zeckner, G. Tucker-Kellogg, J. Touchman, K. Patel, S. Mousses, M. Bittner, R. Schevitz, M.H. Lai, K.L. Blanchard, and J.E. Thomas. 2007. A transforming mutation in the pleckstrin homology domain of AKT1 in cancer. *Nature*. 448:439-444.

Carvajal-Gonzalez, J.M., D. Gravotta, R. Mattera, F. Diaz, A. Perez Bay, A.C. Roman, R.P. Schreiner, R. Thuenauer, J.S. Bonifacino, and E. Rodriguez-Boulan. 2012. Basolateral sorting of the coxsackie and adenovirus receptor through interaction of a canonical YXXPhi motif with the clathrin adaptors AP-1A and AP-1B. *Proceedings of the National Academy of Sciences of the United States of America*. 109:3820-3825.

Caswell, P.T., M. Chan, A.J. Lindsay, M.W. McCaffrey, D. Boettiger, and J.C. Norman. 2008. Rab-coupling protein coordinates recycling of alpha5beta1 integrin and EGFR1 to promote cell migration in 3D microenvironments. *The Journal of cell biology*. 183:143-155.

Chen, S., P. Novick, and S. Ferro-Novick. 2013. ER structure and function. *Current opinion in cell biology*. 25:428-433.

Chen, W., Y. Feng, D. Chen, and A. Wandinger-Ness. 1998. Rab11 is required for trans-golgi network-to-plasma membrane transport and a preferential target for GDP dissociation inhibitor. *Molecular biology of the cell*. 9:3241-3257.

Cheng, P., C.S. Lau, A. Lai, E. Ho, P. Leung, F. Chan, A. Wong, and W. Lim. 2009. A novel reovirus isolated from a patient with acute respiratory disease. *Journal of clinical virology : the official publication of the Pan American Society for Clinical Virology*. 45:79-80.

Choy, R.W., Z. Cheng, and R. Schekman. 2012. Amyloid precursor protein (APP) traffics from the cell surface via endosomes for amyloid beta (Abeta) production in the trans-Golgi network. *Proceedings of the National Academy of Sciences of the United States of America*. 109:E2077-2082.

Chua, K.B., G. Crameri, A. Hyatt, M. Yu, M.R. Tompang, J. Rosli, J. McEachern, S. Crameri, V. Kumarasamy, B.T. Eaton, and L.F. Wang. 2007. A previously unknown reovirus of bat origin is associated with an acute respiratory disease in humans. *Proceedings of the National Academy of Sciences of the United States of America*. 104:11424-11429.

Chua, K.B., K. Voon, G. Crameri, H.S. Tan, J. Rosli, J.A. McEachern, S. Suluraju, M. Yu, and L.F. Wang. 2008. Identification and characterization of a new orthoreovirus from patients with acute respiratory infections. *PloS one*. 3:e3803.

Chua, K.B., K. Voon, M. Yu, C. Keniscope, K. Abdul Rasid, and L.F. Wang. 2011. Investigation of a potential zoonotic transmission of orthoreovirus associated with acute influenza-like illness in an adult patient. *PloS one*. 6:e25434.

Ciechonska, M., and R. Duncan. 2014. Reovirus FAST proteins: virus-encoded cellular fusogens. *Trends in microbiology*. 22:715-724.

Ciechonska, M., T. Key, and R. Duncan. 2014. Efficient reovirus- and measles virus-mediated pore expansion during syncytium formation is dependent on annexin A1 and intracellular calcium. *Journal of virology*. 88:6137-6147.

Clancy, E.K., C. Barry, M. Ciechonska, and R. Duncan. 2010. Different activities of the reovirus FAST proteins and influenza hemagglutinin in cell-cell fusion assays and in response to membrane curvature agents. *Virology*. 397:119-129.

Cobbold, C., A.P. Monaco, A. Sivaprasadarao, and S. Ponnambalam. 2003. Aberrant trafficking of transmembrane proteins in human disease. *Trends in cell biology*. 13:639-647.

Collins, B.M. 2008. The structure and function of the retromer protein complex. *Traffic*. 9:1811-1822.

Collins, B.M., A.J. McCoy, H.M. Kent, P.R. Evans, and D.J. Owen. 2002. Molecular architecture and functional model of the endocytic AP2 complex. *Cell*. 109:523-535.

Corcoran, J.A., E.K. Clancy, and R. Duncan. 2011. Homomultimerization of the reovirus p14 fusion-associated small transmembrane protein during transit through the ER-Golgi complex secretory pathway. *The Journal of general virology*. 92:162-166.

Corcoran, J.A., and R. Duncan. 2004. Reptilian reovirus utilizes a small type III protein with an external myristylated amino terminus to mediate cell-cell fusion. *Journal of virology*. 78:4342-4351.

Corcoran, J.A., J. Salsman, R. de Antueno, A. Touhami, M.H. Jericho, E.K. Clancy, and R. Duncan. 2006. The p14 fusion-associated small transmembrane (FAST) protein effects membrane fusion from a subset of membrane microdomains. *The Journal of biological chemistry*. 281:31778-31789.

Corcoran, J.A., R. Syvitski, D. Top, R.M. Epand, R.F. Epand, D. Jakeman, and R. Duncan. 2004. Myristoylation, a protruding loop, and structural plasticity are essential features of a nonenveloped virus fusion peptide motif. *The Journal of biological chemistry*. 279:51386-51394.

Cosson, P., and F. Letourneur. 1994. Coatomer interaction with di-lysine endoplasmic reticulum retention motifs. *Science*. 263:1629-1631.

Costes, S.V., D. Daelemans, E.H. Cho, Z. Dobbin, G. Pavlakis, and S. Lockett. 2004. Automatic and quantitative measurement of protein-protein colocalization in live cells. *Biophysical journal*. 86:3993-4003.

Cukierman, E., I. Huber, M. Rotman, and D. Cassel. 1995. The ARF1 GTPase-activating protein: zinc finger motif and Golgi complex localization. *Science*. 270:1999-2002.

Cullen, P.J. 2008. Endosomal sorting and signalling: an emerging role for sorting nexins. *Nat.Rev.Mol.Cell Biol.* 9:574-582.

Czech, M.P. 2000. PIP2 and PIP3: complex roles at the cell surface. *Cell*. 100:603-606.

D'Souza, R.S., R. Semus, E.A. Billings, C.B. Meyer, K. Conger, and J.E. Casanova. 2014. Rab4 orchestrates a small GTPase cascade for recruitment of adaptor proteins to early endosomes. *Current biology : CB*. 24:1187-1198.

Dahan, S., J.P. Ahluwalia, L. Wong, B.I. Posner, and J.J. Bergeron. 1994. Concentration of intracellular hepatic apolipoprotein E in Golgi apparatus saccular distensions and endosomes. *The Journal of cell biology*. 127:1859-1869.

Dai, J., J. Li, E. Bos, M. Porcionatto, R.T. Premont, S. Bourgoin, P.J. Peters, and V.W. Hsu. 2004. ACAP1 promotes endocytic recycling by recognizing recycling sorting signals. *Developmental cell*. 7:771-776.

Dawe, S., J.A. Corcoran, E.K. Clancy, J. Salsman, and R. Duncan. 2005. Unusual topological arrangement of structural motifs in the baboon reovirus fusion-associated small transmembrane protein. *Journal of virology*. 79:6216-6226.

Dawe, S., and R. Duncan. 2002. The S4 genome segment of baboon reovirus is bicistronic and encodes a novel fusion-associated small transmembrane protein. *Journal of virology*. 76:2131-2140.

De Matteis, M.A., and A. Luini. 2008. Exiting the Golgi complex. *Nature reviews. Molecular cell biology*. 9:273-284.

Deora, A.A., D. Gravotta, G. Kreitzer, J. Hu, D. Bok, and E. Rodriguez-Boulan. 2004. The basolateral targeting signal of CD147 (EMMPRIN) consists of a single leucine and is not recognized by retinal pigment epithelium. *Molecular biology of the cell*. 15:4148-4165.

Diaz, F., D. Gravotta, A. Deora, R. Schreiner, J. Schoggins, E. Falck-Pedersen, and E. Rodriguez-Boulan. 2009. Clathrin adaptor AP1B controls adenovirus infectivity of epithelial cells. *Proceedings of the National Academy of Sciences of the United States of America*. 106:11143-11148.

Dong, C., C.D. Nichols, J. Guo, W. Huang, N.A. Lambert, and G. Wu. 2012. A triple arg motif mediates alpha(2B)-adrenergic receptor interaction with Sec24C/D and export. *Traffic*. 13:857-868.

Dong, C., and G. Wu. 2006. Regulation of anterograde transport of alpha2-adrenergic receptors by the N termini at multiple intracellular compartments. *The Journal of biological chemistry*. 281:38543-38554.

Duden, R. 2003. ER-to-Golgi transport: COP I and COP II function (Review). *Molecular membrane biology*. 20:197-207.

Duncan, R. 1999. Extensive sequence divergence and phylogenetic relationships between the fusogenic and nonfusogenic orthoreoviruses: a species proposal. *Virology*. 260:316-328.

Duncan, R., J. Corcoran, J. Shou, and D. Stoltz. 2004. Reptilian reovirus: a new fusogenic orthoreovirus species. *Virology*. 319:131-140.

Duncan, R., and K. Sullivan. 1998. Characterization of two avian reoviruses that exhibit strain-specific quantitative differences in their syncytium-inducing and pathogenic capabilities. *Virology*. 250:263-272.

Dunn, K.W., M.M. Kamocka, and J.H. McDonald. 2011. A practical guide to evaluating colocalization in biological microscopy. *American journal of physiology. Cell physiology*. 300:C723-742.

Dunphy, W.G., and J.E. Rothman. 1985. Compartmental organization of the Golgi stack. *Cell*. 42:13-21.

Dupre, D.J., M. Robitaille, N. Ethier, L.R. Villeneuve, A.M. Mamarbachi, and T.E. Hebert. 2006. Seven transmembrane receptor core signaling complexes are assembled prior to plasma membrane trafficking. *The Journal of biological chemistry*. 281:34561-34573.

Duronio, V. 2008. The life of a cell: apoptosis regulation by the PI3K/PKB pathway. *The Biochemical journal*. 415:333-344.

Duvernay, M.T., C. Dong, X. Zhang, M. Robitaille, T.E. Hebert, and G. Wu. 2009a. A single conserved leucine residue on the first intracellular loop regulates ER export of G protein-coupled receptors. *Traffic*. 10:552-566.

Duvernay, M.T., C. Dong, X. Zhang, F. Zhou, C.D. Nichols, and G. Wu. 2009b. Anterograde trafficking of G protein-coupled receptors: function of the C-terminal F(X)6LL motif in export from the endoplasmic reticulum. *Molecular pharmacology*. 75:751-761.

Duvernay, M.T., F. Zhou, and G. Wu. 2004. A conserved motif for the transport of G protein-coupled receptors from the endoplasmic reticulum to the cell surface. *J.Biol.Chem.* 279:30741-30750.

Eathiraj, S., A. Mishra, R. Prekeris, and D.G. Lambright. 2006. Structural basis for Rab11-mediated recruitment of FIP3 to recycling endosomes. *Journal of molecular biology*. 364:121-135.

Engelman, J.A., J. Luo, and L.C. Cantley. 2006. The evolution of phosphatidylinositol 3-kinases as regulators of growth and metabolism. *Nature reviews. Genetics*. 7:606-619.

Espenshade, P., R.E. Gimeno, E. Holzmacher, P. Teung, and C.A. Kaiser. 1995. Yeast SEC16 gene encodes a multidomain vesicle coat protein that interacts with Sec23p. *The Journal of cell biology*. 131:311-324.

Esseltine, J.L., L.B. Dale, and S.S. Ferguson. 2011. Rab GTPases bind at a common site within the angiotensin II type I receptor carboxyl-terminal tail: evidence that Rab4 regulates receptor phosphorylation, desensitization, and resensitization. *Molecular pharmacology*. 79:175-184.

Faini, M., R. Beck, F.T. Wieland, and J.A. Briggs. 2013. Vesicle coats: structure, function, and general principles of assembly. *Trends in cell biology*. 23:279-288.

Farhan, H., V. Reiterer, V.M. Korkhov, J.A. Schmid, M. Freissmuth, and H.H. Sitte. 2007. Concentrative export from the endoplasmic reticulum of the gamma-aminobutyric acid transporter 1 requires binding to SEC24D. *The Journal of biological chemistry*. 282:7679-7689.

Farhan, H., M. Weiss, K. Tani, R.J. Kaufman, and H.P. Hauri. 2008. Adaptation of endoplasmic reticulum exit sites to acute and chronic increases in cargo load. *The EMBO journal*. 27:2043-2054.

Farquhar, M.G. 1985. Progress in unraveling pathways of Golgi traffic. *Annual review of cell biology*. 1:447-488.

Farquhar, M.G., and G.E. Palade. 1981. The Golgi apparatus (complex)-(1954-1981)-from artifact to center stage. *The Journal of cell biology*. 91:77s-103s.

Favaloro, V., F. Vilardi, R. Schlecht, M.P. Mayer, and B. Dobberstein. 2010. Asna1/TRC40-mediated membrane insertion of tail-anchored proteins. *Journal of cell science*. 123:1522-1530.

Feige, J.N., D. Sage, W. Wahli, B. Desvergne, and L. Gelman. 2005. PixFRET, an ImageJ plug-in for FRET calculation that can accommodate variations in spectral bleed-throughs. *Microscopy research and technique*. 68:51-58.

Ferguson, K.M., M.A. Lemmon, J. Schlessinger, and P.B. Sigler. 1995. Structure of the high affinity complex of inositol trisphosphate with a phospholipase C pleckstrin homology domain. *Cell*. 83:1037-1046.

Ferguson, S.M., A. Raimondi, S. Paradise, H. Shen, K. Mesaki, A. Ferguson, O. Destaing, G. Ko, J. Takasaki, O. Cremona, O.T. E, and P. De Camilli. 2009. Coordinated actions of actin and BAR proteins upstream of dynamin at endocytic clathrin-coated pits. *Developmental cell*. 17:811-822.

Fiedler, K., and K. Simons. 1995. The role of N-glycans in the secretory pathway. *Cell*. 81:309-312.

Fjorback, A.W., M. Seaman, C. Gustafsen, A. Mehmedbasic, S. Gokool, C. Wu, D. Militz, V. Schmidt, P. Madsen, J.R. Nyengaard, T.E. Willnow, E.I. Christensen, W.B. Mobley, A. Nykjaer, and O.M. Andersen. 2012. Retromer binds the FANSHY sorting motif in SorLA to regulate amyloid precursor protein sorting and processing. *The Journal of neuroscience : the official journal of the Society for Neuroscience*. 32:1467-1480.

Foote, C., and S.F. Nothwehr. 2006. The clathrin adaptor complex 1 directly binds to a sorting signal in Ste13p to reduce the rate of its trafficking to the late endosome of yeast. *The Journal of cell biology*. 173:615-626.

Fotin, A., Y. Cheng, N. Grigorieff, T. Walz, S.C. Harrison, and T. Kirchhausen. 2004. Structure of an auxilin-bound clathrin coat and its implications for the mechanism of uncoating. *Nature*. 432:649-653.

Fratti, R.A., Y. Jun, A.J. Merz, N. Margolis, and W. Wickner. 2004. Interdependent assembly of specific regulatory lipids and membrane fusion proteins into the vertex ring domain of docked vacuoles. *The Journal of cell biology*. 167:1087-1098.

Frigerio, G., N. Grimsey, M. Dale, I. Majoul, and R. Duden. 2007. Two human ARFGAPs associated with COP-I-coated vesicles. *Traffic*. 8:1644-1655.

Gage, R.M., K.A. Kim, T.T. Cao, and M. von Zastrow. 2001. A transplantable sorting signal that is sufficient to mediate rapid recycling of G protein-coupled receptors. *The Journal of biological chemistry*. 276:44712-44720.

Garbes, L., K. Kim, A. Riess, H. Hoyer-Kuhn, F. Beleggia, A. Bevot, M.J. Kim, Y.H. Huh, H.S. Kweon, R. Savarirayan, D. Amor, P.M. Kakadia, T. Lindig, K.O. Kagan, J. Becker, S.A. Boyadjiev, B. Wollnik, O. Semler, S.K. Bohlander, J. Kim, and C. Netzer. 2015. Mutations in SEC24D, Encoding a Component of the COPII Machinery, Cause a Syndromic Form of Osteogenesis Imperfecta. *American journal of human genetics*. 96:432-439.

Ghosh, P., and S. Kornfeld. 2003. AP-1 binding to sorting signals and release from clathrin-coated vesicles is regulated by phosphorylation. *The Journal of cell biology*. 160:699-708.

Gilchrist, A., C.E. Au, J. Hiding, A.W. Bell, J. Fernandez-Rodriguez, S. Lesimple, H. Nagaya, L. Roy, S.J. Gosline, M. Hallett, J. Paiement, R.E. Kearney, T. Nilsson, and J.J. Bergeron. 2006. Quantitative proteomics analysis of the secretory pathway. *Cell*. 127:1265-1281.

Gillingham, A.K., and S. Munro. 2007. The small G proteins of the Arf family and their regulators. *Annual review of cell and developmental biology*. 23:579-611.

Gimeno, R.E., P. Espenshade, and C.A. Kaiser. 1996. COPII coat subunit interactions: Sec24p and Sec23p bind to adjacent regions of Sec16p. *Molecular biology of the cell*. 7:1815-1823.

Giraudo, C.G., and H.J. Maccioni. 2003. Endoplasmic reticulum export of glycosyltransferases depends on interaction of a cytoplasmic dibasic motif with Sar1. *Molecular biology of the cell*. 14:3753-3766.

Glick, B.S., and A. Luini. 2011. Models for Golgi traffic: a critical assessment. *Cold Spring Harbor perspectives in biology*. 3:a005215.

Glick, B.S., and V. Malhotra. 1998. The curious status of the Golgi apparatus. *Cell*. 95:883-889.

Goder, V., and M. Spiess. 2001. Topogenesis of membrane proteins: determinants and dynamics. *FEBS letters*. 504:87-93.

Godi, A., C.A. Di, A. Konstantakopoulos, T.G. Di, D.R. Alessi, G.S. Kular, T. Daniele, P. Marra, J.M. Lucocq, and M.A. De Matteis. 2004. FAPPs control Golgi-to-cell-surface membrane traffic by binding to ARF and PtdIns(4)P. *Nat.Cell Biol.* 6:393-404.

Goldenring, J.R., K.R. Shen, H.D. Vaughan, and I.M. Modlin. 1993. Identification of a small GTP-binding protein, Rab25, expressed in the gastrointestinal mucosa, kidney, and lung. *The Journal of biological chemistry*. 268:18419-18422.

Gonzalez, A., and E. Rodriguez-Boulan. 2009. Clathrin and AP1B: key roles in basolateral trafficking through trans-endosomal routes. *FEBS letters*. 583:3784-3795.

Gorvel, J.P., P. Chavrier, M. Zerial, and J. Gruenberg. 1991. rab5 controls early endosome fusion in vitro. *Cell*. 64:915-925.

Goud, B., and P.A. Gleeson. 2010. TGN golgins, Rabs and cytoskeleton: regulating the Golgi trafficking highways. *Trends in cell biology*. 20:329-336.

Guo, H., X. Sun, L. Yan, L. Shao, and Q. Fang. 2013. The NS16 protein of aquareovirus-C is a fusion-associated small transmembrane (FAST) protein, and its activity can be enhanced by the nonstructural protein NS26. *Virus research*. 171:129-137.

Gut, A., F. Kappeler, N. Hyka, M.S. Balda, H.P. Hauri, and K. Matter. 1998. Carbohydrate-mediated Golgi to cell surface transport and apical targeting of membrane proteins. *The EMBO journal*. 17:1919-1929.

Haft, C.R., M. de la Luz Sierra, R. Bafford, M.A. Lesniak, V.A. Barr, and S.I. Taylor. 2000. Human orthologs of yeast vacuolar protein sorting proteins Vps26, 29, and 35: assembly into multimeric complexes. *Molecular biology of the cell*. 11:4105-4116.

Hales, C.M., J.P. Vaerman, and J.R. Goldenring. 2002. Rab11 family interacting protein 2 associates with Myosin Vb and regulates plasma membrane recycling. *The Journal of biological chemistry*. 277:50415-50421.

Hamelin, E., C. Theriault, G. Laroche, and J.L. Parent. 2005. The intracellular trafficking of the G protein-coupled receptor TPbeta depends on a direct interaction with Rab11. *The Journal of biological chemistry*. 280:36195-36205.

Hammad, M.M., Y.Q. Kuang, A. Morse, and D.J. Dupre. 2012. Rab1 interacts directly with the beta2-adrenergic receptor to regulate receptor anterograde trafficking. *Biological chemistry*. 393:541-546.

Hanada, K., K. Kumagai, N. Tomishige, and T. Yamaji. 2009. CERT-mediated trafficking of ceramide. *Biochimica et biophysica acta*. 1791:684-691.

Hara-Kuge, S., O. Kuge, L. Orci, M. Amherdt, M. Ravazzola, F.T. Wieland, and J.E. Rothman. 1994. En bloc incorporation of coatomer subunits during the assembly of COP-coated vesicles. *The Journal of cell biology*. 124:883-892.

Hardt, B., B. Kalz-Fuller, R. Aparicio, C. Volker, and E. Bause. 2003. (Arg)3 within the N-terminal domain of glucosidase I contains ER targeting information but is not required absolutely for ER localization. *Glycobiology*. 13:159-168.

Harrison, M.S., C.S. Hung, T.T. Liu, R. Christiano, T.C. Walther, and C.G. Burd. 2014. A mechanism for retromer endosomal coat complex assembly with cargo. *Proceedings of the National Academy of Sciences of the United States of America*. 111:267-272.

Harterink, M., F. Port, M.J. Lorenowicz, I.J. McGough, M. Silhankova, M.C. Betist, J.R. van Weering, R.G. van Heesbeen, T.C. Middelkoop, K. Basler, P.J. Cullen, and H.C. Korswagen. 2011. A SNX3-dependent retromer pathway mediates retrograde transport of the Wnt sorting receptor Wntless and is required for Wnt secretion. *Nature cell biology*. 13:914-923.

Haruki, H., J. Nishikawa, and U.K. Laemmli. 2008. The anchor-away technique: rapid, conditional establishment of yeast mutant phenotypes. *Molecular cell*. 31:925-932.

Hauri, H.P., F. Kappeler, H. Andersson, and C. Appenzeller. 2000. ERGIC-53 and traffic in the secretory pathway. *Journal of cell science*. 113 (Pt 4):587-596.

Hayer, A., M. Stoeber, D. Ritz, S. Engel, H.H. Meyer, and A. Helenius. 2010. Caveolin-1 is ubiquitinated and targeted to intralumenal vesicles in endolysosomes for degradation. *The Journal of cell biology*. 191:615-629.

He, J., J.L. Scott, A. Heroux, S. Roy, M. Lenoir, M. Overduin, R.V. Stahelin, and T.G. Kutateladze. 2011. Molecular basis of phosphatidylinositol 4-phosphate and ARF1 GTPase recognition by the FAPP1 pleckstrin homology (PH) domain. *The Journal of biological chemistry*. 286:18650-18657.

He, X., W.P. Chang, G. Koelsch, and J. Tang. 2002. Memapsin 2 (beta-secretase) cytosolic domain binds to the VHS domains of GGA1 and GGA2: implications on the endocytosis mechanism of memapsin 2. *FEBS letters*. 524:183-187.

He, X., F. Li, W.P. Chang, and J. Tang. 2005. GGA proteins mediate the recycling pathway of memapsin 2 (BACE). *The Journal of biological chemistry*. 280:11696-11703.

Hegde, R.S., and H.D. Bernstein. 2006. The surprising complexity of signal sequences. *Trends in biochemical sciences*. 31:563-571.

Heldwein, E.E., E. Macia, J. Wang, H.L. Yin, T. Kirchhausen, and S.C. Harrison. 2004. Crystal structure of the clathrin adaptor protein 1 core. *Proceedings of the National Academy of Sciences of the United States of America*. 101:14108-14113.

Henne, W.M., E. Boucrot, M. Meinecke, E. Evergren, Y. Vallis, R. Mittal, and H.T. McMahon. 2010. FCHo proteins are nucleators of clathrin-mediated endocytosis. *Science*. 328:1281-1284.

Higy, M., T. Junne, and M. Spiess. 2004. Topogenesis of membrane proteins at the endoplasmic reticulum. *Biochemistry*. 43:12716-12722.

Hinshaw, J.E., and S.L. Schmid. 1995. Dynamin self-assembles into rings suggesting a mechanism for coated vesicle budding. *Nature*. 374:190-192.

Hirst, J., L.D. Barlow, G.C. Francisco, D.A. Sahlender, M.N. Seaman, J.B. Dacks, and M.S. Robinson. 2011. The fifth adaptor protein complex. *PLoS biology*. 9:e1001170.

Hirst, J., C. Irving, and G.H. Borner. 2013. Adaptor protein complexes AP-4 and AP-5: new players in endosomal trafficking and progressive spastic paraplegia. *Traffic*. 14:153-164.

Honing, S., D. Ricotta, M. Krauss, K. Spate, B. Spolaore, A. Motley, M. Robinson, C. Robinson, V. Haucke, and D.J. Owen. 2005. Phosphatidylinositol-(4,5)-bisphosphate regulates sorting signal recognition by the clathrin-associated adaptor complex AP2. *Molecular cell*. 18:519-531.

Hope, H.R., and L.J. Pike. 1996. Phosphoinositides and phosphoinositide-utilizing enzymes in detergent-insoluble lipid domains. *Molecular biology of the cell*. 7:843-851.

Horgan, C.P., and M.W. McCaffrey. 2009. The dynamic Rab11-FIPs. *Biochemical Society transactions*. 37:1032-1036.

Horgan, C.P., and M.W. McCaffrey. 2012. Endosomal trafficking in animal cytokinesis. *Frontiers in bioscience*. 4:547-555.

Hu, J., Y. Shibata, C. Voss, T. Shemesh, Z. Li, M. Coughlin, M.M. Kozlov, T.A. Rapoport, and W.A. Prinz. 2008. Membrane proteins of the endoplasmic reticulum induce high-curvature tubules. *Science*. 319:1247-1250.

Huang, M., J.T. Weissman, S. Beraud-Dufour, P. Luan, C. Wang, W. Chen, M. Aridor, I.A. Wilson, and W.E. Balch. 2001. Crystal structure of Sar1-GDP at 1.7 A resolution and the role of the NH2 terminus in ER export. *The Journal of cell biology*. 155:937-948.

Hughes, H., A. Budnik, K. Schmidt, K.J. Palmer, J. Mantell, C. Noakes, A. Johnson, D.A. Carter, P. Verkade, P. Watson, and D.J. Stephens. 2009. Organisation of human ER-exit sites: requirements for the localisation of Sec16 to transitional ER. *Journal of cell science*. 122:2924-2934.

Hunziker, W., and C. Fumey. 1994. A di-leucine motif mediates endocytosis and basolateral sorting of macrophage IgG Fc receptors in MDCK cells. *The EMBO journal*. 13:2963-2969.

Huotari, J., and A. Helenius. 2011. Endosome maturation. *The EMBO journal*. 30:3481-3500.

Hutagalung, A.H., and P.J. Novick. 2011. Role of Rab GTPases in membrane traffic and cell physiology. *Physiological reviews*. 91:119-149.

Iinuma, T., A. Shiga, K. Nakamoto, M.B. O'Brien, M. Aridor, N. Arimitsu, M. Tagaya, and K. Tani. 2007. Mammalian Sec16/p250 plays a role in membrane traffic from the endoplasmic reticulum. *The Journal of biological chemistry*. 282:17632-17639.

Inoue, M., T. Shiba, K. Ihara, Y. Yamada, S. Hirano, H. Kamikubo, M. Kataoka, M. Kawasaki, R. Kato, K. Nakayama, and S. Wakatsuki. 2007. Molecular basis for autoregulatory interaction between GAE domain and hinge region of GGA1. *Traffic*. 8:904-913.

Itin, C., A.C. Roche, M. Monsigny, and H.P. Hauri. 1996. ERGIC-53 is a functional mannose-selective and calcium-dependent human homologue of leguminous lectins. *Molecular biology of the cell*. 7:483-493.

Jackson, C.L. 2009. Mechanisms of transport through the Golgi complex. *Journal of cell science*. 122:443-452.

Jackson, L.P., B.T. Kelly, A.J. McCoy, T. Gaffry, L.C. James, B.M. Collins, S. Honing, P.R. Evans, and D.J. Owen. 2010. A large-scale conformational change couples membrane recruitment to cargo binding in the AP2 clathrin adaptor complex. *Cell*. 141:1220-1229.

Jackson, L.P., M. Lewis, H.M. Kent, M.A. Edeling, P.R. Evans, R. Duden, and D.J. Owen. 2012. Molecular basis for recognition of dilysine trafficking motifs by COPI. *Developmental cell*. 23:1255-1262.

Jackson, M.R., T. Nilsson, and P.A. Peterson. 1990. Identification of a consensus motif for retention of transmembrane proteins in the endoplasmic reticulum. *The EMBO journal*. 9:3153-3162.

Jacques, K.M., Z. Nie, S. Stauffer, D.S. Hirsch, L.X. Chen, K.T. Stanley, and P.A. Randazzo. 2002. Arf1 dissociates from the clathrin adaptor GGA prior to being inactivated by Arf GTPase-activating proteins. *The Journal of biological chemistry*. 277:47235-47241.

Jagoe, W.N., A.J. Lindsay, R.J. Read, A.J. McCoy, M.W. McCaffrey, and A.R. Khan. 2006. Crystal structure of rab11 in complex with rab11 family interacting protein 2. *Structure*. 14:1273-1283.

Jahn, R., and R.H. Scheller. 2006. SNAREs--engines for membrane fusion. *Nature reviews. Molecular cell biology*. 7:631-643.

James Morre, D., and H.H. Mollenhauer. 2007. Microscopic morphology and the origins of the membrane maturation model of Golgi apparatus function. *International review of cytology*. 262:191-218.

Jones, B., E.L. Jones, S.A. Bonney, H.N. Patel, A.R. Mensenkamp, S. Eichenbaum-Voline, M. Rudling, U. Myrdal, G. Annesi, S. Naik, N. Meadows, A. Quattrone, S.A. Islam, R.P. Naoumova, B. Angelin, R. Infante, E. Levy, C.C. Roy, P.S. Freemont, J. Scott, and C.C. Shoulders. 2003. Mutations in a Sar1 GTPase of COPII vesicles are associated with lipid absorption disorders. *Nature genetics*. 34:29-31.

Kappeler, F., D.R. Klopfenstein, M. Foguet, J.P. Paccaud, and H.P. Hauri. 1997. The recycling of ERGIC-53 in the early secretory pathway. ERGIC-53 carries a cytosolic endoplasmic reticulum-exit determinant interacting with COPII. *The Journal of biological chemistry*. 272:31801-31808.

Kelly, B.T., S.C. Graham, N. Liska, P.N. Dannhauser, S. Honing, E.J. Ungewickell, and D.J. Owen. 2014. Clathrin adaptors. AP2 controls clathrin polymerization with a membrane-activated switch. *Science*. 345:459-463.

Kelly, B.T., and D.J. Owen. 2011. Endocytic sorting of transmembrane protein cargo. *Current opinion in cell biology*. 23:404-412.

Kelly, E.E., C.P. Horgan, and M.W. McCaffrey. 2012. Rab11 proteins in health and disease. *Biochemical Society transactions*. 40:1360-1367.

Key, T., and R. Duncan. 2014. A compact, multifunctional fusion module directs cholesterol-dependent homomultimerization and syncytiogenic efficiency of reovirus p10 FAST proteins. *PLoS pathogens*. 10:e1004023.

Key, T., M. Sarker, R. de Antueno, J.K. Rainey, and R. Duncan. 2015. The p10 FAST protein fusion peptide functions as a cystine noose to induce cholesterol-dependent liposome fusion without liposome tubulation. *Biochimica et biophysica acta*. 1848:408-416.

Kikuchi, A., T. Yamashita, M. Kawata, K. Yamamoto, K. Ikeda, T. Tanimoto, and Y. Takai. 1988. Purification and characterization of a novel GTP-binding protein with a molecular weight of 24,000 from bovine brain membranes. *The Journal of biological chemistry*. 263:2897-2904.

Kinsella, B.T., and W.A. Maltese. 1992. rab GTP-binding proteins with three different carboxyl-terminal cysteine motifs are modified in vivo by 20-carbon isoprenoids. *The Journal of biological chemistry*. 267:3940-3945.

Kleene, R., and E.G. Berger. 1993. The molecular and cell biology of glycosyltransferases. *Biochimica et biophysica acta*. 1154:283-325.

Kliouchnikov, L., J. Bigay, B. Mesmin, A. Parnis, M. Rawet, N. Goldfeder, B. Antonny, and D. Cassel. 2009. Discrete determinants in ArfGAP2/3 conferring Golgi localization and regulation by the COPI coat. *Molecular biology of the cell*. 20:859-869.

Klumperman, J., A. Schweizer, H. Clausen, B.L. Tang, W. Hong, V. Oorschot, and H.P. Hauri. 1998. The recycling pathway of protein ERGIC-53 and dynamics of the ER-Golgi intermediate compartment. *Journal of cell science*. 111 (Pt 22):3411-3425.

Knodler, A., S. Feng, J. Zhang, X. Zhang, A. Das, J. Peranen, and W. Guo. 2010. Coordination of Rab8 and Rab11 in primary ciliogenesis. *Proceedings of the National Academy of Sciences of the United States of America*. 107:6346-6351.

Kohl, C., R. Lesnik, A. Brinkmann, A. Ebinger, A. Radonic, A. Nitsche, K. Muhldorfer, G. Wibbelt, and A. Kurth. 2012. Isolation and characterization of three mammalian orthoreoviruses from European bats. *PloS one*. 7:e43106.

Koivisto, U.M., A.L. Hubbard, and I. Mellman. 2001. A novel cellular phenotype for familial hypercholesterolemia due to a defect in polarized targeting of LDL receptor. *Cell*. 105:575-585.

Kuehn, M.J., and R. Schekman. 1997. COPII and secretory cargo capture into transport vesicles. *Current opinion in cell biology*. 9:477-483.

Kumichel, A., K. Kapp, and E. Knust. 2015. A conserved di-basic motif of Drosophila Crumbs contributes to efficient ER export. *Traffic*.

Kung, L.F., S. Pagant, E. Futai, J.G. D'Arcangelo, R. Buchanan, J.C. Dittmar, R.J. Reid, R. Rothstein, S. Hamamoto, E.L. Snapp, R. Schekman, and E.A. Miller. 2012. Sec24p and Sec16p cooperate to regulate the GTP cycle of the COPII coat. *The EMBO journal*. 31:1014-1027.

Kurokawa, K., M. Okamoto, and A. Nakano. 2014. Contact of cis-Golgi with ER exit sites executes cargo capture and delivery from the ER. *Nature communications*. 5:3653.

Kutateladze, T.G., K.D. Ogburn, W.T. Watson, B.T. de, S.D. Emr, C.G. Burd, and M. Overduin. 1999. Phosphatidylinositol 3-phosphate recognition by the FYVE domain. *Mol.Cell*. 3:805-811.

Kutay, U., E. Hartmann, and T.A. Rapoport. 1993. A class of membrane proteins with a C-terminal anchor. *Trends in cell biology*. 3:72-75.

Laflamme, C., G. Assaker, D. Ramel, J.F. Dorn, D. She, P.S. Maddox, and G. Emery. 2012. Evi5 promotes collective cell migration through its Rab-GAP activity. *The Journal of cell biology*. 198:57-67.

Lai, F., L. Stubbs, and K. Artzt. 1994. Molecular analysis of mouse Rab11b: a new type of mammalian YPT/Rab protein. *Genomics*. 22:610-616.

Lamirande, E.W., D.K. Nichols, J.W. Owens, J.M. Gaskin, and E.R. Jacobson. 1999. Isolation and experimental transmission of a reovirus pathogenic in ratsnakes (Elaphe species). *Virus research*. 63:135-141.

Landgraf, K.E., C. Pilling, and J.J. Falke. 2008. Molecular mechanism of an oncogenic mutation that alters membrane targeting: Glu17Lys modifies the PIP lipid specificity of the AKT1 PH domain. *Biochemistry*. 47:12260-12269.

Lane, K.T., and L.S. Beese. 2006. Thematic review series: lipid posttranslational modifications. Structural biology of protein farnesyltransferase and geranylgeranyltransferase type I. *Journal of lipid research*. 47:681-699.

Lapierre, L.A., and J.R. Goldenring. 2005. Interactions of myosin vb with rab11 family members and cargoes traversing the plasma membrane recycling system. *Methods in enzymology*. 403:715-723.

Lavoie, C., J. Paiement, M. Dominguez, L. Roy, S. Dahan, J.N. Gushue, and J.J. Bergeron. 1999. Roles for alpha(2)p24 and COPI in endoplasmic reticulum cargo exit site formation. *The Journal of cell biology*. 146:285-299.

Lee, C., and J. Goldberg. 2010. Structure of coatomer cage proteins and the relationship among COPI, COPII, and clathrin vesicle coats. *Cell*. 142:123-132.

Leland, M.M., G.B. Hubbard, H.T. Sentmore, 3rd, K.F. Soike, and J.K. Hilliard. 2000. Outbreak of Orthoreovirus-induced meningoencephalomyelitis in baboons. *Comparative medicine*. 50:199-205.

Lemmon, M.A. 2007. Pleckstrin homology (PH) domains and phosphoinositides. *Biochemical Society symposium*:81-93.

Li, J., P.J. Peters, M. Bai, J. Dai, E. Bos, T. Kirchhausen, K.V. Kandror, and V.W. Hsu. 2007. An ACAP1-containing clathrin coat complex for endocytic recycling. *The Journal of cell biology*. 178:453-464.

Lindsay, A.J., and M.W. McCaffrey. 2002. Rab11-FIP2 functions in transferrin recycling and associates with endosomal membranes via its COOH-terminal domain. *The Journal of biological chemistry*. 277:27193-27199.

Lippincott-Schwartz, J., and R.D. Phair. 2010. Lipids and cholesterol as regulators of traffic in the endomembrane system. *Annual review of biophysics*. 39:559-578.

Liu, T.T., T.S. Gomez, B.K. Sackey, D.D. Billadeau, and C.G. Burd. 2012. Rab GTPase regulation of retromer-mediated cargo export during endosome maturation. *Molecular biology of the cell*. 23:2505-2515.

Lohia, M., Y. Qin, and I.G. Macara. 2012. The Scribble polarity protein stabilizes E-cadherin/p120-catenin binding and blocks retrieval of E-cadherin to the Golgi. *PloS one*. 7:e51130.

Losev, E., C.A. Reinke, J. Jellen, D.E. Strongin, B.J. Bevis, and B.S. Glick. 2006. Golgi maturation visualized in living yeast. *Nature*. 441:1002-1006.

Lu, L., R.N. Hannoush, B.C. Goess, S. Varadarajan, M.D. Shair, and T. Kirchhausen. 2013. The small molecule dispergo tubulates the endoplasmic reticulum and inhibits export. *Molecular biology of the cell*. 24:1020-1029.

Lubben, N.B., D.A. Sahlender, A.M. Motley, P.J. Lehner, P. Benaroch, and M.S. Robinson. 2007. HIV-1 Nef-induced down-regulation of MHC class I requires AP-1 and clathrin but not PACS-1 and is impeded by AP-2. *Molecular biology of the cell*. 18:3351-3365.

Ma, D., T.K. Taneja, B.M. Hagen, B.Y. Kim, B. Ortega, W.J. Lederer, and P.A. Welling. 2011. Golgi export of the Kir2.1 channel is driven by a trafficking signal located within its tertiary structure. *Cell*. 145:1102-1115.

Ma, D., N. Zerangue, Y.F. Lin, A. Collins, M. Yu, Y.N. Jan, and L.Y. Jan. 2001. Role of ER export signals in controlling surface potassium channel numbers. *Science*. 291:316-319.

Ma, W., and J. Goldberg. 2013. Rules for the recognition of dilysine retrieval motifs by coatomer. *The EMBO journal*. 32:926-937.

Malsam, J., S. Kreye, and T.H. Sollner. 2008. Membrane fusion: SNAREs and regulation. *Cellular and molecular life sciences : CMLS*. 65:2814-2832.

Malsam, J., A. Satoh, L. Pelletier, and G. Warren. 2005. Golgin tethers define subpopulations of COPI vesicles. *Science*. 307:1095-1098.

Mammoto, A., T. Ohtsuka, I. Hotta, T. Sasaki, and Y. Takai. 1999. Rab11BP/Rabphilin-11, a downstream target of rab11 small G protein implicated in vesicle recycling. *The Journal of biological chemistry*. 274:25517-25524.

Mancias, J.D., and J. Goldberg. 2008. Structural basis of cargo membrane protein discrimination by the human COPII coat machinery. *The EMBO journal*. 27:2918-2928.

Manzano-Lopez, J., A.M. Perez-Linero, A. Aguilera-Romero, M.E. Martin, T. Okano, D.V. Silva, P.H. Seeberger, H. Riezman, K. Funato, V. Goder, R.E. Wellinger, and M. Muniz. 2015. COPII coat composition is actively regulated by luminal cargo maturation. *Current biology : CB*. 25:152-162.

Margeta-Mitrovic, M., Y.N. Jan, and L.Y. Jan. 2000. A trafficking checkpoint controls GABA(B) receptor heterodimerization. *Neuron*. 27:97-106.

Martinez-Menarguez, J.A., H.J. Geuze, J.W. Slot, and J. Klumperman. 1999. Vesicular tubular clusters between the ER and Golgi mediate concentration of soluble secretory proteins by exclusion from COPI-coated vesicles. *Cell*. 98:81-90.

Martinez-Menarguez, J.A., R. Prekeris, V.M. Oorschot, R. Scheller, J.W. Slot, H.J. Geuze, and J. Klumperman. 2001. Peri-Golgi vesicles contain retrograde but not anterograde proteins consistent with the cisternal progression model of intra-Golgi transport. *The Journal of cell biology*. 155:1213-1224.

Martoglio, B., and B. Dobberstein. 1998. Signal sequences: more than just greasy peptides. *Trends Cell Biol.* 8:410-415.

Matsuoka, K., R. Schekman, L. Orci, and J.E. Heuser. 2001. Surface structure of the COPII-coated vesicle. *Proceedings of the National Academy of Sciences of the United States of America*. 98:13705-13709.

Matsuura-Tokita, K., M. Takeuchi, A. Ichihara, K. Mikuriya, and A. Nakano. 2006. Live imaging of yeast Golgi cisternal maturation. *Nature*. 441:1007-1010.

Matter, K., and I. Mellman. 1994. Mechanisms of cell polarity: sorting and transport in epithelial cells. *Current opinion in cell biology*. 6:545-554.

Matter, K., E.M. Yamamoto, and I. Mellman. 1994. Structural requirements and sequence motifs for polarized sorting and endocytosis of LDL and Fc receptors in MDCK cells. *The Journal of cell biology*. 126:991-1004.

Mayer, A., D. Scheglmann, S. Dove, A. Glatz, W. Wickner, and A. Haas. 2000. Phosphatidylinositol 4,5-bisphosphate regulates two steps of homotypic vacuole fusion. *Molecular biology of the cell*. 11:807-817.

McDonold, C.M., and J.C. Fromme. 2014. Four GTPases differentially regulate the Sec7 Arf-GEF to direct traffic at the trans-golgi network. *Developmental cell*. 30:759-767.

McEwen, D.P., S.M. Schumacher, Q. Li, M.D. Benson, J.A. Iniguez-Lluhi, K.M. Van Genderen, and J.R. Martens. 2007. Rab-GTPase-dependent endocytic recycling of Kv1.5 in atrial myocytes. *The Journal of biological chemistry*. 282:29612-29620.

McLauchlan, H., J. Newell, N. Morrice, A. Osborne, M. West, and E. Smythe. 1998. A novel role for Rab5-GDI in ligand sequestration into clathrin-coated pits. *Current biology : CB*. 8:34-45.

McMahon, C., S.M. Studer, C. Clendinen, G.P. Dann, P.D. Jeffrey, and F.M. Hughson. 2012. The structure of Sec12 implicates potassium ion coordination in Sar1 activation. *The Journal of biological chemistry*. 287:43599-43606.

McMahon, H.T., and E. Boucrot. 2011. Molecular mechanism and physiological functions of clathrin-mediated endocytosis. *Nature reviews. Molecular cell biology*. 12:517-533.

Mellman, I., and W.J. Nelson. 2008. Coordinated protein sorting, targeting and distribution in polarized cells. *Nature reviews. Molecular cell biology*. 9:833-845.

Mendoza, P., J. Diaz, and V.A. Torres. 2014. On the role of Rab5 in cell migration. *Current molecular medicine*. 14:235-245.

Mercer, J., M. Schelhaas, and A. Helenius. 2010. Virus entry by endocytosis. *Annual review of biochemistry*. 79:803-833.

Meyer, C., D. Zizioli, S. Lausmann, E.L. Eskelinen, J. Hamann, P. Saftig, K. von Figura, and P. Schu. 2000. mu1A-adaptin-deficient mice: lethality, loss of AP-1 binding and rerouting of mannose 6-phosphate receptors. *The EMBO journal*. 19:2193-2203.

Michelsen, K., H. Yuan, and B. Schwappach. 2005. Hide and run. Arginine-based endoplasmic-reticulum-sorting motifs in the assembly of heteromultimeric membrane proteins. *EMBO reports*. 6:717-722.

Miller, E., B. Antonny, S. Hamamoto, and R. Schekman. 2002. Cargo selection into COPII vesicles is driven by the Sec24p subunit. *The EMBO journal*. 21:6105-6113.

Miller, E.A., T.H. Beilharz, P.N. Malkus, M.C. Lee, S. Hamamoto, L. Orci, and R. Schekman. 2003. Multiple cargo binding sites on the COPII subunit Sec24p ensure capture of diverse membrane proteins into transport vesicles. *Cell*. 114:497-509.

Miranda, K.C., T. Khromykh, P. Christy, T.L. Le, C.J. Gottardi, A.S. Yap, J.L. Stow, and R.D. Teasdale. 2001. A dileucine motif targets E-cadherin to the basolateral cell surface in Madin-Darby canine kidney and LLC-PK1 epithelial cells. *The Journal of biological chemistry*. 276:22565-22572.

Mironov, A.A., G.V. Beznoussenko, P. Nicoziani, O. Martella, A. Trucco, H.S. Kweon, D. Di Giandomenico, R.S. Polishchuk, A. Fusella, P. Lupetti, E.G. Berger, W.J. Geerts, A.J. Koster, K.N. Burger, and A. Luini. 2001. Small cargo proteins and large aggregates can traverse the Golgi by a common mechanism without leaving the lumen of cisternae. *The Journal of cell biology*. 155:1225-1238.

Mironov, A.A., A.A. Mironov, Jr., G.V. Beznoussenko, A. Trucco, P. Lupetti, J.D. Smith, W.J. Geerts, A.J. Koster, K.N. Burger, M.E. Martone, T.J. Deerinck, M.H. Ellisman, and A. Luini. 2003. ER-to-Golgi carriers arise through direct en bloc protrusion and multistage maturation of specialized ER exit domains. *Developmental cell*. 5:583-594.

Mitrovic, S., H. Ben-Tekaya, E. Koegler, J. Gruenberg, and H.P. Hauri. 2008. The cargo receptors Surf4, endoplasmic reticulum-Golgi intermediate compartment (ERGIC)-53, and p25 are required to maintain the architecture of ERGIC and Golgi. *Molecular biology of the cell*. 19:1976-1990.

Mossessova, E., L.C. Bickford, and J. Goldberg. 2003. SNARE selectivity of the COPII coat. *Cell*. 114:483-495.

Muhammad, A., I. Flores, H. Zhang, R. Yu, A. Staniszewski, E. Planel, M. Herman, L. Ho, R. Kreber, L.S. Honig, B. Ganetzky, K. Duff, O. Arancio, and S.A. Small. 2008. Retromer deficiency observed in Alzheimer's disease causes hippocampal dysfunction, neurodegeneration, and Abeta accumulation. *Proceedings of the National Academy of Sciences of the United States of America*. 105:7327-7332.

Mullins, C., and J.S. Bonifacino. 2001. Structural requirements for function of yeast GGAs in vacuolar protein sorting, alpha-factor maturation, and interactions with clathrin. *Molecular and cellular biology*. 21:7981-7994.

Muniz, M., C. Nuoffer, H.P. Hauri, and H. Riezman. 2000. The Emp24 complex recruits a specific cargo molecule into endoplasmic reticulum-derived vesicles. *The Journal of cell biology*. 148:925-930.

Nakada-Tsukui, K., Y. Saito-Nakano, V. Ali, and T. Nozaki. 2005. A retromerlike complex is a novel Rab7 effector that is involved in the transport of the virulence factor cysteine protease in the enteric protozoan parasite Entamoeba histolytica. *Molecular biology of the cell*. 16:5294-5303.

Nakatsu, F., and H. Ohno. 2003. Adaptor protein complexes as the key regulators of protein sorting in the post-Golgi network. *Cell structure and function*. 28:419-429.

Nakayama, K., and S. Wakatsuki. 2003. The structure and function of GGAs, the traffic controllers at the TGN sorting crossroads. *Cell structure and function*. 28:431-442.

Ngo, M.H., T.R. Colbourne, and N.D. Ridgway. 2010. Functional implications of sterol transport by the oxysterol-binding protein gene family. *The Biochemical journal*. 429:13-24.

Nibert, M.L., and R. Duncan. 2013. Bioinformatics of recent aqua- and orthoreovirus isolates from fish: evolutionary gain or loss of FAST and fiber proteins and taxonomic implications. *PloS one*. 8:e68607.

Nichols, W.C., U. Seligsohn, A. Zivelin, V.H. Terry, C.E. Hertel, M.A. Wheatley, M.J. Moussalli, H.P. Hauri, N. Ciavarella, R.J. Kaufman, and D. Ginsburg. 1998. Mutations in the ER-Golgi intermediate compartment protein ERGIC-53 cause combined deficiency of coagulation factors V and VIII. *Cell*. 93:61-70.

Nielsen, E., F. Severin, J.M. Backer, A.A. Hyman, and M. Zerial. 1999. Rab5 regulates motility of early endosomes on microtubules. *Nature cell biology*. 1:376-382.

Nielsen, M.S., P. Madsen, E.I. Christensen, A. Nykjaer, J. Gliemann, D. Kasper, R. Pohlmann, and C.M. Petersen. 2001. The sortilin cytoplasmic tail conveys Golgi-endosome transport and binds the VHS domain of the GGA2 sorting protein. *The EMBO journal*. 20:2180-2190.

Nilsson, J., B. Persson, and G. von Heijne. 2005. Comparative analysis of amino acid distributions in integral membrane proteins from 107 genomes. *Proteins*. 60:606-616.

Nilsson, T., C.E. Au, and J.J. Bergeron. 2009. Sorting out glycosylation enzymes in the Golgi apparatus. *FEBS letters*. 583:3764-3769.

Nishimura, N., and W.E. Balch. 1997. A di-acidic signal required for selective export from the endoplasmic reticulum. *Science*. 277:556-558.

Nishimura, N., S. Bannykh, S. Slabough, J. Matteson, Y. Altschuler, K. Hahn, and W.E. Balch. 1999. A di-acidic (DXE) code directs concentration of cargo during export from the endoplasmic reticulum. *The Journal of biological chemistry*. 274:15937-15946.

Nothwehr, S.F., S.A. Ha, and P. Bruinsma. 2000. Sorting of yeast membrane proteins into an endosome-to-Golgi pathway involves direct interaction of their cytosolic domains with Vps35p. *The Journal of cell biology*. 151:297-310.

Novick, P., C. Field, and R. Schekman. 1980. Identification of 23 complementation groups required for post-translational events in the yeast secretory pathway. *Cell*. 21:205-215.

Nufer, O., F. Kappeler, S. Guldbrandsen, and H.P. Hauri. 2003. ER export of ERGIC-53 is controlled by cooperation of targeting determinants in all three of its domains. *Journal of cell science*. 116:4429-4440.

O'Donnell, J., K. Maddox, and S. Stagg. 2011. The structure of a COPII tubule. *Journal of structural biology*. 173:358-364.

O'Keeffe, M.B., H.M. Reid, and B.T. Kinsella. 2008. Agonist-dependent internalization and trafficking of the human prostacyclin receptor: a direct role for Rab5a GTPase. *Biochimica et biophysica acta*. 1783:1914-1928.

Ohno, H. 2006. Clathrin-associated adaptor protein complexes. *Journal of cell science*. 119:3719-3721.

Orci, L., M. Ravazzola, P. Meda, C. Holcomb, H.P. Moore, L. Hicke, and R. Schekman. 1991. Mammalian Sec23p homologue is restricted to the endoplasmic reticulum transitional cytoplasm. *Proceedings of the National Academy of Sciences of the United States of America*. 88:8611-8615.

Orci, L., M. Ravazzola, A. Volchuk, T. Engel, M. Gmachl, M. Amherdt, A. Perrelet, T.H. Sollner, and J.E. Rothman. 2000. Anterograde flow of cargo across the golgi stack potentially mediated via bidirectional "percolating" COPI vesicles. *Proceedings of the National Academy of Sciences of the United States of America*. 97:10400-10405.

Orci, L., M. Stamnes, M. Ravazzola, M. Amherdt, A. Perrelet, T.H. Sollner, and J.E. Rothman. 1997. Bidirectional transport by distinct populations of COPI-coated vesicles. *Cell*. 90:335-349.

Ostermann, J., L. Orci, K. Tani, M. Amherdt, M. Ravazzola, Z. Elazar, and J.E. Rothman. 1993. Stepwise assembly of functionally active transport vesicles. *Cell*. 75:1015-1025.

Paczkowski, J.E., B.C. Richardson, and J.C. Fromme. 2015. Cargo adaptors: structures illuminate mechanisms regulating vesicle biogenesis. *Trends in cell biology*.

Pagant, S., A. Wu, S. Edwards, F. Diehl, and E.A. Miller. 2015. Sec24 is a coincidence detector that simultaneously binds two signals to drive ER export. *Current biology : CB*. 25:403-412.

Pandey, K.N., H.T. Nguyen, R. Garg, M.L. Khurana, and J. Fink. 2005. Internalization and trafficking of guanylyl (guanylate) cyclase/natriuretic peptide receptor A is regulated by an acidic tyrosine-based cytoplasmic motif GDAY. *The Biochemical journal*. 388:103-113.

Parachoniak, C.A., Y. Luo, J.V. Abella, J.H. Keen, and M. Park. 2011. GGA3 functions as a switch to promote Met receptor recycling, essential for sustained ERK and cell migration. *Developmental cell*. 20:751-763.

Parent, A., E. Hamelin, P. Germain, and J.L. Parent. 2009. Rab11 regulates the recycling of the beta2-adrenergic receptor through a direct interaction. *The Biochemical journal*. 418:163-172.

Park, W.S., W.D. Heo, J.H. Whalen, N.A. O'Rourke, H.M. Bryan, T. Meyer, and M.N. Teruel. 2008. Comprehensive identification of PIP3-regulated PH domains from C. elegans to H. sapiens by model prediction and live imaging. *Molecular cell*. 30:381-392.

Parmar, H.B., C. Barry, and R. Duncan. 2014a. Polybasic trafficking signal mediates golgi export, ER retention or ER export and retrieval based on membrane-proximity. *PloS one*. 9:e94194.

Parmar, H.B., C. Barry, F. Kai, and R. Duncan. 2014b. Golgi complex-plasma membrane trafficking directed by an autonomous, tribasic Golgi export signal. *Molecular biology of the cell*. 25:866-878.

Patterson, G.H., K. Hirschberg, R.S. Polishchuk, D. Gerlich, R.D. Phair, and J. Lippincott-Schwartz. 2008. Transport through the Golgi apparatus by rapid partitioning within a two-phase membrane system. *Cell*. 133:1055-1067.

Pelham, H.R., and J.E. Rothman. 2000. The debate about transport in the Golgi--two sides of the same coin? *Cell*. 102:713-719.

Pevzner, I., J. Strating, L. Lifshitz, A. Parnis, F. Glaser, A. Herrmann, B. Brugger, F. Wieland, and D. Cassel. 2012. Distinct role of subcomplexes of the COPI coat in the regulation of ArfGAP2 activity. *Traffic*. 13:849-856.

Pfeffer, S.R. 2013. Rab GTPase regulation of membrane identity. *Current opinion in cell biology*. 25:414-419.

Piccolo, E., P.F. Innominato, M.A. Mariggio, T. Maffucci, S. Iacobelli, and M. Falasca. 2002. The mechanism involved in the regulation of phospholipase Cgamma1 activity in cell migration. *Oncogene*. 21:6520-6529.

Pilling, C., K.E. Landgraf, and J.J. Falke. 2011. The GRP1 PH domain, like the AKT1 PH domain, possesses a sentry glutamate residue essential for specific targeting to plasma membrane PI(3,4,5)P(3). *Biochemistry*. 50:9845-9856.

Pocha, S.M., T. Wassmer, C. Niehage, B. Hoflack, and E. Knust. 2011. Retromer controls epithelial cell polarity by trafficking the apical determinant Crumbs. *Current biology : CB*. 21:1111-1117.

Popova, N.V., I.E. Deyev, and A.G. Petrenko. 2013. Clathrin-mediated endocytosis and adaptor proteins. *Acta naturae*. 5:62-73.

Preuss, D., J. Mulholland, A. Franzusoff, N. Segev, and D. Botstein. 1992. Characterization of the Saccharomyces Golgi complex through the cell cycle by immunoelectron microscopy. *Molecular biology of the cell*. 3:789-803.

Puertollano, R., R.C. Aguilar, I. Gorshkova, R.J. Crouch, and J.S. Bonifacino. 2001a. Sorting of mannose 6-phosphate receptors mediated by the GGAs. *Science*. 292:1712-1716.

Puertollano, R., P.A. Randazzo, J.F. Presley, L.M. Hartnell, and J.S. Bonifacino. 2001b. The GGAs promote ARF-dependent recruitment of clathrin to the TGN. *Cell*. 105:93-102.

Purvanov, V., A. Koval, and V.L. Katanaev. 2010. A direct and functional interaction between Go and Rab5 during G protein-coupled receptor signaling. *Science signaling*. 3:ra65.

Quintero, C.A., C.G. Giraudo, M. Villarreal, G. Montich, and H.J. Maccioni. 2010. Identification of a site in Sar1 involved in the interaction with the cytoplasmic tail of glycolipid glycosyltransferases. *The Journal of biological chemistry*. 285:30340-30346.

Rabouille, C., N. Hui, F. Hunte, R. Kieckbusch, E.G. Berger, G. Warren, and T. Nilsson. 1995. Mapping the distribution of Golgi enzymes involved in the construction of complex oligosaccharides. *Journal of cell science*. 108 (Pt 4):1617-1627.

Rabouille, C., and J. Klumperman. 2005. Opinion: The maturing role of COPI vesicles in intra-Golgi transport. *Nature reviews. Molecular cell biology*. 6:812-817.

Rabu, C., V. Schmid, B. Schwappach, and S. High. 2009. Biogenesis of tail-anchored proteins: the beginning for the end? *Journal of cell science*. 122:3605-3612.

Racine, T., T. Hurst, C. Barry, J. Shou, F. Kibenge, and R. Duncan. 2009. Aquareovirus effects syncytiogenesis by using a novel member of the FAST protein family translated from a noncanonical translation start site. *Journal of virology*. 83:5951-5955.

Rapoport, I., W. Boll, A. Yu, T. Bocking, and T. Kirchhausen. 2008. A motif in the clathrin heavy chain required for the Hsc70/auxilin uncoating reaction. *Molecular biology of the cell*. 19:405-413.

Rapoport, T.A. 2007. Protein translocation across the eukaryotic endoplasmic reticulum and bacterial plasma membranes. *Nature*. 450:663-669.

Reider, A., S.L. Barker, S.K. Mishra, Y.J. Im, L. Maldonado-Baez, J.H. Hurley, L.M. Traub, and B. Wendland. 2009. Syp1 is a conserved endocytic adaptor that contains domains involved in cargo selection and membrane tubulation. *The EMBO journal*. 28:3103-3116.

Reinhard, C., M. Schweikert, F.T. Wieland, and W. Nickel. 2003. Functional reconstitution of COPI coat assembly and disassembly using chemically defined components. *Proceedings of the National Academy of Sciences of the United States of America*. 100:8253-8257.

Rejman Lipinski, A., J. Heymann, C. Meissner, A. Karlas, V. Brinkmann, T.F. Meyer, and D. Heuer. 2009. Rab6 and Rab11 regulate Chlamydia trachomatis development and golgin-84-dependent Golgi fragmentation. *PLoS pathogens*. 5:e1000615.

Ren, X., G.G. Farias, B.J. Canagarajah, J.S. Bonifacino, and J.H. Hurley. 2013. Structural basis for recruitment and activation of the AP-1 clathrin adaptor complex by Arf1. *Cell*. 152:755-767.

Renard, H.F., M. Simunovic, J. Lemiere, E. Boucrot, M.D. Garcia-Castillo, S. Arumugam, V. Chambon, C. Lamaze, C. Wunder, A.K. Kenworthy, A.A. Schmidt, H.T. McMahon, C. Sykes, P. Bassereau, and L. Johannes. 2015. Endophilin-A2 functions in membrane scission in clathrin-independent endocytosis. *Nature*. 517:493-496.

Robert, J., E. Clauser, P.X. Petit, and M.A. Ventura. 2005. A novel C-terminal motif is necessary for the export of the vasopressin V1b/V3 receptor to the plasma membrane. *The Journal of biological chemistry*. 280:2300-2308.

Robinson, M.S. 2004. Adaptable adaptors for coated vesicles. *Trends in cell biology*. 14:167-174.

Robinson, M.S., D.A. Sahlender, and S.D. Foster. 2010. Rapid inactivation of proteins by rapamycin-induced rerouting to mitochondria. *Developmental cell*. 18:324-331.

Rodriguez-Boulan, E., and A. Musch. 2005. Protein sorting in the Golgi complex: shifting paradigms. *Biochimica et biophysica acta*. 1744:455-464.

Rojas, R., T. van Vlijmen, G.A. Mardones, Y. Prabhu, A.L. Rojas, S. Mohammed, A.J. Heck, G. Raposo, P. van der Sluijs, and J.S. Bonifacino. 2008. Regulation of retromer recruitment to endosomes by sequential action of Rab5 and Rab7. *The Journal of cell biology*. 183:513-526.

Rossanese, O.W., J. Soderholm, B.J. Bevis, I.B. Sears, J. O'Connor, E.K. Williamson, and B.S. Glick. 1999. Golgi structure correlates with transitional endoplasmic reticulum organization in Pichia pastoris and Saccharomyces cerevisiae. *The Journal of cell biology*. 145:69-81.

Rothman, J.E. 1981. The golgi apparatus: two organelles in tandem. *Science*. 213:1212-1219.

Rothman, J.E., and F.T. Wieland. 1996. Protein sorting by transport vesicles. *Science*. 272:227-234.

Rubino, M., M. Miaczynska, R. Lippe, and M. Zerial. 2000. Selective membrane recruitment of EEA1 suggests a role in directional transport of clathrin-coated vesicles to early endosomes. *The Journal of biological chemistry*. 275:3745-3748.

Rzomp, K.A., L.D. Scholtes, B.J. Briggs, G.R. Whittaker, and M.A. Scidmore. 2003. Rab GTPases are recruited to chlamydial inclusions in both a species-dependent and species-independent manner. *Infection and immunity*. 71:5855-5870.

Sakurada, K., K. Uchida, K. Yamaguchi, K. Aisaka, S. Ito, T. Ohmori, Y. Takeyama, T. Ueda, Y. Hori, H. Ohyanagi, and et al. 1991. Molecular cloning and characterization of a ras p21-like GTP-binding protein (24KG) from rat liver. *Biochemical and biophysical research communications*. 177:1224-1232.

Salsman, J., D. Top, C. Barry, and R. Duncan. 2008. A virus-encoded cell-cell fusion machine dependent on surrogate adhesins. *PLoS pathogens*. 4:e1000016.

Salsman, J., D. Top, J. Boutilier, and R. Duncan. 2005. Extensive syncytium formation mediated by the reovirus FAST proteins triggers apoptosis-induced membrane instability. *Journal of virology*. 79:8090-8100.

Samal, S.K., H. Attoui, F. Mohd Jaafer, and P.P.C. Mertens. 2005. *Aquareovirus, Reoviridae*. Elsevier/Academic Press, London, United Kingdom.

Saraogi, I., and S.O. Shan. 2011. Molecular mechanism of co-translational protein targeting by the signal recognition particle. *Traffic*. 12:535-542.

Sasaki, T., A. Kikuchi, S. Araki, Y. Hata, M. Isomura, S. Kuroda, and Y. Takai. 1990. Purification and characterization from bovine brain cytosol of a protein that inhibits the dissociation of GDP from and the subsequent binding of GTP to smg p25A, a ras p21-like GTP-binding protein. *The Journal of biological chemistry*. 265:2333-2337.

Scheele, U., C. Kalthoff, and E. Ungewickell. 2001. Multiple interactions of auxilin 1 with clathrin and the AP-2 adaptor complex. *The Journal of biological chemistry*. 276:36131-36138.

Schindelin, J., I. Arganda-Carreras, E. Frise, V. Kaynig, M. Longair, T. Pietzsch, S. Preibisch, C. Rueden, S. Saalfeld, B. Schmid, J.Y. Tinevez, D.J. White, V. Hartenstein, K. Eliceiri, P. Tomancak, and A. Cardona. 2012. Fiji: an open-source platform for biological-image analysis. *Nature methods*. 9:676-682.

Schlossman, D.M., S.L. Schmid, W.A. Braell, and J.E. Rothman. 1984. An enzyme that removes clathrin coats: purification of an uncoating ATPase. *The Journal of cell biology*. 99:723-733.

Schonteich, E., G.M. Wilson, J. Burden, C.R. Hopkins, K. Anderson, J.R. Goldenring, and R. Prekeris. 2008. The Rip11/Rab11-FIP5 and kinesin II complex regulates endocytic protein recycling. *Journal of cell science*. 121:3824-3833.

Schulein, R., R. Hermosilla, A. Oksche, M. Dehe, B. Wiesner, G. Krause, and W. Rosenthal. 1998. A dileucine sequence and an upstream glutamate residue in the intracellular carboxyl terminus of the vasopressin V2 receptor are essential for cell surface transport in COS.M6 cells. *Molecular pharmacology*. 54:525-535.

Schweizer, F.E., T. Schafer, and M.M. Burger. 1991. Intracellular mechanisms in exocytotic secretion. *Biochemical pharmacology*. 41:163-169.

Scott, D.B., T.A. Blanpied, G.T. Swanson, C. Zhang, and M.D. Ehlers. 2001. An NMDA receptor ER retention signal regulated by phosphorylation and alternative splicing. *J.Neurosci.* 21:3063-3072.

Seabra, M.C., Y. Reiss, P.J. Casey, M.S. Brown, and J.L. Goldstein. 1991. Protein farnesyltransferase and geranylgeranyltransferase share a common alpha subunit. *Cell*. 65:429-434.

Seabra, M.C., and C. Wasmeier. 2004. Controlling the location and activation of Rab GTPases. *Current opinion in cell biology*. 16:451-457.

Seachrist, J.L., S.A. Laporte, L.B. Dale, A.V. Babwah, M.G. Caron, P.H. Anborgh, and S.S. Ferguson. 2002. Rab5 association with the angiotensin II type 1A receptor promotes Rab5 GTP binding and vesicular fusion. *The Journal of biological chemistry*. 277:679-685.

Seaman, M.N. 2007. Identification of a novel conserved sorting motif required for retromer-mediated endosome-to-TGN retrieval. *Journal of cell science*. 120:2378-2389.

Seaman, M.N. 2012. The retromer complex - endosomal protein recycling and beyond. *Journal of cell science*. 125:4693-4702.

Seaman, M.N., M.E. Harbour, D. Tattersall, E. Read, and N. Bright. 2009. Membrane recruitment of the cargo-selective retromer subcomplex is catalysed by the small GTPase Rab7 and inhibited by the Rab-GAP TBC1D5. *Journal of cell science*. 122:2371-2382.

Seaman, M.N., J.M. McCaffery, and S.D. Emr. 1998. A membrane coat complex essential for endosome-to-Golgi retrograde transport in yeast. *The Journal of cell biology*. 142:665-681.

Seet, L.F., and W. Hong. 2006. The Phox (PX) domain proteins and membrane traffic. *Biochimica et biophysica acta*. 1761:878-896.

Sekar, R.B., and A. Periasamy. 2003. Fluorescence resonance energy transfer (FRET) microscopy imaging of live cell protein localizations. *The Journal of cell biology*. 160:629-633.

Semerdjieva, S., B. Shortt, E. Maxwell, S. Singh, P. Fonarev, J. Hansen, G. Schiavo, B.D. Grant, and E. Smythe. 2008. Coordinated regulation of AP2 uncoating from clathrin-coated vesicles by rab5 and hRME-6. *The Journal of cell biology*. 183:499-511.

Sevier, C.S., O.A. Weisz, M. Davis, and C.E. Machamer. 2000. Efficient export of the vesicular stomatitis virus G protein from the endoplasmic reticulum requires a signal in the cytoplasmic tail that includes both tyrosine-based and di-acidic motifs. *Molecular biology of the cell*. 11:13-22.

Shan, S.O., and P. Walter. 2005. Co-translational protein targeting by the signal recognition particle. *FEBS letters*. 579:921-926.

Shao, S., and R.S. Hegde. 2011. Membrane protein insertion at the endoplasmic reticulum. *Annual review of cell and developmental biology*. 27:25-56.

Shaywitz, D.A., P.J. Espenshade, R.E. Gimeno, and C.A. Kaiser. 1997. COPII subunit interactions in the assembly of the vesicle coat. *The Journal of biological chemistry*. 272:25413-25416.

Shikano, S., and M. Li. 2003. Membrane receptor trafficking: evidence of proximal and distal zones conferred by two independent endoplasmic reticulum localization signals. *Proceedings of the National Academy of Sciences of the United States of America*. 100:5783-5788.

Shmulevitz, M., J. Corcoran, J. Salsman, and R. Duncan. 2004. Cell-cell fusion induced by the avian reovirus membrane fusion protein is regulated by protein degradation. *Journal of virology*. 78:5996-6004.

Shmulevitz, M., and R. Duncan. 2000. A new class of fusion-associated small transmembrane (FAST) proteins encoded by the non-enveloped fusogenic reoviruses. *The EMBO journal*. 19:902-912.

Shmulevitz, M., J. Salsman, and R. Duncan. 2003. Palmitoylation, membrane-proximal basic residues, and transmembrane glycine residues in the reovirus p10 protein are essential for syncytium formation. *Journal of virology*. 77:9769-9779.

Siegenthaler, B.M., and L. Rajendran. 2012. Retromers in Alzheimer's disease. *Neuro-degenerative diseases*. 10:116-121.

Simon, S.M. 2008. Golgi governance: the third way. *Cell*. 133:951-953.

Sipos, L., and G. von Heijne. 1993. Predicting the topology of eukaryotic membrane proteins. *European journal of biochemistry / FEBS*. 213:1333-1340.

Sivars, U., D. Aivazian, and S. Pfeffer. 2005. Purification and properties of Yip3/PRA1 as a Rab GDI displacement factor. *Methods in enzymology*. 403:348-356.

Small, S.A., K. Kent, A. Pierce, C. Leung, M.S. Kang, H. Okada, L. Honig, J.P. Vonsattel, and T.W. Kim. 2005. Model-guided microarray implicates the retromer complex in Alzheimer's disease. *Annals of neurology*. 58:909-919.

Smith, I., and L.F. Wang. 2013. Bats and their virome: an important source of emerging viruses capable of infecting humans. *Current opinion in virology*. 3:84-91.

Stagg, S.M., C. Gurkan, D.M. Fowler, P. LaPointe, T.R. Foss, C.S. Potter, B. Carragher, and W.E. Balch. 2006. Structure of the Sec13/31 COPII coat cage. *Nature*. 439:234-238.

Stahlschmidt, W., M.J. Robertson, P.J. Robinson, A. McCluskey, and V. Haucke. 2014. Clathrin terminal domain-ligand interactions regulate sorting of mannose 6-phosphate receptors mediated by AP-1 and GGA adaptors. *The Journal of biological chemistry*. 289:4906-4918.

Starcevic, M., R. Nazarian, and E.C. Dell'Angelica. 2002. The molecular machinery for the biogenesis of lysosome-related organelles: lessons from Hermansky-Pudlak syndrome. *Seminars in cell & developmental biology*. 13:271-278.

Stefanovic, S., and R.S. Hegde. 2007. Identification of a targeting factor for posttranslational membrane protein insertion into the ER. *Cell*. 128:1147-1159.

Steinberg, F., M. Gallon, M. Winfield, E.C. Thomas, A.J. Bell, K.J. Heesom, J.M. Tavare, and P.J. Cullen. 2013. A global analysis of SNX27-retromer assembly and cargo specificity reveals a function in glucose and metal ion transport. *Nature cell biology*. 15:461-471.

Stenmark, H. 2009. Rab GTPases as coordinators of vesicle traffic. *Nature reviews. Molecular cell biology*. 10:513-525.

Stephens, D.J., and R. Pepperkok. 2001. Illuminating the secretory pathway: when do we need vesicles? *Journal of cell science*. 114:1053-1059.

Stephens, D.J., and R. Pepperkok. 2002. Imaging of procollagen transport reveals COPI-dependent cargo sorting during ER-to-Golgi transport in mammalian cells. *Journal of cell science*. 115:1149-1160.

Steyer, A., I. Gutierrez-Aguire, M. Kolenc, S. Koren, D. Kutnjak, M. Pokorn, M. Poljsak-Prijatelj, N. Racki, M. Ravnikar, M. Sagadin, A. Fratnik Steyer, and N. Toplak. 2013. High similarity of novel orthoreovirus detected in a child hospitalized with acute gastroenteritis to mammalian orthoreoviruses found in bats in Europe. *Journal of clinical microbiology*. 51:3818-3825.

Stimpson, H.E., C.P. Toret, A.T. Cheng, B.S. Pauly, and D.G. Drubin. 2009. Early-arriving Syp1p and Ede1p function in endocytic site placement and formation in budding yeast. *Molecular biology of the cell*. 20:4640-4651.

Stockklausner, C., and N. Klocker. 2003. Surface expression of inward rectifier potassium channels is controlled by selective Golgi export. *The Journal of biological chemistry*. 278:17000-17005.

Stockklausner, C., J. Ludwig, J.P. Ruppersberg, and N. Klocker. 2001. A sequence motif responsible for ER export and surface expression of Kir2.0 inward rectifier K(+) channels. *FEBS letters*. 493:129-133.

Strutt, D., and J.P. Vincent. 2010. Frizzled signaling: Galphao and Rab5 at the crossroads of the canonical and PCP pathways? *Science signaling*. 3:pe43.

Sucic, S., A. El-Kasaby, O. Kudlacek, S. Sarker, H.H. Sitte, P. Marin, and M. Freissmuth. 2011. The serotonin transporter is an exclusive client of the coat protein complex II (COPII) component SEC24C. *The Journal of biological chemistry*. 286:16482-16490.

Sun, Z., F. Anderl, K. Frohlich, L. Zhao, S. Hanke, B. Brugger, F. Wieland, and J. Bethune. 2007. Multiple and stepwise interactions between coatomer and ADP-ribosylation factor-1 (Arf1)-GTP. *Traffic*. 8:582-593.

Sundborger, A., C. Soderblom, O. Vorontsova, E. Evergren, J.E. Hinshaw, and O. Shupliakov. 2011. An endophilin-dynamin complex promotes budding of clathrin-coated vesicles during synaptic vesicle recycling. *Journal of cell science*. 124:133-143.

Sung, C.H., and A.W. Tai. 2000. Rhodopsin trafficking and its role in retinal dystrophies. *International review of cytology*. 195:215-267.

Supek, F., D.T. Madden, S. Hamamoto, L. Orci, and R. Schekman. 2002. Sec16p potentiates the action of COPII proteins to bud transport vesicles. *The Journal of cell biology*. 158:1029-1038.

Surma, M.A., C. Klose, and K. Simons. 2012. Lipid-dependent protein sorting at the trans-Golgi network. *Biochimica et biophysica acta*. 1821:1059-1067.

Sweitzer, S.M., and J.E. Hinshaw. 1998. Dynamin undergoes a GTP-dependent conformational change causing vesiculation. *Cell*. 93:1021-1029.

Takahashi, M., T. Ishiko, H. Kamohara, H. Hidaka, O. Ikeda, M. Ogawa, and H. Baba. 2007. Curcumin (1,7-bis(4-hydroxy-3-methoxyphenyl)-1,6-heptadiene-3,5-dione) blocks the chemotaxis of neutrophils by inhibiting signal transduction through IL-8 receptors. *Mediators of inflammation*. 2007:10767.

Takatsu, H., Y. Katoh, Y. Shiba, and K. Nakayama. 2001. Golgi-localizing, gamma-adaptin ear homology domain, ADP-ribosylation factor-binding (GGA) proteins interact with acidic dileucine sequences within the cytoplasmic domains of sorting receptors through their Vps27p/Hrs/STAM (VHS) domains. *The Journal of biological chemistry*. 276:28541-28545.

Tanigawa, G., L. Orci, M. Amherdt, M. Ravazzola, J.B. Helms, and J.E. Rothman. 1993. Hydrolysis of bound GTP by ARF protein triggers uncoating of Golgi-derived COP-coated vesicles. *The Journal of cell biology*. 123:1365-1371.

Taylor, M.J., D. Perrais, and C.J. Merrifield. 2011. A high precision survey of the molecular dynamics of mammalian clathrin-mediated endocytosis. *PLoS biology*. 9:e1000604.

Teasdale, R.D., and M.R. Jackson. 1996. Signal-mediated sorting of membrane proteins between the endoplasmic reticulum and the golgi apparatus. *Annu.Rev.Cell Dev.Biol.* 12:27-54.

Temkin, P., B. Lauffer, S. Jager, P. Cimermancic, N.J. Krogan, and M. von Zastrow. 2011. SNX27 mediates retromer tubule entry and endosome-to-plasma membrane trafficking of signalling receptors. *Nature cell biology*. 13:715-721.

Thalmann, C.M., D.M. Cummins, M. Yu, R. Lunt, L.I. Pritchard, E. Hansson, S. Crameri, A. Hyatt, and L.F. Wang. 2010. Broome virus, a new fusogenic Orthoreovirus species isolated from an Australian fruit bat. *Virology*. 402:26-40.

Thomas, D.C., and M.G. Roth. 1994. The basolateral targeting signal in the cytoplasmic domain of glycoprotein G from vesicular stomatitis virus resembles a variety of intracellular targeting motifs related by primary sequence but having diverse targeting activities. *The Journal of biological chemistry*. 269:15732-15739.

Top, D., C. Barry, T. Racine, C.L. Ellis, and R. Duncan. 2009. Enhanced fusion pore expansion mediated by the trans-acting Endodomain of the reovirus FAST proteins. *PLoS pathogens*. 5:e1000331.

Top, D., R. de Antueno, J. Salsman, J. Corcoran, J. Mader, D. Hoskin, A. Touhami, M.H. Jericho, and R. Duncan. 2005. Liposome reconstitution of a minimal protein-mediated membrane fusion machine. *The EMBO journal*. 24:2980-2988.

Top, D., J.A. Read, S.J. Dawe, R.T. Syvitski, and R. Duncan. 2012. Cell-cell membrane fusion induced by p15 fusion-associated small transmembrane (FAST) protein requires a novel fusion peptide motif containing a myristoylated polyproline type II helix. *The Journal of biological chemistry*. 287:3403-3414.

Traub, L.M. 2009. Tickets to ride: selecting cargo for clathrin-regulated internalization. *Nature reviews. Molecular cell biology*. 10:583-596.

Traub, L.M. 2011. Regarding the amazing choreography of clathrin coats. *PLoS biology*. 9:e1001037.

Trucco, A., R.S. Polishchuk, O. Martella, A. Di Pentima, A. Fusella, D. Di Giandomenico, E. San Pietro, G.V. Beznoussenko, E.V. Polishchuk, M. Baldassarre, R. Buccione, W.J. Geerts, A.J. Koster, K.N. Burger, A.A. Mironov, and A. Luini. 2004. Secretory traffic triggers the formation of tubular continuities across Golgi sub-compartments. *Nature cell biology*. 6:1071-1081.

Ullrich, O., H. Stenmark, K. Alexandrov, L.A. Huber, K. Kaibuchi, T. Sasaki, Y. Takai, and M. Zerial. 1993. Rab GDP dissociation inhibitor as a general regulator for the membrane association of rab proteins. *The Journal of biological chemistry*. 268:18143-18150.

Ungewickell, E., H. Ungewickell, S.E. Holstein, R. Lindner, K. Prasad, W. Barouch, B. Martin, L.E. Greene, and E. Eisenberg. 1995. Role of auxilin in uncoating clathrin-coated vesicles. *Nature*. 378:632-635.

Urbe, S., L.A. Huber, M. Zerial, S.A. Tooze, and R.G. Parton. 1993. Rab11, a small GTPase associated with both constitutive and regulated secretory pathways in PC12 cells. *FEBS letters*. 334:175-182.

van de Graaf, S.F., Q. Chang, A.R. Mensenkamp, J.G. Hoenderop, and R.J. Bindels. 2006. Direct interaction with Rab11a targets the epithelial Ca2+ channels TRPV5 and TRPV6 to the plasma membrane. *Molecular and cellular biology*. 26:303-312.

van Kerkhof, P., J. Lee, L. McCormick, E. Tetrault, W. Lu, M. Schoenfish, V. Oorschot, G.J. Strous, J. Klumperman, and G. Bu. 2005. Sorting nexin 17 facilitates LRP recycling in the early endosome. *The EMBO journal*. 24:2851-2861.

van Weering, J.R., P. Verkade, and P.J. Cullen. 2012. SNX-BAR-mediated endosome tubulation is co-ordinated with endosome maturation. *Traffic*. 13:94-107.

Vardarajan, B.N., S.Y. Bruesegem, M.E. Harbour, R. Inzelberg, R. Friedland, P. St George-Hyslop, M.N. Seaman, and L.A. Farrer. 2012. Identification of Alzheimer disease-associated variants in genes that regulate retromer function. *Neurobiology of aging*. 33:2231 e2215-2231 e2230.

Varnai, P., T. Bondeva, P. Tamas, B. Toth, L. Buday, L. Hunyady, and T. Balla. 2005. Selective cellular effects of overexpressed pleckstrin-homology domains that recognize PtdIns(3,4,5)P3 suggest their interaction with protein binding partners. *Journal of cell science*. 118:4879-4888.

Verges, M., F. Luton, C. Gruber, F. Tiemann, L.G. Reinders, L. Huang, A.L. Burlingame, C.R. Haft, and K.E. Mostov. 2004. The mammalian retromer regulates transcytosis of the polymeric immunoglobulin receptor. *Nature cell biology*. 6:763-769.

Verstreken, P., T.W. Koh, K.L. Schulze, R.G. Zhai, P.R. Hiesinger, Y. Zhou, S.Q. Mehta, Y. Cao, J. Roos, and H.J. Bellen. 2003. Synaptojanin is recruited by endophilin to promote synaptic vesicle uncoating. *Neuron*. 40:733-748.

Vieler, E., W. Baumgartner, W. Herbst, and G. Kohler. 1994. Characterization of a reovirus isolate from a rattle snake, Crotalus viridis, with neurological dysfunction. *Archives of virology*. 138:341-344.

Vilardi, F., H. Lorenz, and B. Dobberstein. 2011. WRB is the receptor for TRC40/Asna1-mediated insertion of tail-anchored proteins into the ER membrane. *Journal of cell science*. 124:1301-1307.

Vilarino-Guell, C., C. Wider, O.A. Ross, J.C. Dachsel, J.M. Kachergus, S.J. Lincoln, A.I. Soto-Ortolaza, S.A. Cobb, G.J. Wilhoite, J.A. Bacon, B. Behrouz, H.L. Melrose, E. Hentati, A. Puschmann, D.M. Evans, E. Conibear, W.W. Wasserman, J.O. Aasly, P.R. Burkhard, R. Djaldetti, J. Ghika, F. Hentati, A. Krygowska-Wajs, T. Lynch, E. Melamed, A. Rajput, A.H. Rajput, A. Solida, R.M. Wu, R.J. Uitti, Z.K. Wszolek, F. Vingerhoets, and M.J. Farrer. 2011. VPS35 mutations in Parkinson disease. *American journal of human genetics*. 89:162-167.

Vincent, M.J., A.S. Martin, and R.W. Compans. 1998. Function of the KKXX motif in endoplasmic reticulum retrieval of a transmembrane protein depends on the length and structure of the cytoplasmic domain. *The Journal of biological chemistry*. 273:950-956.

Vivanco, I., and C.L. Sawyers. 2002. The phosphatidylinositol 3-Kinase AKT pathway in human cancer. *Nature reviews. Cancer*. 2:489-501.

Voeltz, G.K., W.A. Prinz, Y. Shibata, J.M. Rist, and T.A. Rapoport. 2006. A class of membrane proteins shaping the tubular endoplasmic reticulum. *Cell*. 124:573-586.

von Arnim, C.A., M.M. Tangredi, I.D. Peltan, B.M. Lee, M.C. Irizarry, A. Kinoshita, and B.T. Hyman. 2004. Demonstration of BACE (beta-secretase) phosphorylation and its interaction with GGA1 in cells by fluorescence-lifetime imaging microscopy. *Journal of cell science*. 117:5437-5445.

von Heijne, G. 1986. Net N-C charge imbalance may be important for signal sequence function in bacteria. *Journal of molecular biology*. 192:287-290.

von Heijne, G. 1989. Control of topology and mode of assembly of a polytopic membrane protein by positively charged residues. *Nature*. 341:456-458.

Vonderheit, A., and A. Helenius. 2005. Rab7 associates with early endosomes to mediate sorting and transport of Semliki forest virus to late endosomes. *PLoS biology*. 3:e233.

Wahle, T., K. Prager, N. Raffler, C. Haass, M. Famulok, and J. Walter. 2005. GGA proteins regulate retrograde transport of BACE1 from endosomes to the trans-Golgi network. *Molecular and cellular neurosciences*. 29:453-461.

Wandinger-Ness, A., and M. Zerial. 2014. Rab proteins and the compartmentalization of the endosomal system. *Cold Spring Harbor perspectives in biology*. 6:a022616.

Wang, X., J. Matteson, Y. An, B. Moyer, J.S. Yoo, S. Bannykh, I.A. Wilson, J.R. Riordan, and W.E. Balch. 2004. COPII-dependent export of cystic fibrosis transmembrane conductance regulator from the ER uses a di-acidic exit code. *The Journal of cell biology*. 167:65-74.

Wang, Y.J., J. Wang, H.Q. Sun, M. Martinez, Y.X. Sun, E. Macia, T. Kirchhausen, J.P. Albanesi, M.G. Roth, and H.L. Yin. 2003. Phosphatidylinositol 4 phosphate regulates targeting of clathrin adaptor AP-1 complexes to the Golgi. *Cell*. 114:299-310.

Warren, G., and I. Mellman. 1999. Bulk flow redux? *Cell*. 98:125-127.

Watson, P., A.K. Townley, P. Koka, K.J. Palmer, and D.J. Stephens. 2006. Sec16 defines endoplasmic reticulum exit sites and is required for secretory cargo export in mammalian cells. *Traffic*. 7:1678-1687.

Wattenberg, B., and T. Lithgow. 2001. Targeting of C-terminal (tail)-anchored proteins: understanding how cytoplasmic activities are anchored to intracellular membranes. *Traffic*. 2:66-71.

Waugh, M.G. 2015. PIPs in neurological diseases. *Biochimica et biophysica acta*.

Wehrle-Haller, B., and B.A. Imhof. 2001. Stem cell factor presentation to c-Kit. Identification of a basolateral targeting domain. *The Journal of biological chemistry*. 276:12667-12674.

Weimer, C., R. Beck, P. Eckert, I. Reckmann, J. Moelleken, B. Brugger, and F. Wieland. 2008. Differential roles of ArfGAP1, ArfGAP2, and ArfGAP3 in COPI trafficking. *The Journal of cell biology*. 183:725-735.

Welsh, G.I., S.E. Leney, B. Lloyd-Lewis, M. Wherlock, A.J. Lindsay, M.W. McCaffrey, and J.M. Tavare. 2007. Rip11 is a Rab11- and AS160-RabGAP-binding protein required for insulin-stimulated glucose uptake in adipocytes. *Journal of cell science*. 120:4197-4208.

Welz, T., J. Wellbourne-Wood, and E. Kerkhoff. 2014. Orchestration of cell surface proteins by Rab11. *Trends in cell biology*. 24:407-415.

Wen, L., F.L. Tang, Y. Hong, S.W. Luo, C.L. Wang, W. He, C. Shen, J.U. Jung, F. Xiong, D.H. Lee, Q.G. Zhang, D. Brann, T.W. Kim, R. Yan, L. Mei, and W.C. Xiong. 2011. VPS35 haploinsufficiency increases Alzheimer's disease neuropathology. *The Journal of cell biology*. 195:765-779.

Westlake, C.J., J.R. Junutula, G.C. Simon, M. Pilli, R. Prekeris, R.H. Scheller, P.K. Jackson, and A.G. Eldridge. 2007. Identification of Rab11 as a small GTPase binding protein for the Evi5 oncogene. *Proceedings of the National Academy of Sciences of the United States of America*. 104:1236-1241.

White, J.M., S.E. Delos, M. Brecher, and K. Schornberg. 2008. Structures and mechanisms of viral membrane fusion proteins: multiple variations on a common theme. *Critical reviews in biochemistry and molecular biology*. 43:189-219.

Wieland, F.T., M.L. Gleason, T.A. Serafini, and J.E. Rothman. 1987. The rate of bulk flow from the endoplasmic reticulum to the cell surface. *Cell*. 50:289-300.

Wikstrom, K., H.M. Reid, M. Hill, K.A. English, M.B. O'Keeffe, C.C. Kimbembe, and B.T. Kinsella. 2008. Recycling of the human prostacyclin receptor is regulated through a direct interaction with Rab11a GTPase. *Cellular signalling*. 20:2332-2346.

Wong, A.H., P.K. Cheng, M.Y. Lai, P.C. Leung, K.K. Wong, W.Y. Lee, and W.W. Lim. 2012. Virulence potential of fusogenic orthoreoviruses. *Emerging infectious diseases*. 18:944-948.

Wooding, S., and H.R. Pelham. 1998. The dynamics of golgi protein traffic visualized in living yeast cells. *Molecular biology of the cell*. 9:2667-2680.

Wu, Y.W., L.K. Oesterlin, K.T. Tan, H. Waldmann, K. Alexandrov, and R.S. Goody. 2010. Membrane targeting mechanism of Rab GTPases elucidated by semisynthetic protein probes. *Nature chemical biology*. 6:534-540.

Xia, Z., and Y. Liu. 2001. Reliable and global measurement of fluorescence resonance energy transfer using fluorescence microscopes. *Biophysical journal*. 81:2395-2402.

Xing, Y., T. Bocking, M. Wolf, N. Grigorieff, T. Kirchhausen, and S.C. Harrison. 2010. Structure of clathrin coat with bound Hsc70 and auxilin: mechanism of Hsc70-facilitated disassembly. *The EMBO journal*. 29:655-665.

Yamamoto, Y., and T. Sakisaka. 2012. Molecular machinery for insertion of tail-anchored membrane proteins into the endoplasmic reticulum membrane in mammalian cells. *Molecular cell*. 48:387-397.

Yamanaka, A., A. Iwakiri, T. Yoshikawa, K. Sakai, H. Singh, D. Himeji, I. Kikuchi, A. Ueda, S. Yamamoto, M. Miura, Y. Shioyama, K. Kawano, T. Nagaishi, M. Saito, M. Minomo, N. Iwamoto, Y. Hidaka, H. Sohma, T. Kobayashi, Y. Kanai, T. Kawagishi, N. Nagata, S. Fukushi, T. Mizutani, H. Tani, S. Taniguchi, A. Fukuma, M. Shimojima, I. Kurane, T. Kageyama, T. Odagiri, M. Saijo, and S. Morikawa. 2014. Imported case of acute respiratory tract infection associated with a member of species nelson bay orthoreovirus. *PloS one*. 9:e92777.

Yeaman, C., A.H. Le Gall, A.N. Baldwin, L. Monlauzeur, A. Le Bivic, and E. Rodriguez-Boulan. 1997. The O-glycosylated stalk domain is required for apical sorting of neurotrophin receptors in polarized MDCK cells. *The Journal of cell biology*. 139:929-940.

Yorimitsu, T., and K. Sato. 2012. Insights into structural and regulatory roles of Sec16 in COPII vesicle formation at ER exit sites. *Molecular biology of the cell*. 23:2930-2942.

Yu, X., M. Breitman, and J. Goldberg. 2012. A structure-based mechanism for Arf1-dependent recruitment of coatomer to membranes. *Cell*. 148:530-542.

Yuan, T.L., and L.C. Cantley. 2008. PI3K pathway alterations in cancer: variations on a theme. *Oncogene*. 27:5497-5510.

Yuasa, K., S. Yamagami, M. Nagahama, and A. Tsuji. 2008. Trafficking of cGMP-dependent protein kinase II via interaction with Rab11. *Biochemical and biophysical research communications*. 374:522-526.

Zelazny, E., M. Santambrogio, M. Pourcher, P. Chambrier, A. Berne-Dedieu, I. Fobis-Loisy, C. Miege, Y. Jaillais, and T. Gaude. 2013. Mechanisms governing the endosomal membrane recruitment of the core retromer in Arabidopsis. *The Journal of biological chemistry*. 288:8815-8825.

Zerangue, N., M.J. Malan, S.R. Fried, P.F. Dazin, Y.N. Jan, L.Y. Jan, and B. Schwappach. 2001. Analysis of endoplasmic reticulum trafficking signals by combinatorial screening in mammalian cells. *Proceedings of the National Academy of Sciences of the United States of America*. 98:2431-2436.

Zerangue, N., B. Schwappach, Y.N. Jan, and L.Y. Jan. 1999. A new ER trafficking signal regulates the subunit stoichiometry of plasma membrane K(ATP) channels. *Neuron*. 22:537-548.

Zeuschner, D., W.J. Geerts, E. van Donselaar, B.M. Humbel, J.W. Slot, A.J. Koster, and J. Klumperman. 2006. Immuno-electron tomography of ER exit sites reveals the existence of free COPII-coated transport carriers. *Nature cell biology*. 8:377-383.

Zhang, X., C. Dong, Q.J. Wu, W.E. Balch, and G. Wu. 2011. Di-acidic motifs in the membrane-distal C termini modulate the transport of angiotensin II receptors from the endoplasmic reticulum to the cell surface. *The Journal of biological chemistry*. 286:20525-20535.

Zhao, L., J.B. Helms, B. Brugger, C. Harter, B. Martoglio, R. Graf, J. Brunner, and F.T. Wieland. 1997. Direct and GTP-dependent interaction of ADP ribosylation factor 1 with coatomer subunit beta. *Proceedings of the National Academy of Sciences of the United States of America*. 94:4418-4423.

Zhou, B., Y. Wu, and X. Lin. 2011. Retromer regulates apical-basal polarity through recycling Crumbs. *Developmental biology*. 360:87-95.

Zhu, Y., B. Doray, A. Poussu, V.P. Lehto, and S. Kornfeld. 2001. Binding of GGA2 to the lysosomal enzyme sorting motif of the mannose 6-phosphate receptor. *Science*. 292:1716-1718.

Zurek, N., L. Sparks, and G. Voeltz. 2011. Reticulon short hairpin transmembrane domains are used to shape ER tubules. *Traffic*. 12:28-41.

APPENDIX A

COPYRIGHT PERMISSION LETTERS

American Society for Cell Biology LICENSE TERMS AND CONDITIONS

Apr 24, 2015

This is a License Agreement between Hirendrasinh Parmar ("You") and American Society for Cell Biology ("American Society for Cell Biology") provided by Copyright Clearance Center ("CCC"). The license consists of your order details, the terms and conditions provided by American Society for Cell Biology, and the payment terms and conditions.

All payments must be made in full to CCC. For payment instructions, please see information listed at the bottom of this form.

License Number	3615500612467
License date	Apr 24, 2015
Licensed content publisher	American Society for Cell Biology
Licensed content title	MOLECULAR BIOLOGY OF THE CELL. ONLINE
Licensed content date	Dec 31, 1969
Type of Use	Thesis/Dissertation
Requestor type	Academic institution
Format	Print, Electronic
Portion	chart/graph/table/figure
Number of charts/graphs/tables/figures	10
Title or numeric reference of the portion(s)	Figures 1-10
Title of the article or chapter the portion is from	Golgi complex-plasma membrane trafficking directed by an autonomous, tribasic Golgi export signal
Editor of portion(s)	Adam Linstedt
Author of portion(s)	Hirendrasinh B. Parmar, Christopher Barry, FuiBoon Kai, and Roy Duncan
Volume of serial or monograph.	25
Issue, if republishing an article from a serial	6
Page range of the portion	866-78
Publication date of portion	March 2014
Rights for	Main product

Duration of use	Life of current edition
Creation of copies for the disabled	no
With minor editing privileges	yes
For distribution to	Canada
In the following language(s)	Original language of publication
With incidental promotional use	no
The lifetime unit quantity of new product	Up to 499
Made available in the following markets	Education
Specified additional information	I am the lead author of this article.
The requesting person/organization is:	Hirendrasinh Parmar
Order reference number	None
Author/Editor	Hirendrasinh Parmar
The standard identifier	hr425141
Title	The Ins and Outs of Protein Trafficking Pathways: Insights from the FAST Proteins
Publisher	Dalhousie University
Expected publication date	May 2015
Estimated size (pages)	200
Total (may include CCC user fee)	0.00 USD
Terms and Conditions	

TERMS AND CONDITIONS

The following terms are individual to this publisher:

None

Other Terms and Conditions:

None

STANDARD TERMS AND CONDITIONS

1. Description of Service; Defined Terms. This Republication License enables the User to obtain licenses for republication of one or more copyrighted works as described in detail on the relevant Order Confirmation (the "Work(s)"). Copyright Clearance Center, Inc. ("CCC") grants licenses through the Service on behalf of the rightsholder identified on the Order Confirmation (the "Rightsholder"). "Republication", as used herein, generally

means the inclusion of a Work, in whole or in part, in a new work or works, also as described on the Order Confirmation. “User”, as used herein, means the person or entity making such republication.

2. The terms set forth in the relevant Order Confirmation, and any terms set by the Rightsholder with respect to a particular Work, govern the terms of use of Works in connection with the Service. By using the Service, the person transacting for a republication license on behalf of the User represents and warrants that he/she/it (a) has been duly authorized by the User to accept, and hereby does accept, all such terms and conditions on behalf of User, and (b) shall inform User of all such terms and conditions. In the event such person is a “freelancer” or other third party independent of User and CCC, such party shall be deemed jointly a “User” for purposes of these terms and conditions. In any event, User shall be deemed to have accepted and agreed to all such terms and conditions if User republishes the Work in any fashion.

3. Scope of License; Limitations and Obligations.

3.1 All Works and all rights therein, including copyright rights, remain the sole and exclusive property of the Rightsholder. The license created by the exchange of an Order Confirmation (and/or any invoice) and payment by User of the full amount set forth on that document includes only those rights expressly set forth in the Order Confirmation and in these terms and conditions, and conveys no other rights in the Work(s) to User. All rights not expressly granted are hereby reserved.

3.2 General Payment Terms: You may pay by credit card or through an account with us payable at the end of the month. If you and we agree that you may establish a standing account with CCC, then the following terms apply: Remit Payment to: Copyright Clearance Center, Dept 001, P.O. Box 843006, Boston, MA 02284-3006. Payments Due: Invoices are payable upon their delivery to you (or upon our notice to you that they are available to you for downloading). After 30 days, outstanding amounts will be subject to a service charge of 1-1/2% per month or, if less, the maximum rate allowed by applicable law. Unless otherwise specifically set forth in the Order Confirmation or in a separate written agreement signed by CCC, invoices are due and payable on “net 30” terms. While User may exercise the rights licensed immediately upon issuance of the Order Confirmation, the license is automatically revoked and is null and void, as if it had never been issued, if complete payment for the license is not received on a timely basis either from User directly or through a payment agent, such as a credit card company.

3.3 Unless otherwise provided in the Order Confirmation, any grant of rights to User (i) is “one-time” (including the editions and product family specified in the license), (ii) is non-exclusive and non-transferable and (iii) is subject to any and all limitations and restrictions (such as, but not limited to, limitations on duration of use or circulation) included in the Order Confirmation or invoice and/or in these terms and conditions. Upon completion of the licensed use, User shall either secure a new permission for further use of the Work(s) or immediately cease any new use of the Work(s) and shall render inaccessible (such as by deleting or by removing or severing links or other locators) any

further copies of the Work (except for copies printed on paper in accordance with this license and still in User's stock at the end of such period).

3.4 In the event that the material for which a republication license is sought includes third party materials (such as photographs, illustrations, graphs, inserts and similar materials) which are identified in such material as having been used by permission, User is responsible for identifying, and seeking separate licenses (under this Service or otherwise) for, any of such third party materials; without a separate license, such third party materials may not be used.

3.5 Use of proper copyright notice for a Work is required as a condition of any license granted under the Service. Unless otherwise provided in the Order Confirmation, a proper copyright notice will read substantially as follows: “Republished with permission of [Rightsholder’s name], from [Work's title, author, volume, edition number and year of copyright]; permission conveyed through Copyright Clearance Center, Inc. ” Such notice must be provided in a reasonably legible font size and must be placed either immediately adjacent to the Work as used (for example, as part of a by-line or footnote but not as a separate electronic link) or in the place where substantially all other credits or notices for the new work containing the republished Work are located. Failure to include the required notice results in loss to the Rightsholder and CCC, and the User shall be liable to pay liquidated damages for each such failure equal to twice the use fee specified in the Order Confirmation, in addition to the use fee itself and any other fees and charges specified.

3.6 User may only make alterations to the Work if and as expressly set forth in the Order Confirmation. No Work may be used in any way that is defamatory, violates the rights of third parties (including such third parties' rights of copyright, privacy, publicity, or other tangible or intangible property), or is otherwise illegal, sexually explicit or obscene. In addition, User may not conjoin a Work with any other material that may result in damage to the reputation of the Rightsholder. User agrees to inform CCC if it becomes aware of any infringement of any rights in a Work and to cooperate with any reasonable request of CCC or the Rightsholder in connection therewith.

4. Indemnity. User hereby indemnifies and agrees to defend the Rightsholder and CCC, and their respective employees and directors, against all claims, liability, damages, costs and expenses, including legal fees and expenses, arising out of any use of a Work beyond the scope of the rights granted herein, or any use of a Work which has been altered in any unauthorized way by User, including claims of defamation or infringement of rights of copyright, publicity, privacy or other tangible or intangible property.

5. Limitation of Liability. UNDER NO CIRCUMSTANCES WILL CCC OR THE RIGHTSHOLDER BE LIABLE FOR ANY DIRECT, INDIRECT, CONSEQUENTIAL OR INCIDENTAL DAMAGES (INCLUDING WITHOUT LIMITATION DAMAGES FOR LOSS OF BUSINESS PROFITS OR INFORMATION, OR FOR BUSINESS INTERRUPTION) ARISING OUT OF THE USE OR INABILITY TO USE A WORK, EVEN IF ONE OF THEM HAS BEEN ADVISED OF THE POSSIBILITY OF SUCH DAMAGES. In any event, the total liability of the Rightsholder and CCC (including their

respective employees and directors) shall not exceed the total amount actually paid by User for this license. User assumes full liability for the actions and omissions of its principals, employees, agents, affiliates, successors and assigns.

6. Limited Warranties. THE WORK(S) AND RIGHT(S) ARE PROVIDED “AS IS”. CCC HAS THE RIGHT TO GRANT TO USER THE RIGHTS GRANTED IN THE ORDER CONFIRMATION DOCUMENT. CCC AND THE RIGHTSHOLDER DISCLAIM ALL OTHER WARRANTIES RELATING TO THE WORK(S) AND RIGHT(S), EITHER EXPRESS OR IMPLIED, INCLUDING WITHOUT LIMITATION IMPLIED WARRANTIES OF MERCHANTABILITY OR FITNESS FOR A PARTICULAR PURPOSE. ADDITIONAL RIGHTS MAY BE REQUIRED TO USE ILLUSTRATIONS, GRAPHS, PHOTOGRAPHS, ABSTRACTS, INSERTS OR OTHER PORTIONS OF THE WORK (AS OPPOSED TO THE ENTIRE WORK) IN A MANNER CONTEMPLATED BY USER; USER UNDERSTANDS AND AGREES THAT NEITHER CCC NOR THE RIGHTSHOLDER MAY HAVE SUCH ADDITIONAL RIGHTS TO GRANT.

7. Effect of Breach. Any failure by User to pay any amount when due, or any use by User of a Work beyond the scope of the license set forth in the Order Confirmation and/or these terms and conditions, shall be a material breach of the license created by the Order Confirmation and these terms and conditions. Any breach not cured within 30 days of written notice thereof shall result in immediate termination of such license without further notice. Any unauthorized (but licensable) use of a Work that is terminated immediately upon notice thereof may be liquidated by payment of the Rightsholder's ordinary license price therefor; any unauthorized (and unlicensable) use that is not terminated immediately for any reason (including, for example, because materials containing the Work cannot reasonably be recalled) will be subject to all remedies available at law or in equity, but in no event to a payment of less than three times the Rightsholder's ordinary license price for the most closely analogous licensable use plus Rightsholder's and/or CCC's costs and expenses incurred in collecting such payment.

8. **Miscellaneous.**

8.1 User acknowledges that CCC may, from time to time, make changes or additions to the Service or to these terms and conditions, and CCC reserves the right to send notice to the User by electronic mail or otherwise for the purposes of notifying User of such changes or additions; provided that any such changes or additions shall not apply to permissions already secured and paid for.

8.2 Use of User-related information collected through the Service is governed by CCC’s privacy policy, available online here:http://www.copyright.com/content/cc3/en/tools/footer/privacypolicy.html.

8.3 The licensing transaction described in the Order Confirmation is personal to User. Therefore, User may not assign or transfer to any other person (whether a natural person or an organization of any kind) the license created by the Order Confirmation and these

terms and conditions or any rights granted hereunder; provided, however, that User may assign such license in its entirety on written notice to CCC in the event of a transfer of all or substantially all of User's rights in the new material which includes the Work(s) licensed under this Service.

8.4 No amendment or waiver of any terms is binding unless set forth in writing and signed by the parties. The Rightsholder and CCC hereby object to any terms contained in any writing prepared by the User or its principals, employees, agents or affiliates and purporting to govern or otherwise relate to the licensing transaction described in the Order Confirmation, which terms are in any way inconsistent with any terms set forth in the Order Confirmation and/or in these terms and conditions or CCC's standard operating procedures, whether such writing is prepared prior to, simultaneously with or subsequent to the Order Confirmation, and whether such writing appears on a copy of the Order Confirmation or in a separate instrument.

8.5 The licensing transaction described in the Order Confirmation document shall be governed by and construed under the law of the State of New York, USA, without regard to the principles thereof of conflicts of law. Any case, controversy, suit, action, or proceeding arising out of, in connection with, or related to such licensing transaction shall be brought, at CCC's sole discretion, in any federal or state court located in the County of New York, State of New York, USA, or in any federal or state court whose geographical jurisdiction covers the location of the Rightsholder set forth in the Order Confirmation. The parties expressly submit to the personal jurisdiction and venue of each such federal or state court.If you have any comments or questions about the Service or Copyright Clearance Center, please contact us at 978-750-8400 or send an e-mail to info@copyright.com.

v 1.1

Questions? customercare@copyright.com or +1-855-239-3415 (toll free in the US) or +1-978-646-2777.

Gratis licenses (referencing $0 in the Total field) are free. Please retain this printable license for your reference. No payment is required.

ELSEVIER LICENSE
TERMS AND CONDITIONS

Apr 23, 2015

This is a License Agreement between Hirendrasinh Parmar ("You") and Elsevier ("Elsevier") provided by Copyright Clearance Center ("CCC"). The license consists of your order details, the terms and conditions provided by Elsevier, and the payment terms and conditions.

All payments must be made in full to CCC. For payment instructions, please see information listed at the bottom of this form.

Supplier	Elsevier Limited The Boulevard,Langford Lane Kidlington,Oxford,OX5 1GB,UK
Registered Company Number	1982084
Customer name	Hirendrasinh Parmar
Customer address	7S1-5850 College St Halifax, NS B3H 4R2
License number	3614890714621
License date	Apr 23, 2015
Licensed content publisher	Elsevier
Licensed content publication	Trends in Cell Biology
Licensed content title	TGN golgins, Rabs and cytoskeleton: regulating the Golgi trafficking highways
Licensed content author	Bruno Goud,Paul A. Gleeson
Licensed content date	June 2010
Licensed content volume number	20
Licensed content issue number	6
Number of pages	8
Start Page	329
End Page	336
Type of Use	reuse in a thesis/dissertation
Intended publisher of new work	other
Portion	figures/tables/illustrations

Number of figures/tables/illustrations	1
Format	both print and electronic
Are you the author of this Elsevier article?	No
Will you be translating?	No
Original figure numbers	Figure 2
Title of your thesis/dissertation	The Ins and Outs of Protein Trafficking Pathways: Insights from the FAST Proteins
Expected completion date	May 2015
Estimated size (number of pages)	200
Elsevier VAT number	GB 494 6272 12
Permissions price	0.00 USD
VAT/Local Sales Tax	0.00 USD / 0.00 GBP
Total	0.00 USD

ELSEVIER LICENSE
TERMS AND CONDITIONS

Apr 23, 2015

This is a License Agreement between Hirendrasinh Parmar ("You") and Elsevier ("Elsevier") provided by Copyright Clearance Center ("CCC"). The license consists of your order details, the terms and conditions provided by Elsevier, and the payment terms and conditions.

All payments must be made in full to CCC. For payment instructions, please see information listed at the bottom of this form.

Supplier	Elsevier Limited The Boulevard,Langford Lane Kidlington,Oxford,OX5 1GB,UK
Registered Company Number	1982084
Customer name	Hirendrasinh Parmar
Customer address	7S1-5850 College St Halifax, NS B3H 4R2
License number	3614871379577
License date	Apr 23, 2015
Licensed content publisher	Elsevier
Licensed content publication	Trends in Cell Biology
Licensed content title	Signals for COPII-dependent export from the ER: what's the ticket out?
Licensed content author	Charles Barlowe
Licensed content date	June 2003
Licensed content volume number	13
Licensed content issue number	6
Number of pages	6
Start Page	295
End Page	300
Type of Use	reuse in a thesis/dissertation
Intended publisher of new work	other
Portion	figures/tables/illustrations

Number of figures/tables/illustrations	1
Format	both print and electronic
Are you the author of this Elsevier article?	No
Will you be translating?	No
Original figure numbers	Figure 3
Title of your thesis/dissertation	The Ins and Outs of Protein Trafficking Pathways: Insights from the FAST Proteins
Expected completion date	May 2015
Estimated size (number of pages)	200
Elsevier VAT number	GB 494 6272 12
Permissions price	0.00 USD
VAT/Local Sales Tax	0.00 USD / 0.00 GBP
Total	0.00 USD

ELSEVIER LICENSE
TERMS AND CONDITIONS

Apr 23, 2015

This is a License Agreement between Hirendrasinh Parmar ("You") and Elsevier ("Elsevier") provided by Copyright Clearance Center ("CCC"). The license consists of your order details, the terms and conditions provided by Elsevier, and the payment terms and conditions.

All payments must be made in full to CCC. For payment instructions, please see information listed at the bottom of this form.

Supplier	Elsevier Limited The Boulevard,Langford Lane Kidlington,Oxford,OX5 1GB,UK
Registered Company Number	1982084
Customer name	Hirendrasinh Parmar
Customer address	7S1-5850 College St Halifax, NS B3H 4R2
License number	3614880160935
License date	Apr 23, 2015
Licensed content publisher	Elsevier
Licensed content publication	Trends in Cell Biology
Licensed content title	Cargo adaptors: structures illuminate mechanisms regulating vesicle biogenesis
Licensed content author	None
Licensed content date	Available online 17 March 2015
Licensed content volume number	n/a
Licensed content issue number	n/a
Number of pages	1
Start Page	0
End Page	0
Type of Use	reuse in a thesis/dissertation
Intended publisher of new work	other
Portion	figures/tables/illustrations

Number of figures/tables/illustrations	1
Format	both print and electronic
Are you the author of this Elsevier article?	No
Will you be translating?	No
Original figure numbers	Figure 1
Title of your thesis/dissertation	The Ins and Outs of Protein Trafficking Pathways: Insights from the FAST Proteins
Expected completion date	May 2015
Estimated size (number of pages)	200
Elsevier VAT number	GB 494 6272 12
Permissions price	0.00 USD
VAT/Local Sales Tax	0.00 USD / 0.00 GBP
Total	0.00 USD

ELSEVIER LICENSE
TERMS AND CONDITIONS

Apr 23, 2015

This is a License Agreement between Hirendrasinh Parmar ("You") and Elsevier ("Elsevier") provided by Copyright Clearance Center ("CCC"). The license consists of your order details, the terms and conditions provided by Elsevier, and the payment terms and conditions.

All payments must be made in full to CCC. For payment instructions, please see information listed at the bottom of this form.

Supplier	Elsevier Limited The Boulevard,Langford Lane Kidlington,Oxford,OX5 1GB,UK
Registered Company Number	1982084
Customer name	Hirendrasinh Parmar
Customer address	7S1-5850 College St Halifax, NS B3H 4R2
License number	3614581230839
License date	Apr 23, 2015
Licensed content publisher	Elsevier
Licensed content publication	Trends in Microbiology
Licensed content title	Reovirus FAST proteins: virus-encoded cellular fusogens
Licensed content author	None
Licensed content date	December 2014
Licensed content volume number	22
Licensed content issue number	12
Number of pages	10
Start Page	715
End Page	724
Type of Use	reuse in a thesis/dissertation
Portion	figures/tables/illustrations
Number of figures/tables/illustrations	1
Format	both print and electronic

Are you the author of this Elsevier article?	No
Will you be translating?	No
Original figure numbers	Figure 2
Title of your thesis/dissertation	The Ins and Outs of Protein Trafficking Pathways: Insights from the FAST Proteins
Expected completion date	May 2015
Estimated size (number of pages)	200
Elsevier VAT number	GB 494 6272 12
Permissions price	0.00 USD
VAT/Local Sales Tax	0.00 USD / 0.00 GBP
Total	0.00 USD

ELSEVIER LICENSE
TERMS AND CONDITIONS

Apr 24, 2015

This is a License Agreement between Hirendrasinh Parmar ("You") and Elsevier ("Elsevier") provided by Copyright Clearance Center ("CCC"). The license consists of your order details, the terms and conditions provided by Elsevier, and the payment terms and conditions.

All payments must be made in full to CCC. For payment instructions, please see information listed at the bottom of this form.

Supplier	Elsevier Limited The Boulevard,Langford Lane Kidlington,Oxford,OX5 1GB,UK
Registered Company Number	1982084
Customer name	Hirendrasinh Parmar
Customer address	7S1-5850 College St Halifax, NS B3H 4R2
License number	3615641249992
License date	Apr 24, 2015
Licensed content publisher	Elsevier
Licensed content publication	Current Opinion in Cell Biology
Licensed content title	ER structure and function
Licensed content author	None
Licensed content date	August 2013
Licensed content volume number	25
Licensed content issue number	4
Number of pages	6
Start Page	428
End Page	433
Type of Use	reuse in a thesis/dissertation
Portion	figures/tables/illustrations
Number of figures/tables/illustrations	1
Format	both print and electronic

Are you the author of this Elsevier article?	No
Will you be translating?	No
Original figure numbers	Figure 2
Title of your thesis/dissertation	The Ins and Outs of Protein Trafficking Pathways: Insights from the FAST Proteins
Expected completion date	May 2015
Estimated size (number of pages)	200
Elsevier VAT number	GB 494 6272 12
Permissions price	0.00 USD
VAT/Local Sales Tax	0.00 USD / 0.00 GBP
Total	0.00 USD

ELSEVIER LICENSE
TERMS AND CONDITIONS

Apr 24, 2015

This is a License Agreement between Hirendrasinh Parmar ("You") and Elsevier ("Elsevier") provided by Copyright Clearance Center ("CCC"). The license consists of your order details, the terms and conditions provided by Elsevier, and the payment terms and conditions.

All payments must be made in full to CCC. For payment instructions, please see information listed at the bottom of this form.

Supplier	Elsevier Limited The Boulevard,Langford Lane Kidlington,Oxford,OX5 1GB,UK
Registered Company Number	1982084
Customer name	Hirendrasinh Parmar
Customer address	7S1-5850 College St Halifax, NS B3H 4R2
License number	3615641480142
License date	Apr 24, 2015
Licensed content publisher	Elsevier
Licensed content publication	Virology
Licensed content title	Different activities of the reovirus FAST proteins and influenza hemagglutinin in cell–cell fusion assays and in response to membrane curvature agents
Licensed content author	Eileen K. Clancy,Chris Barry,Marta Ciechonska,Roy Duncan
Licensed content date	5 February 2010
Licensed content volume number	397
Licensed content issue number	1
Number of pages	11
Start Page	119
End Page	129
Type of Use	reuse in a thesis/dissertation
Intended publisher of new work	other
Portion	figures/tables/illustrations
Number of figures/tables/illustrations	1
Format	both print and electronic

Are you the author of this Elsevier article?	No
Will you be translating?	No
Original figure numbers	Figure 8A
Title of your thesis/dissertation	The Ins and Outs of Protein Trafficking Pathways: Insights from the FAST Proteins
Expected completion date	May 2015
Estimated size (number of pages)	200
Elsevier VAT number	GB 494 6272 12
Permissions price	0.00 USD
VAT/Local Sales Tax	0.00 USD / 0.00 GBP
Total	0.00 USD
Terms and Conditions	

INTRODUCTION

1. The publisher for this copyrighted material is Elsevier. By clicking "accept" in connection with completing this licensing transaction, you agree that the following terms and conditions apply to this transaction (along with the Billing and Payment terms and conditions established by Copyright Clearance Center, Inc. ("CCC"), at the time that you opened your Rightslink account and that are available at any time at http://myaccount.copyright.com).

GENERAL TERMS

2. Elsevier hereby grants you permission to reproduce the aforementioned material subject to the terms and conditions indicated.

3. Acknowledgement: If any part of the material to be used (for example, figures) has appeared in our publication with credit or acknowledgement to another source, permission must also be sought from that source. If such permission is not obtained then that material may not be included in your publication/copies. Suitable acknowledgement to the source must be made, either as a footnote or in a reference list at the end of your publication, as follows:

"Reprinted from Publication title, Vol /edition number, Author(s), Title of article / title of chapter, Pages No., Copyright (Year), with permission from Elsevier [OR APPLICABLE SOCIETY COPYRIGHT OWNER]." Also Lancet special credit - "Reprinted from The Lancet, Vol. number, Author(s), Title of article, Pages No., Copyright (Year), with permission from Elsevier."

4. Reproduction of this material is confined to the purpose and/or media for which permission is hereby given.

5. Altering/Modifying Material: Not Permitted. However figures and illustrations may be altered/adapted minimally to serve your work. Any other abbreviations, additions, deletions and/or any other alterations shall be made only with prior written authorization of Elsevier Ltd. (Please contact Elsevier at permissions@elsevier.com)

6. If the permission fee for the requested use of our material is waived in this instance, please be advised that your future requests for Elsevier materials may attract a fee.

7. Reservation of Rights: Publisher reserves all rights not specifically granted in the combination of (i) the license details provided by you and accepted in the course of this licensing transaction, (ii) these terms and conditions and (iii) CCC's Billing and Payment terms and conditions.

8. License Contingent Upon Payment: While you may exercise the rights licensed immediately upon issuance of the license at the end of the licensing process for the transaction, provided that you have disclosed complete and accurate details of your proposed use, no license is finally effective unless and until full payment is received from you (either by publisher or by CCC) as provided in CCC's Billing and Payment terms and conditions. If full payment is not received on a timely basis, then any license preliminarily granted shall be deemed automatically revoked and shall be void as if never granted. Further, in the event that you breach any of these terms and conditions or any of CCC's Billing and Payment terms and conditions, the license is automatically revoked and shall be void as if never granted. Use of materials as described in a revoked license, as well as any use of the materials beyond the scope of an unrevoked license, may constitute copyright infringement and publisher reserves the right to take any and all action to protect its copyright in the materials.

9. Warranties: Publisher makes no representations or warranties with respect to the licensed material.

10. Indemnity: You hereby indemnify and agree to hold harmless publisher and CCC, and their respective officers, directors, employees and agents, from and against any and all claims arising out of your use of the licensed material other than as specifically authorized pursuant to this license.

11. No Transfer of License: This license is personal to you and may not be sublicensed, assigned, or transferred by you to any other person without publisher's written permission.

12. No Amendment Except in Writing: This license may not be amended except in a writing signed by both parties (or, in the case of publisher, by CCC on publisher's behalf).

13. Objection to Contrary Terms: Publisher hereby objects to any terms contained in any purchase order, acknowledgment, check endorsement or other writing prepared by you, which terms are inconsistent with these terms and conditions or CCC's Billing and

Payment terms and conditions. These terms and conditions, together with CCC's Billing and Payment terms and conditions (which are incorporated herein), comprise the entire agreement between you and publisher (and CCC) concerning this licensing transaction. In the event of any conflict between your obligations established by these terms and conditions and those established by CCC's Billing and Payment terms and conditions, these terms and conditions shall control.

14. Revocation: Elsevier or Copyright Clearance Center may deny the permissions described in this License at their sole discretion, for any reason or no reason, with a full refund payable to you. Notice of such denial will be made using the contact information provided by you. Failure to receive such notice will not alter or invalidate the denial. In no event will Elsevier or Copyright Clearance Center be responsible or liable for any costs, expenses or damage incurred by you as a result of a denial of your permission request, other than a refund of the amount(s) paid by you to Elsevier and/or Copyright Clearance Center for denied permissions.

LIMITED LICENSE

The following terms and conditions apply only to specific license types:

15. **Translation**: This permission is granted for non-exclusive world **English** rights only unless your license was granted for translation rights. If you licensed translation rights you may only translate this content into the languages you requested. A professional translator must perform all translations and reproduce the content word for word preserving the integrity of the article. If this license is to re-use 1 or 2 figures then permission is granted for non-exclusive world rights in all languages.

16. **Posting licensed content on any Website**: The following terms and conditions apply as follows: Licensing material from an Elsevier journal: All content posted to the web site must maintain the copyright information line on the bottom of each image; A hyper-text must be included to the Homepage of the journal from which you are licensing athttp://www.sciencedirect.com/science/journal/xxxxx or the Elsevier homepage for books athttp://www.elsevier.com; Central Storage: This license does not include permission for a scanned version of the material to be stored in a central repository such as that provided by Heron/XanEdu.

Licensing material from an Elsevier book: A hyper-text link must be included to the Elsevier homepage at http://www.elsevier.com . All content posted to the web site must maintain the copyright information line on the bottom of each image.

Posting licensed content on Electronic reserve: In addition to the above the following clauses are applicable: The web site must be password-protected and made available only to bona fide students registered on a relevant course. This permission is granted for 1 year only. You may obtain a new license for future website posting.

17. **For journal authors:** the following clauses are applicable in addition to the above:

Preprints:

A preprint is an author's own write-up of research results and analysis, it has not been peer-reviewed, nor has it had any other value added to it by a publisher (such as formatting, copyright, technical enhancement etc.).

Authors can share their preprints anywhere at any time. Preprints should not be added to or enhanced in any way in order to appear more like, or to substitute for, the final versions of articles however authors can update their preprints on arXiv or RePEc with their Accepted Author Manuscript (see below).

If accepted for publication, we encourage authors to link from the preprint to their formal publication via its DOI. Millions of researchers have access to the formal publications on ScienceDirect, and so links will help users to find, access, cite and use the best available version. Please note that Cell Press, The Lancet and some society-owned have different preprint policies. Information on these policies is available on the journal homepage.

Accepted Author Manuscripts: An accepted author manuscript is the manuscript of an article that has been accepted for publication and which typically includes author-incorporated changes suggested during submission, peer review and editor-author communications.

Authors can share their accepted author manuscript:

- – immediately
    - via their non-commercial person homepage or blog
    - by updating a preprint in arXiv or RePEc with the accepted manuscript
    - via their research institute or institutional repository for internal institutional uses or as part of an invitation-only research collaboration work-group
    - directly by providing copies to their students or to research collaborators for their personal use
    - for private scholarly sharing as part of an invitation-only work group on commercial sites with which Elsevier has an agreement
- – after the embargo period
    - via non-commercial hosting platforms such as their institutional repository
    - via commercial sites with which Elsevier has an agreement

In all cases accepted manuscripts should:

- – link to the formal publication via its DOI
- – bear a CC-BY-NC-ND license - this is easy to do

- – if aggregated with other manuscripts, for example in a repository or other site, be shared in alignment with our hosting policy not be added to or enhanced in any way to appear more like, or to substitute for, the published journal article.

Published journal article (JPA): A published journal article (PJA) is the definitive final record of published research that appears or will appear in the journal and embodies all value-adding publishing activities including peer review co-ordination, copy-editing, formatting, (if relevant) pagination and online enrichment.

Policies for sharing publishing journal articles differ for subscription and gold open access articles:

Subscription Articles: If you are an author, please share a link to your article rather than the full-text. Millions of researchers have access to the formal publications on ScienceDirect, and so links will help your users to find, access, cite, and use the best available version.

Theses and dissertations which contain embedded PJAs as part of the formal submission can be posted publicly by the awarding institution with DOI links back to the formal publications on ScienceDirect.

If you are affiliated with a library that subscribes to ScienceDirect you have additional private sharing rights for others' research accessed under that agreement. This includes use for classroom teaching and internal training at the institution (including use in course packs and courseware programs), and inclusion of the article for grant funding purposes.

Gold Open Access Articles: May be shared according to the author-selected end-user license and should contain a CrossMark logo, the end user license, and a DOI link to the formal publication on ScienceDirect.

Please refer to Elsevier's posting policy for further information.

18. **For book authors** the following clauses are applicable in addition to the above: Authors are permitted to place a brief summary of their work online only. You are not allowed to download and post the published electronic version of your chapter, nor may you scan the printed edition to create an electronic version. **Posting to a repository:** Authors are permitted to post a summary of their chapter only in their institution's repository.

19. **Thesis/Dissertation**: If your license is for use in a thesis/dissertation your thesis may be submitted to your institution in either print or electronic form. Should your thesis be published commercially, please reapply for permission. These requirements include permission for the Library and Archives of Canada to supply single copies, on demand, of the complete thesis and include permission for Proquest/UMI to supply single copies, on demand, of the complete thesis. Should your thesis be published commercially, please reapply for permission. Theses and dissertations which contain embedded PJAs as part

CC BY NC ND: The CC BY-NC-ND license allows users to copy and distribute the Article, provided this is not done for commercial purposes and further does not permit distribution of the Article if it is changed or edited in any way, and provided the user gives appropriate credit (with a link to the formal publication through the relevant DOI), provides a link to the license, and that the licensor is not represented as endorsing the use made of the work. The full details of the license are available at http://creativecommons.org/licenses/by-nc-nd/4.0. Any commercial reuse of Open Access articles published with a CC BY NC SA or CC BY NC ND license requires permission from Elsevier and will be subject to a fee.

Commercial reuse includes:

- – Associating advertising with the full text of the Article
- – Charging fees for document delivery or access
- – Article aggregation
- – Systematic distribution via e-mail lists or share buttons

Posting or linking by commercial companies for use by customers of those companies.

20. **Other Conditions**:

v1.7

Questions? customercare@copyright.com or +1-855-239-3415 (toll free in the US) or +1-978-646-2777.

Gratis licenses (referencing $0 in the Total field) are free. Please retain this printable license for your reference. No payment is required.

FW: CSHL Press Reprint Permission Request Form

Brown, Carol <brown@cshl.edu>

Thu 4/23/2015 4:14 PM
Inbox
To:Hirendrasinh Parmar <H.Parmar@Dal.Ca>;
Permission granted.

Regards,

Carol C. Brown
Books Development, Marketing and Sales
Cold Spring Harbor Laboratory Press
500 Sunnyside Blvd
Woodbury, New York 11797
516 422 4038 ph.
516 422 4095 fx.
brown@cshl.edu

-----Original Message-----
From: reprint@cshl.edu [mailto:reprint@cshl.edu]
Sent: Thursday, April 23, 2015 1:29 PM
To: Reprint
Subject: CSHL Press Reprint Permission Request Form

Default Intro
Default Intro - line2

Name: Hirendrasinh Parmar
CompanyInstitution: Dalhousie University
Library Address: 7S1-5850 College St
Library Address (line 2):
City: Halifax
State (US and Canada): Nova Scotia
Country: Canada
Zip: B3H 4R2
Title:
Lab/Department: Dept. of Microbiology & Immunology
Phone: +19024942630
Fax:
Email: h.parmar@dal.ca
Title of Publication: The Ins and Outs of Protein Trafficking Pathways: Insights from the FAST Proteins
Authors/Editors: Hirendrasinh Parmar

Date of Publication: May 2015
Publisher: Dalhousie University
Title of CSHLP Journal/Book: Cold Spring Harbor Perspectives in Biology
Title of Article/Chapter: Models for Golgi Traffic: A Critical Assessment
CSHL Authors/Editors: Benjamin S. Glick and Alberto Luini
Page Numbers: 1-15
Figure Numbers: Figure 1, Figure 2
Figure Page Numbers:
Copyright Date:
Language: English
Territory: Canada
Format: Electronic and print
Additional comments: I would like to use these two figures for my PhD thesis.

ipaddress: 134.190.237.236
view here: http://www.cshlpress.com/subs_admin.tpl

Journal of cell science

- **Order detail ID:** 66821507
- **Order date:** 04/23/2015
- **Order License Id:** 3614870833341
- **ISSN:**0021-9533
- **Publication Type:** Journal
- **Volume:**
- **Issue:**
- **Start page:**
- **Publisher:** Company of Biologists Ltd.
- **Author/Editor:** COMPANY OF BIOLOGISTS
- **Permission Status:** **Granted**
- **Permission type:** Republish or display content
- **Type of use:** Republish in a thesis/dissertation

Requestor type	Academic institution
Format	Print, Electronic
Portion	chart/graph/table/figure
Number of charts/graphs/tables/figures	1
Title or numeric reference of the portion(s)	Figure 3(A)
Title of the article or chapter the portion is from	Mechanisms of transport through the Golgi complex
Editor of portion(s)	N/A
Author of portion(s)	Catherine L. Jackson
Volume of serial or monograph	122
Issue, if republishing an article from a serial	4
Page range of portion	443-452
Publication date of portion	February 15, 2009
Rights for	Main product
Duration of use	Life of current edition

Creation of copies for the disabled	no
With minor editing privileges	yes
For distribution to	Canada
In the following language(s)	Original language of publication
With incidental promotional use	no
Lifetime unit quantity of new product	Up to 499
Made available in the following markets	Education
The requesting person/organization	Hirendrasinh Parmar
Order reference number	
Author/Editor	Hirendrasinh Parmar
The standard identifier	hr425141
Title	The Ins and Outs of Protein Trafficking Pathways: Insights from the FAST Proteins
Publisher	Dalhousie University
Expected publication date	May 2015
Estimated size (pages)	200

Note: This item will be invoiced or charged separately through CCC's **RightsLink** service. More info**$ 0.00**

This is not an invoice.
Total order items: 1
Order Total: 0.00 USD

Confirmation Number: 11346286

Special Rightsholder Terms & Conditions

The following terms & conditions apply to the specific publication under which they are listed

Journal of cell science
Permission type: Republish or display content
Type of use: Republish in a thesis/dissertation

TERMS AND CONDITIONS

The following terms are individual to this publisher:

The acknowledgement should state "Reproduced / adapted with permission" and give the source journal name. The acknowledgement should either provide full citation details or refer to the relevant citation in the article reference list. The full citation details should include authors, journal, year, volume, issue and page citation.

Where appearing online or in other electronic media, a link should be provided to the original article (e.g. via DOI):

Development: dev.biologists.org

Disease Models & Mechanisms: dmm.biologists.org

Journal of Cell Science: jcs.biologists.org

The Journal of Experimental Biology: jeb.biologists.org

Other Terms and Conditions:

None

STANDARD TERMS AND CONDITIONS

1. Description of Service; Defined Terms. This Republication License enables the User to obtain licenses for republication of one or more copyrighted works as described in detail on the relevant Order Confirmation (the "Work(s)"). Copyright Clearance Center, Inc. ("CCC") grants licenses through the Service on behalf of the rightsholder identified on the Order Confirmation (the "Rightsholder"). "Republication", as used herein, generally means the inclusion of a Work, in whole or in part, in a new work or works, also as described on the Order Confirmation. "User", as used herein, means the person or entity making such republication.

2. The terms set forth in the relevant Order Confirmation, and any terms set by the Rightsholder with respect to a particular Work, govern the terms of use of Works in connection with the Service. By using the Service, the person transacting for a republication license on behalf of the User represents and warrants that he/she/it (a) has been duly authorized by the User to accept, and hereby does accept, all such terms and conditions on behalf of User, and (b) shall inform User of all such terms and conditions. In the event such person is a "freelancer" or other third party independent of User and CCC, such party shall be deemed jointly a "User" for purposes of these terms and conditions. In any event, User shall be deemed to have accepted and agreed to all such terms and conditions if User republishes the Work in any fashion.

3. Scope of License; Limitations and Obligations.

3.1 All Works and all rights therein, including copyright rights, remain the sole and exclusive property of the Rightsholder. The license created by the exchange of an Order Confirmation (and/or any invoice) and payment by User of the full amount set forth on that document includes only those rights expressly set forth in the Order Confirmation and in these terms and conditions, and conveys no other rights in the Work(s) to User. All rights not expressly granted are hereby reserved.

3.2 General Payment Terms: You may pay by credit card or through an account with us payable at the end of the month. If you and we agree that you may establish a standing account with CCC, then the following terms apply: Remit Payment to: Copyright Clearance Center, Dept 001, P.O. Box 843006, Boston, MA 02284-3006. Payments Due: Invoices are payable upon their delivery to you (or upon our notice to you that they are available to you for downloading). After 30 days, outstanding amounts will be subject to a service charge of 1-1/2% per month or, if less, the maximum rate allowed by applicable law. Unless otherwise specifically set forth in the Order Confirmation or in a separate written agreement signed by CCC, invoices are due and payable on "net 30" terms. While User may exercise the rights licensed immediately upon issuance of the Order Confirmation, the license is automatically revoked and is null and void, as if it had never been issued, if complete payment for the license is not received on a timely basis either from User directly or through a payment agent, such as a credit card company.

3.3 Unless otherwise provided in the Order Confirmation, any grant of rights to User (i) is "one-time" (including the editions and product family specified in the license), (ii) is non-exclusive and non-transferable and (iii) is subject to any and all limitations and restrictions (such as, but not limited to, limitations on duration of use or circulation) included in the Order Confirmation or invoice and/or in these terms and conditions. Upon completion of the licensed use, User shall either secure a new permission for further use of the Work(s) or immediately cease any new use of the Work(s) and shall render inaccessible (such as by deleting or by removing or severing links or other locators) any further copies of the Work (except for copies printed on paper in accordance with this license and still in User's stock at the end of such period).

3.4 In the event that the material for which a republication license is sought includes third party materials (such as photographs, illustrations, graphs, inserts and similar materials) which are identified in such material as having been used by permission, User is responsible for identifying, and seeking separate licenses (under this Service or otherwise) for, any of such third party materials; without a separate license, such third party materials may not be used.

3.5 Use of proper copyright notice for a Work is required as a condition of any license granted under the Service. Unless otherwise provided in the Order Confirmation, a proper copyright notice will read substantially as follows: "Republished with permission of [Rightsholder's name], from [Work's title, author, volume, edition number and year of copyright]; permission conveyed through Copyright Clearance Center, Inc. " Such notice must be provided in a reasonably legible font size and must be placed either immediately adjacent to the Work as used (for example, as part of a by-line or footnote but not as a separate electronic link) or in the place where substantially all other credits or notices for the new work containing the republished Work are located. Failure to include the required notice results in loss to the Rightsholder and CCC, and the User shall be liable to pay liquidated damages for each such failure equal to twice the use fee specified in the Order Confirmation, in addition to the use fee itself and any other fees and charges specified.

3.6 User may only make alterations to the Work if and as expressly set forth in the Order Confirmation. No Work may be used in any way that is defamatory, violates the rights of third parties (including such third parties' rights of copyright, privacy, publicity, or other tangible or intangible property), or is otherwise illegal, sexually explicit or obscene. In addition, User may not conjoin a Work with any other material that may result in damage to the reputation of the Rightsholder. User agrees to inform CCC if it becomes aware of any infringement of any rights in a Work and to cooperate with any reasonable request of CCC or the Rightsholder in connection therewith.

4. Indemnity. User hereby indemnifies and agrees to defend the Rightsholder and CCC, and their respective employees and directors, against all claims, liability, damages, costs and expenses, including legal fees and expenses, arising out of any use of a Work beyond the scope of the rights granted herein, or any use of a Work which has been altered in any unauthorized way by User, including claims of defamation or infringement of rights of copyright, publicity, privacy or other tangible or intangible property.

5. Limitation of Liability. UNDER NO CIRCUMSTANCES WILL CCC OR THE RIGHTSHOLDER BE LIABLE FOR ANY DIRECT, INDIRECT, CONSEQUENTIAL OR INCIDENTAL DAMAGES (INCLUDING WITHOUT LIMITATION DAMAGES FOR LOSS OF BUSINESS PROFITS OR INFORMATION, OR FOR BUSINESS INTERRUPTION) ARISING OUT OF THE USE OR INABILITY TO USE A WORK, EVEN IF ONE OF THEM HAS BEEN ADVISED OF THE POSSIBILITY OF SUCH DAMAGES. In any event, the total liability of the Rightsholder and CCC (including their respective employees and directors) shall not exceed the total amount actually paid by User for this license. User assumes full liability for the actions and omissions of its principals, employees, agents, affiliates, successors and assigns.

6. Limited Warranties. THE WORK(S) AND RIGHT(S) ARE PROVIDED "AS IS". CCC HAS THE RIGHT TO GRANT TO USER THE RIGHTS GRANTED IN THE ORDER CONFIRMATION DOCUMENT. CCC AND THE RIGHTSHOLDER DISCLAIM ALL OTHER WARRANTIES RELATING TO THE WORK(S) AND RIGHT(S), EITHER EXPRESS OR IMPLIED, INCLUDING WITHOUT LIMITATION IMPLIED WARRANTIES OF MERCHANTABILITY OR FITNESS FOR A PARTICULAR PURPOSE. ADDITIONAL RIGHTS MAY BE REQUIRED TO USE ILLUSTRATIONS, GRAPHS, PHOTOGRAPHS, ABSTRACTS, INSERTS OR OTHER PORTIONS OF THE WORK (AS OPPOSED TO THE ENTIRE WORK) IN A MANNER CONTEMPLATED BY USER; USER UNDERSTANDS AND AGREES THAT NEITHER CCC NOR THE RIGHTSHOLDER MAY HAVE SUCH ADDITIONAL RIGHTS TO GRANT.

7. Effect of Breach. Any failure by User to pay any amount when due, or any use by User of a Work beyond the scope of the license set forth in the Order Confirmation and/or these terms and conditions, shall be a material breach of the license created by the Order Confirmation and these terms and conditions. Any breach not cured within 30 days of written notice thereof shall result in immediate termination of such license without further notice. Any unauthorized (but licensable) use of a Work that is terminated immediately upon notice thereof may be liquidated by payment of the Rightsholder's ordinary license price therefor; any unauthorized (and unlicensable) use that is not terminated immediately for any reason (including, for example, because materials containing the Work cannot reasonably be recalled) will be subject to all remedies available at law or in equity, but in no event to a payment of less than three times the Rightsholder's ordinary license price for the most closely analogous licensable use plus Rightsholder's and/or CCC's costs and expenses incurred in collecting such payment.

8. **Miscellaneous.**

8.1 User acknowledges that CCC may, from time to time, make changes or additions to the Service or to these terms and conditions, and CCC reserves the right to send notice to the User by electronic mail or otherwise for the purposes of notifying User of such changes or additions; provided that any such changes or additions shall not apply to permissions already secured and paid for.

8.2 Use of User-related information collected through the Service is governed by CCC's privacy policy, available online here:
http://www.copyright.com/content/cc3/en/tools/footer/privacypolicy.html.

8.3 The licensing transaction described in the Order Confirmation is personal to User. Therefore, User may not assign or transfer to any other person (whether a natural person or an organization of any kind) the license created by the Order Confirmation and these terms and conditions or any rights granted hereunder; provided, however, that User may assign such license in its entirety on written notice to CCC in the event of a transfer of all or substantially all of User's rights in the new material which includes the Work(s) licensed under this Service.

8.4 No amendment or waiver of any terms is binding unless set forth in writing and signed by the parties. The Rightsholder and CCC hereby object to any terms contained in any writing prepared by the User or its principals, employees, agents or affiliates and purporting to govern or otherwise relate to the licensing transaction described in the Order Confirmation, which terms are in any way inconsistent with any terms set forth in the Order Confirmation and/or in these terms and conditions or CCC's standard operating procedures, whether such writing is prepared prior to, simultaneously with or subsequent to the Order Confirmation, and whether such writing appears on a copy of the Order Confirmation or in a separate instrument.

8.5 The licensing transaction described in the Order Confirmation document shall be governed by and construed under the law of the State of New York, USA, without regard to the principles thereof of conflicts of law. Any case, controversy, suit, action, or proceeding arising out of, in connection with, or related to such licensing transaction shall be brought, at CCC's sole discretion, in any federal or state court located in the County of New York, State of New York, USA, or in any federal or state court whose geographical jurisdiction covers the location of the Rightsholder set forth in the Order Confirmation. The parties expressly submit to the personal jurisdiction and venue of each such federal or state court.If you have any comments or questions about the Service or Copyright Clearance Center, please contact us at 978-750-8400 or send an e-mail to info@copyright.com.

v 1.1